Methods in Molecular Biology 1569

Springer Protocols

Thomas Dandekar
Muhammad Naseem *Editors*

Auxins and Cytokinins in Plant Biology

Methods and Protocols

EXTRAS ONLINE

Humana Press

METHODS IN MOLECULAR BIOLOGY

Series Editor
John M. Walker
School of Life and Medical Sciences
University of Hertfordshire
Hatfield, Hertfordshire, AL10 9AB, UK

For further volumes:
http://www.springer.com/series/7651

Auxins and Cytokinins in Plant Biology

Methods and Protocols

Edited by

Thomas Dandekar

Deptartment of Bioinformatics, Biocenter University of Würzburg Am Hubland Würzburg Germany, Julius-Maximilians-Universität Würzburg, Würzburg, Germany

Muhammad Naseem

Deptartment of Bioinformatics, Biocenter University of Würzburg Am Hubland Würzburg Germany, Julius-Maximilians-Universität Würzburg, Würzburg, Germany; Department of Molecular Biology and Genetics, Boğaziçi University, Istanbul, Turkey

Humana Press

Editors
Thomas Dandekar
Deptartment of Bioinformatics
Biocenter University of Würzburg Am Hubland
Würzburg Germany
Julius-Maximilians-Universität Würzburg
Würzburg, Germany

Muhammad Naseem
Deptartment of Bioinformatics
Biocenter University of Würzburg Am Hubland
Würzburg Germany
Julius-Maximilians-Universität Würzburg
Wurzburg, Germany

Department of Molecular Biology and Genetics
Boğaziçi University
Istanbul, Turkey

ISSN 1064-3745 ISSN 1940-6029 (electronic)
Methods in Molecular Biology
ISBN 978-1-4939-6829-9 ISBN 978-1-4939-6831-2 (eBook)
DOI 10.1007/978-1-4939-6831-2

Library of Congress Control Number: 2017931659

Printed on acid-free paper

This Humana Press imprint is published by Springer Nature
The registered company is Springer Science+Business Media LLC
The registered company address is: 233 Spring Street, New York, NY 10013, U.S.A.

Preface

It has been several decades since Skoog and Miller described the contrasting behavior of auxin and cytokinin in influencing the growth of root and shoot in plants. Since then, a profound understanding concerning the implications of auxin and cytokinin for plant growth and development has been achieved. Complex processes such as the maintenance of stem cell in niches such as root apical meristem, shoot apical meristem, and lateral root meristems have recently been unearthed. Robust stem cell signaling networks, leaf position determination, and emergence of leaf primordia, lateral root formation, and de novo hormone-induced organogenesis are the processes that are stringently fine-tuned by a balance between auxin and cytokinins in plants.

More intriguingly, for various plant processes synergistic and antagonistic interactions have been demonstrated for auxin and cytokinins. Auxin exerts its inhibition on cytokinins at several levels; mechanisms range from its biosynthesis to the suppression of its signaling. Reciprocally, cytokinins antagonistically impact the flux, distribution, and signaling of auxin. Not only in growth and development but both these hormones have recently been shown to modulate plant regulatory networks that govern the adaptation of plants to biotic and abiotic stresses. The interaction between cytokinin and salicylic acid and that of auxin and jasmonate have opened new avenues in the study of plant-pathogen interactions. Furthermore, reports also highlight the emerging role of cytokinin in abiotic stresses as well as its crosstalk to stress hormone abscisic acid.

All these groundbreaking discoveries concerning the biology of auxin and cytokinins are by the virtue of dedicated efforts made by the plant science community. Besides phenomenal description of these important plant hormones in many publications, a methodological focus on tools, assays, and techniques that enhance our understanding of the functional role of auxin and cytokinins is worth a special compilation. To accomplish this task, we aimed at collecting vital protocols with their background information as well as potential applications in the form of this volume of Methods in Molecular Biology (MiMB). We are thankful to our humble authors who did spare time and efforts to contribute to this timely topic of plant biology. We hope that this volume will provide a unique opportunity to plant scientists, graduate and undergraduate students in adopting these vital methods in addressing their biological questions pertinent to the functional implications of auxin and cytokinins.

Würzburg, Germany — *Thomas Dandekar*
Würzburg, Germany — *Muhammad Naseem*

Contents

Preface . . . . . *v*
Contributors . . . . . *ix*

1 Methodological Advances in Auxin and Cytokinin Biology 1
Andrej Hurný and Eva Benková

2 Analytical Determination of Auxins and Cytokinins 31
Petre I. Dobrev, Klára Hoyerová, and Jan Petrášek

3 Manipulation of Auxin and Cytokinin Balance During the *Plasmodiophora brassicae–Arabidopsis thaliana* Interaction 41
Jutta Ludwig-Müller, Susann Auer, Sabine Jülke, and Sabine Marschollek

4 Microbial Manipulation of Auxins and Cytokinins in Plants 61
Anwar Hussain, Ihsan Ullah, and Shahida Hasnain

5 A Standardized Method to Assess Infection Rates of Root-Knot and Cyst Nematodes in *Arabidopsis thaliana* Mutants with Alterations in Root Development Related to Auxin and Cytokinin Signaling 73
Rocío Olmo, Ana Cláudia Silva, Fernando E. Díaz-Manzano, Javier Cabrera, Carmen Fenoll, and Carolina Escobar

6 Reconstruction of an Immune Dynamic Model to Simulate the Contrasting Role of Auxin and Cytokinin in Plant Immunity 83
Martin Kaltdorf, Thomas Dandekar, and Muhammad Naseem

7 Interplay Between Auxin and Cytokinin and Its Impact on Mitogen Activated Protein Kinase (MAPK) 93
Pallavi Singh and Alok Krishna Sinha

8 Quantification of Cytokinin Levels and Responses in Abiotic Stresses 101
Alfonso Albacete

9 Assessment of Cytokinin-Induced Immunity Through Quantification of *Hyaloperonospora arabidopsidis* Infection in *Arabidopsis thaliana* 113
Ruth A. Watson and Cristiana T. Argueso

10 Real-Time Genetic Manipulations of the Cytokinin Pathway: A Tool for Laboratory and Field Studies 127
Martin Schäfer and Stefan Meldau

11 Modulating the Levels of Plant Hormone Cytokinins at the Host-Pathogen Interface 141
Muhammad Naseem, Shabana Shams, and Thomas Roitsch

12 Analyzing Cytokinin Responses During Plant-Nematode Interactions 151
Florian M.W. Grundler and Shahid Siddique

13 Examining H_2O_2 Production in *Arabidopsis* Leaves Upon Challenge by Cytokinin 159
Shahjahan Shabbir Ahmed, Ihsan Ullah, Shazia Irfan, and Nazeer Ahmed

14 A Systems Biology Methodology Combining Transcriptome and Interactome Datasets to Assess the Implications of Cytokinin Signaling for Plant Immune Networks. 165
Meik Kunz, Thomas Dandekar, and Muhammad Naseem

15 Monitoring of Crosstalk Between Jasmonate and Auxin in the Framework of Plant Stress Responses of Roots. 175
Víctor Carrasco Loba, Marta-Marina Pérez Alonso, and Stephan Pollmann

16 High-Throughput Protoplast Trans-Activation (PTA) Screening to Define Transcription Factors in Auxin-Mediated Gene Regulation 187
Nora Wehner, Jörn Herfert, Wolfgang Dröge-Laser, and Christoph Weiste

Index *203*

Contributors

Nazeer Ahmed • *Department of Biotechnology, Balochistan University of IT, Engineering and Management Sciences, Quetta, Pakistan*

Shahjahan Shabbir Ahmed • *Department of Biotechnology, Balochistan University of IT, Engineering and Management Sciences, Quetta, Pakistan*

Alfonso Albacete • *Department of Plant Nutrition, CEBAS-CSIC, Murcia, Spain*

Cristiana T. Argueso • *Department of Bioagricultural Sciences and Pest Management, Colorado State University, Fort Collins, CO, USA*

Susann Auer • *Institut für Botanik, Technische Universität Dresden, Dresden, Germany*

Eva Benková • *Institute of Science and Technology, Klosterneuburg, Austria*

Javier Cabrera • *Facultad de Ciencias Ambientales y Bioquímica, Universidad de Castilla-La Mancha, Toledo, Spain*

Thomas Dandekar • *Deptartment of Bioinformatics, Biocenter University of Würzburg Am Hubland Würzburg Germany, Julius-Maximilians-Universität Würzburg, Würzburg, Germany*

Fernando E. Díaz-Manzano • *Facultad de Ciencias Ambientales y Bioquímica, Universidad de Castilla-La Mancha, Toledo, Spain*

Petre I. Dobrev • *Laboratory of Hormonal Regulations in Plants, Institute of Experimental Botany, CAS, Praha, Czech Republic*

Wolfgang Dröge-Laser • *Pharmazeutische Biologie, Julius-von-Sachs-Institut, Julius-Maximilians-Universität Würzburg, Würzburg, Germany*

Carolina Escobar • *Facultad de Ciencias Ambientales y Bioquímica, Universidad de Castilla-La Mancha, Toledo, Spain*

Carmen Fenoll • *Facultad de Ciencias Ambientales y Bioquímica, Universidad de Castilla-La Mancha, Toledo, Spain*

Florian M.W. Grundler • *Department of Molecular Phytomedicine, Rheinische Friedrich-Wilhelms-University of Bonn, Bonn, Germany*

Shahida Hasnain • *Department of Microbiology and Molecular Genetics, University of the Punjab, Lahore, Pakistan*

Jörn Herfert • *Pharmazeutische Biologie, Julius-von-Sachs-Institut, Julius-Maximilians-Universität Würzburg, Würzburg, Germany*

Klára Hoyerová • *Laboratory of Hormonal Regulations in Plants, Institute of Experimental Botany, CAS, Praha, Czech Republic*

Andrej Hurný • *Institute of Science and Technology, Klosterneuburg, Austria*

Anwar Hussain • *Department of Botany, Garden Campus, Abdul Wali Khan University, Mardan, Pakistan*

Shazia Irfan • *Department of Biotechnology, Balochistan University of IT, Engineering and Management Sciences, Quetta, Pakistan*

Sabine Jülke • *Institut für Botanik, Technische Universität Dresden, Dresden, Germany*

Martin Kaltdorf • *Functional Genomics & Systems Biology Group, Department of Bioinformatics, Biocenter, University of Würzburg, Wuerzburg, Germany*

Meik Kunz • *Functional Genomics & Systems Biology Group, Department of Bioinformatics, Biocenter, University of Würzburg, Wuerzburg, Germany*

Víctor Carrasco Loba • *Centro de Biotecnología y Genómica de Plantas, Universidad Politécnica de Madrid (UPM)-Instituto Nacional de Investigación y Tecnología Agraria y Alimentación (INIA), Campus de Montegancedo, Madrid, Spain*
Jutta Ludwig-Müller • *Institut für Botanik, Technische Universität Dresden, Dresden, Germany*
Sabine Marschollek • *Institut für Botanik, Technische Universität Dresden, Dresden, Germany*
Stefan Meldau • *Research & Development, KWS SAAT SE, Grimsehlstrasse, Einbeck, Germany*
Muhammad Naseem • *Deptartment of Bioinformatics, Biocenter University of Würzburg Am Hubland Würzburg Germany, Julius-Maximilians-Universität Würzburg, Würzburg, Germany; Department of Molecular Biology and Genetics, Boğaziçi University, Bebek, Istanbul, Turkey*
Rocío Olmo • *Facultad de Ciencias Ambientales y Bioquímica, Universidad de Castilla-La Mancha, Toledo, Spain*
Marta-Marina Pérez Alonso • *Centro de Biotecnología y Genómica de Plantas, Universidad Politécnica de Madrid (UPM)-Instituto Nacional de Investigación y Tecnología Agraria y Alimentación (INIA), Campus de Montegancedo, Madrid, Spain*
Jan Petrášek • *Laboratory of Hormonal Regulations in Plants, Institute of Experimental Botany, CAS, Prague, Czech Republic; Department of Experimental Plant Biology, Faculty of Science, Charles University, Prague, Czech Republic*
Stephan Pollmann • *Centro de Biotecnología y Genómica de Plantas, Universidad Politécnica de Madrid (UPM)-Instituto Nacional de Investigación y Tecnología Agraria y Alimentación (INIA), Campus de Montegancedo, Madrid, Spain*
Thomas Roitsch • *Department of Plant and Environmental Sciences, Copenhagen Plant Science Centre, University of Copenhagen, Taastrup, Denmark; Global Change Research Centre, Czech Globe AS CR, Drásov, Czech Republic*
Martin Schäfer • *Department of Molecular Ecology, Max-Planck-Institute for Chemical Ecology, Jena, Germany*
Shabana Shams • *Department of Animal Sciences, Quaid-i-Azam University, Islamabad, Pakistan*
Shahid Siddique • *Department of Molecular Phytomedicine, Rheinische Friedrich-Wilhelms-University of Bonn, Bonn, Germany*
Ana Cláudia Silva • *Facultad de Ciencias Ambientales y Bioquímica, Universidad de Castilla-La Mancha, Toledo, Spain*
Pallavi Singh • *National Institute of Plant Genome Research, New Delhi, India*
Alok Krishna Sinha • *National Institute of Plant Genome Research, New Delhi, India*
Ihsan Ullah • *Department of Environmental Science, Islamic International University, Islamabad, Pakistan*
Ruth A. Watson • *Department of Bioagricultural Sciences and Pest Management, Colorado State University, Fort Collins, CO, USA*
Nora Wehner • *Pharmazeutische Biologie, Julius-von-Sachs-Institut, Julius-Maximilians-Universität Würzburg, Würzburg, Germany*
Christoph Weiste • *Pharmazeutische Biologie, Julius-von-Sachs-Institut, Julius-Maximilians-Universität Würzburg, Würzburg, Germany*

Chapter 1

Methodological Advances in Auxin and Cytokinin Biology

Andrej Hurný and Eva Benková

Abstract

The history of auxin and cytokinin biology including the initial discoveries by father–son duo Charles Darwin and Francis Darwin (1880), and Gottlieb Haberlandt (1919) is a beautiful demonstration of unceasing continuity of research. Novel findings are integrated into existing hypotheses and models and deepen our understanding of biological principles. At the same time new questions are triggered and hand to hand with this new methodologies are developed to address these new challenges.

Key words Auxin and cytokinins, Auxin signaling and metabolism, Auxin transport, Cytokinin signaling

1 Introduction

The concept of plant hormones as chemical messengers that control plant growth and development is not a new one. Already in 1758, Duhamel du Monceau's experiments suggested communication between plant organs and showed that sap moving from the leaves controls root growth [1]. More than a century later Julius-von-Sachs proposed that plants produce "organ-forming substances"-molecules moving to different parts of the plant where they control initiation and development of specific plant organs [2]. Finally, Charles and Francis Darwin, with their experiments on phototropism of coleoptiles (described in "The Power of Movement in Plants" [3]) that later led to the discovery of auxin by Went [4], fully launched the modern research in plant growth substances.

The first note about cytokinin comes from 1913 when Gottlieb Haberlandt observed that compounds from phloem could stimulate cell division in potato parenchyma cells [5]. In the 1950s, kinetin, an active compound stimulating cell division, was isolated from herring sperm [6]. The first naturally occurring cytokinin in plants named zeatin was isolated from immature maize endosperm [7].

Thomas Dandekar and Muhammad Naseem (eds.), *Auxins and Cytokinins in Plant Biology: Methods and Protocols*, Methods in Molecular Biology, vol. 1569, DOI 10.1007/978-1-4939-6831-2_1,

Since these initial discoveries, a great number of studies have demonstrated an essential role of both auxin and cytokinin in the regulation of many aspects of plant growth and development including embryogenesis [8, 9], postembryonic organogenic processes such as root [10–14], and shoot branching [15–17], root [18–21] and shoot apical meristem activity and phyllotaxis [22–25] vasculature development [26–28] as well as tropic responses [29–31]. Importantly, a classic series of experiments by Skoog and Miller [32] demonstrated that the ratio of cytokinin to auxin profoundly influences the morphogenesis of roots and shoots in plant tissue culture. This was one of the first studies revealing auxin and cytokinin interaction in the differentiation of plant organs and pointed at hormonal cross talk as an important aspect of auxin and cytokinin regulatory functions (reviewed in [33–35]).

Nevertheless, it has been primarily the recent boom of modern technologies and approaches including analytical chemistry, biochemistry, molecular biology, genetics, cell and developmental biology that have enabled rapid progress in deciphering the auxin and cytokinin activities at the molecular level. Due to ongoing improvements and development of new methods, we are gaining deeper insights into mechanisms that control auxin and cytokinin biosynthesis, distribution, perception, and signal transduction as well as insights into their functions in the regulation of plant growth and development. In this review, we briefly discuss the major recent progress made in this area, and highlight the importance of continuous methodological improvements.

2 Discovery of Auxin and Cytokinin

Discovery of auxin is tightly linked with Darwin's early studies on coleoptiles. Based on the bending of coleoptiles toward unilateral light, the existence of a messenger molecule named auxein (from the Greek "auxein" meaning "to grow") was predicted, which was apparently transported from the site of light perception at the tip of coleoptile towards the site of response where bending occurs [3]. Later, it was demonstrated that an asymmetric accumulation of auxin at the non-illuminated side compared to the illuminated side correlated with differential cell growth and organ bending [36]. A model implementing a role for auxin and its asymmetric distribution in the regulation of plant tropic responses was proposed [4, 37, 38]. Although the existence of auxin as a molecule controlling plant growth had been predicted already by Darwin in 1880, its chemical identity remained unknown for a long time. In 1928, Went succeeded in capturing this growth substance from coleoptile tips into agar blocks and demonstrated its biological activity [4]. However, due to insufficient analytical methods for detecting low amounts of the hormone, the first auxin (indole-3-acetic acid,

IAA) was purified from human urine and culture filtrates of several fungi, both of which are rich sources of substances with auxin activity when tested in the bioassays [39, 40]. A decade later IAA was eventually discovered in a plant (*Zea mays*) [41].

The first experimental indication of the existence of cytokinins was reported by Gottlieb Haberlandt [5], who observed that phloem sap can stimulate division of potato parenchyma cells. Further studies showed that compounds which trigger cell division are present in various other plant species [42, 43]. The first molecule with the ability to promote cell division was purified from autoclaved herring sperm DNA. The compound 6-(furfurylamino) purine was named kinetin, and although it is one of the most biologically active cytokinins, it is formed as a DNA degradation product and is not detected in plant tissues [6, 44]. The first naturally occurring cytokinin, zeatin, was almost simultaneously isolated from *Zea mays* by Miller [45] and Letham [7]. Since then, many naturally occurring cytokinins have been isolated and found to be ubiquitous to all plant species [46].

The discovery and identification of auxin and cytokinins triggered the interest of researchers, who then diversified to explore pathways that underlie auxin and cytokinin biosynthesis and metabolism, their distribution, as well as perception and signal transduction of these two plant hormones. The establishment of *Arabidopsis thaliana* as a model organism for plant molecular biology was one of the important milestones in hormone molecular biology. The use of *Arabidopsis* for mutant screens based on sensitivities to auxin and cytokinin enabled the identification of genes and pathways controlling their metabolism, transport, perception and signaling. These in combination with novel technologies and approaches, such as large-scale transcriptome profiling, proteomics, chemical genomics, and most recently mathematical modeling, resulted in major breakthroughs in our understanding of auxin and cytokinin biology.

3 Auxin and Cytokinin: Insights into Biosynthesis

Although IAA had been recognized as the main native auxin already in 1935 [40], the question as to how auxin is synthesized remained unanswered for more than 70 years afterwards. Using genetic and biochemical tools, it has been found that IAA is mainly synthesized from L-tryptophan (Trp) via indole-3-pyruvate (IPA) in a two-step reaction catalyzed by TRYPTOPHAN AMINOTRANSFERASE OF ARABIDOPSIS (TAA) and YUCCA (YUC) (Fig. 1a). The TAA family of amino transferases which mediate the first step of the pathway was isolated from independent genetic screens for mutants affected in shade, ethylene, and responses to the auxin transport inhibitor NPA [47–49].

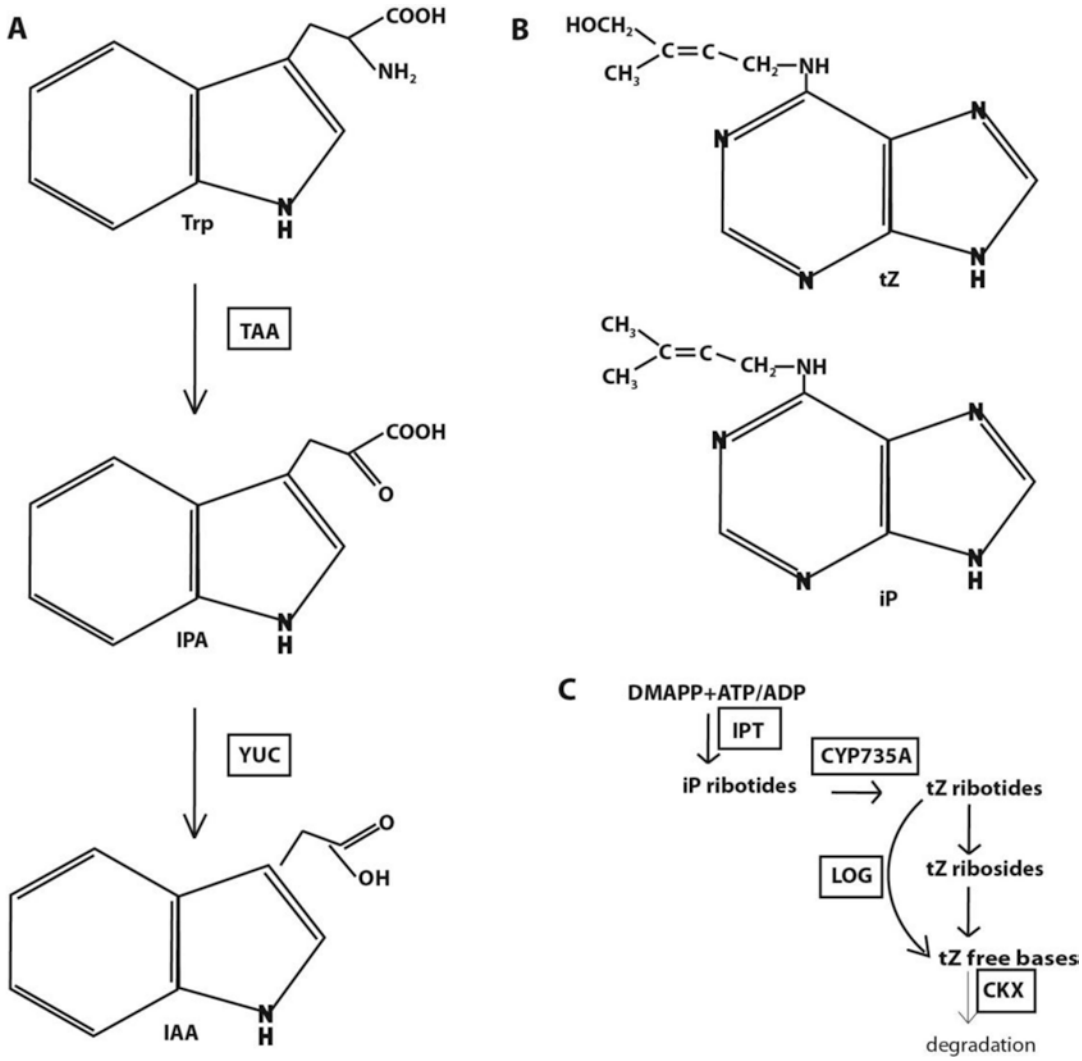

Fig. 1 Biosynthesis of auxin and cytokinins. (**a**) Auxin (IAA) is synthesized from tryptophan (Trp) precursor in two step pathway catalyzed by TAA and YUCCA. (**b**) Common plant cytokinins *trans*-zeatin (tZ) and isopentenyladenine (iP). (**c**) Core steps of cytokinin metabolism. Biosynthesis of tZ cytokinin is initiated by adenosine phosphate-isopentenyltransferase (IPT) using dimethylallyl diphosphate (DMAPP) and adenosine 5′-diphosphate (ADP), or adenosine 5′-triphosphate (ATP) to form iP-ribotides which are converted to the corresponding tZ-ribotides by cytochrome P450 monooxygenases (CYP735As). tZ-ribotides can be dephosphorylated to tZ-ribosides or directly converted to active free bases by cytokinin nucleoside 5′-monophosphate phosphoribohydrolase (LOG)

Severe auxin deficient phenotypes (in developmental processes such as embryogenesis, seedling growth, flower development, vascular patterning, root branching, tropisms, and shade avoidance) as well as reduced endogenous auxin levels were observed in mutants lacking activity of TAA1 and the homologous TAR1 and TAR2, which indicated their function in auxin homeostasis

maintenance [47]. The phenotypic defects observed in TAA1/TAR deficient mutants were partially rescued by auxin, whereas induction of TAA1 led to the accumulation of endogenous IPA. Importantly, the recombinant TAA1 protein has been found to catalyze the conversion of Trp into IPA in vitro, thus providing evidence for its direct involvement in auxin biosynthesis [47, 48].

Similarly to *TAA1*, *YUC* genes were originally identified by a genetic screen in *Arabidopsis*. Using an activation-tagged mutant library, a flavin-containing monooxygenase *YUC1* was isolated. The *YUC1* (*yuc1D*) gain-of-function mutant exhibits increase in endogenous IAA and phenotypic alterations mimicking high auxin activity. Disruption of several *YUC* genes in *Arabidopsis* leads to defects in embryogenesis, seedling growth, flower development, and vascular pattern formation [50, 51]. The developmental defects of the loss-of-function *yuc* mutants are rescued by the bacterial auxin biosynthesis gene *iaaM*, supporting *YUC* genes function in auxin biosynthesis [50].

Although previously proposed to act in two independent pathways, recent genetic and biochemical studies showed that the TAAs and YUCs catalyze two consecutive reactions in the same pathway that converts Trp to IAA. Multiple lines of evidence support this model including similarities of both *taa* and *yuc* mutants phenotypes [52] and enhancement of the auxin related phenotypes when both *YUC* and *TAA* are overexpressed in the same plants [53]. Additionally, the YUC auxin overproduction phenotypes are suppressed in the *taa* mutant backgrounds, indicating that TAA acts upstream of YUC-mediated auxin biosynthesis [52]. Direct measurement of IPA levels reveals that *yuc* mutants accumulate IPA whereas *taa* mutants are partially IPA deficient, suggesting that TAAs catalyzes synthesis of IPA which is converted by YUCs to IAA [52, 53]. Finally, in vitro biochemical assays have demonstrated that TAA can convert Trp to IPA and that YUCs produce IAA using IPA as a substrate [53].

Early physiological studies on auxin biosynthesis suggested that auxin is primarily synthesized in the young developing organs such as leaves, shoot apical meristems, and developing fruits and seeds [54, 55]. The expression pattern of *TAA* and *YUC* genes modifies this established view on auxin biosynthesis. Local auxin production seems to take place in very distinct cell types, including root and apical embryo meristems, the root cap, quiescent center (QC), root proximal meristem, vasculature of hypocotyls, as well as apical hooks, thus hinting at the spatiotemporal control of the IAA biosynthesis throughout plant growth and development [47, 48, 50, 51]. Several transcription factors which control *TAA* and *YUC* genes expression have been identified and thus might determine spatiotemporal pattern of the IAA biosynthesis. *LEAFY COTYLEDON2* (*LEC2*) [56], *SHORT INTERNODES/STYLISH* (*SHI/STY*) [57], *PHYTOCHROME-INTERACTING FACTORs*

(*PIFs*) [58, 59], *INDETERMINATE DOMAIN* (*IDD*) [60], and *PLETHORA* family members [61] have been reported as transcriptional activators of *YUC* and *TAA1* genes. In contrast, the *SPOROCYTELESS/NOZZLE* (*SPL/NZZ*) transcription factor, has been shown to negatively regulate some of *YUC* genes [62].

Chemical biology-based studies provided additional support for the central role of the IPA pathway in IAA production. Chemical screens for auxin inhibitors uncovered L-kynurenine and L-aminooxyphenylpropionic acid (L-AOPP) as TAA inhibitors and yucasin as a YUC inhibitor. Application of these compounds reduces endogenous IAA levels and results in phenotype alterations mimicking mutants deficient in auxin biosynthesis [63–65].

Overall, genetic and biochemical analyses support the YUCs/TAAs mediated auxin biosynthesis as the major pathway used to produce auxin during plant development, whereas other pathways catalyzed by CYP79B2/B3, nitrilases, aldehyde oxidases, and pyruvate decarboxylases might not be the main pathways in auxin biosynthesis [23].

The great progress in elucidation of the cytokinin biosynthesis pathway occurred almost 20 years after identification of the chemical nature of cytokinins by Miller [45] and Letham [7]. In 1978, Taya and coworkers reported biosynthesis of free cytokinins in vitro and demonstrated that cell-free extracts of the slime mold *Dictyostelium discoideum* converts adenosine monophosphate (AMP) and dimethylallyl pyrophosphate (DMAPP) to the active cytokinin iPMP (*N*6-(D2-isopentenyl)adenosine-5′-monophosphate [66]. Subsequently, the *ISOPENTENYLTRANSFERASE* (*IPT*) gene from *Agrobacterium tumefaciens* was shown to encode an enzyme with similar activity [67]. Later, nine *IPT*-homologs genes were identified by an in silico search in the *A. thaliana* genome. The expression of *IPT* genes (except *AtIPT2* and *AtIPT9*) in *E. coli* resulted in the secretion of the cytokinins isopentenyladenine (iP) and zeatin, confirming their function as cytokinin biosynthetic enzymes [68]. *IPT* genes display distinct, tissue-specific patterns of expression, indicative of cytokinin production sites [69, 70].

Free iP-riboside generated via the IPT pathway, as well as the corresponding base, are further stereospecifically hydroxylated to *trans*-zeatin forms. The *CYP735A1* and *CYP735A2* encoding cytochrome P450 monooxygenases with cytokinin trans-hydroxylase enzymatic activity were identified in *A. thaliana* by a screen employing an (*AtIPT4*)/*P450* co-expression system in *Saccharomyces cerevisiae* [71].

The final step in cytokinin biosynthesis, conversion of the cytokinin ribotides to their active, free base forms is catalyzed by the cytokinin nucleoside 5′-monophosphate phosphoribohydrolase LONELY GUY (LOG). These were first identified in rice by a genetic screen for defects in the maintenance of shoot meristems [72].

In *A. thaliana*, seven homologous genes that encode active LOG enzymes were detected. The *LOG* genes are differentially expressed in various tissues during plant development. In accordance with their predicted function the conditional overexpression of *LOG*s in *Arabidopsis* reduced the content of iP riboside 5′-phosphates and increased the levels of iP and the glucosides [73]. Alternatively, the cytokinin ribotides are dephosphorylated to the ribosides and subsequently converted to free-base cytokinins [74, 75], however the corresponding genes have not yet been identified (Fig. 1b, c).

Levels of active cytokinins in plant cells are tightly controlled. They might be either converted to storage forms through conjugation to glucose [76] or inactivated through irreversible cleavage by cytokinin oxidases [77, 78] (Fig. 1c). Development of highly sensitive analytical methods was instrumental in the detection of numerous cytokinins metabolites and in deciphering complex cytokinin metabolism, followed by identification of the corresponding metabolic enzymes and genes [79–81].

4 Transport of Auxin and Cytokinin

By definition, hormones are chemical messengers that are transported to distant tissues and organs to regulate their physiology and development. Darwin's early experiments on coleoptiles had already indicated that controlled transport of auxin from the tip of coleoptile to the bending region might be an essential part of the mechanism through which auxin executes its regulatory function. Later, based on the transport studies, it was proposed that cytokinins and auxin are synthesized only in root tips and shoot apices, respectively, and translocated to target tissues. Although the recent detailed investigations of expression patterns of auxin and cytokinin biosynthesis genes questions this oversimplified model, the tight control of hormone distribution through organs and tissues is considered to be the crucial component of their regulatory mechanisms. Nowadays, the broadly accepted concept is that both hormones are synthesized and act at various sites in a plant body and that they have coordinated functions as long-distance messengers as well as local signals.

The classical transport assays using radioactively labeled auxins outlined main routes of auxin movement in plants [82]. To transport auxin, plants use two distinct pathways: a nonpolar passive distribution through phloem and an active cell-to-cell polar auxin transport (PAT). In the first pathway, most of the auxin and auxin derivatives are rapidly transported via unregulated flow in the mature phloem over long distances in both basipetal and acropetal directions [83]. The second pathway is slower and acts over shorter distances, transporting auxin in a cell-to-cell manner from the shoot towards the root. In contrast to phloem transport, PAT is

specific for active free auxins, occurs in a cell-to-cell manner and is strictly unidirectional. The main PAT stream from the apex towards the root occurs in the cambium and the adjacent partially differentiated xylem elements [82, 84]. In roots, the auxin stream continues acropetally towards the root tip, where part of the auxin is redirected backwards and transported through the root epidermis to the elongation zone [85].

Based on the chemical nature of auxin and the physiology of PAT, the model of cell-to-cell auxin of transport has been proposed, known as the chemiosmotic hypothesis [86, 87]. As a weak acid, a fraction of IAA exists in the acidic environment of the apoplast as the protonated, neutral form (IAAH), which may diffuse through the plasma membrane. In the more basic cytosol, auxin becomes deprotonated (IAA^-) and is unable to pass passively through the plasma membrane. The chemiosmotic hypothesis predicted that the exit of auxin anions from the cell is mediated by active efflux carriers and that the passive diffusion of auxin can be further facilitated by influx carriers. The polar membrane localization of the auxin efflux carriers in a file of adjacent cells would determine directionality of the auxin flow (Fig. 2a).

It has been primarily genetic studies that led to discovery of genes required for auxin influx and efflux [31, 88–91]. An auxin influx transporter *AUXIN RESISTANT1* (*AUX1*), *encoding* an amino acid permease-like protein, was found in a screen for auxin resistant plants [92]. Strong insensitivity to membrane-impermeable auxin (2,4-D) suggested that the *aux1* mutation interferes with auxin uptake [88], which was confined by the transport assays using a *Xenopus* oocyte expression system [93]. The *A. thaliana* genome encodes four auxin influx transporters: *AUXIN RESISTANT1* (*AUX1*) and three *Like AUX1* (*LAX1*, *LAX2*, *LAX3*) [94–96]. Thorough exploration of mutants lacking AUX1/LAX activity revealed the essential role of the auxin uptake in the regulation of gravitropism, phototropism, root branching, phyllotaxis, and root hair development [88, 95–99].

Genetic screens were also instrumental in identifying molecular components of auxin efflux. In the early 1990s, the *A. thaliana* mutant, *pin-formed1* (*pin1*) with needle-like inflorescence was described. The characteristic phenotype similar to wild type plants treated with chemical inhibitors of auxin efflux indicated defects in auxin transport. Auxin transport assays in *pin1* stem segments confirmed severe reduction of the basipetal flow of auxin and pointed to a function for PIN1 in auxin efflux [100]. Indeed, identification of the mutant locus revealed that *PIN1* encodes a putative transmembrane protein with a predicted topology of transporter proteins [89]. Auxin transport assays in *Arabidopsis* and tobacco cell suspension culture as well as in heterologous non-plant systems including yeast, mammalian HeLa cells and *Xenopus* oocytes have provided evidence for an auxin efflux capacity of PIN

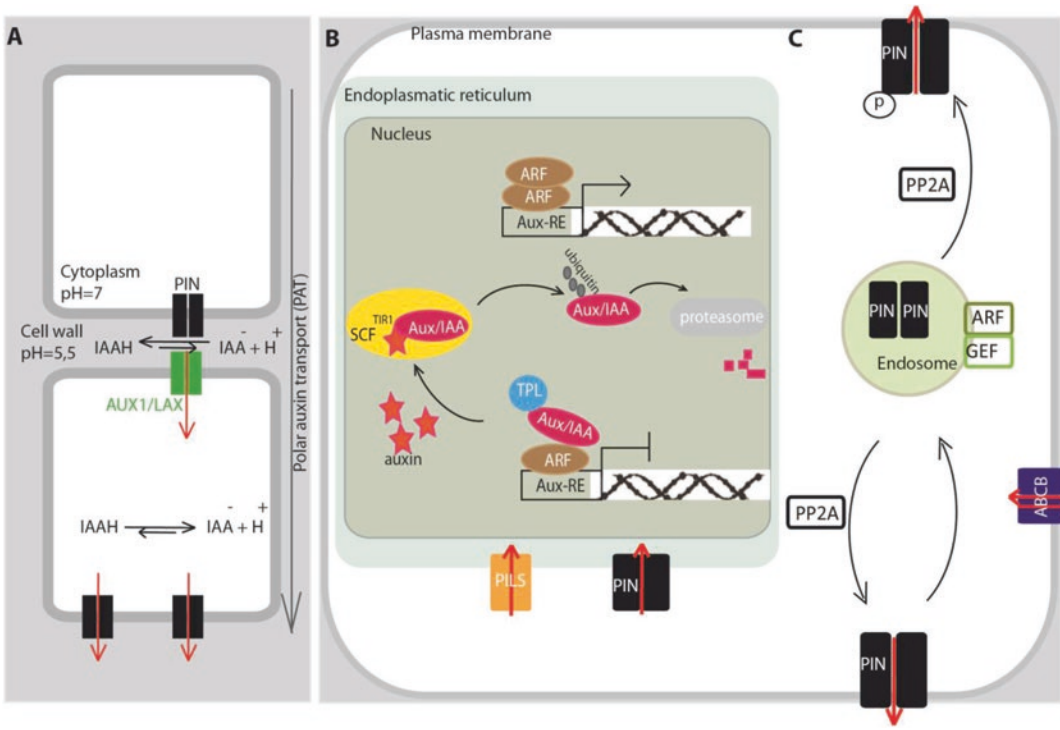

Fig. 2 Model of auxin transport and signaling. (**a**) Chemiosmotic hypothesis for polar auxin transport. In the acidic apoplast auxin is protonated. The protonated auxin either passively diffuses through the plasma membrane or is actively transported by AUX1/LAX influx carriers into the cell. In the neutral cytosol auxin becomes deprotonated and can leave the cell only by auxin efflux carriers such as PIN proteins and PGP transporters. (**b**) Under low auxin conditions, Aux/IAAs form a complex with ARF transcription factors and the TPL corepressor, thereby inhibiting AuxRE-mediated gene transcription. At higher concentrations, auxin stimulates ubiquitin-mediated proteolysis of Aux/IAA catalyzed by an SCF^{TIR1} E3 ubiquitin ligase. Degradation of Aux/IAAs relieves the ARF repression and allows transcription. (**c**) Outside the nucleus PIN auxin efflux transporters cycle between endosomes and the plasma membrane. The exocytosis requires the activity of GNOM, an ADP-ribosylation factor GTPase guanine nucleotide exchange factor (ARF-GEF), whereas endocytosis occurs in a clathrin-dependent manner. The PIN phosphorylation status, controlled by PINOID kinase (PID) and protein phosphatase 2A (PP2A), determines PINs recruitment to apical or basal targeting pathways. The short PIN proteins and PILS located in the ER might regulate intracellular auxin homeostasis

proteins [101–104]. The *Arabidopsis PIN* gene family consists of eight members [105, 106]. Based on the localization and domain organization, these were divided into two groups. The first group consists of PIN1, PIN2, PIN3, PIN4, and PIN7 and is located at the plasma membrane. The second group comprising PIN5, PIN6, and PIN8 has a reduced middle hydrophilic loop and is located at the endoplasmic reticulum (ER), where they presumably control auxin flow between the cytosol and ER lumen, thus possibly affecting subcellular auxin homeostasis [107, 108]. Similarly, PIN-LIKES proteins (PILS) are located in the ER and might play a role in regulation of intracellular auxin homeostasis [109] (Fig. 2).

In addition to the PIN family of plant-specific auxin transporters, plant orthologs of the mammalian ATP-binding cassette subfamily B (ABCB)-type transporters of the multidrug resistance/phosphoglycoprotein (ABCB/MDR/PGP) protein family [110, 111] have been implicated in auxin transport. Biochemical evidence for the ABCB proteins auxin transport activity has been demonstrated both in plant and non-plant systems. In contrast to polar localization of PINs, which corresponds with known direction of auxin flow, the ABCBs presumably act in nondirectional long-distance auxin transport controlling amount of auxin in these streams [110–112].

The chemiosmotic hypothesis predicted that the polar membrane localization of auxin transporters determines the directionality of the auxin flow. This concept was supported by observations of a polar subcellular localization for PIN proteins [31, 89] and a tight correlation between PIN polarity and directions of auxin flow [113]. Phosphorylation of PINs controlled by a set of kinases and phosphatases [104, 114–118], Ca^{2+} signaling [119], cell wall [120], or mechanical signals orienting the plant microtubule network [121] were found to determine PIN protein activity and polarity. Cell-biological studies revealed that PIN auxin efflux transporters may not solely reside at the plasma membrane since they undergo constitutive cycles of endocytosis and recycling back to the plasma membrane [122, 123] (Fig. 2c). The constitutive endocytosis and recycling of PIN proteins depends on complex subcellular trafficking machinery including the coat protein clathrin [123–125], ADP-ribosylation factor guanine-nucleotide exchange factors ARF-GEFs [122, 126–129]; ARF-GTPase-activating protein VASCULAR NETWORK DEFECTIVE3 [130], the related ARF-GEF GNOM-LIKE1 [131] and small GTPase Rab1b [132]. Downstream of endocytosis, the early endosomal trafficking of PINs is controlled by another ARF-GEF, BFA-visualized endocytic trafficking defective1, and the Sec1/Munc18 family protein BEN2 [133, 134]. The endocytosis and constitutive recycling of PIN proteins has been implicated in the maintenance of PIN polar localization and as a mechanism for rapid modifications of PIN polarity during various developmental processes including embryogenesis [8, 135], lateral root organogenesis [11, 136], or tropic responses [18, 137–139].

Like auxin, cytokinins are highly mobile molecules. However, in contrast to the well-characterized transport machinery of auxin, the nature of cytokinin transport is less clear. Long-distance transport of cytokinin is supported by the discovery of cytokinins in xylem and phloem sap [140–142]. In xylem sap, the major form of cytokinin is tZ-riboside (tZR) [68, 143, 144], while in phloem sap iP-type cytokinins, such as iP-ribosides and iP-ribotides are

detected [144, 145]. Accordingly, grafting experiments between wild-type plants and cytokinin biosynthesis mutants showed preferential transport of different cytokinins; *trans*-zeatin tZ-type cytokinins were transported from the root to the shoot, while iP-type cytokinins moved from the shoot to the root [146]. Thus, plants might use tZ-type as an acropetal messenger and iP-type cytokinins as basipetal messengers [147]. Recently, transport assays using radiolabeled cytokinins confirmed basipetal movement of cytokinin through the phloem and revealed that basipetal transport of cytokinin occurs through symplastic connections in the phloem [28]. Reverse genetics approaches applied to systematically characterize the ATP-binding cassette transporter proteins in *A. thaliana* yielded the identification of ABCG14 as a transporter involved in the long-distance acropetal (root to shoot) translocation of the root-synthesized cytokinin. Plasma membrane-located ABCG14 is expressed primarily in the central cylinder of roots and loss of ABCG14 activity interferes with the translocation of tZ-type cytokinins from roots to shoots. *In planta* feeding of radiolabeled tZ suggests that ABCG14 acts as an efflux pump [148].

Mechanisms of cytokinin uptake into cells have been studied using radiolabeled cytokinins in *Arabidopsis* cell cultures. Experiments predicted the presence of proton-coupled high-, medium-, and low affinity cytokinin transport systems [141, 149]. So far, the equilibrative nucleoside transporter (ENT) family and the purine permease (PUP) family have been found to facilitate cytokinin transport [141, 144, 150]. Among *Arabidopsis* PUP family proteins [140], active uptake of free cytokinin bases and several adenine derivatives by PUP1 and PUP2 was demonstrated using a yeast system [141]. Expression of PUP2 in the phloem of *Arabidopsis* leaves suggested a role for PUP2 in phloem loading and unloading for long-distance transport of adenine and possibly cytokinins [141]. Among the plant ENT transporters, competitive uptake studies in yeast cells showed that *Arabidopsis* ENT3, ENT6, ENT7 and rice ENT2 can facilitate uptake of iP-riboside and tZ-riboside [144, 150]. Furthermore, mutants lacking either ENT3 or ENT8 exhibit reduced cytokinin uptake efficiency [151]. Distinct expression patterns of *ENT* genes detected in root, leaf, and flower vasculature suggest that they may act differently during plant growth and development [150–152], however their function as cytokinin transporters *in planta* needs to be experimentally supported. In summary, in contrast to high substrate specificity of the auxin transport system, translocation of cytokinins *in planta* seems to be mediated through transporters with affinities to a broader spectrum of molecules such as purine derivatives and nucleosides.

5 Perception and Signal Transduction of Auxin and Cytokinin

Solving the puzzle of auxin and cytokinin perception mechanism has been undoubtedly one of the biggest challenges of the last years. Establishment of the *Arabidopsis* genetic model has provided excellent tools to address this long-standing question and it has been forward genetic screens in *Arabidopsis* that have led to the identification of backbone elements of both auxin and cytokinin signal transduction cascades. Genetics in combination with advanced molecular and biochemical approaches enabled the achievement of a comprehensive view on the molecular principles of auxin and cytokinin perception and signal transduction.

Several independent forward genetic screens for mutants insensitive to auxin [29, 153, 154] and expression profiling to isolate auxin inducible genes [155–158] led to identification of all key molecular components required for auxin response such as TIR1 (encoding for F-box component of the E3 ubiquitin ligase $SCF^{TIR1/AFBs}$), the auxin early inducible *Aux/IAA* genes as well as the ARF transcription factors that recognize auxin response elements in the promoters of the *Aux/IAAs* [159, 160]. However, how these genes might constitute the pathway sensing and transducing hormonal signal was not obvious. Using advanced genetic and biochemical approaches the auxin signaling circuit has been resolved and TIR1 identified as the auxin receptor. It has been shown that auxin mediates interaction between TIR1/AFBs and Aux/IAA proteins which stimulates Aux/IAAs ubiquitination by $SCF^{TIR1/AFBs}$ E3-ubiquitin ligases for subsequent degradation by the proteasome. This leads to de-repression of ARFs, and transcriptional regulation of downstream response genes. At low auxin concentration, Aux/IAAs form a complex with ARF transcription factors and the transcriptional corepressor TOPLESS (TPL), thus preventing the ARFs from regulating target genes [161–166] (Fig. 2b).

Although the framework which outlines the core molecular mechanism of auxin perception and signal transduction has been recognized, the question as to how *TIR1/AFB*, *Aux/IAAs* and *ARF* families, each comprising many homologous members, mediate specific developmental output remains to be answered. As indicated by recent studies, multiple levels of control appear to exist, including spatiotemporal specific expression of individual auxin signaling pathway components [167, 168], as well as differences in affinities of the TIR1/AFB auxin receptors for the Aux/IAA repressors [169, 170], of Aux/IAA repressors for the ARFs transcription factors [171–175], and of ARFs for their binding motifs in promoters of the target genes [176], which may allow fine tuning of auxin responses.

After a period of biochemical attempts in the early 1970s to identify the cytokinin receptors, the forward genetic screens turned out to be successful strategies. In a screen of the activation tagged

Arabidopsis mutants for cytokinin independent growth, the sensor histidine kinase CKI1 was recovered. This finding suggested that the multistep phosphorelay similar to bacterial two-component signaling system might underlie the cytokinin signal transduction [177]. Another screen for cytokinin insensitive mutants led to identification of the *CRE1* (*CYTOKININ RESISTANT 1*) encoding a sensor histidine kinase related to CKI1 [178]. At about the same time, the *WOODEN LEG* (*WOL*) mutant allele of the AHK4/CRE1 gene (exhibiting severe defects in the vasculature differentiation [179]) was identified, along with the AHK2 and AHK3 homologs required for cytokinin response [180–183]. Elegant experiments in yeast and bacteria provided first evidence that CRE1/AHK4 functions as a cytokinin receptor [178, 181, 184]; later corroborated by direct binding assays with radiolabeled cytokinins [185–187].

Subsequent studies focusing on the downstream signaling cascade revealed that genes with high similarity to molecular elements of the multistep phosphorelay pathway including sensor histidine kinases (AHKs), histidine phosphotransfer proteins (AHPs) and response regulators (ARRs) are present in the *Arabidopsis* genome [188, 189]. Genetic and biochemical characterization of their functions in the cytokinin response yielded the current model of the cytokinin signaling pathway. In brief, a cascade of autophosphorylation and transphosphorylation events triggered by cytokinin leads to activation of AHK receptors and transduction of the signal to downstream components. Downstream of the AHK receptors, the AHPs continuously translocate between cytosol and nucleus to mediate signaling by activating type-B ARABIDOPSIS RESPONSE REGULATORS (ARRs), transcription factors which then trigger the transcription of specific genes. A negative feedback loop is provided by type-A ARRs, which inhibit the activity of type-B ARRs by an unknown mechanism [180, 190–195]. Furthermore, a family of F-box proteins, called the KISS ME DEADLY (KMD) family, targets type-B ARR proteins for degradation and attenuates cytokinin pathway activity [196] (Fig. 3). The large majority of cytokinin receptors localize to the ER, suggesting a central role of this compartment in cytokinin signaling [197, 198]; nevertheless, a small part of the cytokinin receptors might perceive a signal from the plasma membrane [198].

Recently, a set of cytokinin-regulated transcription factors named cytokinin response factors (CRFs) have been described as a potential branch emerging from the classical multistep phosphorelay parallel to that of type-B ARRs [199]. CRFs are members of the AP2/EREBP family of transcription factors, containing a single AP2–DNA binding domain, distinct from both DREB and AP2 proteins. There are eight members of CRF family in *Arabidopsis* (CRF1-CRF8) with CRF7 and CRF8 being atypical as they lack C-terminal extensions [200–202]. The transcript abundance of

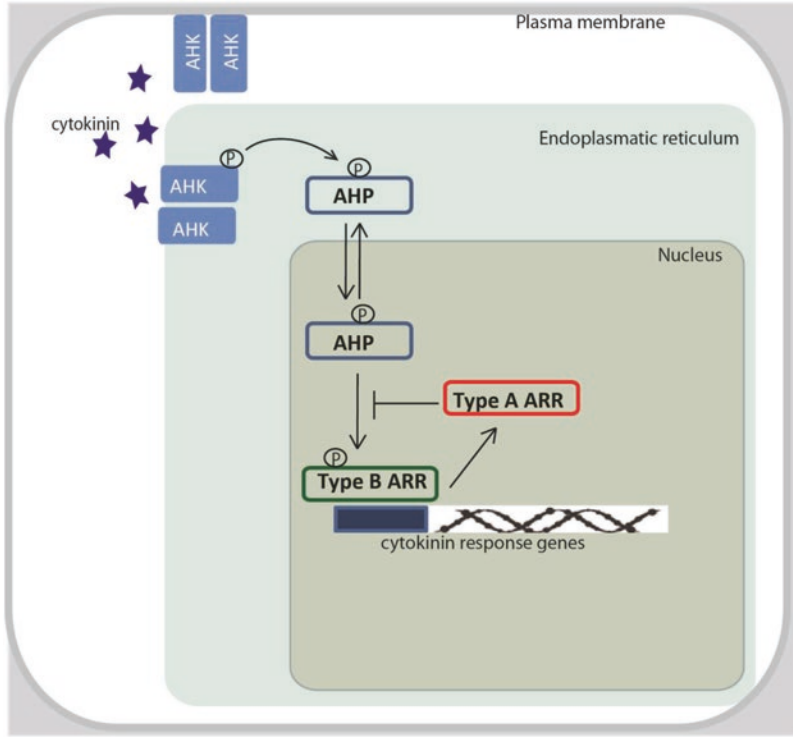

Fig. 3 Model of cytokinin signaling pathway. Cytokinin binds to cytokinin receptor (AHKs) and initiates the phosphorelay signal transduction cascade. The phosphate is transferred from receptor to histidine phosphotransfer proteins (AHPs) followed by the phosphorylation and activation of the type B response regulator (ARR) proteins in the nucleus. A negative feedback loop is provided by type-A ARRs, which inhibits the activity of type-B ARRs

certain *CRFs* (*CRF2*, *CRF5*, and *CRF6*) is rapidly upregulated by cytokinin [199]. Protein–protein interaction analysis indicated that CRFs are able to interact with each other to form homodimers and/or heterodimers as well as with components of the classical cytokinin signaling pathway. Transcriptome analysis has revealed a large overlap in CRFs and type B ARR targets, pointing at a close link between both branches of the cytokinin signaling pathway.

However, how the specificity of cytokinin response is achieved by the signaling cascade, where each step is supported by a gene family comprising several members, awaits further investigation.

Importantly, elucidation of the molecular elements and mechanistic principles of auxin and cytokinin transduction pathways has enabled the development of specific sensors for monitoring auxin and cytokinin *in planta*. Nowadays, highly sensitive reporters such as *DR5* [203]; DII-VENUS [204, 205], and *TCS* [9] are extensively used for mapping auxin and cytokinin activities, respectively, and demonstrate a great potential of these tools for better understanding of the roles of auxin and cytokinin in plant development.

6 Auxin and Cytokinin Interaction in Regulation of Plant Development

Since the initial discovery of auxin and cytokinin, the number of reports supporting their regulatory role in various aspects of plant development has accumulated. Moreover, studies of auxin and cytokinin function in plant cell suspension growth provided the first evidence of hormonal interaction and its role in directing plant development. The experiments of Skoog and Miller [32] demonstrated that both auxin and cytokinin are not only required to induce and maintain cell division and growth in plant tissue culture, but that the auxin–cytokinin ratio determines distinct organogenic pathways. A high ratio of cytokinin to auxin stimulated formation of shoots, whereas a low ratio induced root regeneration. Tight communication between auxin and cytokinin is crucial for proper establishment of meristems in early embryogenesis [9, 206], ovule development [207], shoot apical meristem activity and phyllotaxis [22, 23, 78, 208], shoot and root branching [13, 14, 209–212], root growth and meristem maintenance [20]. Hence the deciphering of molecular and mechanistic bases of auxin and cytokinin interaction became one of the major themes in plant biology. Over the years, research on developmental processes in plants has uncovered genes and networks, giving first insights into molecular mechanisms of auxin and cytokinin cross talk in the context of these complex developmental programs. Here, a few examples of auxin–cytokinin cross talk mechanisms and their relevance in coordination of specific developmental processes are discussed.

It has been shown that specification of the root pole during the early phases of embryogenesis is dependent on the tightly balanced activity of auxin and cytokinin. Auxin was found to stimulate expression of the cytokinin signaling repressors *ARR7* and *ARR15* and thus to attenuate the output of the cytokinin pathway. Lack of this auxin-driven negative feedback loop resulted in the upregulation of the cytokinin response and severe patterning defects at the embryonic root pole [9]. Interestingly, recent observations hint at another auxin–cytokinin regulatory module acting in the early embryogenesis. Among the transcriptional targets of AUXIN RESPONSE FACTOR (ARF5/MP), previously linked with embryonic root specification [213, 214], TARGET OF MONOPTEROS (TMO3), coding for the CRF2 was identified [215]. Expression of CRF2 and homologous genes is cytokinin responsive and interference with their functions leads to severe embryonic defects [199]. Furthermore, two auxin efflux transporters (*PIN1* and *PIN7*), both shown to control distribution of auxin during early embryogenesis [8], were identified as CRF2 transcriptional targets [216]. However, how these two regulatory circuits jointly coordinate early embryogenesis requires further investigation.

Auxin and cytokinin act in an antagonistic manner to define the root apical meristem size by promoting cell division and differentiation, respectively [21, 217]. A complex network of auxin and cytokinin interactions has been implicated in the root meristem activity control. Cytokinin modulates the auxin pathway by affecting the expression of its signaling components. Cytokinin (through the AHK3 receptor and ARR1 and ARR12 response regulators) was shown to directly activate transcription of the auxin repressor *IAA3/SHORT HYPOCOTYL 2* (*SHY2*). This leads to the attenuation of auxin responses and reduced expression of *PIN* auxin efflux transporters [20, 21, 218, 219]. Consequently, a decreased abundance of PINs limits the auxin supply to the root apical meristem, thereby restricting its meristematic activity [20, 21]. Besides this transcription-based regulation of auxin activity and distribution, cytokinin was also found to modulate the endocytic trafficking of PIN1 by redirecting this membrane protein for lytic degradation in the vacuoles [212, 220]. This alternative mode of cytokinin action provides a mechanism for rapid control of auxin fluxes; and as recently suggested, the enhanced depletion of PIN1 at specific polar domains by cytokinin might also modulate direction of the auxin flow [221].

Another mechanism through which auxin and cytokinin balance each other's activities occurs by a cross talk between their metabolic pathways. High cytokinin levels promote auxin biosynthesis [222] and auxin, in turn, gives feedback on the cytokinin metabolism by inducing CYTOKININ OXIDASE (CKX) thereby decreasing cytokinin levels [223–225]. On the other hand, in the root apical meristem, auxin enhances (in an IAA3/SHY2-dependent manner) the expression of ISOPENTENYL TRANSFERASE5 (IPT5), which encodes a rate limiting enzyme in the cytokinin biosynthesis, eventually resulting in the local upregulation of cytokinin levels [20, 69].

Both auxin and cytokinin exhibit specific functions in the shoot apical meristem. High cytokinin promotes proliferation of undifferentiated cells, whereas auxin coordinates organogenesis in the peripheral zone [35]. Cytokinin participates in the WUSCHEL/WUS-CLAVATA/CLV, the core regulatory loop controlling shoot apical meristem activity, by stimulating WUS expression [226]. By direct repression of the ARR7 and ARR15 cytokinin signaling repressors, WUS further reinforces the cytokinin promoting effect on the WUS-mediated pathway [208]. An important additional input in this cytokinin-driven regulation is provided by auxin. In mutants defective in auxin biosynthesis, transport, and signaling, expression of *ARR7* and *ARR15* was found to be enhanced, and the *ARF5/MP* transcription factor was identified as a direct repressor of their transcription [23]. This constitutes a regulatory circuit in which auxin enhances cytokinin response by attenuating the expression of the cytokinin signaling repressors, and consequently promoting WUS activity in the WUS-CLV loop.

At the peripheral zone of the shoot apical meristem, new organ formation is triggered by auxin [22]. Studies following pathways regulated by auxin transport and response revealed that initiation of the lateral organs is accompanied by modulations in the polarity of PIN1 and redirection of the auxin towards incipient primordia [227]. The accumulation of auxin correlates with a decrease in *SHOOT MERISTEMLESS* (*STM*) expression, which eventually results in lower cytokinin at the peripheral zone [228]. How PIN1 polarization throughout the shoot apical meristem is coordinated and whether cytokinin contributes to the regulation of polar auxin transport through mechanisms analogous to these detected in root is unknown. Nevertheless, a reduced level of PIN1 in the maize *ARR* repressor ortholog mutant *abphyl 1* supports such a scenario [229]. Recently, Besnard et al. [230] provide further evidence for cytokinin function in the peripheral zone and coordination of lateral organ initiation. Analysis of *AHP6* expression patterns along with monitoring of auxin and cytokinin sensitive reporters indicates that AHP6, which acts as a repressor of cytokinin signaling [26], regulates the spatiotemporal pattern of cytokinin activity at the shoot apical meristem periphery. The cytokinin inhibitory fields generated downstream of auxin by AHP6 might stabilize auxin fields, thereby increasing robustness of the phyllotactic patterning [230].

Studies of auxin–cytokinin cross talk directing other developmental process (including initiation and organogenesis of ovules; vasculature differentiation, shoot and root meristem activity and lateral branching (reviewed in [33–35]) point towards specific as well as common aspects of mechanisms mediating mutual communication between these two hormonal pathways.

With increasing amounts of confirmed molecular interactions and circuits that determine hormone activity at the level of metabolism, transport, perception, and signaling, the prediction of hormone regulatory network behavior and output becomes unfeasible Modeling and mathematical simulations provide a novel means to address these issues and help to achieve better understanding of the complexity and dynamics of hormone action [231].

For example, studies of the transcription factor *PHABULOSA* (*PHB*) and cytokinin in controlling the root meristem size showed that cytokinin regulates *microRNA165/166* and that both cytokinin and *microRNA165/166* jointly regulate *PHB*. In return, PHB promotes cytokinin biosynthesis by stimulation *IPT7* expression [232]. One-dimensional model and mathematical simulations provided insights into the functioning of such a complicated molecular network, showing that this regulatory loop restrains the reduction and accelerates the recovery of PHB levels, thus providing robustness against cytokinin fluctuations [232].

A combination of experimental and modeling approaches has also been applied to integrate auxin and cytokinin pathways in the specification of vascular patterning. A two-dimensional multicellular model of Muraro et al. [233] incorporated previous findings of

a mutually inhibitory interaction between auxin and cytokinin, mediated through the auxin inducible repressor of the cytokinin signaling AHP6; cytokinin feedback on the PIN auxin efflux carriers and SHORT ROOT (SHR) promoted expression of the mobile *microRNA165/166* which silences *PHB* to form a gradient of *PHB* mRNA that controls the specification of xylem and inhibits *AHP6* expression [28, 234]. Mathematical simulations revealed that this gene regulatory network is not sufficient to establish proper expression patterns of key marker genes as observed experimentally, and predicted additional negative regulators of cytokinin signaling and the mutual degradation of both *microRNA165/6* and *PHB* mRNA [233].

A genetic network tested in the model simulation of De Rybel et al. [235] integrated two incoherent feed-forward loops and evaluated their impact on the patterning of vascular tissues. One of the feed-forward loops implements auxin–cytokinin antagonistic regulations of PIN mediated auxin efflux [26, 28]. A second loop is based on the experimental identification of interaction between MONOPTEROS/ARF5 and TARGET OF MONOPTEROS5/LONESOME HIGHWAY (TMO5)/LHW) and LONELY GUY4 (LOG4) which mediates auxin-dependent control of the cytokinin biosynthesis [236]. The authors show that the individual subnetworks provide specific regulatory inputs, one generating a high-auxin domain whereas a second defines sharp boundaries between the high auxin domain and the neighboring cytokinin response domain. Integration of both regulatory circuits is sufficient to generate distinct hormonal zones and establishment of stable patterns within a vascular tissue [235].

7 Conclusion

The history of auxin and cytokinin biology including the initial discoveries by father–son duo Charles Darwin and Francis Darwin [3], and Gottlieb Haberlandt [5] is a beautiful demonstration of unceasing continuity of research. Novel findings are integrated into existing hypotheses and models and deepen our understanding of biological principles. At the same time new questions are triggered and hand to hand with this new methodologies are developed to address these new challenges.

Acknowledgments

We thank Melinda Abas and Jiri Friml for critical reading of the manuscript. As only a limited number of original articles are cited and discussed, we apologize to authors whose works are not cited because of space restrictions. This work was supported by the Austrian Science Fund (FWF01_I1774S) to E.B. and A.H.

References

1. Du Monceau D (1758) La physique des arbres, vol I. HL Guérin & LF Delatour, Paris
2. Sachs J (1880) Stoff und Form der Pflanzenorgane I. Arb Bot Inst Würzburg 2: 452–488
3. Darwin C (1880) The power of movement in plants. John Murray, London
4. Went F (1928) Wuchsstoff und Wachstum. Receuil Des Travaux Botaniques Neerlandais 25:1–116
5. Haberlandt G (1913) Zur physiologie der zellteilung. Sitzungsber Akad Wiss Berlin Phys Math C 1:318–345
6. Miller CO, Skoog F, von Saltza M, Strong FM (1955) Kinetin, a cell division factor from deoxyribonucleic acid. J Am Chem Soc 77: 1392
7. Letham DS (1963) Zeatin, a factor inducing cell division isolated from Zea mays. Life Sci 8:569–573
8. Friml J, Vieten A, Sauer M, Weijers D, Schwarz H, Hamann T, Offringa R, Jurgens G (2003) Efflux-dependent auxin gradients establish the apical-basal axis of *Arabidopsis*. Nature 426:147–153
9. Müller B, Sheen J (2008) Cytokinin and auxin interaction in root stem-cell specification during early embryogenesis. Nature 453:1094–1097
10. Fukaki H, Tameda S, Masuda H, Tasaka M (2002) Lateral root formation is blocked by a gain-of-function mutation in the SOLITARY-ROOT/IAA14 gene of *Arabidopsis*. Plant J 29:153–168
11. Benkova E, Michniewicz M, Sauer M, Teichmann T, Seifertova D, Jurgens G, Friml J (2003) Local, efflux-dependent auxin gradients as a common module for plant organ formation. Cell 115:591–602
12. De Smet I, Tetsumura T, De Rybel B, Frey NF, Laplaze L, Casimiro I, Swarup R, Naudts M, Vanneste S, Audenaert D, Inze D, Bennett MJ, Beeckman T (2007) Auxin-dependent regulation of lateral root positioning in the basal meristem of *Arabidopsis*. Development 134:681–690
13. Laplaze L, Benkova E, Casimiro I, Maes L, Vanneste S, Swarup R, Weijers D, Calvo V, Parizot B, Herrera-Rodriguez MB, Offringa R, Graham N, Doumas P, Friml J, Bogusz D, Beeckman T, Bennett M (2007) Cytokinins act directly on lateral root founder cells to inhibit root initiation. Plant Cell 19:3889–3900
14. Bielach A, Podlešáková K, Marhavý P, Duclercq J, Cuesta C, Müller B, Grunewald W, Tarkowski P, Benková E (2012) Spatiotemporal regulation of lateral root organogenesis in *Arabidopsis* by cytokinin. Plant Cell 24:3967–3981
15. Leyser O (2009) The control of shoot branching, an example of plant information processing. Plant Cell Environ 32:694–703
16. Shimizu-Sato S, Tanaka M, Mori H (2009) Auxin-cytokinin interactions in the control of shoot branching. Plant Mol Biol 69:429–435
17. Müller D, Waldie T, Miyawaki K, To JP, Melnyk CW, Kieber JJ, Kakimoto T, Leyser O (2015) Cytokinin is required for escape but not release from auxin mediated apical dominance. Plant J 82:874–886
18. Friml J, Benkova E, Blilou I, Wisniewska J, Hamann T, Ljung K, Woody S, Sandberg G, Scheres B, Jurgens G, Palme K (2002) AtPIN4 mediates sink-driven auxin gradients and root patterning in *Arabidopsis*. Cell 108:661–673
19. Blilou I, Xu J, Wildwater M, Willemsen V, Paponov I, Friml J, Heidstra R, Aida M, Palme K, Scheres B (2005) The PIN auxin efflux facilitator network controls growth and patterning in *Arabidopsis* roots. Nature 433:39–44
20. Dello Ioio R, Nakamura K, Moubayidin L, Perilli S, Taniguchi M, Morita MT, Aoyama T, Costantino P, Sabatini S (2008) A genetic framework for the control of cell division and differentiation in the root meristem. Science 322:1380–1384
21. Růžička K, Simaskova M, Duclercq J, Petrasek J, Zazimalova E, Simon S, Friml J, Van Montagu MC, Benkova E (2009) Cytokinin regulates root meristem activity via modulation of the polar auxin transport. Proc Natl Acad Sci U S A 106:4284–4289
22. Reinhardt D, Pesce ER, Stieger P, Mandel T, Baltensperger K, Bennett M, Traas J, Friml J, Kuhlemeier C (2003) Regulation of phyllotaxis by polar auxin transport. Nature 426: 255–260
23. Zhao Z, Andersen SU, Ljung K, Dolezal K, Miotk A, Schultheiss SJ, Lohmann JU (2010) Hormonal control of the shoot stem-cell niche. Nature 465:1089–1092
24. Yoshida S, Mandel T, Kuhlemeier C (2011) Stem cell activation by light guides plant organogenesis. Genes Dev 25:1439–1450
25. Chickarmane VS, Gordon SP, Tarr PT, Heisler MG, Meyerowitz EM (2012) Cytokinin signaling as a positional cue for patterning the apical–basal axis of the growing *Arabidopsis* shoot meristem. Proc Natl Acad Sci U S A 109:4002–4007

26. Mähönen AP, Bishopp A, Higuchi M, Nieminen KM, Kinoshita K, Tormakangas K, Ikeda Y, Oka A, Kakimoto T, Helariutta Y (2006) Cytokinin signaling and its inhibitor AHP6 regulate cell fate during vascular development. Science 311:94–98
27. Hejátko J, Ryu H, Kim GT, Dobesová R, Choi S, Choi SM, Soucek P, Horák J, Pekárová B, Palme K, Brzobohaty B, Hwang I (2009) The histidine kinases CYTOKININ-INDEPENDENT1 and ARABIDOPSIS HISTIDINE KINASE2 and 3 regulate vascular tissue development in *Arabidopsis* shoots. Plant Cell 21:2008–2021
28. Bishopp A, Lehesranta S, Vaten A, Help H, El-Showk S, Scheres B, Helariutta K, Mahonen AP, Sakakibara H, Helariutta Y (2011) Phloem-transported cytokinin regulates polar auxin transport and maintains vascular pattern in the root meristem. Curr Biol 21:927–932
29. Rouse D, Mackay P, Stirnberg P, Estelle M, Leyser O (1998) Changes in auxin response from mutations in an *AUX/IAA* gene. Science 279:1371–1373
30. Müller A, Guan C, Gälweiler L, Tanzler P, Huijser P, Marchant A, Parry G, Bennett M, Wisman E, Palme K (1998) AtPIN2 defines a locus of *Arabidopsis* for root gravitropism control. EMBO J 17:6903–6911
31. Luschnig C, Gaxiola RA, Grisafi P, Fink GR (1998) EIR1, a root-specific protein involved in auxin transport, is required for gravitropism in *Arabidopsis thaliana*. Genes Dev 12:2175–2187
32. Skoog F, Miller C (1957) Chemical regulation of growth and organ formation in plant tissue cultured in vitro. Symp Soc Exp Biol 11:118–131
33. Moubayidin L, Di Mambro R, Sabatini S (2009) Cytokinin-auxin crosstalk. Trends Plant Sci 14:557–562
34. Depuydt S, Hardtke CS (2011) Hormone signalling crosstalk in plant growth regulation. Curr Biol 21:R365–R373
35. Schaller GE, Bishopp A, Kieber JJ (2015) The yin-yang of hormones, cytokinin and auxin interactions in plant development. Plant Cell 27:44–63
36. Boysen-Jensen P (1911) La transmission de l'irritation phototropique dans l'avena. Bulletin Academie Des Sciences et Lettres de Montpellier 3:1–24
37. Cholodny N (1927) Wuchshormone und Tropismen bei den Pflanzen. Biol Zentralbl 47:604–626
38. Cholodny N (1928) Beiträge zur hormonalen Theorie von Tropismen. Planta 6:118–134
39. Kögl F, Erxleben H, Haagen-Smit AJ (1934) Über die Isolierung der Auxine a und b aus pfl anzlichen Materialien. 9. Mitteilung über pfl anzliche Wachstumsstoffe. Hoppe Seylers Z Physiol Chem 225:215–229
40. Thimann KV, Koepfli JB (1935) Identity of the growth-promoting and root-forming substances of plants. Nature 135:101
41. Haagen-Smit AJ, Dandliker WB, Wittwer SH, Murneek AE (1946) Isolation of 3-indoleacetic acid from immature corn kernels. Am J Bot 33:118–120
42. Van Overbeek J, Conklin ME, Blakeslee AF (1941) Factors in coconut milk essential for growth and development of very young datura embryos. Science 94:350–351
43. Jablonski JR, Skoog F (1954) Cell enlargement and cell division in excised tobacco pith tissue. Physiol Plant 7:16–24
44. Hall RH, De Ropp RS (1955) Formation of 6-furfurylaminopurine from DNA breakdown products. J Am Chem Soc 77:6400
45. Miller CO (1961) Kinetin-like compound in maize. Proc Natl Acad Sci U S A 47:170–174
46. Salisbury FB, Ross CW (1992) Plant physiology, 4th edn. Wadsworth, Inc., Belmont, CA
47. Stepanova AN, Robertson-Hoyt J, Yun J, Benavente LM, Xie DY, Dolezal K, Schlereth A, Jurgens G, Alonso JM (2008) TAA1-mediated auxin biosynthesis is essential for hormone crosstalk and plant development. Cell 133:177–191
48. Tao Y, Ferrer JL, Ljung K, Pojer F, Hong F, Long JA, Li L, Moreno JE, Bowman ME, Ivans LJ, Cheng Y, Lim J, Zhao Y, Ballaré CL, Sandberg G, Noel JP, Chory J (2008) Rapid synthesis of auxin via a new tryptophan-dependent pathway is required for shade avoidance in plants. Cell 133:164–176
49. Yamada M, Greenham K, Prigge MJ, Jensen PJ, Estelle M (2009) The *TRANSPORT INHIBITOR RESPONSE2* gene is required for auxin synthesis and diverse aspects of plant development. Plant Physiol 151:168–179
50. Cheng Y, Dai X, Zhao Y (2006) Auxin biosynthesis by the YUCCA flavin monooxygenases controls the formation of floral organs and vascular tissues in *Arabidopsis*. Genes Dev 20:1790–1799
51. Cheng Y, Dai X, Zhao Y (2007) Auxin synthesized by the YUCCA flavin monooxygenases is essential for embryogenesis and leaf formation in *Arabidopsis*. Plant Cell 19:2430–2439
52. Won C, Shen X, Mashiguchi K, Zheng Z, Dai X, Cheng Y, Kasahara H, Kamiya Y, Chory J, Zhao Y (2011) Conversion of tryptophan to indole-3-acetic acid by TRYPTOPHAN

AMINOTRANSFERASES OF ARABIDOPSIS and YUCCAs in *Arabidopsis*. Proc Natl Acad Sci U S A 108:18518–18523

53. Mashiguchi K, Tanaka K, Sakai T, Sugawara S, Kawaide H, Natsume M, Hanada A, Yaeno T, Shirasu K, Yao H, McSteen P, Zhao Y, Hayashi K, Kamiya Y, Kasahara H (2011) The main auxin biosynthesis pathway in Arabidopsis. Proc Natl Acad Sci U S A 108: 18512–18517
54. Bartel B (1997) Auxin biosynthesis. Annu Rev Plant Physiol Plant Mol Biol 48:51–66
55. Ljung K, Bhalerao RP, Sandberg G (2001) Sites and homeostatic control of auxin biosynthesis in *Arabidopsis* during vegetative growth. Plant J 28:465–474
56. Stone SL, Braybrook SA, Paula SL, Kwong LW, Meuser J, Pelletier J, Hsieh TF, Fischer RL, Goldberg RB, Harada J (2008) *Arabidopsis* LEAFY COTYLEDON2 induces maturation traits and auxin activity, implications for somatic embryogenesis. Proc Natl Acad Sci U S A 105:3151–3156
57. Eklund DM, Ståldal V, Valsecchi I, Cierlik I, Eriksson C, Hiratsu K, Ohme-Takagi M, Sundström JF, Thelander M, Ezcurra I, Sundberg E (2010) The *Arabidopsis thaliana* STYLISH1 protein acts as a transcriptional activator regulating auxin biosynthesis. Plant Cell 22:349–363
58. Franklin KA, Lee SH, Patel D, Kumar SV, Spartz AK, Gu C, Ye S, Yu P, Breen G, Cohen JD, Wigge PA, Gray WM (2011) Phytochrome-interacting factor 4 (PIF4) regulates auxin biosynthesis at high temperature. Proc Natl Acad Sci U S A 108:20231–20235
59. Sun J, Qi L, Li Y, Chu J, Li C (2012) PIF4-mediated activation of *YUCCA8* expression integrates temperature into the auxin pathway in regulating *Arabidopsis* hypocotyl growth. PLoS Genet 8:e1002594
60. Cui D, Zhao J, Jing Y, Fan M, Liu J, Wang Z, Xin W, Hu Y (2013) The *Arabidopsis* IDD14, IDD15, and IDD16 cooperatively regulate lateral organ morphogenesis and gravitropism by promoting auxin biosynthesis and transport. PLoS Genet 9:e1003759
61. Pinon V, Prasad K, Grigg SP, Sanchez-Perez GF, Scheres B (2013) Local auxin biosynthesis regulation by PLETHORA transcription factors controls phyllotaxis in *Arabidopsis*. Proc Natl Acad Sci U S A 110:1107–1112
62. Li LC, Qin GJ, Tsuge T, Hou XH, Ding MY, Aoyama T, Oka A, Chen Z, Gu H, Zhao Y, Qu LJ (2008) SPOROCYTELESS modulates YUCCA expression to regulate the development of lateral organs in *Arabidopsis*. New Phytol 179:751–764
63. Soeno K, Goda H, Ishii T, Ogura T, Tachikawa T, Sasaki E, Yoshida S, Fujioka S, Asami T, Shimada Y (2010) Auxin biosynthesis inhibitors, identified by a genomics-based approach, provide insights into auxin biosynthesis. Plant Cell Physiol 51:524–536
64. He W, Brumos J, Li H, Ji Y, Ke M, Gong X, Zeng Q, Li W, Zhang X, An F, Wen X, Li P, Chu J, Sun X, Yan C, Yan N, Xie DY, Raikhel N, Yang Z, Stepanova AN, Alonso JM, Guo H (2011) A small-molecule screen identifies L-kynurenine as a competitive inhibitor of TAA1/TAR activity in ethylene-directed auxin biosynthesis and root growth in *Arabidopsis*. Plant Cell 23:3944–3960
65. Nishimura T, Hayashi K, Suzuki H, Gyohda A, Takaoka C, Sakaguchi Y, Matsumoto S, Kasahara H, Sakai T, Kato J, Kamiya Y, Koshiba T (2014) Yucasin is a potent inhibitor of YUCCA, a key enzyme in auxin biosynthesis. Plant J 77:352–366
66. Taya Y, Tanaka Y, Nishimura S (1978) 5′-AMP is a direct precursor of cytokinin in *Dictyostelium discoideum*. Nature 271:545–547
67. Akiyoshi DE, Klee H, Amasino RM, Nester EW, Gordon MP (1984) T-DNA of *Agrobacterium tumefaciens* encodes an enzyme of cytokinin biosynthesis. Proc Natl Acad Sci U S A 81:5994–5998
68. Takei K, Sakakibara H, Sugiyama T (2001) Identification of genes encoding adenylate isopentenyltransferase, a cytokinin biosynthesis enzyme, in *Arabidopsis thaliana*. J Biol Chem 276:26405–26410
69. Miyawaki K, Matsumoto-Kitano M, Kakimoto T (2004) Expression of cytokinin biosynthetic isopentenyltransferase genes in *Arabidopsis*, tissue specificity and regulation by auxin, cytokinin, and nitrate. Plant J 37:128–138
70. Takei K, Ueda N, Aoki K, Kuromori T, Hirayama T, Shinozaki K, Yamaya T, Sakakibara H (2004) *AtIPT*3, an Arabidopsis isopentenyltransferase gene, is a key determinant of macronutrient-responsive cytokinin biosynthesis. Plant Cell Physiol 45:1053–1062
71. Takei K, Yamaya T, Sakakibara H (2004) *Arabidopsis CYP735A1* and *CYP735A2* encode cytokinin hydroxylases that catalyze the biosynthesis of trans-zeatin. J Biol Chem 279:41866–41872
72. Kurakawa T, Ueda N, Maekawa M, Kobayashi K, Kojima M, Nagato Y, Sakakibara H, Kyozuka J (2007) Direct control of shoot meristem activity by a cytokinin-activating enzyme. Nature 445:652–655
73. Kuroha T, Tokunaga H, Kojima M, Ueda N, Ishida T, Nagawa S, Fukuda H, Sugimoto K, Sakakibara H (2009) Functional analyses of

LONELY GUY cytokinin-activating enzymes reveal the importance of the direct activation pathway in Arabidopsis. Plant Cell 21: 3152–3169

74. Chen CM, Kristopeit SM (1981) Metabolism of cytokinin, dephosphorylation of cytokinin ribonucleotide by 5′-nucleotidases from wheat germ cytosol. Plant Physiol 67:494–498
75. Chen CM, Kristopeit SM (1981) Metabolism of cytokinin, deribosylation of cytokinin ribonucleoside by adenine nucleosidase from wheat germ cells. Plant Physiol 68:1020–1023
76. Hou B, Lim EK, Higgins G, Bowles DJ (2004) N-Glucosylation of cytokinins by glycosyltransferases of *Arabidopsis thaliana*. J Biol Chem 279:47822–47832
77. Werner T, Motyka V, Strnad M, Schmulling T (2001) Regulation of plant growth by cytokinin. Proc Natl Acad Sci U S A 98: 10487–10492
78. Werner T, Motyka V, Laucou V, Smets R, Van Onckelen H, Schmulling T (2003) Cytokinin-deficient transgenic *Arabidopsis* plants show multiple developmental alterations indicating opposite functions of cytokinins in the regulation of shoot and root meristem activity. Plant Cell 15:2532–2550
79. Letham DS, Palni LMS (1983) The biosynthesis and metabolism of cytokinins. Annu Rev Plant Physiol 34:163–197
80. Mok DW, Mok MC (2001) Cytokinin metabolism and action. Annu Rev Plant Physiol Plant Mol Biol 52:89–118
81. Tarkowski P, Ge L, Wan Hong Yong J, Tan SN (2009) Analytical methods for cytokinins. Trends Anal Chem 28(3):323–335
82. Morris DA, Thomas AG (1978) A microautoradiographic study of auxin transport in the stem of intact pea seedlings (*Pisum sativum L.*). J Exp Bot 29:147–157
83. Nowacki J, Bandurski RS (1980) Myo-inositol esters of indole-3-acetic acid as seed auxin precursors of Zea mays L. Plant Physiol 65:422–427
84. Lomax TL, Muday GK, Rubery PH (1995) Auxin transport. In: Davies PJ (ed) Plant hormones, physiology, biochemistry and molecular biology. Kluwer, Dordrecht, Netherlands, pp 509–530
85. Rashotte AM, Brady S, Reed R, Ante S, Muday GK (2000) Basipetal auxin transport is required for gravitropism in roots of *Arabidopsis*. Plant Physiol 122:481–490
86. Rubery PH, Sheldrake AR (1974) Carrier-mediated auxin transport. Planta 118:101–121
87. Raven JA (1975) Transport of indoleacetic acid in plant cells in relation to pH and electrical potential gradients, and its significance for polar IAA transport. New Phytol 74:163–172
88. Bennett MJ, Marchant A, Green HG, May ST, Ward SP, Millner PA, Walker AR, Schulz B, Feldmann KA (1996) *Arabidopsis AUX1* gene, a permease-like regulator of root gravitropism. Science 273:948–950
89. Gälweiler L, Guan C, Muller A, Wisman E, Mendgen K, Yephremov A, Palme K (1998) Regulation of polar auxin transport by AtPIN1 in *Arabidopsis* vascular tissue. Science 282:2226–2230
90. Geisler M, Blakeslee JJ, Bouchard R, Lee OR, Vincenzetti V, Bandyopadhyay A, Titapiwatanakun B, Peer WA, Bailly A, Richards EL, Ejendal KF, Smith AP, Baroux C, Grossniklaus U, Muller A, Hrycyna CA, Dudler R, Murphy AS, Martinoia E (2005) Cellular efflux of auxin catalyzed by the *Arabidopsis* MDR/PGP transporter AtPGP1. Plant J 44:179–194
91. Cho M, Lee SH, Cho HT (2007) P-glycoprotein4 displays auxin efflux transporter-like action in *Arabidopsis* root hair cells and tobacco cells. Plant Cell 19:3930–3943
92. Pickett FB, Wilson AK, Estelle M (1990) The *aux1* mutation of *Arabidopsis* confers both auxin and ethylene resistance. Plant Physiol 94:1462–1466
93. Yang Y, Hammes UZ, Taylor CG, Schachtman DP, Nielsen E (2006) High-affinity auxin transport by the AUX1 influx carrier protein. Curr Biol 16:1123–1127
94. Parry G, Delbarre A, Marchant A, Swarup R, Napier R, Perrot-Rechenmann C, Bennett MJ (2001) Novel auxin transport inhibitors phenocopy the auxin influx carrier mutation *aux1*. Plant J 25:399–406
95. Swarup K, Benkova E, Swarup R, Casimiro I, Peret B, Yang Y, Parry G, Nielsen E, De Smet I, Vanneste S, Levesque MP, Carrier D, James N, Calvo V, Ljung K, Kramer E, Roberts R, Graham N, Marillonnet S, Patel K, Jones JD, Taylor CG, Schachtman DP, May S, Sandberg G, Benfey P, Friml J, Kerr I, Beeckman T, Laplaze L, Bennett MJ (2008) The auxin influx carrier LAX3 promotes lateral root emergence. Nat Cell Biol 10: 946–954
96. Péret B, Swarup K, Ferguson A, Seth M, Yang Y, Dhondt S, James N, Casimiro I, Perry P, Syed A, Yang H, Reemmer J, Venison E, Howells C, Perez-Amador MA, Yun J, Alonso J, Beemster GT, Laplaze L, Murphy A, Bennett MJ, Nielsen E, Swarup R (2012) *AUX/LAX* genes encode a family of auxin influx transporters that perform distinct functions during *Arabidopsis* development. Plant Cell 24:2874–2885

97. Bainbridge K, Guyomarc'h S, Bayer E, Swarup R, Bennett M, Mandel T, Kuhlemeier C (2008) Auxin influx carriers stabilize phyllotactic patterning. Genes Dev 22:810–823
98. Stone BB, Stowe-Evans EL, Harper RM, Celaya RB, Ljung K, Sandberg G, Liscum E (2008) Disruptions in AUX1-dependent auxin influx alter hypocotyl phototropism in *Arabidopsis*. Mol Plant 1:129–144
99. Jones AR, Kramer EM, Knox K, Swarup R, Bennett MJ, Lazarus CM, Leyser HM, Grierson CS (2009) Auxin transport through non-hair cells sustains root-hair development. Nat Cell Biol 11:78–84
100. Okada K, Ueda J, Komaki MK, Bell CJ, Shimura Y (1991) Requirement of the auxin polar transport system in early stages of Arabidopsis floral bud formation. Plant Cell 3:677–684
101. Petrášek J, Mravec J, Bouchard R, Blakeslee JJ, Abas M, Seifertova D, Wisniewska J, Tadele Z, Kubes M, Covanova M, Dhonukshe P, Skupa P, Benkova E, Perry L, Krecek P, Lee OR, Fink GR, Geisler M, Murphy AS, Luschnig C, Zazimalova E, Friml J (2006) PIN proteins perform a rate-limiting function in cellular auxin efflux. Science 312:914–918
102. Yang H, Murphy AS (2009) Functional expression and characterization of *Arabidopsis* ABCB, AUX 1 and PIN auxin transporters in *Schizosaccharomyces pombe*. Plant J 59:179–191
103. Barbez E, Lanková M, Parezová M, Maizel A, Zazímalová E, Petrášek J, Friml J, Kleine-Vehn J (2013) Single-cell-based system to monitor carrier driven cellular auxin homeostasis. BMC Plant Biol 13:20
104. Zourelidou M, Absmanner B, Weller B, Barbosa IC, Willige BC, Fastner A, Streit V, Port SA, Colcombet J, de la Fuente van Bentem S, Hirt H, Kuster B, Schulze WX, Hammes UZ, Schwechheimer C (2014) Auxin efflux by PIN-FORMED proteins is activated by two different protein kinases, D6 PROTEIN KINASE and PINOID. Elife 3
105. Zažímalová E, Krecek P, Skupa P, Hoyerova K, Petrasek J (2007) Polar transport of the plant hormone auxin—the role of PIN-FORMED (PIN) proteins. Cell Mol Life Sci 64:1621–1637
106. Adamowski M, Friml J (2015) PIN-dependent auxin transport, action, regulation, and evolution. Plant Cell 27:20–32
107. Mravec J, Skůpa P, Bailly A, Hoyerová K, Krecek P, Bielach A, Petrásek J, Zhang J, Gaykova V, Stierhof YD, Dobrev PI, Schwarzerová K, Rolcík J, Seifertová D, Luschnig C, Benková E, Zazímalová E, Geisler M, Friml J (2009) Subcellular homeostasis of phytohormone auxin is mediated by the ER-localized PIN5 transporter. Nature 459:1136–1140
108. Ding Z, Wang B, Moreno I, Dupláková N, Simon S, Carraro N, Reemmer J, Pěnčík A, Chen X, Tejos R, Skůpa P, Pollmann S, Mravec J, Petrášek J, Zažímalová E, Honys D, Rolčík J, Murphy A, Orellana A, Geisler M, Friml J (2012) ER-localized auxin transporter PIN8 regulates auxin homeostasis and male gametophyte development in *Arabidopsis*. Nat Commun 3:941
109. Barbez E, Kubeš M, Rolčík J, Béziat C, Pěnčík A, Wang B, Rosquete MR, Zhu J, Dobrev PI, Lee Y, Zažímalovà E, Petrášek J, Geisler M, Friml J, Kleine-Vehn J (2012) A novel putative auxin carrier family regulates intracellular auxin homeostasis in plants. Nature 485: 119–122
110. Noh B, Murphy AS, Spalding EP (2001) Multidrug resistance-like genes of *Arabidopsis* required for auxin transport and auxin-mediated development. Plant Cell 13: 2441–2454
111. Verrier PJ, Bird D, Burla B, Dassa E, Forestier C, Geisler M, Klein M, Kolukisaoglu U, Lee Y, Martinoia E, Murphy A, Rea PA, Samuels L, Schulz B, Spalding EJ, Yazaki K, Theodoulou FL (2008) Plant ABC proteins—a unified nomenclature and updated inventory. Trends Plant Sci 13:151–159
112. Peer WA, Blakeslee JJ, Yang H, Murphy AS (2011) Seven things we think we know about auxin transport. Mol Plant 4:487–504
113. Wisniewska J, Xu J, Seifertova D, Brewer PB, Ruzicka K, Blilou I, Rouquie D, Benkova E, Scheres B, Friml J (2006) Polar PIN localization directs auxin flow in plants. Science 312:883
114. Benjamins R, Quint A, Weijers D, Hooykaas P, Offringa R (2001) The PINOID protein kinase regulates organ development in *Arabidopsis* by enhancing polar auxin transport. Development 128:4057–4067
115. Friml J, Yang X, Michniewicz M, Weijers D, Quint A, Tietz O, Benjamins R, Ouwerkerk PB, Ljung K, Sandberg G, Hooykaas PJ, Palme K, Offringa R (2004) A PINOID-dependent binary switch in apical-basal PIN polar targeting directs auxin efflux. Science 306:862–865
116. Michniewicz M, Zago MK, Abas L, Weijers D, Schweighofer A, Meskiene I, Heisler MG, Ohno C, Zhang J, Huang F, Schwab R, Weigel D, Meyerowitz EM, Luschnig C, Offringa R, Friml J (2007) Antagonistic regulation of PIN phosphorylation by PP2A and PINOID directs auxin flux. Cell 130: 1044–1056

117. Zhang J, Nodzynski T, Pencik A, Rolcik J, Friml J (2010) PIN phosphorylation is sufficient to mediate PIN polarity and direct auxin transport. Proc Natl Acad Sci U S A 107: 918–922
118. Huang F, Zago MK, Abas L, van Marion A, Galvan-Ampudia CS, Offringa R (2010) Phosphorylation of conserved PIN motifs directs *Arabidopsis* PIN1 polarity and auxin transport. Plant Cell 22:1129–1142
119. Zhang J, Vanneste S, Brewer PB, Michniewicz M, Grones P, Kleine-Vehn J, Löfke C, Teichmann T, Bielach A, Cannoot B, Hoyerová K, Chen X, Xue HW, Benková E, Zažímalová E, Friml J (2011) Inositol trisphosphate-induced Ca^{2+} signaling modulates auxin transport and PIN polarity. Dev Cell 20:855–866
120. Feraru E, Feraru MI, Kleine-Vehn J, Martinière A, Mouille G, Vanneste S, Vernhettes S, Runions J, Friml J (2011) PIN polarity maintenance by the cell wall in *Arabidopsis*. Curr Biol 21:338–343
121. Heisler MG, Hamant O, Krupinski P, Uyttewaal M, Ohno C, Jönsson H, Traas J, Meyerowitz EM (2010) Alignment between PIN1 polarity and microtubule orientation in the shoot apical meristem reveals a tight coupling between morphogenesis and auxin transport. PLoS Biol 8:e1000516
122. Geldner N, Friml J, Stierhof YD, Jurgens G, Palme K (2001) Auxin transport inhibitors block PIN1 cycling and vesicle trafficking. Nature 413:425–428
123. Dhonukshe P, Aniento F, Hwang I, Robinson DG, Mravec J, Stierhof YD, Friml J (2007) Clathrin-mediated constitutive endocytosis of PIN auxin efflux carriers in Arabidopsis. Curr Biol 17:520–527
124. Kitakura S, Vanneste S, Robert S, Löfke C, Teichmann T, Tanaka H, Friml J (2011) Clathrin mediates endocytosis and polar distribution of PIN auxin transporters in *Arabidopsis*. Plant Cell 23:1920–1931
125. Wang C, Yan X, Chen Q, Jiang N, Fu W, Ma B, Liu J, Li C, Bednarek SY, Pan J (2013) Clathrin light chains regulate clathrin-mediated trafficking, auxin signaling, and development in *Arabidopsis*. Plant Cell 25: 499–516
126. Geldner N, Anders N, Wolters H, Keicher J, Kornberger W, Muller P, Delbarre A, Ueda T, Nakano A, Jurgens G (2003) The *Arabidopsis* GNOM ARF-GEF mediates endosomal recycling, auxin transport, and auxin-dependent plant growth. Cell 112:219–230
127. Kleine-Vehn J, Dhonukshe P, Sauer M, Brewer PB, Wisniewska J, Paciorek T, Benkova E, Friml J (2008) ARF GEF-dependent transcytosis and polar delivery of PIN auxin carriers in *Arabidopsis*. Curr Biol 18:526–531
128. Kleine-Vehn J, Friml J (2008) Polar targeting and endocytic recycling in auxin-dependent plant development. Annu Rev Cell Dev Biol 24:447–473
129. Naramoto S, Otegui MS, Kutsuna N, de Rycke R, Dainobu T, Karampelias M, Fujimoto M, Feraru E, Miki D, Fukuda H, Nakano A, Friml J (2014) Insights into the localization and function of the membrane trafficking regulator GNOM ARF-GEF at the Golgi apparatus in *Arabidopsis*. Plant Cell 26:3062–3076
130. Naramoto S, Kleine-Vehn J, Robert S, Fujimoto M, Dainobu T, Paciorek T, Ueda T, Nakano A, Van Montagu MCE, Fukuda H, Friml J (2010) ADP-ribosylation factor machinery mediates endocytosis in plant cells. Proc Natl Acad Sci U S A 107:21890–21895
131. Teh OK, Moore I (2007) An ARF-GEF acting at the Golgi and in selective endocytosis in polarized plant cells. Nature 448:493–496
132. Feraru E, Paciorek T, Feraru MI, Zwiewka M, De Groodt R, De Rycke R, Kleine-Vehn J, Friml J (2010) The AP-3 b adaptin mediates the biogenesis and function of lytic vacuoles in *Arabidopsis*. Plant Cell 22:2812–2824
133. Tanaka H, Kitakura S, De Rycke R, De Groodt R, Friml J (2009) Fluorescence imaging-based screen identifies ARF GEF component of early endosomal trafficking. Curr Biol 19:391–397
134. Tanaka H, Kitakura S, Rakusová H, Uemura T, Feraru MI, De Rycke R, Robert S, Kakimoto T, Friml J (2013) Cell polarity and patterning by PIN trafficking through early endosomal compartments in *Arabidopsis thaliana*. PLoS Genet 9:e1003540
135. Robert HS, Grones P, Stepanova AN, Robles LM, Lokerse AS, Alonso JM, Weijers D, Friml J (2013) Local auxin sources orient the apical-basal axis in *Arabidopsis* embryos. Curr Biol 23:2506–2512
136. Dubrovsky JG, Sauer M, Napsucialy-Mendivil S, Ivanchenko MG, Friml J, Shishkova S, Celenza J, Benková E (2008) Auxin acts as a local morphogenetic trigger to specify lateral root founder cells. Proc Natl Acad Sci U S A 105:8790–8794
137. Kleine-Vehn J, Ding Z, Jones AR, Tasaka M, Morita MT, Friml J (2010) Gravity-induced PIN transcytosis for polarization of auxin fluxes in gravity-sensing root cells. Proc Natl Acad Sci U S A 107:22344–22349
138. Ding Z, Galván-Ampudia CS, Demarsy E, Łangowski Ł, Kleine-Vehn J, Fan Y, Morita MT, Tasaka M, Fankhauser C, Offringa R, Friml J (2011) Light-mediated polarization

of the PIN3 auxin transporter for the phototropic response in *Arabidopsis*. Nat Cell Biol 13:447–452

139. Rakusová H, Gallego-Bartolomé J, Vanstraelen M, Robert HS, Alabadí D, Blázquez MA, Benková E, Friml J (2011) Polarization of PIN3-dependent auxin transport for hypocotyl gravitropic response in *Arabidopsis thaliana*. Plant J 67:817–826
140. Gillissen B, Burkle L, Andre B, Kuhn C, Rentsch D, Brandl B, Frommer WB (2000) A new family of high-affinity transporters for adenine, cytosine, and purine derivatives in *Arabidopsis*. Plant Cell 12:291–300
141. Burkle L, Cedzich A, Dopke C, Stransky H, Okumoto S, Gillissen B, Kuhn C, Frommer WB (2003) Transport of cytokinins mediated by purine transporters of the PUP family expressed in phloem, hydathodes, and pollen of Arabidopsis. Plant J 34:13–26
142. Bishopp A, Benkova E, Helariutta Y (2011) Sending mixed messages, auxin-cytokinin crosstalk in roots. Curr Opin Plant Biol 14:10–16
143. Beveridge CA, Murfet IC, Kerhoas L, Sotta B, Miginiac E, Rameau C (1997) The shoot controls zeatin riboside export from pea roots. Evidence from the branching mutant *rms4*. Plant J 11:339–345
144. Hirose N, Makita N, Yamaya T, Sakakibara H (2005) Functional characterization and expression analysis of a gene, OsENT2, encoding an equilibrative nucleoside transporter in rice suggest a function in cytokinin transport. Plant Physiol 138:196–206
145. Corbesier L, Prinsen E, Jacqmard A, Lejeune P, Van Onckelen H, Périlleux C, Bernier G (2003) Cytokinin levels in leaves, leaf exudate and shoot apical meristem of *Arabidopsis thaliana* during floral transition. J Exp Bot 54:2511–2517
146. Matsumoto-Kitano M, Kusumoto T, Tarkowski P, Kinoshita-Tsujimura K, Václavíková K, Miyawaki K, Kakimoto T (2008) Cytokinins are central regulators of cambial activity. Proc Natl Acad Sci U S A 105:20027–20031
147. Kudo T, Kiba T, Sakakibara H (2010) Metabolism and long-distance translocation of cytokinins. J Integr Plant Biol 52:53–60
148. Zhang K, Novak O, Wei Z, Gou M, Zhang X, Yu Y, Yang H, Cai Y, Strnad M, Liu CJ (2014) *Arabidopsis* ABCG14 protein controls the acropetal translocation of root-synthesized cytokinins. Nat Commun 5:3274
149. Cedzich A, Stransky H, Schulz B, Frommer WB (2008) Characterization of cytokinin and adenine transport in *Arabidopsis* cell cultures. Plant Physiol 148:1857–1867
150. Li G, Liu K, Baldwin SA, Wang D (2003) Equilibrative nucleoside transporters of *Arabidopsis thaliana*. cDNA cloning, expression pattern, and analysis of transport activities. J Biol Chem 278:35732–35742
151. Sun J, Hirose N, Wang X, Wen P, Xue L, Sakakibara H, Zuo J (2005) *Arabidopsis SOI33/AtENT8* gene encodes a putative equilibrative nucleoside transporter that is involved in cytokinin transport in planta. J Integr Plant Biol 47:588–603
152. Hirose N, Takei K, Kuroha T, Kamada-Nobusada T, Hayashi H, Sakakibara H (2008) Regulation of cytokinin biosynthesis, compartmentalization and translocation. J Exp Bot 59:75–83
153. Ruegger M, Dewey E, Gray WM, Hobbie L, Turner J, Estelle M (1998) The TIR1 protein of *Arabidopsis* functions in auxin response and is related to human SKP2 and yeast grr1p. Genes Dev 12:198–207
154. Ruegger M, Dewey E, Hobbie L, Brown D, Bernasconi P, Turner J, Muday G, Estelle M (1997) Reduced naphthylphthalamic acid binding in the *tir3* mutant of *Arabidopsis* is associated with a reduction in polar auxin transport and diverse morphological defects. Plant Cell 9:745–757
155. Abel S, Nguyen MD, Theologis A (1995) The PS-IAA4/5-like family of early auxin-inducible mRNAs in *Arabidopsis thaliana*. J Mol Biol 251:533–549
156. Hagen G, Guilfoyle T (2002) Auxin-responsive gene expression, genes, promoters and regulatory factors. Plant Mol Biol 49:373–385
157. Abel S, Theologis A (1996) Early genes and auxin action. Plant Physiol 111:9–17
158. Ulmasov T, Hagen G, Guilfoyle TJ (1997) ARF1, a transcription factor that binds auxin response elements. Science 276:1865–1868
159. Gray WM, del Pozo JC, Walker L, Hobbie L, Risseeuw E, Banks T, Crosby WL, Yang M, Ma H, Estelle M (1999) Identification of an SCF ubiquitin-ligase complex required for auxin response in *Arabidopsis thaliana*. Genes Dev 13:1678–1691
160. Abel S, Theologis A (2010) Odyssey of auxin. Cold Spring Harb Perspect Biol 2:a004572
161. Gray WM, Kepinski S, Rouse D, Leyser O, Estelle M (2001) Auxin regulates SCF(TIR1)-dependent degradation of AUX/IAA proteins. Nature 414:271–276
162. Dharmasiri N, Dharmasiri S, Estelle M (2005) The F-box protein TIR1 is an auxin receptor. Nature 435:441–445
163. Dharmasiri N, Dharmasiri S, Weijers D, Lechner E, Yamada M, Hobbie L, Ehrismann

JS, Jurgens G, Estelle M (2005) Plant development is regulated by a family of auxin receptor F box proteins. Dev Cell 9:109–119

164. Kepinski S, Leyser O (2005) The Arabidopsis F-box protein TIR1 is an auxin receptor. Nature 435:446–451
165. Tan X, Calderon-Villalobos LI, Sharon M, Zheng C, Robinson CV, Estelle M, Zheng N (2007) Mechanism of auxin perception by the TIR1 ubiquitin ligase. Nature 446:640–645
166. Szemenyei H, Hannon M, Long JA (2008) TOPLESS mediates auxin-dependent transcriptional repression during *Arabidopsis* embryogenesis. Science 319:1384–1386
167. Overvoorde PJ, Okushima Y, Alonso JM, Chan A, Chang C, Ecker JR, Hughes B, Liu A, Onodera C, Quach H, Smith A, Yu G, Theologis A (2005) Functional genomic analysis of the *AUXIN/INDOLE-3-ACETIC ACID* gene family members in *Arabidopsis thaliana*. Plant Cell 17:3282–3300
168. Okushima Y, Overvoorde PJ, Arima K, Alonso JM, Chan A, Chang C, Ecker JR, Hughes B, Lui A, Nguyen D, Onodera C, Quach H, Smith A, Yu G, Theologis A (2005) Functional genomic analysis of the *AUXIN RESPONSE FACTOR* gene family members in *Arabidopsis thaliana*, unique and overlapping functions of ARF7 and ARF19. Plant Cell 17:444–463
169. Calderón Villalobos LI, Lee S, De Oliveira C, Ivetac A, Brandt W, Armitage L, Sheard LB, Tan X, Parry G, Mao H, Zheng N, Napier R, Kepinski S, Estelle M (2012) A combinatorial TIR1/AFB-Aux/IAA co-receptor system for differential sensing of auxin. Nat Chem Biol 8:477–485
170. Moss BL, Mao H, Guseman JM, Hinds TR, Hellmuth A, Kovenock M, Noorassa A, Lanctot A, Villalobos LI, Zheng N, Nemhauser JL (2015) Rate motifs tune auxin/indole-3-acetic acid degradation dynamics. Plant Physiol 169:803–813
171. Vernoux T, Brunoud G, Farcot E, Morin V, Van den Daele H, Legrand J, Oliva M, Das P, Larrieu A, Wells D, Guédon Y, Armitage L, Picard F, Guyomarch S, Cellier C, Parry G, Koumproglou R, Doonan JH, Estelle M, Godin C, Kepinski S, Bennett M, De Veylder L, Traas J (2011) The auxin signalling network translates dynamic input into robust patterning at the shoot apex. Mol Syst Biol 7:508
172. Lee S, Sundaram S, Armitage L, Evans JP, Hawkes T, Kepinski S, Ferro N, Napier RM (2014) Defining binding efficiency and specificity of auxins for SCF(TIR1/AFB)-Aux/IAA co-receptor complex formation. ACS Chem Biol 9:673–682
173. Korasick DA, Westfall CS, Lee SG, Nanao MH, Dumas R, Hagen G, Guilfoyle TJ, Jez JM, Strader LC (2014) Molecular basis for AUXIN RESPONSE FACTOR protein interaction and the control of auxin response repression. Proc Natl Acad Sci U S A 111: 5427–5432
174. Nanao MH, Vinos-Poyo T, Brunoud G, Thévenon E, Mazzoleni M, Mast D, Lainé S, Wang S, Hagen G, Li H, Guilfoyle TJ, Parcy F, Vernoux T, Dumas R (2014) Structural basis for oligomerization of auxin transcriptional regulators. Nat Commun 7:3617
175. Shimizu-Mitao Y, Kakimoto T (2014) Auxin sensitivities of all *Arabidopsis* Aux/IAAs for degradation in the presence of every TIR1/AFB. Plant Cell Physiol 55:1405–1459
176. Boer DR, Freire-Rios A, van den Berg WA, Saaki T, Manfield IW, Kepinski S, López-Vidrieo I, Franco-Zorrilla JM, de Vries SC, Solano R, Weijers D, Coll M (2014) Structural basis for DNA binding specificity by the auxin-dependent ARF transcription factors. Cell 156:577–589
177. Kakimoto T (1996) CKI1, a histidine kinase homolog implicated in cytokinin signal transduction. Science 274:982–985
178. Inoue T, Higuchi M, Hashimoto Y, Seki M, Kobayashi M, Kato T, Tabata S, Shinozaki K, Kakimoto T (2001) Identification of CRE1 as a cytokinin receptor from *Arabidopsis*. Nature 409:1060–1063
179. Mähönen AP, Bonke M, Kauppinen L, Riikonen M, Benfey PN, Helariutta Y (2000) A novel two-component hybrid molecule regulates vascular morphogenesis of the *Arabidopsis* root. Genes Dev 14: 2938–2943
180. Hwang I, Sheen J (2001) Two-component circuitry in *Arabidopsis* cytokinin signal transduction. Nature 413:383–389
181. Ueguchi C, Sato S, Kato T, Tabata S (2001) The AHK4 gene involved in the cytokinin-signaling pathway as a direct receptor molecule in *Arabidopsis thaliana*. Plant Cell Physiol 42:751–755
182. Higuchi M, Pischke MS, Mahonen AP, Miyawaki K, Hashimoto Y, Seki M, Kobayashi M, Shinozaki K, Kato T, Tabata S, Helariutta Y, Sussman MR, Kakimoto T (2004) In planta functions of the *Arabidopsis* cytokinin receptor family. Proc Natl Acad Sci U S A 101:8821–8826
183. Nishimura C, Ohashi Y, Sato S, Kato T, Tabata S, Ueguchi C (2004) Histidine kinase homologs that act as cytokinin receptors possess overlapping functions in the regulation of shoot and root growth in *Arabidopsis*. Plant Cell 16:1365–1377

184. Suzuki T, Miwa K, Ishikawa K, Yamada H, Aiba H, Mizuno T (2001) The Arabidopsis sensor His-kinase, AHK4, can respond to cytokinins. Plant Cell Physiol 42:107–113
185. Romanov GA, Spíchal L, Lomin SN, Strnad M, Schmülling T (2005) A live cell hormone-binding assay on transgenic bacteria expressing a eukaryotic receptor protein. Anal Biochem 347:129–134
186. Romanov GA, Lomin SN, Schmülling T (2006) Biochemical characteristics and ligand-binding properties of *Arabidopsis* cytokinin receptor AHK3 compared to CRE1/AHK4 as revealed by a direct binding assay. J Exp Bot 57:4051–4058
187. Stolz A, Riefler M, Lomin SN, Achazi K, Romanov GA, Schmülling T (2011) The specificity of cytokinin signalling in *Arabidopsis thaliana* is mediated by differing ligand affinities and expression profiles of the receptors. Plant J 67:157–168
188. Mizuno T (2005) Two-component phosphorelay signal transduction systems in plants: from hormone responses to circadian rhythms. Biosci Biotechnol Biochem 69(12):2263–2276
189. Schaller GE, Kieber JJ, Shiu S-H (2008) Two-component signaling elements and histidyl-aspartyl phosphorelays. In: Somerville C, Meyerowitz E (eds) The Arabidopsis book. American Society of Plant Biologists, Rockville, MD
190. Sakai H, Honma T, Aoyama T, Sato S, Kato T, Tabata S, Oka A (2001) ARR1, a transcription factor for genes immediately responsive to cytokinins. Science 294:1519–1521
191. Mason MG, Mathews DE, Argyros DA, Maxwell BB, Kieber JJ, Alonso JM, Ecker JR, Schaller GE (2005) Multiple type-B response regulators mediate cytokinin signal transduction in Arabidopsis. Plant Cell 17:3007–3018
192. Hutchison CE, Li J, Argueso C, Gonzalez M, Lee E, Lewis MW, Maxwell BB, Perdue TD, Schaller GE, Alonso JM, Ecker JR, Kieber JJ (2006) The Arabidopsis histidine phosphotransfer proteins are redundant positive regulators of cytokinin signaling. Plant Cell 18:3073–3087
193. To JP, Deruere J, Maxwell BB, Morris VF, Hutchison CE, Ferreira FJ, Schaller GE, Kieber JJ (2007) Cytokinin regulates type-A Arabidopsis Response Regulator activity and protein stability via two-component phosphorelay. Plant Cell 19:3901–3914
194. Argyros RD, Mathews DE, Chiang YH, Palmer CM, Thibault DM, Etheridge N, Argyros DA, Mason MG, Kieber JJ, Schaller GE (2008) Type B response regulators of *Arabidopsis* play key roles in cytokinin signaling and plant development. Plant Cell 20:2102–2116
195. Kieber JJ, Schaller GE (2014) Cytokinins. The Arabidopsis Book 12, e0168
196. Kim HJ, Chiang YH, Kieber JJ, Schaller GE (2013) SCF(KMD) controls cytokinin signaling by regulating the degradation of type-B response regulators. Proc Natl Acad Sci U S A 110:10028–10033
197. Caesar K, Thamm AM, Witthoft J, Elgass K, Huppenberger P, Grefen C, Horak J, Harter K (2011) Evidence for the localization of the *Arabidopsis* cytokinin receptors AHK3 and AHK4 in the endoplasmic reticulum. J Exp Bot 62:5571–5580
198. Wulfetange K, Lomin SN, Romanov GA, Stolz A, Heyl A, Schmulling T (2011) The cytokinin receptors of *Arabidopsis* are located mainly to the endoplasmic reticulum. Plant Physiol 156:1808–1818
199. Rashotte AM, Mason MG, Hutchison CE, Ferreira FJ, Schaller GE, Kieber JJ (2006) A subset of *Arabidopsis* AP2 transcription factors mediates cytokinin responses in concert with a two-component pathway. Proc Natl Acad Sci U S A 103:11081–11085
200. Sakuma Y, Liu Q, Dubouzet JG, Abe H, Shinozaki K, Yamaguchi-Shinozaki K (2002) DNA-binding specificity of the ERF/AP2 domain of Arabidopsis DREBs, transcription factors involved in dehydration- and cold-inducible gene expression. Biochem Biophys Res Commun 290:998–1009
201. Nakano T, Suzuki K, Fujimura T, Shinshi H (2006) Genome-wide analysis of the ERF gene family in *Arabidopsis* and rice. Plant Physiol 140:411–432
202. Rashotte AM, Goertzen LR (2010) The CRF domain defines cytokinin response factor proteins in plants. BMC Plant Biol 10:74
203. Ulmasov T, Murfett J, Hagen G, Guilfoyle TJ (1997) Aux/IAA proteins repress expression of reporter genes containing natural and highly active synthetic auxin response elements. Plant Cell 9:1963–1971
204. Band LR, Wells DM, Larrieu A, Sun J, Middleton AM, French AP, Brunoud G, Sato EM, Wilson MH, Péret B, Oliva M, Swarup R, Sairanen I, Parry G, Ljung K, Beeckman T, Garibaldi JM, Estelle M, Owen MR, Vissenberg K, Hodgman TC, Pridmore TP, King JR, Vernoux T, Bennett MJ (2012) Root gravitropism is regulated by a transient lateral auxin gradient controlled by a tipping-point mechanism. Proc Natl Acad Sci U S A 109:4668–4673

205. Brunoud G, Wells DM, Oliva M, Larrieu A, Mirabet V, Burrow AH, Beeckman T, Kepinski S, Traas J, Bennett MJ, Vernoux T (2012) A novel sensor to map auxin response and distribution at high spatio-temporal resolution. Nature 482:103–106
206. Su YH, Liu YB, Zhang XS (2011) Auxin-cytokinin interaction regulates meristem development. Mol Plant 4:616–625
207. Bencivenga S, Simonini S, Benková E, Colombo L (2012) The transcription factors BEL1 and SPL are required for cytokinin and auxin signaling during ovule development in *Arabidopsis*. Plant Cell 24:2886–2897
208. Leibfried A, To JP, Busch W, Stehling S, Kehle A, Demar M, Kieber JJ, Lohmann JU (2005) WUSCHEL controls meristem function by direct regulation of cytokinin-inducible response regulators. Nature 438: 1172–1175
209. Domagalska MA, Leyser O (2011) Signal integration in the control of shoot branching. Nat Rev Mol Cell Biol 12:211–221
210. Laskowski MJ, Williams ME, Nusbaum HC, Sussex IM (1995) Formation of lateral root meristems is a two-stage process. Development 121:3303–3310
211. Laskowski M, Grieneisen VA, Hofhuis H, Hove CA, Hogeweg P, Maree AF, Scheres B (2008) Root system architecture from coupling cell shape to auxin transport. PLoS Biol 6:e307
212. Marhavý P, Bielach A, Abas L, Abuzeineh A, Duclercq J, Tanaka H, Pařezová M, Petrášek J, Friml J, Kleine-Vehn J, Benková E (2011) Cytokinin modulates endocytic trafficking of PIN1 auxin efflux carrier to control plant organogenesis. Dev Cell 21:796–804
213. Hardtke CS, Berleth T (1998) The *Arabidopsis* gene MONOPTEROS encodes a transcription factor mediating embryo axis formation and vascular development. EMBO J 17:1405–1411
214. Hamann T, Benkova E, Baurle I, Kientz M, Jurgens G (2002) The *Arabidopsis* BODENLOS gene encodes an auxin response protein inhibiting MONOPTEROS-mediated embryo patterning. Genes Dev 16:1610–1615
215. Schlereth A, Möller B, Liu W, Kientz M, Flipse J, Rademacher EH, Schmid M, Jürgens G, Weijers D (2010) MONOPTEROS controls embryonic root initiation by regulating a mobile transcription factor. Nature 464: 913–916
216. Šimášková M, O'Brien JA, Khan M, Van Noorden G, Ötvös K, Vieten A, De Clercq I, Van Haperen JM, Cuesta C, Hoyerová K, Vanneste S, Marhavý P, Wabnik K, Van Breusegem F, Nowack M, Murphy A, Friml J, Weijers D, Beeckman T, Benková E (2015) Cytokinin response factors regulate PIN-FORMED auxin transporters. Nat Commun 6:8717
217. Dello Ioio R, Linhares FS, Scacchi E, Casamitjana-Martinez E, Heidstra R, Costantino P, Sabatini S (2007) Cytokinins determine *Arabidopsis* root-meristem size by controlling cell differentiation. Curr Biol 17:678–682
218. Vieten A, Vanneste S, Wisniewska J, Benkova E, Benjamins R, Beeckman T, Luschnig C, Friml J (2005) Functional redundancy of PIN proteins is accompanied by auxin-dependent cross-regulation of PIN expression. Development 132:4521–4531
219. Pernisová M, Klima P, Horak J, Valkova M, Malbeck J, Soucek P, Reichman P, Hoyerova K, Dubova J, Friml J, Zazimalova E, Hejatko J (2009) Cytokinins modulate auxin-induced organogenesis in plants via regulation of the auxin efflux. Proc Natl Acad Sci U S A 106:3609–3614
220. Zhang W, To JP, Cheng CY, Eric Schaller G, Kieber JJ (2011) Type-A response regulators are required for proper root apical meristem function through the post-transcriptional regulation of PIN auxin efflux carriers. Plant J 68:1–10
221. Marhavý P, Duclercq J, Weller B, Feraru E, Bielach A, Offringa R, Friml J, Schwechheimer C, Murphy A, Benková E (2014) Cytokinin controls polarity of PIN1-dependent auxin transport during lateral root organogenesis. Curr Biol 24:1031–1037
222. Jones B, Gunneras SA, Petersson SV, Tarkowski P, Graham N, May S, Dolezal K, Sandberg G, Ljung K (2010) Cytokinin regulation of auxin synthesis in *Arabidopsis* involves a homeostatic feedback loop regulated via auxin and cytokinin signal transduction. Plant Cell 22:2956–2969
223. Eklöf S, Åstot C, Blackwell J, Moritz T, Olsson O, Sandberg G (1997) Auxin-cytokinin interactions in wild-type and transgenic tobacco. Plant Cell Physiol 38: 225–235
224. Nordström A, Tarkowski P, Tarkowska D, Norbaek R, Astot C, Dolezal K, Sandberg G (2004) Auxin regulation of cytokinin biosynthesis in Arabidopsis thaliana: a factor of potential importance for auxin-cytokinin-regulated development. Proc Natl Acad Sci U S A 101:8039–8044
225. Carabelli M, Possenti M, Sessa G, Ciolfi A, Sassi M, Morelli G, Ruberti I (2007) Canopy shade causes a rapid and transient arrest in leaf

development through auxin-induced cytokinin oxidase activity. Genes Dev 21:1863–1868

226. Gordon SP, Chickarmane VS, Ohno C, Meyerowitz EM (2009) Multiple feedback loops through cytokinin signaling control stem cell number within the *Arabidopsis* shoot meristem. Proc Natl Acad Sci U S A 106: 16529–16534
227. Heisler MG, Ohno C, Das P, Sieber P, Reddy GV, Long JA, Meyerowitz EM (2005) Patterns of auxin transport and gene expression during primordium development revealed by live imaging of the *Arabidopsis* inflorescence meristem. Curr Biol 15:1899–1911
228. Hamant O, Nogué F, Belles-Boix E, Jublot D, Grandjean O, Traas J, Pautot V (2002) The KNAT2 homeodomain protein interacts with ethylene and cytokinin signaling. Plant Physiol 130:657–665
229. Lee BH, Johnston R, Yang Y, Gallavotti A, Kojima M, Travençolo BA, Costa LF, Sakakibara H, Jackson D (2009) Studies of aberrant *phyllotaxy1* mutants of maize indicate complex interactions between auxin and cytokinin signaling in the shoot apical meristem. Plant Physiol 150:205–216
230. Besnard F, Refahi Y, Morin V, Marteaux B, Brunoud G, Chambrier P, Rozier F, Mirabet V, Legrand J, Lainé S, Thévenon E, Farcot E, Cellier C, Das P, Bishopp A, Dumas R, Parcy F, Helariutta Y, Boudaoud A, Godin C, Traas J, Guédon Y, Vernoux T (2014) Cytokinin signalling inhibitory fields provide robustness to phyllotaxis. Nature 16:417–421
231. Voß U, Bishopp A, Farcot E, Bennett MJ (2014) Modelling hormonal response and development. Trends Plant Sci 19:311–319
232. Dello Ioio R, Galinha C, Fletcher AG, Grigg SP, Molnar A, Willemsen V, Scheres B, Sabatini S, Baulcombe D, Maini PK, Tsiantis M (2012) A PHABULOSA/cytokinin feedback loop controls root growth in *Arabidopsis*. Curr Biol 22:1699–1704
233. Muraro D, Mellor N, Pound MP, Help H, Lucas M, Chopard J, Byrne HM, Godin C, Hodgman TC, King JR, Pridmore TP, Helariutta Y, Bennett MJ, Bishopp A (2014) Integration of hormonal signaling networks and mobile microRNAs is required for vascular patterning in *Arabidopsis* roots. Proc Natl Acad Sci U S A 111:857–862
234. Carlsbecker A, Lee JY, Robertsm CJ, Dettmer J, Lehesranta S, Zhou J, Lindgren O, Moreno-Risueno MA, Vatén A, Thitamadee S, Campilho A, Sebastian J, Bowman JL, Helariutta Y, Benfey PN (2010) Cell signalling by *microRNA165/6* directs gene dose-dependent root cell fate. Nature 465: 316–321
235. De Rybel B, Adibi M, Breda AS, Wendrich JR, Smit ME, Novák O, Yamaguchi N, Yoshida S, Van Isterdael G, Palovaara J, Nijsse B, Boekschoten MV, Hooiveld G, Beeckman T, Wagner D, Ljung K, Fleck C, Weijers D (2014) Plant development. Integration of growth and patterning during vascular tissue formation in Arabidopsis. Science 345: 1255215
236. De Rybel B, Möller B, Yoshida S, Grabowicz I, Barbier de Reuille P, Boeren S, Smith RS, Borst JW, Weijers D (2013) A bHLH complex controls embryonic vascular tissue establishment and indeterminate growth in *Arabidopsis*. Dev Cell 24:426–437

Chapter 2

Analytical Determination of Auxins and Cytokinins

Petre I. Dobrev, Klára Hoyerová, and Jan Petrášek

Abstract

Parallel determination of auxin and cytokinin levels within plant organs and tissues represents an invaluable tool for studies of their physiological effects and mutual interactions. Thanks to their different chemical structures, auxins, cytokinins and their metabolites are often determined separately, using specialized procedures of sample purification, extraction, and quantification. However, recent progress in the sensitivity of analytical methods of liquid chromatography coupled to mass spectrometry (LC-MS) allows parallel analysis of multiple compounds. Here we describe a method that is based on single step purification protocol followed by LC-MS separation and detection for parallel analysis of auxins, cytokinins and their metabolites in various plant tissues and cell cultures.

Key words Auxin, Cytokinins, Phytohormones, Liquid chromatography, Mass spectrometry

1 Introduction

Plant hormones as small molecules occurring in minute concentrations are of decisive importance for major physiological processes in plants. Of those, auxin and cytokinins through their specific cross talk are important cell fate modulators [1]. Indole-3-acetic acid (IAA), the major endogenous auxin, is an indole derivative with weak acidity due to the exocyclic carboxylic acid group (Fig. 1a). IAA-associated metabolites include its precursors, i.e., tryptophan, indole pyruvic acid, indole acetonitrile, indole acetamide, conjugates with amino acids (mostly with aspartate and glutamate) and carbohydrates (IAA-glucosyl ester), and oxidative catabolites represented by oxindole-3-acetic acid [2]. Cytokinins, with their common natural representative *trans*-zeatin (*t*Z, Fig. 1a) are adenine derivatives with five carbon side chain connected to the exocyclic amino group. The exocyclic amino group determines the alkaline character of cytokinins. Common cytokinin metabolites include *N*9-ribosides, *N*9-ribotides, *N*7-glucosides, and *O*-glucosides [3].

Thomas Dandekar and Muhammad Naseem (eds.), *Auxins and Cytokinins in Plant Biology: Methods and Protocols*, Methods in Molecular Biology, vol. 1569, DOI 10.1007/978-1-4939-6831-2_2,

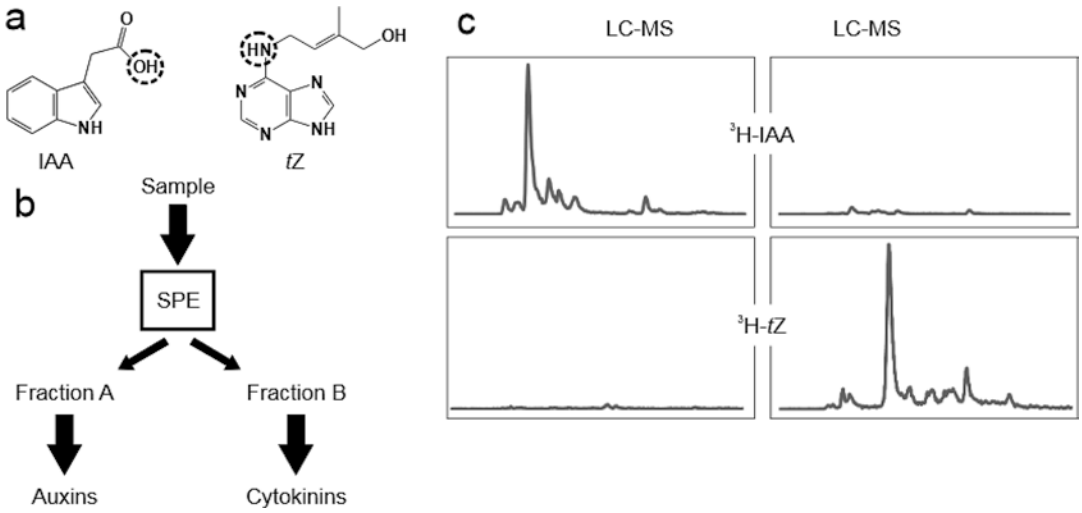

Fig. 1 Structures of IAA and *tZ*. (**a**) Structures of IAA and *tZ* with depicted ionisable parts that affect their isolation. (**b**) Simplified purification scheme (SPE, solid phase extraction) with splitting of plant extract into two fractions, fraction A containing auxins, and fraction B containing cytokinins. (**c**) HPLC separation of metabolites of ^{3}H-IAA and ^{3}H-*tZ* applied to 14-day-old *Arabidopsis thaliana* seedlings for 4 h from fractions A and B according to the scheme above. Each fraction was run on HPLC coupled with online radiodetector

The determination of endogenous levels of auxin and cytokinins underwent significant progress in recent years. The trend of plant hormone analysis is to switch from tedious multistep purification, derivatization, and immunodetection or nonselective instrumental detection of limited number of compounds, to minimalistic purification, consisting of few or even one step, followed by sensitive and selective detection of many compounds [4–9]. This "metabolite profiling" relies on the LC-MS and allows tracking the whole metabolic paths and networks of phytohormones.

Here we describe the procedure that is applied in our laboratory for determination of auxin, cytokinins and their metabolites in plants and cell cultures. It is based on single step purification, followed by LC-MS set at multiple reaction monitoring (MRM) mode for simultaneous measurement of hormonal precursors, active forms, and metabolites in single sample. Simplified scheme of the procedure is shown in Fig. 1b. The purification step splits the extract into two fractions, fraction A containing compounds of neutral and acidic character, and fraction B containing basic compounds. Since auxin and its major metabolites are acidic or neutral, they remain in fraction A. On the other hand, cytokinins as weak bases elute in fraction B. As shown here for samples purified from *Arabidopsis thaliana* seedlings incubated with either ^{3}H-*tZ* or ^{3}H-IAA for 4 h, the majority of IAA metabolites are found in fraction A, without any appreciable radioactivity in fraction B, and vice versa for the *tZ* (Fig. 1c). This separation of auxin and cytokinins and their metabolites is crucial for their metabolic profiling by LC-MS, as documented in our studies [7, 10].

2 Materials

Prepare all water solutions using MilliQ deionized water. For in vitro prepared plant material, all culture media should be sterilized as well as equipment for handling cells, seeds, or seedlings (*see* **Note 1**).

2.1 Plant Material

The methods of sampling, extraction or purification may differ with respect to particular material. Leaf tissue of approximately 100 mg FW is most common representative of processed samples thus the method of its extraction and purification is described in detail in Subheadings 3.2 and 3.3. For procedures analyzing plant hormones in liquid media or tiny materials of low weights, e.g., root tips, parts of very young seedlings or etiolated ones (*see* **Note 6**).

2.2 Sampling, Extraction, and Purification

1. Liquid nitrogen.
2. Methanol, deionized water, ammonium hydroxide 25%, formic acid, all p.a. grade.
3. Mixer mill MM301 Retsch, Teflon adapter racks for 2 mL vials, 5 mm zirconium oxide grinding balls.
4. Pipettes, 50 µL, 1 mL.
5. Analytical balances.
6. Stable isotope labeled internal standards, 0.2 µM dissolved into 50% methanol in water (*see* **Note 2**).
7. 2 mL microcentifuge tubes.
8. Benchtop cooled centrifuge.
9. Freezers (−20 °C, −80 °C).
10. Solid phase extraction columns (SPE Oasis MCX), 1 mL/30 mg, Waters.
11. SPE vacuum manifold, 12 or 24 port.
12. Rotary vacuum evaporator, SpeedVac.

2.3 LC-MS

1. Acetic acid and acetonitrile, both LC-MS grade.
2. Deionized water, MilliQ.
3. Autosampler vials, 0.5 mL.
4. HPLC column, e.g., Luna C18, 3 µm, 100 × 2 mm, Phenomenex.
5. HPLC system, e.g., Ultimate 3000, Dionex.
6. MS detector, e.g., 3200 QTRAP LC/MS/MS, AB Sciex.

2.4 Solvent Preparation

1. Extraction solvent: mix the following p.a. grade solvents: methanol–water–formic acid = 15/4/1, v/v/v, store at −20 °C.
2. SPE load solvent: 1 M formic acid, dilute 3.8 mL of 99% formic acid with water to 100 mL.

3. SPE elute 1 solvent: methanol, 100%, p.a. grade.
4. SPE elute 2 solvent: 0.35 M ammonium hydroxide in 70% methanol: to 70 mL methanol add 2.5 mL 25% ammonium hydroxide and fill to 100 mL with water; prepare fresh.
5. LC-MS solvent A: 5 mM acetic acid in 5% acetonitrile, to 50 mL acetonitrile for LC-MS add 286 µL acetic acid (99%, for LC-MS) and fill to 1000 mL with MilliQ water.
6. LC-MS solvent B: 5 mM acetic acid in 95% acetonitrile, to 50 mL MilliQ water add 286 µL acetic acid (99%, for LC-MS) and fill to 1000 mL with acetonitrile for LC-MS.

3 Methods

3.1 Plant Material Sampling

1. Collect about 100 mg FW plant material and put it into labeled and tared 2 mL microcentrifuge tube. Weigh and record the precise weight of sample (*see* **Note 3**).
2. Add one 5 mm zirconium oxide grinding ball (*see* **Note 4**) and close the tube.
3. Quickly freeze the sample into liquid nitrogen bath (*see* **Note 5**). Store samples at −80 °C.
4. Extremely small and tiny samples is worth to collect directly into microcentrifuge tube with methanol (about 300 µL) precisely weighted before sample addition. In certain cases the collecting of the samples may cause a loss of methanol due to the quick evaporation then the counting must be related to the number of collected parts instead of FW.

3.2 Homogenization and Extraction

Homogenization and extraction can be skipped in certain special cases (*see* **Note 6**).

1. Place samples into Teflon adapter and leave at −80 °C to cool down, at least for 15 min.
2. Mount the cold adapter with tubes into the arms of mixer mill MM 301. Apply frequency 25 Hz for 2 min. Repeat if tissue is not fully homogenized. Add 0.5 mL cold (−20 °C) extraction solvent (*see* **Note 7**).
3. Add 50 µL internal standards (*see* **Note 8**), mix and leave at −20 °C for 1 h. Centrifuge at 20,000 × *g* at 4 °C for 20 min. Transfer the supernatant into new 2 mL tube.
4. Re-extract the pellet with additional 0.5 mL extraction solvent for 30 min (*see* **Note 9**) and centrifuge as above.
5. Evaporate pooled supernatants in SpeedVac at 10 mBar and 40 °C to ¼ of initial volume (less than 0.25 mL, *see* **Note 10**).

3.3 Purification (See Note 11)

Purification can be skipped in certain special cases (*see* **Note 6**).

1. Mount Oasis MCX column on SPE vacuum manifold. Equilibrate the column by washing it with 1 mL methanol, followed by 1 mL SPE load solvent.
2. Dilute partially evaporated sample extract in 0.5 mL of SPE load solvent and apply to column. Discard flow-through.
3. Wash the column with 0.5 mL SPE load solvent, followed by 1 mL water. Discard flow-through.
4. Apply 0.5 mL SPE elute 1 solvent, collect the flow-through into new 2 mL microcentrifuge tube, which represents fraction A.
5. Apply 0.5 mL SPE elute 2 solvent, collect the flow-through into new 2 mL microcentrifuge tube, which represents fraction B.
6. Evaporate the collected fractions in SpeedVac at 10 mBar and 40 °C to dryness. Store dried fractions at −20 °C till LC-MS analysis.

3.4 Quantification by LC-MS (See Note 12)

3.4.1 Fraction A

1. Dissolve dried sample into 30 µL 15% acetonitrile in water. Centrifuge at 20,000 × *g*, 4 °C for 20 min. Transfer supernatant into autosampler vial.
2. Inject an aliquot, usually 1/10, of sample into LC-MS (*see* **Note 13**).
3. Run linear gradient of LC-MS solvents A and B; 10–50% LC-MS solvent B in 15 min at flow rate 0.3 mL/min. Flush column with 100% solvent B for 5 min and equilibrate with 10% solvent B for 10 min.
4. Set MS in negative electrospray mode. Ion source parameters: ion spray voltage −4000 V, nebulizer gas 50 psi, heater gas 50 psi, curtain gas 20 psi, gas heater 500 °C.
5. Set MS analyzer in MRM mode with the optimal compound specific parameters like declustering potential, precursor ion *m/z*, product ion *m/z*, collision energy, adjusted for each compound and internal standard.

3.4.2 Fraction B

1. Dissolve dried sample into 30 µL 5% methanol in water. Centrifuge at 20,000 × *g*, 4 °C for 20 min. Transfer supernatant into autosampler vial.
2. Inject an aliquot, usually 1/10, of sample into LC-MS.
3. Run linear gradient of LC-MS solvents A and B; 5–40% LC-MS solvent B in 15 min at flow rate 0.3 mL/min. Flush column with 100% solvent B for 5 min and equilibrate at 10% solvent B for 10 min (*see* **Note 14**).
4. Set MS in positive electrospray mode. Ion source parameters: ion spray voltage +4000 V, nebulizer gas 50 psi, heater gas 50 psi, curtain gas 20 psi, gas heater 500 °C.

5. Set MS analyzer in MRM mode with the optimal compound specific parameters like declustering potential, precursor ion *m/z*, product ion *m/z*, collision energy; adjusted for each compound and internal standard.
6. Inject an appropriate number of calibration standards for determination of the parameters of calibration curve. Quantify the samples based on isotope dilution with calibration curve (*see* **Note 15**).

4 Notes

1. For the reliable analyses of auxins and cytokinins in in vitro cultured plants or cell cultures it is absolutely essential to keep this material in strictly aseptic conditions, i.e., all media and materials should be sterilized before use. Since bacteria and fungi can themselves be a source of auxins and cytokinins, they could greatly influence their levels in analyzed plant samples.
2. For list of internal standards, *see* ref. 7. It should be stressed that chromatographic and MS optimalization of standards is instrument-dependent and should be carefully optimized.
3. The amount collected depends on the sensitivity of quantitation method and on the losses during purification. For our procedure an optimal amount is about 100 mg of fresh plant material. Although most commonly the results are presented in units of hormone amount per gram fresh weight (i.e., pmol/g FW) there are some cases where one has to consider different units. Other alternatives can be hormone amount per gram dry weight, per organ, per cell, per organ distance, etc. Choosing different units of data presentation or even better, having more alternatives, could improve for example the data variability, or could give more biological sense of results. The collected material should be representative of the experiment, and as homogenous as possible. If the amount of plant material is not limited, it is desirable to collect large representative batch from which an aliquot is taken. Extremely small and tiny samples are worth to collect directly into microcentrifuge tube with methanol (about 300 μL) precisely weighted before sample addition. In certain cases the collecting of the samples may cause a loss of methanol due to the quick evaporation then the counting must be related to the number of collected parts instead of FW.
4. We found that zirconium oxide balls are most appropriate for homogenization. The use of wolfram or stainless steel balls leads to significant loses of indole compounds, i.e., auxin and its metabolites.

5. The sample is frozen in liquid nitrogen to stop any metabolic processes.
6. In case of determination of phytohormones secreted into liquid growth media, extraction step is omitted and the medium (up to 1 mL) is acidified below pH 3 with formic acid. Purification starts after addition of internal standards to each sample with application on the SPE column (Subheading 3.3, **step 2**).

   Similarly, in case of tiny plant material (root tips, etiolated parts of seedlings, etc.) and amounts below 50 mg FW per sample the whole purification procedure might be skipped. Internal standards are added to samples collected in methanol and evaporated to dryness as described in Subheading 3.3, **step 6**.
7. The extraction is a process of quantitative release of phytohormones from plant tissue into extraction solvent. Concurrently, the extraction solvent should ideally fix the tissue, i.e., stop any metabolic conversions during extraction. In our protocol the extraction solvent contains organic solvent (methanol, 75 % by volume) and formic acid. High organic and low pH deactivate and precipitate enzymes in the tissue. Low temperature of extraction also diminishes post-extraction reactions.
8. Very important step is the addition of internal standards in the beginning of extraction. Internal standards are compounds with known purity and concentration, which ideally are chemically closest to the compounds of interest thus having same behavior during extraction and purification. The quantitation step should be able to discriminate between the target compound and the internal standard and measure them separately. The best internal standard is the stable isotope labeled equivalent of the target compound that differs only by mass, which can be distinguished by mass spectrometer. Since the concentration of internal standard is used for quantitation calculations, it is important to add precisely known and equal amounts.
9. The primary extraction recovers about 90 % of hormones with re-extraction adding another 8–9 %.
10. It is important to remove the organic solvent from the extraction mixture, because it could interfere with the following purification. Cool down samples at −80 °C before placing them into SpeedVac to avoid sample losses due to splash.
11. Ideally, the purification should remove all unwanted compounds that have been extracted and leave a solution where target compounds dominate. To achieve this, several purification steps can be applied, such as reversed phase, cation exchange, and anion exchange, preferably with orthogonal modes of action. Purification columns used here contain the so-called dual-mode sorbent, having two functionalities: reversed phase and cation exchange. This permits to use single purification column, and by stepwise elution with appropriate

solvents, to separate different groups of hormones into individual fractions. As opposed to the silica based sorbents, the sorbent we use can be air flushed without losing its activity and capacity. We apply air flush between individual elutions to increase the sample recovery and to better split them. The sample is applied to column in aqueous acidic solvent, allowing the hormones to bind to the sorbent by means of hydrophobic (auxins, CKs) and ion exchange (CKs) interactions. Following is the first elution with methanol, which releases from sorbent hydrophobically bound hormones, i.e., auxins. The second elution with ammonia and methanol increases abruptly pH, thus weakening the electrostatic binding of CKs to sorbent and releasing them in solution. As shown in Fig. 1c the metabolites of auxin and cytokinin at least in *Arabidopsis* have the same affinities towards the sorbent, thus elute in the same fraction with their precursor, i.e., the auxin metabolites in first elution (A-fraction) and CK metabolites in second elution (B-fraction). It should be noted that the order of elution solvents is important and should be observed. To avoid significant sample loss due to column overload, the maximal extracted plant material should be below 0.5 g FW.

12. The resulting two fractions of purification step are each analyzed individually on LC-MS. Fraction A containing the auxin and its metabolites are separated on reversed phase HPLC column using gradient of acidified aqueous mobile phase and acetonitrile. The mass spectrometer utilizes electrospray (ESI) interface set at negative mode, the most appropriate for the auxins. The fraction B, containing cytokinins, utilizes essentially same chromatographic conditions, with exception of slightly different gradient and the ESI in positive mode.
13. An aliquot of 1/10 corresponds to an extract from 100 mg FW (typically *Arabidopsis* seedlings or tobacco cell cultures). This aliquot can be adjusted up or down depending on the plant sample amount or the expected hormonal content.
14. Cytokinin metabolites are more demanding chromatographically, because there are several positional isomers like *cis*-Zeatin vs. *trans*-Zeatin, *N7*- vs. *N9*- vs. *O*-glucosides that must be separated.
15. In order to have statistically robust results, it is recommended to have at least three biological repetitions, with optimal five and more repetitions.

Acknowledgment

This work was supported by MEYS CR, projects no. LD14120 (PD), LD15137 (KH), and LO1417 (JP).

References

1. Chandler JW, Werr W (2015) Cytokinin–auxin crosstalk in cell type specification. Trends Plant Sci 20:291–300
2. Tivendale ND, Ross JJ, Cohen JD (2014) The shifting paradigms of auxin biosynthesis. Trends Plant Sci 19:44–51
3. Kaminek M (2015) Tracking the story of cytokinin research. J Plant Growth Regul 34: 723–739
4. Novák O, Hényková E, Sairanen I et al (2012) Tissue-specific profiling of the Arabidopsis thaliana auxin metabolome. Plant J 72: 523–536
5. Kojima M, Sakakibara H (2012) Highly sensitive high-throughput profiling of six phytohormones using MS-probe modification and liquid chromatography-tandem mass spectrometry. In: Normanly J (ed) High-throughput phenotyping in plants: methods and protocols, vol 918, Methods in molecular biology. Springer Science + Business Media, Dordrecht
6. Antoniadi I, Plackova L, Simonovik B, Dolezal K, Turnbull C, Ljung K, Novak O (2015) Cell-type-specific cytokinin distribution within the Arabidopsis primary root apex. Plant Cell 27: 1955–1967
7. Dobrev PI, Vankova R (2012) Quantification of abscisic acid, cytokinin, and auxin content in salt-stressed plant tissues. In: Shabala S, Cuin TA (eds) Plant salt tolerance: methods and protocols, vol 913, Methods in molecular biology. Springer Science + Business Media, Dordrecht
8. Kojima M, Kamada-Nobusada T, Kamatsu H, Takei K, Kuroha T, Mizutani M, Ashikari M, Ueguchi-Tanaka M, Matsuoka M, Suzuki K, Sakakibara H (2009) Highly sensitive and high-throughput analysis of plant hormones using MS-probe modification and liquid chromatogramy-tandem mass spectrometry: an application for hormone profiling in Oryza sativa. Plant Cell Physiol 50:1201–1214
9. Pan X, Welti R, Wang X (2008) Simultaneous quantification of major phytohormones and related compounds in crude plant extracts by liquid chromatography-electrospray tandem mass spectrometry. Phytochemistry 69:1773–1781
10. Djilianov DL, Dobrev PI, Moyankova DP, Vankova R, Georgieva DT, Gajdosova S, Motyka V (2013) Dynamics of endogenous phytohormones during desiccation and recovery of the resurrection plant species Haberlea rhodopensis. J Plant Growth Regul 32:564–574

Chapter 3

Manipulation of Auxin and Cytokinin Balance During the *Plasmodiophora brassicae–Arabidopsis thaliana* Interaction

Jutta Ludwig-Müller, Susann Auer, Sabine Jülke, and Sabine Marschollek

Abstract

The symptoms of the clubroot disease on *Brassica* species caused by the obligate biotrophic protist *Plasmodiophora brassicae* relies, among other factors, on the modulation of plant hormones. Signaling, transport as well as biosynthesis and metabolism are key features how the levels of auxins and cytokinins are controlled. We here describe (a) how to inoculate the model plant *Arabidopsis thaliana* with *P. brassicae*, (b) qualitative and quantitative methods to evaluate disease severity in auxin and cytokinin mutants, (c) molecular methods to monitor changes in plant and pathogen transcripts, (d) prerequisites for the establishment of transgenic lines manipulated in an auxin or cytokinin pathway, and (e) methods for β-glucuronidase staining in root galls and sections of infected roots to determine auxin and cytokinin responsive promoter activities.

Key words *Arabidopsis thaliana*, Auxin, Clubroot, Cytokinins, β-Glucuronidase, Hormone responsive promoter, *Plasmodiophora brassicae*

1 Introduction

The clubroot disease is one of the most damaging diseases of the Brassicaceae family. It is caused by the obligate biotrophic protist *Plasmodiophora brassicae*. In addition to many crop plants such as oilseed rape/canola and vegetable cabbages, the model plant *Arabidopsis thaliana* is a good host for *P. brassicae* [1]. When this particular disease is considered, two major topics are essential to be assessed: first, the life cycle of the pathogen which is quite different from other pathogens (*see* Fig. 1), and second, how to determine disease symptoms in a reliable and reproducible manner.

Susann Auer, Sabine Jülke, and Sabine Marschollek in alphabetical order.

Thomas Dandekar and Muhammad Naseem (eds.), *Auxins and Cytokinins in Plant Biology: Methods and Protocols*, Methods in Molecular Biology, vol. 1569, DOI 10.1007/978-1-4939-6831-2_3,

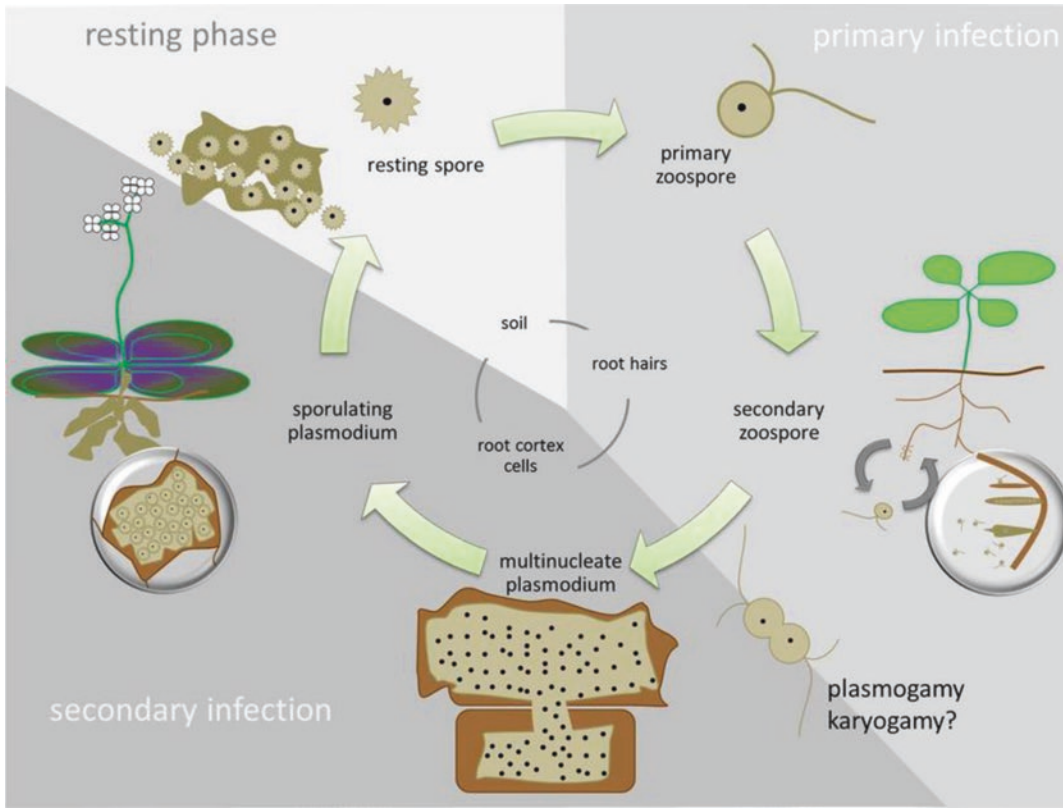

Fig. 1 The life cycle of *Plasmodiophora brassicae* in *Arabidopsis thaliana*. The cycle is similar in other *Brassica* hosts. The resting phase takes place in the soil and consists of the highly durable resting spores. These eventually hatch and the resulting primary zoospores multiply in a root hair of a host plant via a multinucleate primary plasmodium. The secondary zoospores can reinfect root hairs or enter the root cortex. There, they develop into a multinucleate plasmodium that also alters host metabolism, especially the hormonal balance. Disease symptoms are therefore assayed typically during this phase. The plasmodium develops into resting spores which, upon tissue disruption, are released into the soil. During this late stage of infection, the host plant is often highly stressed since water and nutrient supply from the root are compromised

During the life cycle [2] two distinct phases can be described: the first is occurring in the root hair and is mainly used to multiply the inoculum; the second is found in the root cortex and leads in a susceptible interaction to the typical clubroot symptoms. For the phenotypical rating of the disease only stages during the secondary infection are used, while the pathogen can be detected in root hairs as well by using PCR and staining methods. The highly durable resting spores hatch in the soil and the biflagellate zoospores find their host by swimming in capillary water during a small period of a few hours. They encyst when they have attached to a plant and inject their protoplast into the root hair of a suitable host, where it develops into a multinucleate plasmodium. The latter finally forms zoospores again (called secondary zoospores) that repeatedly infect

root hairs or enter the cortex in a yet still unknown procedure. Once in the cortex the structures develop into multinucleate (secondary) plasmodia which reorganize the host root tissue. In the beginning only a few cells are infected and swelling of the roots starts slowly. So, depending on the virulence of the isolate used and also the genotype of the host, first swellings are clearly visible after ca. 18 days after inoculation (dai). Large galls are visible 24 dai and around 28 dai the gall starts to decay. Routinely, gall severity is detected around 26–28 dai [1].

The progress of the disease during the secondary infection cycle is dependent on plant hormones such as auxins, cytokinins and brassinosteroids [3–5]. Cell divisions are controlled by cytokinin and auxin, while the hypertrophied cells are most likely the result of increased auxin levels only.

The contribution of individual hormones to the disease progression can be experimentally evaluated by using mutants and transgenic plants altered in a respective hormone pathway. Auxin biosynthesis, metabolism and signaling mutants [3, 6] as well as cytokinin deficient transgenic plants [4] have been investigated and resulted in a variation of disease symptoms. While nitrilase mutants were partially resistant to the clubroot infection [6], mutants in genes encoding proteins involved in the synthesis of auxin conjugates as well as in auxin receptors were more susceptible [3]. *A. thaliana* lines overexpressing a gene encoding cytokinin oxidase/dehydrogenase were resistant to clubroot, even though the plants were quite dwarfish [5]. Furthermore, it was shown that the auxin and cytokinin response was activated using auxin and cytokinin responsive promoter::reporter lines [5, 7, 8]. However, the thickness of a clubbed root during late infection stages affects histological methods, so that routine laboratory methods need to be adapted. Due to the fact that in large clubbed roots all developmental stages of the pathogen are detectable, it is difficult to analyze individual cell populations for hormone levels. Even though promoter::reporter lines cannot replace transcriptional or hormone analyses on whole roots, they are an alternative to investigate the hormone response by using auxin and cytokinin responsive promoter::reporter plants [4, 7–9].

For the evaluation of the disease protocols are needed to evaluate the disease severity or resistance response of a host plant by using qualitative and quantitative systems. A quantitative system is the so-called disease index [1], which takes different rating classes for infected roots into account. The definition of susceptibility under optimum infection conditions and high spore number (10^6–10^7 spores/ml) for wild type would be a disease index (DI) between 80 and 100. If a susceptible wild type shows such a DI, partial resistance (or sometimes also called tolerance) is defined when the DI is $\leq$75 (although exceptions to this rule also have been reported). A resistance phenotype is categorized to occur with a

DI ≤50. If a higher susceptibility is to be determined, then dilutions of the resting spore solution have to be made. Under such inoculation conditions, the wild type might show a DI ≤60, whereas the mutant line that is more susceptible to infection has a DI ≥70 [10]. It should be also noted in this context that hormone mutants have often an altered phenotype even without infections [1, 3, 4]. This needs to be taken into account when evaluating disease symptoms. A solution, at least when generating transgenic lines, is the use of either tissue specific [11] or inducible promoters.

A qualitative system uses qPCR to detect the DNA of *P. brassicae* in the root of an infected host plant [12]. Sequencing of the *P. brassicae* genome [13] indicated the presence of genes of the protist that could manipulate plant hormones. One example is a member of the so-called GH3 protein family that in plants can conjugate auxin, jasmonic acid and salicylic acid to various amino acids. In plants the synthesis of amino acid conjugates of indole-3-acetic acid (IAA) by members of the GH3 family results in the inactivation of the hormone [14]. However, since *P. brassicae* cannot be transformed so far so that the respective proteins are formed [15], manipulation of plant hormones can be only done by alterations within the host.

In this chapter we therefore describe (a) the inoculation protocol for *A. thaliana* with *P. brassicae*, (b) how to evaluate the severity of the disease in auxin and cytokinin-related mutant and transgenic lines by using the disease index, (c) molecular methods to monitor changes in plant and pathogen transcripts, (d) prerequisites for the generation of transgenic lines altered in an auxin or cytokinin pathway, and (e) histological β-glucuronidase activity staining for auxin and cytokinin responsive promoters (also applicable for other promoters of interest).

2 Materials

2.1 Plant Material

A. thaliana ecotypes (NASC; The European Arabidopsis Stock Centre).

Chinese cabbage *Brassica rapa* var. Graanat (Gatersleben, Germany).

2.2 Plasmodiophora brassicae

Single spore isolate e3 [16, 17].

"Field isolate" [18].

(*see* **Note 1**)

2.3 Culture Substrate

1. Standard soil type "Pikiererde CL P Classic" (Einheitserdewerke Patzer, Germany), blend of weakly decomposed white sphagnum peat (70%), clay and other additives; electrical conductivity: 200–900 µS/cm; pH 3.3–6.3; contains nitrogen (180 mg/l), phosphate (200 mg/l), sulfur (130 mg/l), magnesium (130 mg/l),

potassium (240 mg/l), and <1.5 g/l potassium chloride (*see* **Note 2**).

2. Commercially available children's playing sand, the sand should not be too fine and include few small stones.

2.4 Buffers

1. Potassium buffer for inoculation: 50 mM KH_2PO_4, pH adjusted to 5.5 with 1 M K_2HPO_4.
2. Potassium buffer for GUS staining: 100 mM NaH_2PO_4 ($\times 1H_2O$), 100 mM Na_2HPO_4 ($\times 2H_2O$), pH = 7.4.
3. Incubation buffer for GUS staining: 10 mM Na_2-EDTA; 0.5 mM $K_3[Fe(CN)_6]$; 0.5 mM $K_4[Fe(CN)_6]$; 0.5% Triton X-100; dissolve in potassium buffer for GUS staining, immediately before use add 100 mM X-Gluc (*see* **Note 3**).

3 Methods

3.1 Plant Cultivation

1. Stratify *A. thaliana* seeds in the dark in tap water for 2–4 days. Pre-germinate Chinese cabbage seeds on wet filter paper in petri dishes in the light at room temperature for 2–3 days (*see* **Note 4**).
2. Coarsely sieve the soil through a soil sieve (pore size 1 cm) and steam sterilize it for 120 min (*see* **Note 5**).
3. Mix three parts of soil with one part of sand (*see* **Note 6**) and water it adequately (*see* **Note 7**). Spread the soil mixture in cultivation pots with a size sufficient to grow an adult plant and smooth the surface.
4. Sow *A. thaliana* seeds using a pipette (20 µl) or a toothpick. Place two to three seeds per spot on the soil surface which are later thinned out to one plant per spot. Make sure that the plants are spaced adequately (for *A. thaliana* at least 3.5 cm apart) to ensure normal growth and development of the rosettes and avoid shading effects. Carefully transfer the cabbage seedlings to the pots and make sure the radicle points downwards to help the seedling establish in the soil. Cover with a thin layer of soil.
5. Place a translucent hood on the trays and pots for the first 2 weeks of the growth period to ensure adequate moisture for the seedlings. Skip this step for cabbage seedlings.
6. Place the trays and pots under long day conditions (16 h light, 8 h dark) in the greenhouse or in a climate chamber (23 °C day/18 °C night).

3.2 Inoculation Procedure with Plasmodiophora brassicae

1. Adjust the spore suspension to the desired concentration using potassium buffer for inoculation (*see* **Note 8**).
2. Cabbage plants are inoculated within 5 days after transferring to pots, *A. thaliana* seedlings are inoculated 2 weeks after sow-

ing. Inoculate plants with 1–2 ml resting spores of *P. brassicae* (10^6–10^7 spores/ml in potassium buffer for inoculation) by slowly injecting the soil around the hypocotyl of each plant with the spore suspension using a pipette. Apply the same amount of potassium buffer to a group of control plants. When working with mutants always inoculate the corresponding wild type as well (*see* **Note 9**).

3. Do not water the plants for the next 2 days so that the spore suspension is not diluted.
4. Water the plants regularly throughout the experiment. To obtain resting spores from Chinese cabbage you can fertilize the plants one or two times throughout the growing period with commercial fertilizer to enhance gall size.

3.3 Harvesting of Plant Material

1. To harvest the roots carefully dig out the whole plant at the appropriate time point. Transfer it (with adhesive soil) to a tray with water and start with the cleaning procedure.
2. Use a painters brush to remove soil and other particles from the roots (*see* **Note 10**). Take care not to rupture the fine root system, especially in severely infected plants they are quite fragile. For RNA isolation you should work with highest accuracy to ensure reliable results.
3. Depending on your experiment use the plant parts you are interested in: Isolate spores from galls (*see* Subheading 3.4), use shoot, hypcotyl, and/or roots for RNA isolation (*see* Subheading 3.5) or rate the disease severity of the plants (*see* Subheading 3.6).

3.4 Isolating Resting Spores from P. brassicae

1. Galls can be stored at −20 °C for up to 10 years.
2. To obtain the spores homogenize the galls with a small amount of water in a kitchen blender at the highest speed until a homogeneous liquid forms. Filter the homogenate through gauze (pore size 80 μm).
3. Centrifuge the homogenate at room temperature for 10 min at 2500 × *g* and discard the supernatant. Wash the spores with water and repeat the centrifugation, discard the supernatant and resuspend the spores in a small volume of potassium buffer for inoculation.
4. Determine the spore concentration under a light microscope using a Neubauer counting chamber and a hemocytometer. If necessary dilute the solution 1:10 or 1:100 in order to be able to count the spores.
5. Adjust the spore density with potassium buffer for inoculation to an appropriate dilution for your further experiments. We recommend to store a stock solution of resting spores.
6. Freeze the resting spore suspension in Eppendorf tubes at −20 °C until needed (*see* **Note 11**).

3.5 Extraction of RNA from Galls and PCR Analyses

1. To achieve high RNA quality and integrity when isolating RNA from roots/galls we recommend to grind the freshly harvested material immediately in liquid nitrogen with a mortar and pestle (*see* **Note 12**). The nitrogen will evaporate quickly and must be replaced several times. Do not let the tissue thaw during this process! Store the powder in an adequate solution at −80 °C. RNAzol (Thermo Scientific) gives very good results in our experience. Follow the standard manual for the amount of starting material, incubation time and temperatures and pay attention to standard RNA handling precautions.
2. The RNA can be processed with RNAzol or other methods of your choice. We recommend RNAzol in combination with Directzol RNA MiniPrep (Zymo Research) or the RNeasy Plant Mini Kit (Qiagen) for extraction.
3. Always perform a DNAse digest (1 U/μg RNA) before cDNA synthesis.
4. Check the quality, quantity, and integrity of your RNA for example with a spectrophotometer or a bioanalyzer (Agilent Technologies) before cDNA synthesis. Consider general rules and recommendations for purity and integrity to ensure a reliable result of your analysis.
5. cDNA synthesis can be performed with any suitable kit and primers of your choice. We usually use random hexamer and oligo d(T) primers and transcribe 1 μg RNA to get enough cDNA for detailed qPCR analysis.
6. Do PCR or qPCR using your usual laboratory method (*see* **Note 13**), but keep in mind to check for unspecific amplificates caused by pathogen RNA or DNA (*see* **Note 14**). Test your primers of interest on genomic DNA samples first.
7. Calculate expression data for example with the ΔΔCt-method by Livak and Schmidtgen [19] and compare for example infected vs. uninfected roots or the expression of your gene of interest during disease development.

3.6 Disease Rating

1. Disease rating should be done at 26–28 days after inoculation [1] (*see* **Note 15**).
2. Harvest the roots as described in Subheading 3.3. The rating is based on grouping the roots and their disease symptoms into five different classes ranging from 0 to 4 (*see* Fig. 2):

   Class 0: Plant roots do not show any disease symptoms.

   Class 1: Only minor swellings at the minor and/or secondary roots appear and the typical root structure/architecture is still present.

   Class 2: The primary root is visibly thickened; the fine roots and lateral roots are reduced and also thickened.

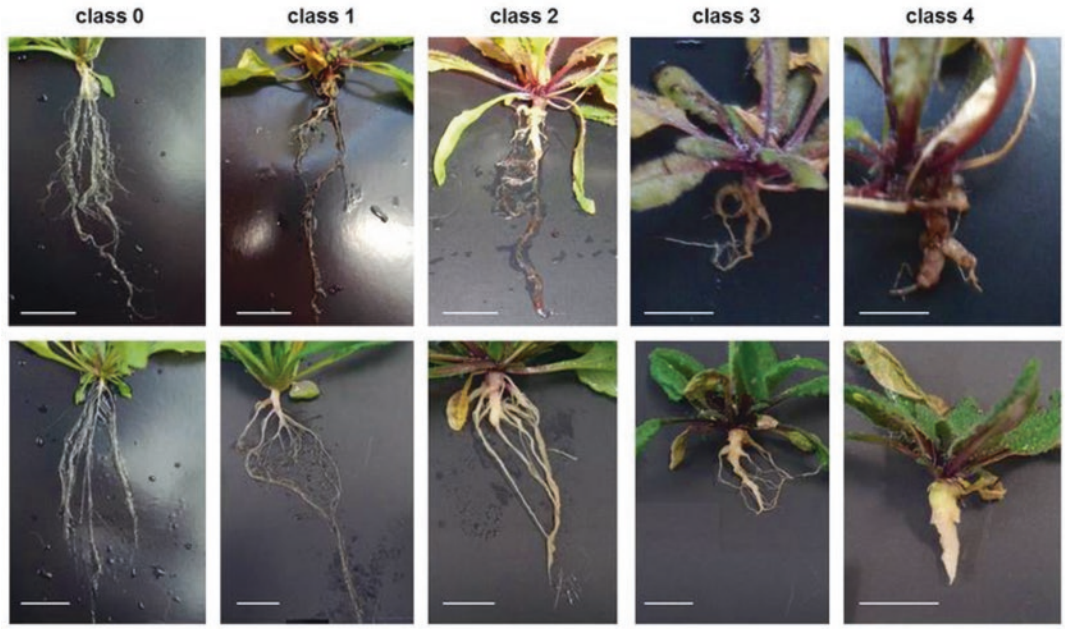

Fig. 2 Typical disease symptoms from clubrooted *A. thaliana* for the different disease classes. Disease classes range from 0 = no symptoms visible to 4 = no fine root system present but one large root gall

Class 3: The root system is strongly reduced. Galls are clearly visible at primary and secondary roots and usually fine roots are no longer available. In part the hypocotyl also shows gall development.

Class 4: The root consists of one big in part brownish gall. Mostly this comes along with wilting and stunting of the green aboveground plant parts.

(*see* **Note 16**)

3. Based on this categorization calculate the disease index (DI) (*see* **Note 17**).

$$\text{Disease Index (DI)} = \frac{(1n_1 + 2n_2 + 3n_3 + 4n_4) \cdot 100}{/\ 4\text{Nt}}$$

n_1 to n_4 = number of plants in the different disease classes
Nt = Number of all inoculated plants per treatment

4. Cut the plant parts above the hypocotyl and determine the shoot fresh weight to calculate the shoot index (SI) to further evaluate disease severity. The SI is the ratio between shoot fresh weights of infected plants to the shoot fresh weight of uninfected plants (*see* **Note 18**).

3.7 Manipulation of Auxin and Cytokinin Balance During Clubroot Disease

1. Choose an appropriate promoter (*see* **Note 19**).
2. Choose an enzyme that can influence the natural hormone metabolism. Clone the corresponding gene behind the chosen promoter to construct an expression cassette for plant transformation (*see* **Note 20**).
3. Transform a clubroot host plant (e.g., *A. thaliana* using floral dip method from Clough and Bent [20]).
4. Select transgenic plants using the appropriate selection marker and verify the mutation by PCR.
5. First, it is recommended to validate the expression of the transgene in uninfected transgenic plants in comparison to wild type plants. Second, if possible, check if the corresponding protein is detectable in the transgenic plants. If the expression of the transgene is confirmed, you can start with further analyses.
6. Analyze the hormone levels (*see* Chapters 12 and 19 by Dobrev and Pollmann in this issue) in the mutants (infected vs. not infected and vs. wild type plants; *see* **Note 21**).
7. Select plants with a strong phenotype (altered hormone level, changed gene expression, etc.) for infection tests (*see* Subheadings 3.2 and 3.6) or analyze downstream processes like gene expression, signaling processes etc. to analyze the role of the altered hormone level during clubroot development. *See* Table 1 for a summary of hormone mutants and their disease severity during clubroot.

3.8 GUS Staining and Embedding

1. The carefully harvested plants (*see* Subheading 3.3) are stained immediately in incubation buffer. For *A. thaliana* we use the whole plant and submerge it in a sufficient volume of buffer. Usually we use 6-well plates and up to 10 ml buffer (*see* **Note 22**).
2. Incubate the plants at 37 °C until you see the expected blue staining. Usually 2 h is a good starting point, for weak promoter activity or thick galls maybe overnight incubation is required (*see* **Note 23**).
3. To stop the reaction discard the incubation buffer and store the plants in potassium buffer for GUS staining. Alternatively you can follow up an ascending ethanol series to fix and dehydrate the sample: Incubate successively at room temperature for minimum 30 min in 30, 50, 70, 90% ethanol. Store the plants at last in 96–100% ethanol (*see* **Note 24**).
4. GUS staining can now be observed and documented by your method of choice (*see* Figs. 3 and 4).
5. To further investigate the cellular localization of GUS activity the samples can be embedded in resin and cut with a microtome. We use Technovit (Heraeus-Kulzer) for this.

Table 1
Disease indices for selected auxin and cytokinin related mutants and transgenic lines after inoculation with *Plasmodiophora brassicae*

Protein/function	Line	Isolate	Spore concentration (ml^{-1})	Outcome based on DI	Reference
Auxin influx carrier	*aux1-7*	e	10^6	Susceptible	[1]
Auxin conjugate hydrolase	*ilr1*	e	10^6	Susceptible	[1]
IAA-glucose conjugate synthesis overexpressor	35S::IAGLU	e	10^6	Susceptible	[1]
Auxin signaling, component of ubiquitin-activating enzyme E1	*axr1-12* *axr1-3*	e e	10^6 10^6	Susceptible Susceptible	[1] [1]
Early step in auxin response	*axr2*	e	10^6	Susceptible	[1]
Cytochrome P450 79B2/B3 Indole glucosinolate synthesis	*cyp79b2,b3*	e3	10^7	Susceptible 100 (100)	[31]
Heterochromatin protein 1; indirect effect on IAA and indole glucosinolate levels	*tu8/tfl1*	IF	10^6 10^7–10^8	Susceptible[a] at lower temperatures (18 °C) Resistant[a]	[1] [32]
Cross talk ethylene–auxin; probably auxin transport	*alh1*	ECD 16-2-12	10^6	Resistant 30 (92)	[8]
Nitrilase auxin synthesis	*nit1*	IF	10^7–10^8	Resistant[a]	[6]
Nitrilase overexpressor	35S::NIT2	IF	10^7–10^8	Susceptible[a]	[6]
Nitrilase antisense	aNIT1 aNIT2	IF IF	10^7 10^7	Tolerant[a] Tolerant[a]	[33] [33]

Auxin conjugate synthetase	*gh3.5*	e3	10^6	Susceptible 72 (70)	[3]
			10^7	susceptible 65 (68)	
	gh3.17	e3	10^5	Susceptible 55 (55)	[3]
			10^6	Susceptible 55 (70)	
			10^7	Susceptible 60 (70)	
	gh3.5,*gh3.17*	e3	10^5	Susceptible 60 (55)	[3]
			10^6	Susceptible 58 (70)	
			10^7	More susceptible[a] 60 (70)	
Auxin receptor	*tir1*	e3	10^4	More susceptible 70 (50)	[3]
			10^5	Susceptible 64 (63)	
			10^6	Susceptible 82 (80)	
	afb1	e3	10^4	More susceptible 60 (50)	[3]
			10^5	Susceptible 65 (63)	
			10^6	Susceptible 84 (80)	
	afb1,*afb2*	e3	10^4	More susceptible 72 (50)	[3]
			10^5	Susceptible 64 (63)	
			10^6	Susceptible 88 (80)	

Table 1
(continued)

Protein/function	Line	Isolate	Spore concentration (ml^{-1})	Outcome based on DI	Reference
Inhibitor of auxin-induced transcription; IAA17	*axr3-1*	Ms6	10^5	Resistant 43 (93)	[34]
			10^6	Resistant 56 (100)	
			10^7	Resistant 69 (100)	
		eH	10^7	Susceptible >94 (100)	
Auxin resistant; aberrant pattern of cell division	*axr6-1*	Ms6	10^7	Susceptible 84–100 (100)	[34]
		eH	10^7	Susceptible >94 (100)	
Hookless; ethylene related; auxin mediated signaling pathway	*hls1*	Ms6	10^7	Susceptible 84–100 (100)	[34]
		eH	10^7	Susceptible >94 (100)	
Cytokinin related					
Cytokinin oxidase overexpressor	35S::CKX1	eH	10^6	Resistant 31 (99)	[4]
		1-CK	10^6	Resistant 51 (100)	
		k1	10^6	Resistant 41 (97)	
		e2	10^6	Resistant 62 (91)	

	35S::CKX2	eH	10^6	Susceptible 90 (99)	[4]
		1-CK	10^6	Susceptible 100 (100)	
		k1	10^6	Susceptible 78 (97)	
		e2	10^6	Susceptible 83 (91)	
	35S::CKX3	eH	10^6	Resistant 62 (99)	[4]
		1-CK	10^6	Tolerant 71 (100)	
		k1	10^6	Tolerant 79 (97)	
		e2	10^6	Tolerant 69 (91)	
Cytokinin-resistant; transcription factor activity	*cyr1*	Ms6	10^7	Susceptible 84–100 (100)	[34]
		eH	10^7	Susceptible >94 (100)	
Response to cytokinin stimulus; stunted plant	*stp1*	Ms6	10^7	Susceptible 84–100 (100)	[34]
		eH	10^7	Susceptible >94 (100)	

The isolate used is given as well as the outcome based on the DI (called infection ratio in (8)) of the wild type (in brackets) and mutant or transgenic line if available. The DI is calculated from four disease classes according to the formula given in Subheading 3.6. If the DI is 100 then all plants are in class 4 (highest disease severity). (Partial) Resistant (or tolerant) plants are considered when the DI is <75. If more susceptible plants are to be evaluated, the spore concentration needs to be lower and in this case the DI of wild type is usually <60 while the DI of more susceptible plants is >70

[a]No DI available; rating based on other methods (i.e., root fresh weight)

Fig. 3 *Arabidopsis thaliana* AtEXPA1 promoter::GUS line showing roots and hypocotyls after GUS staining, *left*: control, *right* 23 days after *Plasmodiophora brassicae* infection

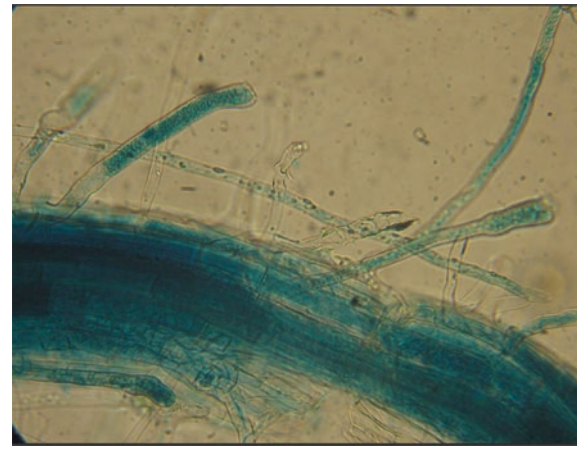

Fig. 4 *A. thaliana* AtEXPA1 promoter::GUS, 10 days after *P. brassicae* infection, root hair with primary plasmodium and GUS activity, embedded in resin and cut with a microtome

According to the manual the samples are pre-infiltrated overnight, infiltrated, and polymerized in the appropriate solutions. Be careful to embed the galls in the right orientation to get the right sectional plane. Fix the sample with the Histobloc system (Hereaus-Kulzer) and cut it with a microtome. Subsequently you can either microscope the GUS staining (*see* Fig. 4) or include another, e.g., *P. brassicae* specific staining (*see* **Note 25**).

4 Notes

1. A lot of different *P. brassicae* isolates are described in the literature and were used to infect plants. These isolates comprise single spore isolates like e_3 as well as mixed field populations with different origins. These different races can vary strongly in terms of pathogenicity and virulence [16]. Please take this into consideration when comparing data like the disease index or gene expression data from the literature (*see* Table 1).
2. In our experience the soil nutrient and mineral content is a critical feature that can influence disease outcome for instance in lowering the infection rate even with virulent isolates.
3. X-Gluc is very light sensitive. Dissolve powder in DMSO and store in small aliquots at −20 °C in the dark. Freshly prepared it is colorless, in our experience it is still active when yellowish but you should discard it when it is turning into a rose color.
4. Around 6–9 weeks after infection Chinese cabbage produces relatively large galls that harbor millions of resting spores which makes this plant ideal for the propagation of *P. brassicae*.
5. We use a soil steam sterilizer manufactured by Friedrich GmbH, Germany. Placing the soil in an autoclave bag and autoclaving it could work as well, however, we prefer steam sterilization.
6. You can either bake the sand for 24 h at 60 °C in an open bucket or you can include it in the right proportion in the soil sterilizing process.
7. Moisture is a critical factor in seedling development and for the successful infection with clubroot. The soil mixture should be thoroughly moist but not dripping wet. The soil water content is correct when you can squeeze the soil and it releases some water drops. You should closely monitor the soil moisture throughout the whole experiment.
8. With the single spore isolate e_3 a spore concentration of 10^6–10^7 spores/ml is usually sufficient to achieve a 100 % infection rate in the *A. thaliana* ecotype Columbia. The wild type from which your mutants originate should reach 100 % infection rate and a disease index of 80–100 (*see* Subheading 1) to ensure that your inoculation protocol works with sufficient efficiency. For this it can be necessary to test different spore concentrations, e.g., 10^5 or 10^6 spores/ml, on your wild type prior to your main experiments.
   For mutants with a higher susceptibility to clubroot you should start with a lower spore concentration first (down to 10^4 spores/ml) whereas for less susceptible cultivars 10^7 spores/ml is a good starting point.

9. It is mandatory for all experiments with mutants always to grow the corresponding wild type as well in the same time frame under the same conditions. Despite constant conditions in the climate chamber we have encountered that the same plants that were grown in different seasons can have a vastly different phenotype. It is therefore necessary to analyze at least 30 plants from separate pots/trays per treatment per trial and repeat each experiment at least twice.
10. For rating and spore extraction you do not have to clean the roots too much whereas for nucleic acid isolation they should be as clean as possible.
11. We typically obtain a spore concentration of 10^9 spores/ml. In our experience the spore suspensions can be stored for at least 5 years or longer and still remain infectious.
12. Grinding small amounts of tissue (up to 300 mg) in liquid nitrogen with a pestle and mortar is the most efficient method to break down the plant cell walls. Mature galls might be quite solid if frozen so homogenizing is difficult, nevertheless it should be done thoroughly. However, do not overdue it as RNA is sensitive to shearing forces.
13. You should use at least two, better three, reference genes for your expression analyses [21]. We highly recommend to use reference genes which show a stable expression during all *P. brassicae* developmental stages in *A. thaliana*. This can be validated by looking into several *A. thaliana* root microarrays (e.g., [4, 22]).
14. Since your samples are a mixture of infected and non-infected plant cells they contain a certain percentage of pathogen cells which can constitute a major part of the sample at late harvest points from 22 dai on. We therefore recommend to retest the primer efficiency of your primers of interest.
15. In most cases disease rating at 26–28 days is reasonable (*see* Subheading 1). However, sometimes the time point has to be adjusted if very strong disease severity is caused or if mutant lines themselves show strong growth disturbance due to their hormone imbalance. Take into account that you need appropriate wild type plants that are also infected and cultivated under the same conditions like the mutant lines analyzed. For *A. thaliana* the ecotype Columbia gives high DI numbers, but other ecotypes could be more or even less susceptible and therefore need prior testing.
16. Since not every infection cycle develops absolutely equal and the disease symptoms used to categorize the plants into the disease classes do not always match perfectly, it can be helpful to sort all the plants ascending or descending according to the disease symptoms. Based on this order it can be easier to define the border lines between the different disease classes.

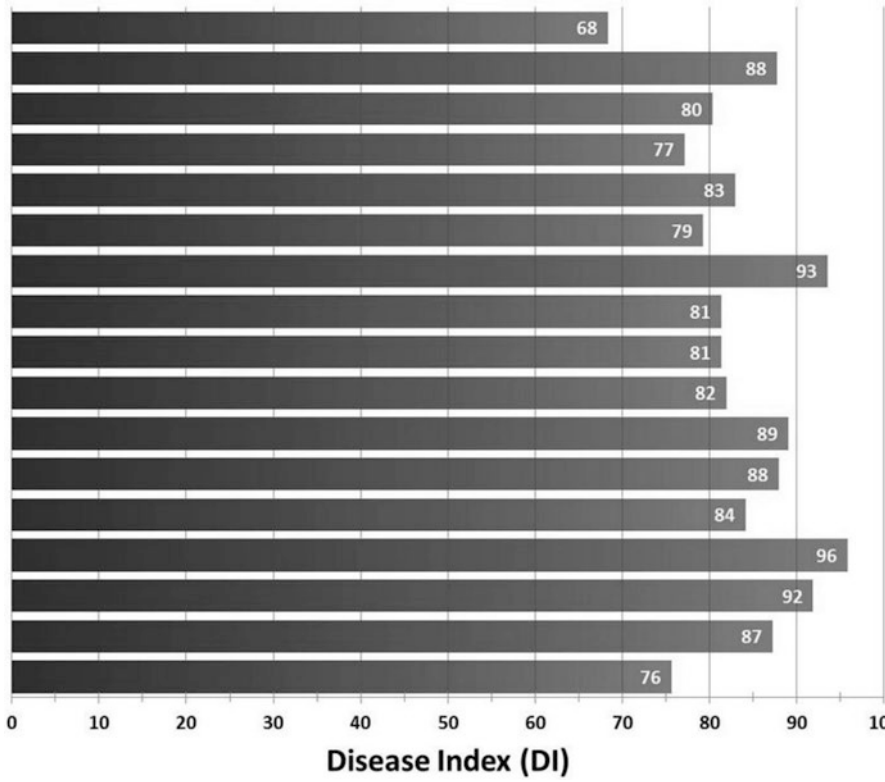

Fig. 5 Variation in the disease index numbers from different biological replicates. *A. thaliana* plants were inoculated with 2 ml spore suspension from *P. brassicae* (10^5 spores/ml; e3 isolate, *see* also Subheading 3.2) and cultivated in the greenhouse at different periods throughout one year. Disease severity was rated at 26 days after inoculation (*see* Subheading 3.7) from the same person. As you can see, the DI varies notably, even if the same inoculation procedure is used and plant cultivation is done under equal conditions

17. The calculated disease index can have a maximum score of 100. This reflects that all plants show the strongest disease symptoms (class 4, *see* Fig. 2). Thus, a high disease index shows susceptibility, whereas a low disease index indicates resistance or tolerance. Susceptible plants should have a disease index between 80 and 100. If the disease index for *A. thaliana* ecotype Columbia wild type plants is below 80 you should try to improve your infection procedure (e.g., inoculum density, composition of soil used). Please note that growth conditions like light, temperature and soil water content also influence disease development. This is why different DI values can be observed in biological replicates of the same plant line, even if the same amount of inoculum is used. Thus, variations in the DI and apparent high standard deviation appear (*see* Fig. 5). To deal with this problem it is necessary that for mutant analyses always wild type plants are also analyzed and compared to elucidate the difference.

18. The shoot index can also be used to evaluate susceptibility or tolerance. A high shoot index reflects a higher vitality of the infected plants, whereas a low shoot index is indicative of clubroot susceptible plants.
19. The usage of an inducible promoter or promoters that confer a local, spatial, or temporal expression is very reasonable, since plants with strong hormonal imbalances often show distinct and abnormal phenotypes. Many plant promoters are known that are induced upon specific stimuli like hormones, abiotic and biotic stimuli, or chemicals that can be applied separately, which allows controlled gene regulation. For the selection of such promoters in silico expression analyses can be performed using tools like Genevestigator [23] or e-FP Browser [24], respectively. Some promoters that were used successfully in the clubroot interaction are the pyk10 promoter [11, 25], cryptic T80 [11, 26] and also the 35S CMV promoter [4].
20. From the model plant *A. thaliana* it is possible to select enzymatically characterized plant enzymes that are able to influence the natural hormone balance like cytokinin oxidases or GH3. Moreover, the recently published *P. brassicae* genome sequence revealed that the protist itself exhibits some enzymes to manipulate plant hormones like auxins, jasmonates and salicylic acid [13, 27]. These enzymes are also interesting candidates to manipulate plant hormones. In contrast to mostly well-characterized enzymes from *A. thaliana*, if enzymes from *P. brassicae* are used, make sure that they really function in hormone metabolism like it was done for PbGH3, an auxin conjugate synthetase [13].
21. If you analyze conjugated IAA in addition to the free IAA levels using the method of alkaline hydrolysis, it is essential that you take into account that *A. thaliana* and other *Brassica* host plants contain indole glucosinolates that can contribute to the values for hydrolyzed IAA [28].
22. Be careful not to use too much plant material per ml buffer. All parts of the plant should swim freely in the buffer.
23. In our experience we never observed an "overstaining" during long incubation durations.
24. If you only want to look at galls and roots, you should cut off and throw away the upper plant parts now. We recommend staining of the whole plant because we observed that injuries can induce GUS expression. We strongly recommend the ethanol treatment if plants should be kept longer than 2 days. Additionally, stained plants can be stored at 4 °C.
25. A typical stain for *P. brassicae* is employing methylene blue, azure II, and basic fuchsin [29, 30].

References

1. Siemens J, Nagel M, Ludwig-Müller J, Sacristán MD (2002) The interaction of *Plasmodiophora brassicae* and *Arabidopsis thaliana*: parameters for disease quantification and screening of mutant lines. J Phytopathol 150: 592–605
2. Kageyama K, Asano T (2009) Life cycle of *Plasmodiophora brassicae*. J Plant Growth Regul 28:203–211
3. Jahn L, Mucha S, Bergmann S, Horn C, Siemens J, Staswick P, Steffens B, Ludwig-Müller J (2013) The clubroot pathogen (*Plasmodiophora brassicae*) influences auxin signaling to regulate auxin homeostasis. Plants 2:726–749
4. Siemens J, Keller I, Sarx J, Kunz S, Schuller A, Nagel W, Schmülling T, Parniske M, Ludwig-Müller J (2006) Transcriptome analysis of *Arabidopsis* clubroots indicate a key role for cytokinins in disease development. Mol Plant Microbe Interact 19:480–494
5. Schuller A, Kehr J, Ludwig-Müller J (2014) Laser microdissection coupled to transcriptional profiling of Arabidopsis roots inoculated by *Plasmodiophora brassicae* indicates a role for brassinosteroids in clubroot formation. Plant Cell Physiol 55:392–411
6. Grsic-Rausch S, Kobelt P, Siemens J, Bischoff M, Ludwig-Müller J (2000) Expression and localization of nitrilase during symptom development of the clubroot disease in *Arabidopsis thaliana*. Plant Physiol 122:369–378
7. Päsold S, Siegel I, Seidel C, Ludwig-Müller J (2010) Flavonoid accumulation in *Arabidopsis thaliana* root galls caused by the obligate biotrophic pathogen *Plasmodiophora brassicae*. Mol Plant Pathol 11:545–562
8. Devos S, Laukens K, Deckers P, Van Der Straeten D, Beeckman T, Inzé D, Van Onckelen H, Witters E, Prinsen E (2006) A hormone and proteome approach to picturing the initial metabolic events during *Plasmodiophora brassicae* infection on *Arabidopsis*. Mol Plant Microbe Interact 19:1431–1443
9. Malinowski R, Smith JA, Fleming AJ, Scholes JD, Rolfe SA (2012) Gall formation in clubroot-infected Arabidopsis results from an increase in existing meristematic activities of the host but is not essential for the completion of the pathogen life cycle. Plant J 71:226–238
10. Knaust A, Ludwig-Müller J (2013) The ethylene signaling pathway is needed to restrict root gall growth in Arabidopsis after infection with the obligate biotrophic protist *Plasmodiophora brassicae*. J Plant Growth Regul 32:9–21
11. Siemens J, Gonzales M-C, Wolf S, Hofmann C, Greiner S, Du Y, Rausch T, Roitsch T, Ludwig-Müller J (2011) Extracellular invertase is involved in the regulation of the clubroot disease in *Arabidopsis thaliana*. Mol Plant Pathol 12:247–262
12. Faggian R, Strelkov SE (2009) Detection and measurement of *Plasmodiophora brassicae*. J Plant Growth Regul 28:282–288
13. Schwelm A, Fogelqvist J, Knaust A, Jülke S, Lilja T, Bonilla-Rosso G, Karlsson M, Shevchenko A, Choi SR, Dhandapani V, Kim HG, Park JY, Lim YP, Ludwig-Müller J, Dixelius C (2015) The *Plasmodiophora brassicae* genome reveals insights in its life cycle and ancestry of chitin synthases. Sci Rep 5:11153. doi:10.1038/srep11153
14. Staswick PE, Serban B, Rowe M, Tiryaki I, Maldonado MT, Maldonado MC, Suza W (2005) Characterization of an Arabidopsis enzyme family that conjugates amino acids to indole-3-acetic acid. Plant Cell 17:616–627
15. Feng J, Hwang SF, Strelkov SE (2013) Genetic transformation of the obligate parasite *Plasmodiophora brassicae*. Phytopathology 103: 1052–1057
16. Fähling M, Graf H, Siemens J (2003) Pathotype-separation of *Plasmodiophora brassicae* by the host plant. J Phytopathol 151:425–430
17. Graf H, Fähling M, Siemens J (2004) Chromosome polymorphism of the obligate biotrophic parasite *Plasmodiophora brassicae*. J Phytopathol 152:86–91
18. Puzio PS, Newe M, Grymaszewska G, Ludwig-Müller J, Grundler FMW (2000) *Plasmodiophora brassicae*-induced expression of pyk20, an *Arabidopsis thaliana* gene with glutamine-rich domain. Physiol Mol Plant Pathol 56:79–84
19. Livak KJ, Schmittgen TD (2001) Analysis of relative gene expression data using real-time quantitative PCR and the $2^{(-\Delta\Delta Ct)}$ method. Methods 2001(25):402–408
20. Clough SJ, Bent AF (1998) Floral dip: a simplified method for Agrobacterium-mediated transformation of *Arabidopsis thaliana*. Plant J 16:735–743
21. Bustin SA, Benes V, Garson JA, Hellemans J, Huggett J, Kubista M, Mueller R, Nolan T, Pfaffl MW, Shipley GL et al (2009) The MIQE guidelines: minimum information for publication of quantitative real-time PCR experiments. Clin Chem 55:611–622

22. Agarwal A, Kaul V, Faggian R, Rookes JE, Ludwig-Müller J, Cahill DM (2011) Analysis of global host gene expression during the primary phase of the *Arabidopsis thaliana*-*Plasmodiophora brassicae* interaction. Funct Plant Biol 38:1–16
23. Hruz T, Laule O, Szabo G, Wessendorp F, Bleuler S, Oertle L, Widmayer P, Gruissem W, Zimmermann P (2008) Genevestigator V3: a reference expression database for the meta-analysis of transcriptomes. Adv Bioinformatics 2008, article ID 420747. doi:10.1155/2008/420747
24. Winter D, Vinegar B, Nahal H, Ammar R, Wilson G, Provart N (2007) An "Electronic Fluorescent Pictograph" browser for exploring and analyzing large-scale biological data sets. PLoS One. doi:10.1371/journal.pone.0000718
25. Nitz I, Berkefeld H, Puzio P, Grundler FMW (2001) Pyk10, a seedling and root specific gene and promoter from *Arabidopsis thaliana*. Plant Sci 161:337–346
26. Mollier P, Hoffmann B, Orsel M, Pelletier G (2000) Tagging of a cryptic promoter that confers root-specific gus expression in *Arabidopsis thaliana*. Plant Cell Rep 19: 1076–1083
27. Ludwig-Müller J, Jülke S, Geiß K, Richter F, Mithöfer A, Šola I, Rusak G, Keenan S, Bulman S (2015) A novel methyltransferase from the intracellular pathogen *Plasmodiophora brassicae* methylates salicylic acid. Mol Plant Pathol 16:349–364
28. Yu P, Lor P, Ludwig-Müller J, Hegeman AD, Cohen JD (2015) Quantitative evaluation of IAA conjugate pools in *Arabidopsis thaliana*. Planta 241:539–548
29. Buczacki ST, Moxham SE (1979) A triple stain for differentiating resin-embedded sections of *Plasmodiophora brassicae* in host tissues under the light microscope. Trans Br Mycol Soc 72:311–347
30. Humphrey CD, Pittman A (1974) Simple methylene blue—azure II—basic fuchsin stain for epoxy-embedded tissue sections. Stain Technol 40(1):9–14
31. Siemens J, Glawischnig E, Ludwig-Müller J (2008) Indole glucosinolates and camalexin do not influence the development of the club-root disease in *Arabidopsis thaliana*. J Phytopathol 156:332–337
32. Ludwig-Müller J, Pieper K, Ruppel M, Cohen JD, Epstein E, Kiddle G, Bennett R (1999) Indole glucosinolate and auxin biosynthesis in *Arabidopsis thaliana* L. glucosinolate mutants and the development of the clubroot disease. Planta 208:409–419
33. Neuhaus K, Grsic-Rausch S, Sauerteig S, Ludwig-Müller J (2000) *Arabidopsis* plants transformed with nitrilase 1 or 2 in antisense direction are delayed in clubroot development. J Plant Physiol 156:756–761
34. Alix K, Lariagon C, Delourme R, Manzanares-Dauleux M (2007) Exploiting natural genetic diversity and mutant resources of *Arabidopsis thaliana* to study the *A. thaliana–Plasmodiophora brassicae* interaction. Plant Breed 126:218–221

Chapter 4

Microbial Manipulation of Auxins and Cytokinins in Plants

Anwar Hussain, Ihsan Ullah, and Shahida Hasnain

Abstract

Microbial associations with plants are crucial for the survival of both the partners. Beside other ways of establishing such associations, phytohormones enjoy a key role in plant–microbe interactions from initial dialog between the two to the establishment of a viable partnership. Cytokinins (CKs) and IAA are among the five classical groups of phytohormones implicated in plant immune response, early signaling, and deciding the fate of interactions between plant and microbes. Here we describe a method to study modulation of Cks and IAA in plant under the influence of a pathogenic bacterium, *Pseudomonas syringae* tomato DC3000. A method for inoculating bacteria on host plant and subsequent determination of Cks and IAA through HPLC-ESI-MS/MS is described.

Key words Cytokinin, Auxins, Plant immunity, *Pseudomonas syringae*, *Arabidopsis*, Plant–microbe interactions

1 Introduction

No organism can survive on its own, thereby undergoing complex interactions with other living organisms not only from closely related groups but also with organisms from distantly related groups. The same principle applies to plants which undergo interactions with a diversity of organisms from other groups, the most important among them are the microbes, both beneficial and harmful [1–3]. To manage their enemies, plants have developed a highly sophisticated defense system that resembles the innate immune system of animals in terms of recognizing nonself molecules or signals from their own cells invaded by the pathogens. Plants respond to such anomalies by activating an effective immune response against the invader encountered [4, 5]. To survive in plants, pathogens establish a prolonged interaction with the host plant by actively interfering with the plant immune system. Beneficial microbes are also initially recognized as potential invaders, so they also have to establish active interference with the plant immune system for entering an intimate mutualistic relationship with the plant [6].

Thomas Dandekar and Muhammad Naseem (eds.), *Auxins and Cytokinins in Plant Biology: Methods and Protocols*, Methods in Molecular Biology, vol. 1569, DOI 10.1007/978-1-4939-6831-2_4,

While interacting with plants, microbes are able to modulate plant metabolism by releasing signaling molecules including phytohormones [7, 8]. Plant metabolism is greatly affected by the in planta absolute and relative concentration of phytohormones and a slight shift of their ratio makes plants vulnerable to biotic and abiotic stresses [9]. Similarly, overall plant health and homeostasis is maintained by the in planta levels of different phytohormones which regulate several fundamental processes of plant growth and development [10, 11]. Among different phytohormones, cytokinins (CKs) and auxins constitute the most important signal regarding plant–microbe interactions [12, 13]. Upon encountering a host plant, microbial partner may modulate host's endogenous phytohormones positively or negatively. Modulation of in planta phytohormone concentration is mostly due to microbial in planta secretion or release into the rhizosphere which is then absorbed by plant root [14, 15]. Many microbes including plant pathogens (Pst) can produce auxins themselves or manipulate the host's auxin signaling [16, 17]. Pathogens exploit auxin-mediated suppression of SA by producing in planta auxin to interfere with plant defense [18].

Contrary to auxins, CKs synergistically act with SA signaling for promoting plant resistance by activating ARR2 transcription factors, which regulate CKs responsive genes. Product of such genes can bind to SA activated transcription TGA3 to promote the expression of PR-1 [19].

Pst can enhance in planta concentration of auxin by upregulating those genes that convert amino acid conjugates of IAA to free IAA and genes for IAA-amido synthases [14]. Pathogens also derepress genes involved in IAA biosynthesis [20]. On contrary, CKs biosynthesis genes are downregulated and promote CKs degradation by promoting the expression of those genes that are responsible for CKs degradation. Hence this pathogens uses host arms against the host by hijacking the immune signaling network of the host [21].

To prolong their mutualistic association with plant, beneficial soil bacteria also have decoy strategies to short-circuit hormone-regulated immune responses that they have to face in the roots once recognized by the host plant. For instance, the beneficial PGPF *Piriformospora indica* recruits the JA pathway to suppress both early and late defenses, including SA-mediated defenses [22]. In addition, many free-living PGPR and PGPF produce substantial amounts of plant hormones, such as auxins and GAs [23, 24], that potentially attenuate SA signaling via hormonal cross talk mechanisms. Production of CKs by microbes has been shown to reduce growth of the primary root and promote the formation of secondary roots along with increase in the number of root hairs [25].

Keeping the importance of CKs and IAA signaling in plant–microbe interactions, it is imperative to evaluate the modulation of these hormones for better understanding of the phenome-

non. For this purpose, concentration of Cks and IAA is determined in plants hosting microbes such as bacteria. In this chapter we report a method of establishing association between plants and bacteria and subsequent determination of Cks and IAA by UPLC-ESI-MS/MS.

2 Materials

2.1 Biologicals

1. *Arabidopsis thaliana* col0.
2. *Arabidopsis ARR5::GUS.*
3. *Arabidopsis* DR5::GUS.
4. *Pseudomonas syringae* tomato DC3000 (Pst).

2.2 Chemicals

1. Make stock of CKs standards and stable isotope-labeled CKs (*see* **Note 1**) in small amount of 1 N NaOH and dilute with deionized water (*see* **Note 2**). Dissolve the required amount of IAA and its stable isotope labeled species D_2IAA in small amount of ethanol and dilute with deionized water. Store at −20 °C.
2. Make 10 mM solution of $MgCl_2$, 0.1% $HgCl_2$, Silwet L-77, acetic acid.
3. Prepare Luria–Bertani (LB) media by adding yeast extract (5 g), tryptone (10 g), and NaCl (10 g) sequentially to distilled water with constant shaking and adjust final volume to 1000 mL. Adjust pH to 7–7.2.
4. Murashige and Skoog basal salt (Sigma-Aldrich) solidified with 1% agar and containing 3% sucrose.
5. To make M9 salts aliquot 800 mL H_2O and add 64 g $Na_2HPO_4{\cdot}7H_2O$, 15 g KH_2PO_4, 2.5 g NaCl, 5.0 g NH_4Cl, 0.2% casaminoacids, 2 pg/L biotin, stir until dissolved, adjust to 1000 mL with distilled H_2O, and sterilize by autoclaving. Add 200 mL of this mixture to approx. 700 mL of autoclaved distilled H_2O and then sequentially add the following: 2 mL of 1 M $MgSO_4$ (autoclaved), 20 mL of 20% glucose, 100 µL of 1 M, $CaCl_2$ (autoclaved) and adjust to 1000 mL with sterilized distilled H_2O.
6. Bieleski buffer contains 60% methanol, 25% $CHCl_3$, 10% HCOOH, and 5% H_2O.
7. Make water-saturated n-butanol by mixing n-butanol and distilled water in equal proportion, shake well and allow the mixture to stand for 30 min, then take the upper water-saturated n-butanol phase.
8. Prepare GUS buffer by mixing 1 mM 5-bromo-4-chloro-3--indolyl-β-D-glucuronide at pH 7.0 (X-Gluc; Molecular Probes, Eugene, OR, USA) with 50 µL dimethylformamide

(DMF). Dilute the mixture by adding 50 mM sodium phosphate buffer pH 7.2 at the rate of 5 mg/mL and supplemented with 0.2 % Triton X-100.

9. 15 mM ammonium formate (pH 4.0).

2.3 Columns and Filters

1. Cellulose acetate filter (Millipore; 22 μm pore size; 47 mm Diameter; Australia Pty Limited, Australia).
2. SPE column (CHROMABOND® HR-XC, 3 mL, and 200 mg).
3. 3-mm tungsten carbide beads (Retsch GmbH & Co. KG, Haan, Germany).

2.4 Instruments

1. MM 301 vibration mill (Retsch GmbH & Co. KG, Haan, Germany).
2. Ultrasonicator.
3. Lyophilizer.
4. Centrifuge.
5. HPLC-ESI-MS/MS (Waters, USA).

3 Methods

3.1 Isolation of Bacteria

Bacteria are grown in the lab on solid media or liquid culture depending on the purpose and future use. To isolate bacteria, media solidified with agar is used. For determining growth of bacteria, obtaining secondary metabolites such as CKs and IAA and their quantification, bacteria are grown in liquid media called broth culture. Common media of choice is Luria–Bertani (LB) called as LB agar or LB broth. This media is prepared by taking 1 % tryptone, 1 % NaCl, and 0.5 % yeast extract in distilled water. The media and the glassware are sterilized by autoclaving at 121 °C for 15 min under 15 lb pressure.

Here we discuss *Pseudomonas syringae* pv tomato DC3000 (Pst) which is a pathogenic bacterium known to cause disease in tomato and related plants. This pathogen can be readily obtained from culture collection or isolated from infected parts of the plants. For isolation, characterization, and identification purpose follow any standard microbiology lab manual.

1. Once you have a pure culture of the pathogen, prepare inoculum by growing bacteria in LB broth culture overnight and harvest the culture next day by spinning at 12,000 rpm (13201 x *g*) for 2 min.
2. Take pellet in equal volume of 10 mM $MgCl_2$, make different dilutions and record OD for all dilutions one by one. Prepare dilutions by taking 4.5 mL sterile distilled water in six screw capped tubes with capacity of holding 10 mL solutions. Label tube 1 with 10^{-1}, tube 2 with 10^{-2}, and so on till the last one

Table 1
Calculation of cfu/mL by plate count experiment

Dilution factor (DF)	No. of colonies on a spread plate (csp)	Cfu/mL = csp × 10/DF
10^{-1}	50	$=50\times10/10^{-1}=5\times10^{3}$
10^{-2}	50	$=50\times10/10^{-2}=5\times10^{4}$
10^{-3}	50	$=50\times10/10^{-3}=5\times10^{5}$
10^{-4}	50	$=50\times10/10^{-4}=5\times10^{6}$
10^{-5}	50	$=50\times10/10^{-5}=5\times10^{7}$
10^{-6}	50	$=50\times10/10^{-6}=5\times10^{8}$

is labeled as 10^{-7}. To tube 1, add 0.5 mL of the bacterial suspension, then transfer 0.5 mL from this mixture to tube 2 and continue in the same way until the final tube labeled as 10^{-7}.

3. Now, spread 100 µL of each dilution on separate LB agar plate in triplicate and count the number colonies appearing on the surface of media next morning. From this data calculate colony forming units per mL (cfu/mL) by multiplying number of colonies by 10. For example if you get 50 colonies in 100 µL then in 1 mL total colonies will be 500. Now divide this number with dilution factor as shown in Table 1. Also note OD of each dilution at 600 nm as reference for future.
4. If you have decided to isolate, select the infected plant parts showing specific symptoms of the disease and remove it from the plant. Surface-sterilize the infected part to remove any contaminant. Crush the infected part in pestle and mortar pre-rinsed with 70% ethanol and then with sterile distilled water. Add phosphate buffer saline to the crushed sample, centrifuge and then serially dilute the supernatant by taking 0.5 mL in 4.5 mL water to make 10^{-1} dilution which is further diluted by taking 0.5 mL of it in 4.5 mL sterile water and the process is repeated till 10^{-6} dilution. Spread 100 µL of each dilution on a separate LB agar plate or selective media for *Pst* tomato (*see* **Note 2**) and incubate at 28 °C overnight. Characterize the obtained colonies under microscope after Gram's staining to check the purity of the colonies.

3.2 Plant Inoculation

Plants can be inoculated by different ways such as soil inoculation, seed priming, root inoculation, and inoculation of aerial parts. Inoculation of aerial parts is done by aerial spray or syringe infiltration. As Pst is an aerial pathogen, it is inoculated by syringe infiltration or aerial spray.

1. Select 6-week-old healthy and uniform seedlings of *A. thialiana* col0 for inoculation purpose.

2. For aerial spray or syringe infiltration make bacterial suspension (10^7 cfu/mL) in 10 mM $MgCl_2$ containing 0.01% of the wetting agent Silwet L-77 (*see* **Note 3**). Spray the suspension on leaves to wet the leaf surface until shortly before droplet run-off occurs. Allow the plants to grow at 22 ± 1° C, 80% relative humidity and long day photoperiod (16 hours light and 8 hours dark cycles).
3. Take bacterial suspension (10^6 cfu/mL) in a 1 mL syringe and infiltrate approximately 200 µL of this suspension on the underside of leaves of *Arabidopsis*.
4. Harvest leaves 24, 48, 72, and 96 h post inoculation and process for phytohormones determination.

3.3 Screening Bacteria for In Planta Modulation of Phytohormones

1. To screen the isolated bacteria for in planta modulation of CKs and IAA, infiltrate leaves of 6-week-old *Arabidopsis* ARR5::GUS and DR5::GUS, respectively (*see* **Note 4**), with bacterial suspension in 10 mM $MgCl_2$. Use 10 mM $MgCl_2$ as mock inoculations.
2. Harvest leaves at 24, 48, 72, 96, and 120 h post inoculation and stain for GUS activity.
3. For GUS staining, shift detached leaves to GUS buffer containing 1 mM 5-bromo-4-chloro-3-indolyl-β-D-glucuronide at pH 7.0 (X-Gluc; Molecular Probes, Eugene, OR, USA) dissolved in 50 µL DMF and diluted in 50 mM sodium phosphate buffer pH 7.2 at the rate of 5 mg/mL and supplemented with 0.2% Triton X-100.
4. Vacuum infiltrate leaves with staining buffer for 10–15 min and then incubate at 37 °C for 3 h.
5. Clear excess stain by vacuum infiltrating stained leaves with clearing solution (70% ethanol) for 2 min and then keep the leaves in the same solution for 24 h [26].
6. Intensity of the localized GUS stain shows the levels of CKs or IAA in the leaves.

3.4 Determination of Auxins and CKs

3.4.1 Extraction of Auxin/CKs from Pst DC3000

1. Grow bacterial strains in M9 medium supplemented with 20% glucose, 0.2% casaminoacids, and 2 pg/L biotin for 72 h at 28 °C (*see* **Note 5**). Centrifuge 100 mL culture at 14,000 rpm (20,800 x *g*) for 10 min at 4 °C, filter through cellulose acetate filter (Millipore; 22 µm pore size; 47 mm Diameter; Australia Pty Limited, Australia) to obtain cells free culture filtrate.
2. Lyophilize the cell free culture filtrate to dryness, redissolve in 10 mL distilled water acidified by adding drops of 7 N HCl and extract three times with 1/2 volume of ethyl acetate having 10 pmol of D_2IAA (internal standard for IAA).
3. Neutralize the aqueous phase to pH 7.0–7.5 with 7 N NaOH and extract three times with 1/2 volume of water-saturated

n-butanol containing appropriate internal standards of CKs [27]. Prepare water-saturated n-butanol by mixing n-butanol and distilled water in equal proportion, shake well and allow the mixture to stand for 30 min, then take the upper water-saturated n-butanol phase. Dry the organic fractions obtained in the extraction steps separately in rotary evaporator, reconstitute in 5 mL deionized water (Millipore), and adjust to pH 3.0 with acetic acid (Sigma).

4. Pass the reconstituted mixtures separately through SPE column (CHROMABOND® HR-XC, 3 mL, and 200 mg) following manufacturer's instructions.
5. Dry the eluent and resuspend it in 15 mM ammonium formate (pH 4.0) for analysis by UPLC-ESI-MS/MS. Analyze CKs and IAA in positive and negative modes respectively.

3.4.2 Extraction of Phytohormones from Plant

1. Take 20–200 mg, FW of *Arabidopsis* leaves (*see* **Note 6**), crush in liquid nitrogen and extract individually in 750–1000 µL of Bieleski buffer by mixing leaves powder with the buffer.
2. Add 3-mm tungsten carbide beads (Retsch GmbH & Co. KG, Haan, Germany) to each tube and vibrate the samples in an MM 301 vibration mill (Retsch GmbH & Co. KG, Haan, Germany) at a frequency of 30 Hz for 3 min.
3. Now, ultrasonicate (*see* **Note 7**) the tube contents for 3 min followed by stirring for 30 min at 4 °C. Centrifuge the mixture for 3 min at 15,000 rpm (20627 x *g*) and 4 °C) and transfer the supernatant into a fresh tube stored at 4 °C.
4. Re-extract the pellets in the same way as mentioned replacing Bieleski buffer by 300 µL of 50% methanol with 2% formic acid. Add stable isotope-labeled CK internal standards to Bieleski buffer or plant samples at the rate of 1 pmol of each compound per sample, to check the recovery during purification and to validate the quantification.
5. For Cks, use the following internal standards (IS): [$^{13}C_5$]tZ, [$^{2}H_5$]tZR, [$^{2}H_5$]tZ9G, [$^{2}H_5$]tZOG, [$^{2}H_5$]tZROG, [$^{13}C_5$]cZ, [$^{2}H_3$]DHZ, [$^{2}H_3$]DHZR, [$^{2}H_3$]DHZ9G, [$^{2}H_6$]iP, [$^{2}H_6$]iPR.
6. For IAA use D_2-IAA as internal standard (*see* **Note 8**).
7. Pool liquid phases obtained during extraction for each sample in a separate tube and pass them individually through 100 mg SCX columns as described earlier.
8. Take the eluate in 15 mM ammonium formate (pH 4.0) for analysis by UPLC-ESI-MS/MS as described earlier.

3.4.3 Calibration Curves

1. To make calibration curves for different CKs and IAA plot ratios of the analyte signal (peak are of Cks or IAA) to the internal standard signal (stable radioisotope-labeled internal standard) against standard analyte concentrations.

2. Use these ratios: for Cks analyte/IS; 0.005, 0.05, 0.5, 5.0, 50.0 pmol/1 pmol and for IAA analyte/IS; 0.005, 0.05, 0.5, 5.0, 50.0/10 pmol.
3. To Plot ratios of analyte/IS against concentration of the analyte, feed the data obtain after analyzing the standards on UPLC-ESI-MS/MS to Excel spread sheet, select data and make scattered *x*,*y* chart.
4. Insert a trend line by selecting linear option along with display equation on the chart.
5. Use the equation to determine the concentration of Cks and IAA in the unknown sample using the ratios.

3.4.4 Limit of Detection (LOD)

1. It is the lowest amount of the analyte in a sample which can be detected but not necessarily quantitated as an exact value. Different approaches may be used to find out LOD including visual evaluation, signal to noise ratio and Standard Deviation of the Response and the Slope.
2. Prepare samples with different known concentrations of the analyte and compare their signals with those of the blank samples. Establish the minimum concentration at which the analyte can be reliably detected. A signal-to-noise ratio between 3 and 2:1 is generally considered acceptable for estimating the detection limit. This means that the height of the peak produced by analyte should be three times greater than that of the blank.

3.4.5 Limit of Quantification

1. The lowest quantifiable amount of the analyte with suitable precision and accuracy is called limit of qetection (LOQ). Concentration of analyte producing a peak ten times higher than that of blank samp i.e. a signal to noise raio equal to 10:1 is normally accepted as limit of quantification.
2. Perform the experiment as described in Subheading 3.4.4, **step 2**.

3.5 Determination of Cks and IAA

1. Inject 5 μL of each sample taken in mobile phase onto UPLC BEH C18 column (2.1 × 50 mm, 1.7 μm; Waters).
2. Eluted the column with a linear gradient of 90:10 A (15 mM ammonium formate): B (methanol) to 50:50 A:B (v/v) at a flow rate of 0.25 mL/min and column temperature of 40 °C.
3. Pass the eluted fractions directly through tandem mass spectrometer equipped with electrospray interface without post-column splitting and quantify by multiple reaction monitoring (MRM).
4. For MRM, conditions should be optimized as follows: capillary voltage, 0.6 kV; source/desolvation gas temperature, 100/350 °C; cone/desolvation gas flow rates, 2.0/550 l/h; LM/HM resolution, 12.5; ion energy 1, 0.3 V; ion energy 2,

Table 2
Optimized product ion scanning, diagnostic transition, cone voltage (CV), collision energy (CE), and dwell time (DT) of the triple quadrupole mass spectrometer (electrospray interface in positive mode) for each of the analyzed CKs and IAA

CKs	Scan mode	Retention time	Transition	CV (V)	CE (eV)	DT (s)
cZ	+	3.57	220.1 > 136.1	22	17	0.07
tZ	+	3.11	220.1 > 136.1	22	17	0.07
[$^2H_5$] tZ	+	3.12	225.1 > 137	24	17	0.07
[$^2H_5$] tZ	+	3.12	225.1 > 136	24	17	0.07
ZR	+	3.9	353.2 > 220.1	30	19	0.18
DHZ	+	3.44	222.1 > 136	24	21	0.07
[$^2H_3$] DHZR	+	4.3	357.1 > 225	24	22	0.07
DHZR	+	4.33	354.1 > 222.1	26	21	0.07
ZOG	+	2.46	382.1 > 220	22	17	0.07
IAA	–	2.18	176.1 > 130	–13	–	–
[$^2H_5$] IAA	–	2.19	178.1 > 132	–14	–	–

1.5 V; entrance, exit and multiplier voltages, 2.0 V, 2.0 V and 650 eV, respectively.

5. Use argon as collision gas at 5×10^{-3} mbar pressure.
6. Optimize dwell times (*see* **Note 9**), cone voltages, and collision energies for particular diagnostic transitions of different compounds (Table 2).

4 Notes

1. Phytohormones do not dissolve in water, so it is best to use ethanol, NaOH, or HCl as solvent and then dilute with water. Normally, 2–5 % of the solvents are used. First completely dissolve the desired phytohormone in a small volume of solvent which makes 2–5 % of the final volume and then add deionized water to bring to final volume.
2. Sometimes selective or differential media are used for isolating a particular bacterium. while for others enrichment media may be required. Selective media are used to culture selective bacteria and avoid contaminations. For example, Pst is kept on media containing antibiotic such as rapamficin so that contaimination by repamficin sensitive is discouraged. Similarly, PHM011 media containing CCTP supplement (HIMEDIA®) can be used to selectively isolate Pst and differentiate it from other

gram-negative bacteria by its small, flat pink colored colonies. However, to confirm the identity of the bacteria molecular techniques such as 16S rDNA homology and hybridization experiments should be done.

3. Wetting agent is used to inoculate bacteria in the form of aerial spray for making it convenient to stay on the leaves and do not wash away. If selective leaves are target on inoculation on the plant, then cover the rest of the leaves with plastic cover such as common plastic bags so that bacterial suspension doesn't fall on the leaves supposed to be uninoculated. Care should be taken not to injure leaf during syringe infiltration. This can be safely done by putting index finger on the upper side of the leaf on the spot to be infiltrated and supporting syringe against the finger followed by slowly pushing the plunger of the syringe. Once the spot on the leaf infiltrated gives wet appearance stop infiltration.
4. The transgenic reporter lines of *Arabidopsis*, i.e., DR5::GUS and ARR5::GUS used to detect any increase in the endogenous concentration of auxins and Cks respectively. These transgenic line harbor auxin or CKs response promoters (DR5 or ARR5) fused to the beta-glucuronidase (GUS) reporter gene. Any change in the concentration of IAA or CKs upregulate or downregulate the expression of GUS under the control of these promoters which can then be detected by GUS staining.
5. Phytohormones are secondary metabolites and are produced maximally during the late stationary phase of bacterial growth normally at 72 h of incubation or later. Production of CKs and IAA by bacteria may be enhanced by providing their respective precursors, i.e., adenine and tryptophan in the growth media. Minimal media is good media of choice for obtaining secondary metabolites from bacteria.
6. Leaves harvested for the determination of phytohormones should be immediately frozen in liquid nitrogen to avoid any post-harvest change in the concentration of plant hormones. Harvest leaves treated in this way may be used directly for phytohormones analysis or stored at −80 °C for future use. The frozen samples must not thaw at any stage. Therefore, frozen samples should be taken in liquid nitrogen-chilled pestle and mortar. Add some liquid nitrogen to mortar containing pestle and allow the nitrogen to evaporate. Frozen moisture on the outer side of the mortar is an indication that it is now ready to receive the frozen samples. Overlay the frozen samples with liquid nitrogen and start crushing by slowly crushing the frozen leaves with pestle against the mortor. Once liquid nitrogen evaporates, forcefully rub the pestle against the mortar to make fine powder of the plant material avoiding sample spill. During this process liquid nitrogen may be added more than once.

Transfer the fine powder with liquid nitrogen-chilled spatula to the Eppendorf containing ice-chilled buffer.

7. Ultrasonication is done for cell lysis and subsequent release of phytohormones to the buffer and homogenization of the tube contents. Ultrasonic bath or VialTweeter at UIS250v (Hielscher Germany) may be used for this purpose.
8. Internal standard is used to improve the quality of data. Internal standard is a closely related compound such as a heavy isotope-labeled compound which produces a peak at a different retention time under similar conditions. In case of internal standard calibrations are based on the ratio of response between the analyte and the IS instead of absolute response.
9. The dwell time of each MRM channel should provide 15–20 scan points per peak for good quantitation. Fewer scan points don't describe the peak adequately resulting in loss of information, for example the top of the peak may be missed. Additionally, reproducibility is also negatively affected. During dwell time adjust the inter-channel delay to 0.1 s and the cycle times to 0.55–0.65 s.

References

1. Bever JD, Dickie IA, Facelli E, Facelli JM, Klironomos J, Moora M, Rillig MC, Stock WD, Tibbett M, Zobel M (2012) Rooting theories of plant community ecology in microbial interactions. Trends Ecol Evol 25: 468–478
2. Hayat R, Ali S, Amara U, Khalid R, Ahmed I (2010) Soil beneficial bacteria and their role in plant growth promotion: a review. Ann Microbiol 60:579–598
3. Misaghi IJ (2011) Physiology and biochemistry of plant-pathogen interactions. Springer Science & Business Media, New York
4. Howe GA, Jander G (2008) Plant immunity to insect herbivores. Annu Rev Plant Biol 59: 41–66
5. Jones JDG, Dangl JL (2006) The plant immune system. Nature 444(7117):323–329
6. Zamioudis C, Pieterse CMJ (2012) Modulation of host immunity by beneficial microbes. Mol Plant Microbe Interact 25:139–150
7. Hussain A, Shah ST, Rahman H, Irshad M, Iqbal A (2015) Effect of IAA on in vitro growth and colonization of Nostoc in plant roots. Front Plant Sci 6:46
8. Kazan K, Lyons R (2014) Intervention of phytohormone pathways by pathogen effectors. Plant Cell 26:2285–2309
9. Hamayun M, Hussain A, Khan SA, Irshad M, Khan AL, Waqas M, Shahzad R, Iqbal A, Ullah N, Rehman G, Kim HY, Lee IJ (2015) Kinetin modulates physio-hormonal attributes and isoflavone contents of soybean grown under salinity stress. Front Plant Sci 6:377
10. Rivas-San Vicente M, Plasencia J (2011) Salicylic acid beyond defence: its role in plant growth and development. J Exp Bot 62:3321–3338
11. Vaňková R, Petrášek J, Zažímalová E, Kamínek M, Motyka V, Ludwig-Müller J (2014) Auxins and cytokinins in plant development and interactions with other phytohormones. J Plant Growth Regul 33:709–714
12. Spaepen S, Vanderleyden J (2011) Auxin and plant-microbe interactions. CSH Perspect Biol 3(4):a001438
13. Giron D, Frago E, Glevarec G, Pieterse CMJ, Dicke M (2013) Cytokinins as key regulators in plant-microbe-insect interactions: connecting plant growth and defence. Funct Ecol 27:599–609

14. Naseem M, Philippi N, Hussain A, Wangorsch G, Ahmed N, Dandekar T (2012) Integrated systems view on networking by hormones in Arabidopsis immunity reveals multiple crosstalk for cytokinin. Plant Cell 24:1793–1814
15. Hussain A, Hasnain S (2011) Interactions of bacterial cytokinins and IAA in the rhizosphere may alter phytostimulatory efficiency of rhizobacteria. World J Microbiol Biotechnol 27: 2645–2654
16. Robert-Seilaniantz A, Grant M, Jones JDG (2011) Hormone crosstalk in plant disease and defense: more than just jasmonate-salicylate antagonism. Annu Rev Phytopathol 49: 317–343
17. Kazan K, Manners JM (2009) Linking development to defense: auxin in plant-pathogen interactions. Trends Plant Sci 14:373–382
18. Chen Z, Agnew JL, Cohen JD, He P, Shan L, Sheen J, Kunkel BN (2007) *Pseudomonas syringae* type III effector AvrRpt2 alters *Arabidopsis thaliana* auxin physiology. Proc Natl Acad Sci 104:20131–20136
19. Pieterse CMJ, Van der Does D, Zamioudis C, Leon-Reyes A, Van Wees SCM (2012) Hormonal modulation of plant immunity. Annu Rev Cell Dev Biol 28:489–521
20. Zhang Z, Li Q, Li Z, Staswick PE, Wang M, Zhu Y, He Z (2007) Dual regulation role of GH3.5 in salicylic acid and auxin signaling during *Arabidopsis-Pseudomonas syringae* interaction. Plant Physiol 145:450–464
21. Naseem M, Dandekar T (2012) The role of auxin-cytokinin antagonism in plant-pathogen interactions. PLoS Pathol 8(11):e1003026. doi:10.1371/journalppat1003026
22. Jacobs S, Zechmann B, Molitor A, Trujillo M, Petutschnig E, Lipka V, Kogel K-H, Schäfer P (2011) Broad-spectrum suppression of innate immunity is required for colonization of *Arabidopsis* roots by the fungus *Piriformospora indica*. Plant Physiol 156:726–740
23. Lugtenberg B, Kamilova F (2009) Plant-growth-promoting rhizobacteria. Annu Rev Microbiol 63:541–556
24. Sirrenberg A, Göbe C, Grond S, Czempinski N, Ratzinger A, Karlovsky P, Santos P, Feussner I, Pawlowski K (2007) *Piriformospora indica* affects plant growth by auxin production. Physiol Plant 131:581–589
25. Ortíz-Castro R, Contreras-Cornejo HA, Macías-Rodrígueza L, López-Bucio J (2009) The role of microbial signals in plant growth and development. Plant Signal Behav 4:701–712
26. Aloni R, Langhans M, Aloni E, Dreieicher E, Ullrich C I (2005). Root-synthesized cytokinin in Arabidopsis is distributed in the shoot by the transpiration stream. J Exp Bot 56(416): 1535–1544.
27. Tien TM, Gaskins MH, Hubbell DH (1979). Plant growth substances produced by *Azospirillum brasilense* and their effect on the growth of pearl millet (*Pennisetum americanum* L.). Appl Environ Microbiol 37(5):1016–1024

Chapter 5

A Standardized Method to Assess Infection Rates of Root-Knot and Cyst Nematodes in *Arabidopsis thaliana* Mutants with Alterations in Root Development Related to Auxin and Cytokinin Signaling

Rocío Olmo*, Ana Cláudia Silva*, Fernando E. Díaz-Manzano, Javier Cabrera, Carmen Fenoll, and Carolina Escobar

Abstract

Plant parasitic nematodes cause a great impact in agricultural systems. The search for effective control methods is partly based on the understanding of underlying molecular mechanisms leading to the formation of nematode feeding sites. In this respect, crosstalk of hormones such as auxins and cytokinins (IAA, CK) between the plant and the nematode seems to be crucial. Thence, the study of loss of function or overexpressing lines with altered IAA and CK functioning is entailed. Those lines frequently show developmental defects in the number, position and/or length of the lateral roots what could generate a bias in the interpretation of the nematode infection parameters. Here we present a protocol to assess differences in nematode infectivity with the lowest interference of root architecture phenotypes in the results. Thus, tailored growth conditions and normalization parameters facilitate the standardized phenotyping of nematode infection.

Key words Auxin, Cytokinin, Root-knot nematodes, Cyst nematodes, Lateral root, Infection assay

1 Introduction

The phytohormones auxin (IAA) and cytokinin (CK) antagonistically regulate the formation and development of the lateral roots in plants. CK negatively regulates the formation of lateral roots while IAA induces their development [1]. Therefore, plant lines carrying

*Author contributed equally with all other contributors.

Electronic supplementary material: The online version of this chapter (doi:10.1007/978-1-4939-6831-2_5) contains supplementary material, which is available to authorized users.

Thomas Dandekar and Muhammad Naseem (eds.), *Auxins and Cytokinins in Plant Biology: Methods and Protocols*, Methods in Molecular Biology, vol. 1569, DOI 10.1007/978-1-4939-6831-2_5, © Springer Science+Business Media LLC 2017

mutations in genes related with the IAA and CK signaling pathways show developmental defects in the number, position, and/or length of the lateral roots [2].

Plant parasitic nematodes, root-knot nematodes (RKN) and the cyst nematodes (CN), constitute a major pest for the agriculture these days, causing important yield losses worldwide per year [3]. RKNs and CNs are obligate parasites and need to establish in the plant roots to complete their life cycle [4, 5]. Therefore, root shape and architecture strongly affect the penetration and establishment capacities of these parasites into the roots. RKNs penetrate intercellularly into the roots through the root tip; therefore the number of available root tips in the plant should be taken into account to measure their infectivity capacity. CNs, however, penetrate intracellularly through any part of the root surface and therefore, root number and length are the parameters to be considered. Several studies reinforce the role of the IAAs and CKs signaling pathways during RKNs and CNs establishment [6–10]. Moreover, it has been demonstrated that the nematode secretions contain IAAs and CKs that could alter the balance of these two phytohormones in the infection site [9, 11, 12]. Additionally, genes directly involved in the IAA signaling pathway leading to the formation of lateral roots are crucial during the CNs and RKNs infection [7, 13, 14].

Infection tests are used routinely for the study of the plant–nematode interactions as a way to infer the impact of the loss or gain of function of a gene during the nematode infection by comparing the number of infections between mutant/transgenic and wild type plants. Plants affected in the IAA and CK signaling or synthesis pathways show developmental defects in the number, position and/or length of the lateral roots [2] what could generate a bias in the interpretation of the nematode infection parameters. Therefore, to assess differences in infectivity with the lowest interference of root architecture in the final data, is unavoidable to design growth conditions and to stablish normalization parameters that could facilitate the standardized phenotyping of nematode infection in these lines with altered root growth. Bearing this in mind, we developed a modified infection test system in which the root phenotypes of wild type and mutant/transgenic plants are equivalent at inoculation time. This method is suitable to assess nematode-infection parameters in most mutant/transgenic plants affected in the IAA and CK signaling pathways with altered root systems. It facilitates the measurement of the number and length of the roots to normalize the number of infections. Moreover, our system could be useful for the study of those plant lines interacting with other root microorganisms.

2 Materials

2.1 Medium Preparation and Arabidopsis thaliana Seeds Sterilization and Sowing

1. Modified Gamborg B5 medium: 15 g/L sucrose, 3.05 g/L Gamborg B5 basal salt mixture including vitamins, 6 g/L Daishin Agar and adjust the pH to 7.0 with 1 M KOH.
2. 90 mm Ø petri dishes.
3. *A. thaliana* mutant/transgenic plants with alterations in root development plus the correspondent wild type accessions for comparison.
4. Sterilization solution: 30% commercial bleach (35 g of active chlorine per L) with 1 μg/μL Triton X-100.
5. 1.5 mL Eppendorf tubes.
6. Nutating mixer.
7. Sterile distilled water.
8. Laminar flow hood cabinet.
9. Micropipettes.
10. Micropipette tips (20–200 μL).
11. Parafilm.
12. Aluminum foil.
13. Growth chamber.

2.2 Nematode Inoculation

1. Sterile cell strainer (70 μm nylon mesh).
2. 50 mL beaker.
3. 300–400 mL glass jar with hermetic lid.
4. Tweezers.
5. Glass bead sterilizer.
6. Sterile tap water.
7. 3 mM $ZnCl_2$ solution.
8. Microscope slides.
9. Stereomicroscope.
10. Modified Gamborg B5 medium (see recipe above).
11. Micropipettes.
12. Micropipette tips.
13. Parafilm®.
14. Aluminum foil.
15. Growth chamber.
16. Gauze.

2.3 Measurement of Infection Parameters

1. Stereomicroscope.
2. Scanner.
3. ImageJ software [15].
4. Microsoft Excel.

3 Methods

3.1 Medium Preparation, Arabidopsis thaliana Seeds Sterilization and Sowing

1. Prepare 1 L of modified Gamborg B5 medium as indicated in the recipe and autoclave (121 °C for 20 min, +1 atm)—*see* **Note 1**.
2. Pour media into 90 mm Ø petri dishes (25 mL/plate) and let them to solidify (*see* **Note 2**).
3. Surface sterilize *A. thaliana* seeds (50–100 seeds) in a 1.5 mL Eppendorf® tube per independent line with 1 mL sterilization solution for 12 min in constant agitation in a nutating mixer.
4. Discard the solution and rinse the seeds 5–6 times, each with 1 mL sterile distilled water in the Eppendorf® tube.
5. Immediately after the last washing step, place 8–10 seeds in a single row with the help of a micropipette in the upper area of the previously prepared modified Gamborg B5 media plates (Fig. 1a)—*see* **Note 3**.
6. Seal the plates with Parafilm® and cover them with aluminum foil. Keep the plates at 4 °C for 2 days for seed stratification, thereby promoting the synchronous germination of all the seeds.
7. Transfer the plates to a growth chamber at 23 °C with a long-day photoperiod (16–8 h light–dark; 0% humidity—*see* **Note 4**—104 μmol/m^2 s light intensity) for 5 days. Place the plates allowing the plants to grow vertically to prevent early appearance of lateral roots. Five days after germination, roots should not show any lateral root (Fig. 1b). Therefore, the root phenotypes of the wild type (controls) and the mutant/transgenic plants for the IAA/CK signaling pathways should be similar regarding lateral root appearance. For infection with CNs root length is also considered (*see* **Note 5**).

3.2 Inoculation with RKNs

1. Prepare a hatching jar with 5 mL of sterile tap water and collect 50 egg masses from previously inoculated cucumber seedlings growth in monoaxenic conditions, accordingly to Díaz-Manzano et al. [16].
2. Inoculate each root tip with around ten nematodes (*see* **Note 6**). Each root tip should be inoculated independently to ensure that each plant is in contact to the same amount of nematodes.

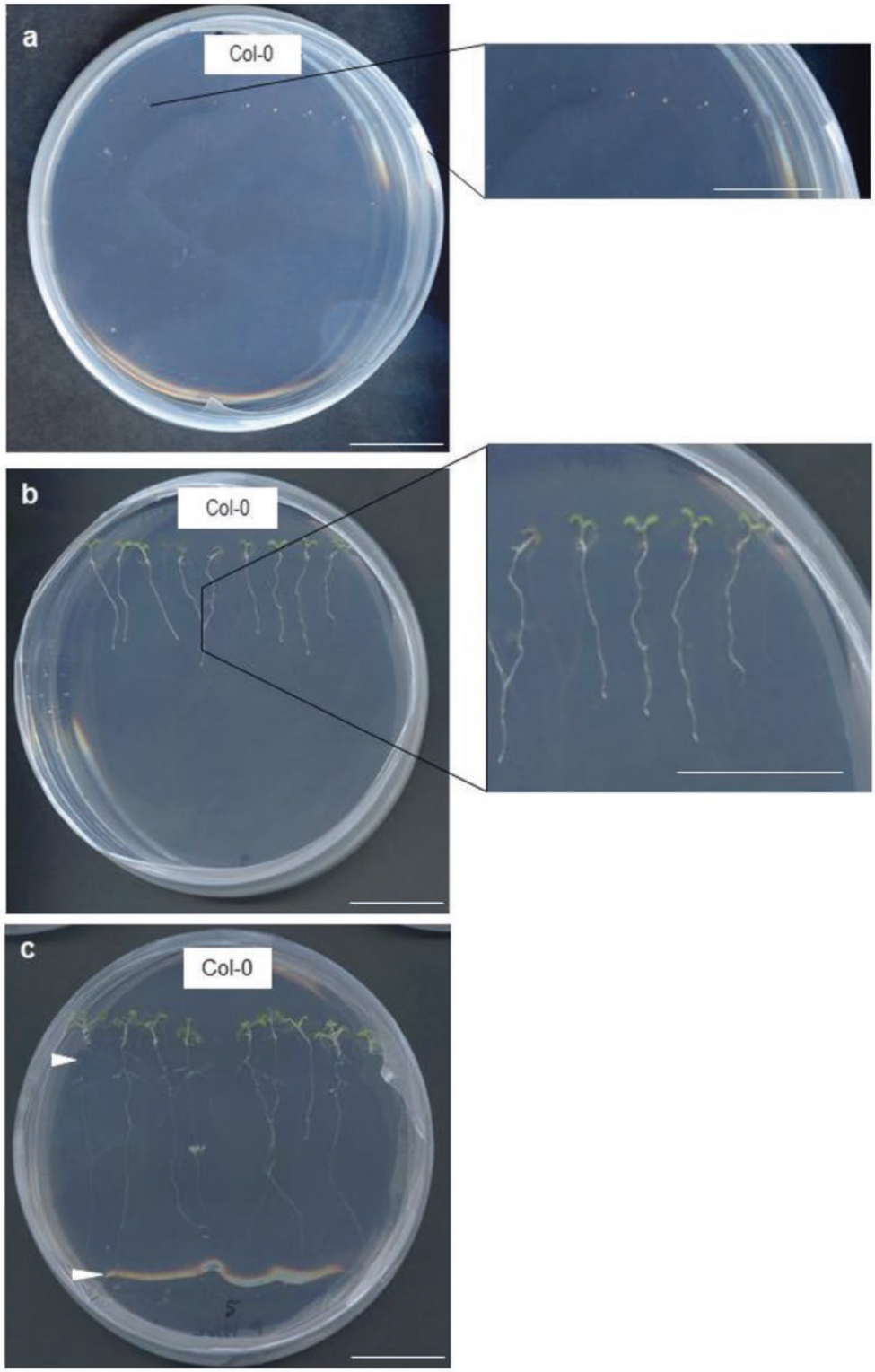

Fig. 1 *Arabidopsis thaliana* plates before inoculation. (**a**) Eight to ten seeds are sown in a single row in the upper part of the plate; *right panel*, enlarged image of sown seeds. (**b**) Plants are placed vertically to avoid early appearance of lateral roots. Up to 5 days after germination (dag); roots should not show any lateral root in all lines treated; *right panel*, enlarged image with detailed view of the seedlings. (**c**) At inoculation time (5 dag), a thin layer of temperate modified Gamborg B5 medium is placed on the roots covering them to facilitate nematode penetration. *White arrow heads* marking start and end of the layer. Scale bars: 2 cm

3. Add 1 mL of a thin layer of temperate modified Gamborg B5 medium on the top of the roots until covering the root tips (*see* **Note 7**), hence facilitating nematode penetration. When the plants are maintained vertically, the roots grow over the medium surface and do not penetrate into the agar (Fig. 1c). RKNs have more difficulties to penetrate into roots grown in the root surface; hence it is necessary to add this temperate medium layer to cover the roots.
4. When the medium is solidified, seal again the plates with Parafilm®, cover them with aluminum foil (*see* **Note 8**) and transfer them to a growth chamber at 23 °C with a long-day photoperiod (16–8 h light–dark; 0% humidity) for 3 days keeping them vertically.
5. Check the plates every 12 h after inoculation under the stereomicroscope for nematode penetration. The first day post infection is established when the nematode is inside the root. It is recommended to label a dot in the back of the plate with a colored marker pen indicative of the T0 infection time.
6. Three days post inoculation; remove the aluminum foil and cover the plates with gauze to protect the plants and the nematodes from an excessive light exposure. Light intensity received by the plants at this point should be around 48 μmol/m² s (Fig. S1) (*see* **Note 9**).

3.3 Inoculation with CNs

1. *Heterodera* spp. juveniles are obtained by the method described by Bohlmann and Wieczorek [17].
2. Inoculate each root with ten nematodes (*see* **Note 6**).
3. Follow the same **steps 3–6** described above for RKNs inoculation.

3.4 Measurement of Infection Parameters for RKNs

1. Count the number of galls at 14 days post inoculation per main root under a stereomicroscope (Fig. 2). Avoid counting those galls induced by RKNs in the lateral roots grown after the inoculation was made.
2. Before the inoculation, the plates should be scanned in order to record the number of main roots per plate and its length by using the imaging software ImageJ [15].
3. Calculate infection rates (number of galls per plant or main root) with the help of a spreadsheet such as Microsoft® Excel and compare the results between the wild type and the mutant line with alterations in root development. This protocol can be also followed for galls phenotyping to check differences in size [18].

3.5 Measurement of Infection Parameters for CNs

1. Count the number of females and males at 14 days post inoculation per main root under a stereomicroscope (Fig. 2). Avoid counting those syncytia induced in the lateral roots grown after the inoculation if present.

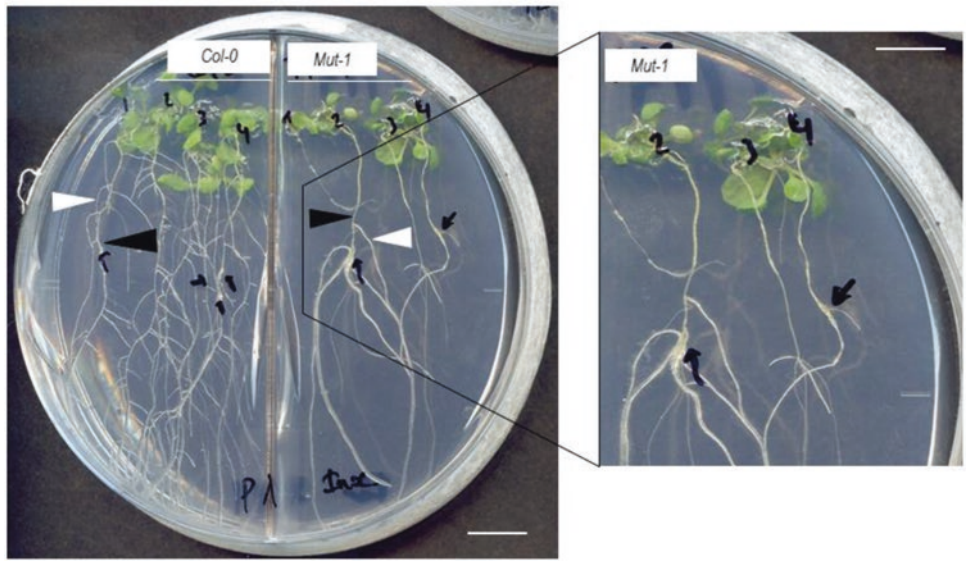

Fig. 2 Infected *Arabidopsis thaliana* plant roots. Two representative lines, including the wild type Col-0, and *mutant 1* as indicated at 19 days after germination (14 days post inoculation) when galls are normally scored to obtain the infection rate. Infective parameter (number of galls per plant per primary root). *Mut-1* shows clearly altered lateral root formation, whereas Col-0 shows profuse lateral root growth. *Right panel*, enlarged area to observe the galls in the infected primary roots. Primary roots (*black arrow heads*) and lateral roots (*white arrow heads*). Galls, *black arrows*. Scale bars: 1 cm

2. Before the inoculation, the plates should be scanned in order to record the number of main roots per plate and its length by using the imaging software ImageJ [15].
3. Calculate infection rates (number of females and males per plant; total number of nematodes per plant and female/male ratio per plant and line) with the help of a spreadsheet such as Microsoft® Excel and compare the results between the wild type and the mutant line with alterations in root development. It is recommended to measure the main root length per plant and refer the infection rates to the root length. As every plant has been imaged, the line tools (straight, segmented or free-hand styles) from the imaging software ImageJ can be used for it. Alternatively measure it directly in the plate with a ruler.

4 Notes

1. From this step onwards, the protocol must be carried out under sterile conditions in a laminar flow cabinet.
2. Plates can be parafilm-sealed and stored at 4 °C if they are not going to be immediately used. Do not allow accumulation of liquid on the medium surface as it will promote future contaminations.

3. It is recommendable to prepare five plates with 8–10 seeds per line and per assay in order to have around 50 plants per line and a good infection rate for each one of them.
4. Humidity in the growth chamber should be set to low humidity, near 0%, to avoid accumulation of water inside the plates and therefore to prevent their contamination.
5. Before inoculation, wild type and mutant line roots should be qualitatively compared. For both CNs and RKNs, the roots that present a considerable different size as compared to the rest within a plate/line should be removed.
6. Take up the necessary volume from the hatching jar containing ten nematodes with an automatic pipette and add it directly into the root tip. The number of J2/mL is normally assessed under a stereomicroscope by counting the number of J2s in three independent 30 μL drops from the hatching jar. The average among the three estimations [16] is considered.
7. The medium should be approximately at 30 °C and should only cover the plant roots and not the aerial part. The temperature could be measured in the laminar flow chamber with an acetone-cleaned thermometer.
8. The plates should be covered with aluminum foil for 3 days in order to facilitate the nematode penetration on the plant roots in darkness.
9. The gauze should replace the aluminum foil in order to avoid etiolation of the plants, while protecting the nematodes from an excessive light exposition detrimental for the infection.

Acknowledgments

This work was supported by the Spanish Government (AGL2013-48787 to CE; and PCIN-2013-053 to CF) and by the Castilla-La Mancha Government (PEII-2014-020-P to CF). FEDM, RO, JC, and ACS acknowledge the European Social Fund, the University of Castilla La Mancha and the MINECO for cofinancing this work.

References

1. Moreira S, Bishopp A, Carvalho H, Campilho A (2013) AHP6 inhibits cytokinin signaling to regulate the orientation of pericycle cell division during lateral root initiation. PLoS One 8(2):e56370
2. Lavenus J, Goh T, Roberts I, Guyomarch S, Lucas M, De Smet I et al (2013) Lateral root development in Arabidopsis: fifty shades of auxin. Trends Plant Sci 18:450–458
3. McCarter JP (2008) Molecular approaches toward resistance to plant-parasitic nematodes. In: Berg RH, Taylor CG (eds) Cell biology of plant nematode parasitism. Springer, Berlin, pp 239–267

4. Bohlmann H (2015) Introductory chapter on the basic biology of cyst nematodes. In: Escobar C, Fenoll C (eds) Advances in botanical research, vol 73. Elsevier Academic Press, Oxford, pp 33–59
5. Escobar C, Barcala M, Cabrera J, Fenoll C (2015) Overview of root-knot nematodes and giant cells. In: Escobar C, Fenoll C (eds) Advances in botanical research, vol 73. Elsevier Academic Press, Oxford, pp 1–32
6. Grunewald W, Van Noorden G, Van Isterdael G, Beeckman T, Gheysen G, Mathesius U (2009) Manipulation of auxin transport in plant roots during Rhizobium symbiosis and nematode parasitism. Plant Cell 21:2553–2562
7. Cabrera J, Diaz-Manzano FE, Sanchez M, Rosso MN, Melillo T, Goh T et al (2014) A role for LATERAL ORGAN BOUNDARIES-DOMAIN 16 during the interaction Arabidopsis-*Meloidogyne* spp. provides a molecular link between lateral root and root-knot nematode feeding site development. New Phytol 203:632–645
8. Cabrera J, Barcala M, Fenoll C, Escobar C (2015) The power of omics to identify plant susceptibility factors and to study resistance to root-knot nematodes. Curr Issues Mol Biol 19:53–72
9. Siddique S, Radakovic ZS, De La Torre CM, Chronis D, Novák O, Ramireddy E et al (2015) A parasitic nematode releases cytokinin that controls cell division and orchestrates feeding site formation in host plants. Proc Natl Acad Sci U S A 112:12669–12674
10. Shanks CM, Rice JH, Zubo Y, Schaller GE, Hewezi T, Kieber JJ (2016) The role of cytokinin during infection of *Arabidopsis thaliana* by the cyst nematode *Heterodera schachtii*. Mol Plant Microbe Interact 29:57–68
11. De Meutter J, Tytgat T, Witters E, Gheysen G, Van Onckelen H, Gheysen G (2003) Identification of cytokinins produced by the plant parasitic nematodes *Heterodera schachtii* and *Meloidogyne incognita*. Mol Plant Pathol 4:271–277
12. De Meutter J, Tytgat T, Prinsen E, Gheysen G, Van Onckelen H, Gheysen G (2005) Production of auxin and related compounds by the plant parasitic nematodes *Heterodera schachtii* and *Meloidogyne incognita*. Commun Agric Appl Biol Sci 70:51–60
13. Grunewald W, Karimi M, Wieczorek K, Beeckman T, Gheysen G, Mathesius U (2008) A role for AtWRKY23 in feeding site establishment of plant-parasitic nematodes. Plant Physiol 148:358–368
14. Cabrera J, Barcala M, García A, Rio-Machín A, Medina C, Jaubert-Possamai S et al (2016) Differentially expressed small RNAs in Arabidopsis galls formed by *Meloidogyne javanica*: a functional role for miR390 and its TAS3-derived tasiRNAs. New Phytol 209: 1625–1640
15. Schneider CA, Rasband WS, Eliceiri KW (2012) NIH Image to ImageJ: 25 years of image analysis. Nat Methods 9:671–675
16. Díaz-Manzano FE, Olmo R, Cabrera J, Barcala M, Escobar C, Fenoll C (2016) Long-term in vitro system for maintenance and amplification of root-knot nematodes in *Cucumis sativus* roots. Front Plant Sci 7:124
17. Bohlmann H, Wieczorek K (2015) Infection assay of cyst nematodes on Arabidopsis roots. Bio-protocol 5(18):e1596
18. Cabrera J, Díaz-Manzano FE, Barcala M, Arganda-Carreras I, de Almeida-Engler J, Engler G et al (2015) Phenotyping nematode feeding sites: three dimensional reconstruction and volumetric measurements of giant cells induced by root-knot nematodes in Arabidopsis. New Phytol 206:868–880

Chapter 6

Reconstruction of an Immune Dynamic Model to Simulate the Contrasting Role of Auxin and Cytokinin in Plant Immunity

Martin Kaltdorf, Thomas Dandekar, and Muhammad Naseem

Abstract

In order to increase our understanding of biological dependencies in plant immune signaling pathways, the known interactions involved in plant immune networks are modeled. This allows computational analysis to predict the functions of growth related hormones in plant–pathogen interaction. The SQUAD (Standardized Qualitative Dynamical Systems) algorithm first determines stable system states in the network and then use them to compute continuous dynamical system states. Our reconstructed Boolean model encompassing hormone immune networks of *Arabidopsis thaliana* (*Arabidopsis*) and pathogenicity factors injected by model pathogen *Pseudomonas syringae* pv. tomato DC3000 (*Pst* DC3000) can be exploited to determine the impact of growth hormones in plant immunity. We describe a detailed working protocol how to use the modified SQUAD-package by exemplifying the contrasting effects of auxin and cytokinins in shaping plant–pathogen interaction.

Key words Plant immunity, Auxin, Cytokinins, Boolean models, Signaling network, Network simulation, Pathway prediction, Hormone immune networks

1 Introduction

The growing abundance of high-throughput omics datasets and the development of complementary tools has enabled the reconstruction of genome scale models. Interactions among genes, proteins, and metabolites constitute the whole cellular interactome that shapes cellular phenotypes in response to internal and external cues. The activating and inhibiting interactions between genes, proteins and signaling molecules orchestrate a highly complex network that can be described as a "gene regulatory networks" (GRNs). The in silico prediction of the GRNs is still a challenging task and needs incredibly higher computational power due to the convoluted nature of genome scale biological networks. The algorithm developed by Mendoza and Xenarios [1] and later on implemented by DiCara et al. [2] in the form of Standardized

Thomas Dandekar and Muhammad Naseem (eds.), *Auxins and Cytokinins in Plant Biology: Methods and Protocols*, Methods in Molecular Biology, vol. 1569, DOI 10.1007/978-1-4939-6831-2_6,

Qualitative Dynamical Systems (SQUAD-package) provides unique opportunity to model biological processes without knowing detailed kinetics of the nodes of the network. The SQUAD package manages to reduce the required computing power to the size of a personal computer by splitting the analysis in sub-steps: (1) calculation of discrete stable system states using Boolean characteristics combined with detailed information on the interactions and (2) hence using the results as a starting point for further analysis by continuous dynamical systems modeling.

Phytohormones act in concert and their signaling crosstalk plays a pivotal role in mediating immune networks in plants. The plant hormone auxin regulates almost every aspect of plant growth and development [3, 4]. The main precursor for indole acetic acid IAA (naturally occurring auxin) is tryptophan (Trp) [3], which is converted to IAA through YUCCA (YUC) family of flavin monooxygenases [5, 6]. In case of low cellular auxin concentrations, auxin repressor proteins (AUX/IAAs) bind to AUXIN RESPONSE FACTORS (ARFs) and repress the transcriptional regulatory function of ARFs. On the contrary, higher cellular auxin concentrations facilitate the degradation of AUX/IAA and thus allow ARFs to initiate the transcription of auxin response genes [7–9]. Plant pathogens manipulate auxin responses to mediate susceptibility of the host [10, 11]. The interaction of pathogen delivered effectors with important auxin pathway proteins AUX/IAA provides mechanistic insight into auxin biology and plant immunity [10, 11]. Altered plant auxin responses have been shown to modulate the central backbone (the antagonistic interaction between salicylic acid (SA) and jasmonate pathways) of plant immunity [12–14].

Cytokinins on the other hand are N^6-substituted adenine derivatives. They bind to the central CHASE (cyclases/histidine kinases associated sensory extracellular) domain of the HISTIDINE KINASE 2–4 (AHK2–4) receptors and initiates a downstream phosphotransfer cascade in a two-component system (TCS) dependent manner [15]. This involves the phosphorylation of *Arabidopsis* response regulators (ARRs) through histidine phosphotransfer proteins (AHPs) [15]. Increased cytokinins responses positively promote plant immune dynamics against infection with various types of biotrophic [16], necrotrophic [17], and hemibiotrophic [18] pathogens. Higher cytokinin accumulation due to infection by microbial pathogens also mediate host susceptibility [19–21]. Mutual antagonism between auxin and cytokinins regulates important developmental processes in plants [4]. Higher plant auxin levels and responses promote the infection of *Pst* DC3000 in *Arabidopsis* [10]. However, increased cytokinin levels and responses have been shown to promote plant immunity against the infection of *Pst* DC3000 [18]. Here, we exemplify these contrasting responses by auxin and cytokinin in modulating plant pathogen

interactions for the infection of model plant *Arabidopsis* by Pst DC3000. We provide a detailed protocol and subsequent notes on the handling of SQUAD based network model and simulations.

2 Materials

2.1 Required Computing Hardware

1. Personal computer running on a current operating system.

2.2 Required Software

1. java RE 1.7 or newly installed version.
2. yEd. yEd [22] a is freeware and accessible for every major operating system. https://www.yworks.com/products/yed/download
3. The simulation software Jimena is provided as a java repository and requires java 1.7 or newer. We recommend the most recent version from February 2015. http://www.bioinfo.biozentrum.uni-wuerzburg.de/computing/jimena [23].

2.3 Required Data

1. Directed interaction data of covered proteins.
2. Experimental data for verification of simulation results.

3 Methods

3.1 Collection of Interaction Data of Proteins and Creation of Network

In order to reconstruct a GRN for simulation using Jimena (*see* **Note 1**), a detailed collection of interaction data is necessary (*see* **Note 2**). Literature survey and previously curated pathway databases are main attributes to network reconstruction phase. In our research we collected literature and consulted various protein-protein-interaction databases for the verification of plant hormone immune interactions (*see* **Note 3**). For instance databases such as Kyoto Encyclopedia for Genes and Genomes (KEGG) [24, 25], STRING based search tool for the retrieval of interacting Genes/Proteins [26, 27] and PMN [28] can be screened to build hormone immune network for reference plant *Arabidopsis*.

3.2 Creation of Network File

1. Reconstruct the network by using yEd text editor.
2. Left click in the program window to create a node.
3. In order to connect two nodes **click + hold** left mouse button on the starting node and drag to target node. Release the mouse button to create the edge.
4. Change edge/connection type according to literature (decision of activation or inhibition) information; arrows indicate activating edges while all edges not ending with an arrowhead are considered inhibitions (*see* **Note 1** and Fig. 1).

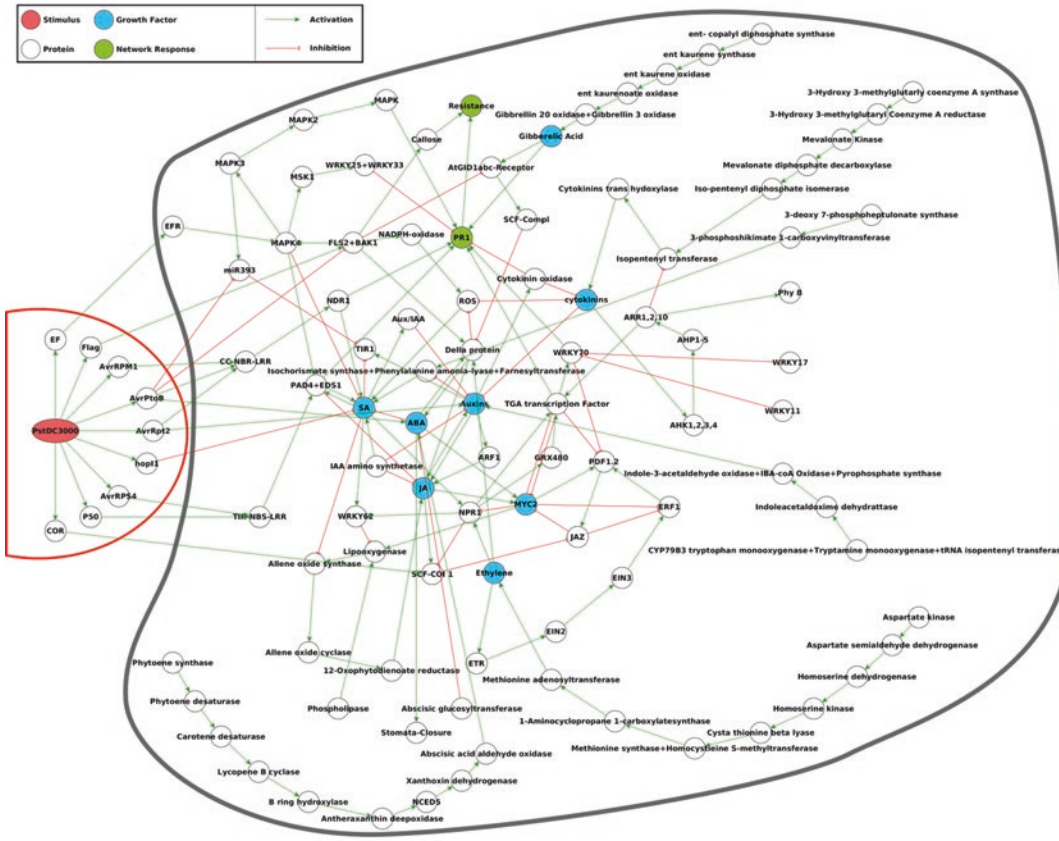

Fig. 1 Network topology illustrating the reconstructed plant hormone-immune network. *Circles* describe proteins and hormones as participating nodes of the network, while *lines* depict the interacting connections as edges of the network. *Blue colored circles* highlight important plant hormones, the *red colored circle* illustrates the Pst DC3000 proteins that invoke immune response in *Arabidopsis. Edges* in *green* show the activation behavour while *red lines* depect inhibitions. Proteins nodes intrinsic to the immune system are surrounded by a *black line*, while all pathogenic proteins are bordered by a *red line* (For network topology and interaction details see Naseem et al. [18])

5. For better visualization you can change color and shape of nodes and edges by selecting and changing them according to the value appearing on parameter window.
6. After completing the task of reconstruction save the network in ".graphml"-file format.

3.3 Analysis and Simulation of the Reconstructed Network

1. Extract jimena.zip on your computer.
2. Open Jimena (on linux operating system use console to type: "java -jar jimena.jar".
3. Import .graphml file already created in yEd (in Subheading 2.2) (in Jimena Window: **Network → Import yEd File**).

4. Set general parameters or use preset values. Simulation Method: preset and suggested is "SQUAD", change in order to use another algorithm. Simulation Time: preset are "50 time units", in most of the simulations "20 time units" are sufficient. Adjust the value according to your simulation results. When your network reaches an equilibrium or steady state, the simulation can be stopped. **dt:** preset and suggested is "0.05", **Max Speed:** preset is "1", can be increased to speed up simulation speed, results will not differ from preset value.
5. Analyze the network for stable steady states (in Jimena Window: **Analysis → Find Stable Steady States**) to calculate valid starting points for the simulation or use the reset-ed state as a starting point.
6. Open "Nodes Table" window (**View → Nodes Table**) to modify the activation values of single nodes. In case that you want to use steady states as starting point, copy the stable steady state you chose to clipboard and paste it into the Nodes Table by selecting the window and pressing "Ctrl + V". During the simulation all nodes values are changed here and still can be altered manually.
7. Run the simulation by selecting the green double arrow button, if you want to run the simulation by single time steps, select the single green arrow button (*see* **Note 3**).
8. To view the dynamic readout, open the "Charts Window" (**View → Charts Window/Data Export**) and select the proteins of interest. Multiple proteins can be selected by pressing and holding the Ctrl-key on your keyboard or pressing "Ctrl + A" to select all nodes.
9. In order to export the simulation results select the "Export Selected" button in the Charts Window and choose the directory you want to save your data.
10. In order to reset the network to import state use the button showing a yellow circular arrow right of the green arrows.

3.4 Analysis and Simulation Using Perturbations

Jimena has incorporated a possibility to additionally simulate the effect of proteins to invasion the effect of knockout mutant or overexpressing transgenic plant.

Open the Perturbations Table (**View → Perturbations Table**) in Jimenas' main window.

1. Chose "Add New Perturbation" and select the targeted node to initialize the perturbation. Furthermore you have to select the type of your perturbation, "On-Off-Perturbation" to simulate knockout/unlimited abundance. "Random Perturbation" and "Sine Perturbation" to simulate random or periodic disturbances to test the robustness of the model.

2. Select "On-Off-Perturbation" and set Start and End timepoint as well as the activity value of the node (between 0 for no activity and 1 for 100% activity).
3. Adjust the "Nodes Table" to your preferred starting point and run simulation.

4 Notes

1. General network evaluation can be achieved by using the Jimenas' built-in function to calculate the models' control centrality values [29]:
   (a) Calculate Network Density $D = \frac{n_{\text{edges}}}{n_{\text{nodes}}}$
   Desirable value range: 1.4–2.75
   (b) Calculate Total Control Centrality*: Indicates Robustness of network (the lower the value, the more robust is the nodes' influence on the network in case of mutations).
   (c) Mean of all TC values*: indicates general vulnerability of the network to mutations (high Mean (TC) = high vulnerability).
   (d) Calculate Value Control Centrality*: Indicates direct influence of the network by a node (the higher the value, the more influence it has on the overall behavior of the network).
   (e) Mean of all TC values*: general control over the network (high Mean (VC) = better steerability).
   *All Control Centrality values have to be seen in relation to the other components' values of the network.
   Overall guideline for quality of Centrality values:
   Generalized Control Centrality scale:
   (a) 1 to 10^{-6}: strong influence
   (b) 10^{-6} to 10^{-8}: intermediate influence
   (c) 10^{-10} and smaller: weak influence
2. *Background information on Jimenas algorithm*:
   In order to analyze the network for steady states, Jimena initiates the processing by calculating the discrete stable states according to differential Eq. 1 (according to Mendoza and Xenarios [1]). Depending on the network topology and the existing connections the boolean characteristics are calculated resulting in a discrete version of the dynamical system representing the network.

Based on the resulting discrete dynamical model the framework is able to efficiently predict stable system states (SSS) with a minimal required computing power. Since the characteristics of continuous dynamical modeling are of a highly nonlinear nature and have to be studied numerically, an efficient analysis is almost unfeasible. Nevertheless it is possible to drastically minimize the required computing space and time in continuous systems by using the resulting steady system states from discrete dynamical modeling (Eq. 2). Hence the analysis can be accomplished even on local personal computers.

$$x_i(t+1)=\begin{cases}\left(x_1^a(t)\vee x_2^a(t)\ldots\vee x_n^a(t)\right)\wedge\neg\left(x_1^i(t)\vee x_2^i(t)\ldots\vee x_m^i(t)\right) & \S\\ \left(x_1^a(t)\vee x_2^a(t)\ldots\vee x_n^a(t)\right) & \S\S\\ \neg\left(x_1^i(t)\vee x_2^i(t)\ldots\vee x_m^i(t)\right) & \S\S\S\end{cases} \tag{1}$$

logical operators : $\vee(\mathrm{OR}),\wedge(\mathrm{AND}),\neg(\mathrm{NOT})$

$x_i\in\{0,1\}$

$\{x_n^a\}$ is the set of activators of x_i

$\{x_m^i\}$ is the set of inhibitors of x_i

$\S$ is used if x_i has activators and inhibitors
$\S\S$ is used if x_i has only activators
$\S\S\S$ is used if x_i has only inhibitors

$$\frac{\mathrm{d}x_i}{\mathrm{d}t}=\frac{-e^{o.5h}+e^{-h(\omega_i-0.5)}}{\left(1-e^{0.5h}\right)\left(1+e^{-h(\omega_i-0.5)}\right)}-\gamma_i x_i$$

$$\omega_i=\begin{cases}\left(\frac{1+\sum\alpha_n}{\sum\alpha_n}\right)\left(\frac{\sum\alpha_n x_n^a}{1+\sum\alpha_n x_n^a}\right)\left(1-\left(\frac{1+\sum\beta_m}{\sum\beta_m}\right)\left(\frac{\sum\beta_m x_m^i}{1+\sum\beta_m x_m^i}\right)\right) & \S\\ \left(\frac{1+\sum\alpha_n}{\sum\alpha_n}\right)\left(\frac{\sum\alpha_n x_n^a}{1+\sum\alpha_n x_n^a}\right) & \S\S\\ \left(1-\left(\frac{1+\sum\beta_m}{\sum\beta_m}\right)\left(\frac{\sum\beta_m x_m^i}{1+\sum\beta_m x_m^i}\right)\right) & \S\S\S\end{cases} \tag{2}$$

$$0\le x_i\le 1$$

$$0\le\omega_i\le 1$$

$$h,\alpha_n,\beta_m,\gamma_i>0$$

$\{x_n^a\}$: set of activators of x_i

$\{x_m^i\}$: set of inhibitors of x_i

§ is used if x_i has activators and inhibitors
§§ is used if x_i has only activators
§§§ is used if x_i has only inhibitor

3. *Network reconstruction encompassing host immune regulatory proteins and pathogenic factors associated diseases development*

   The model is based upon Boolean logic, where each key unit of the involved function is designated as a *node* of the network. The *Pst* DC3000 epitopes such as PAMPs, effectors as well as important host proteins such as *R*-genes proteins, transcription factors, and proteins of host hormone signaling pathways [11] (Fig. 1). The dynamics of the activation of marker node pathogenesis related-1 PR-is a good indicator of the overall immune response strength of the system for this plant–pathogen interaction [11]. The connectivity among nodes in the network is maintained through edges; they either show activation or inhibition. Densely nodes of the network serve as hub-nodes that have central positions in the network and orchestrate the ultimate immune response of the system. The Boolean model can be established using CellDesigner [30]. SQUAD converts the static network model (Boolean based activation and inhibition) into a continuous dynamic system. We simulated the effect of cytokinin and auxin on plant immune system (Fig. 2). The simulation (Fig. 2) shows how various activation levels of auxin and cytokinins impact the immune output in terms of PR-1 gene activation as sigmoid curve. System attains immunity when the activation of cytokinins is maximized, whereas activation of auxin reduces the activation of the immune markers genes and thus approximates decline in the level of immunity. This approach can be extended to other phytohormones as well as other plant process such as growth, development, and response to abiotic stresses. The

Acknowledgments

We thank the German Research Foundation (DFG) for funding (TR124/B1)

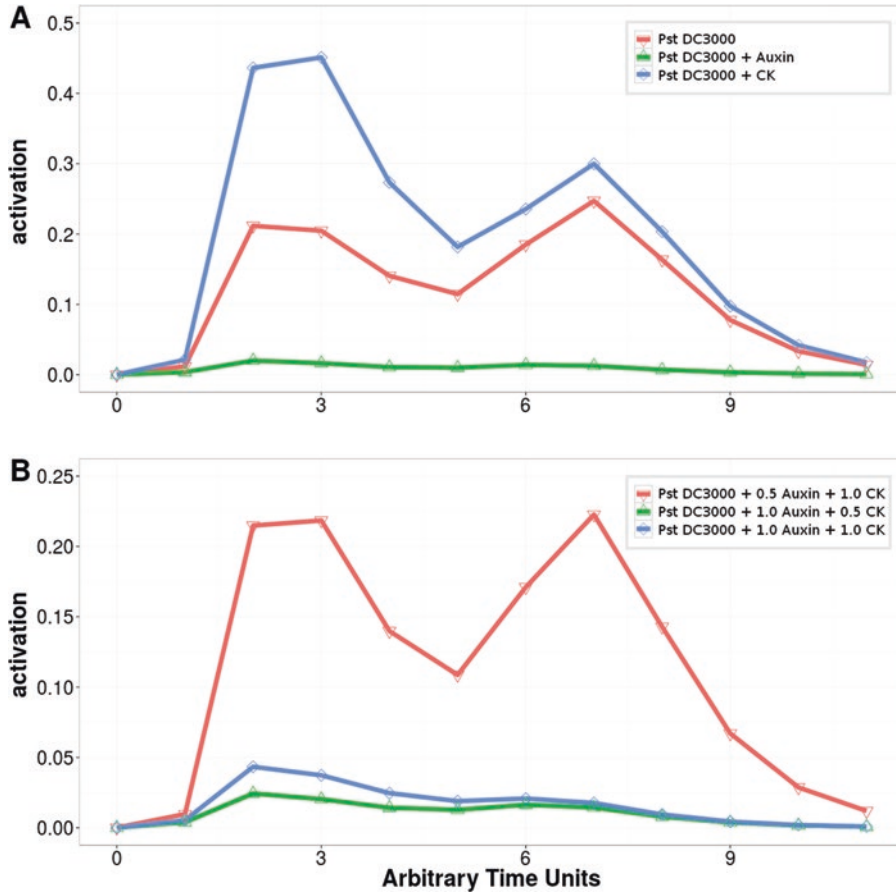

Fig. 2 Simulation result showing the dynamic readout regarding the activity of plant hormone auxin and cytokinins and their effects on plant immunity. PR1 (pathogenesis related protein-1) in response to Pst DC3000 infection serve as index of plant immunity. PR1 activity (*y*-axis) over arbitarry units of time (*x*-axis) in response to Pst DC3000 infection under influence of auxin or cytokinins in comparision to wild type infection (**a**). Effects of various activation states of auxin and cytokinin on PR1 activity during infection of *Arabidopsis* with Pst DC3000 (**b**). *Red line*: auxin activity of 50 % and cytokinin activity of 100 % activation; *green line*: auxin activity of 100 % and cytokinin activity of 50 % activation; *blue line*: both auxin and cytokinin activity of 100 % activation

References

1. Mendoza L, Xenarios I (2006) A method for the generation of standardized qualitative dynamical systems of regulatory networks. Theor Biol Med Model 3:13
2. Di Cara A, Garg A, De Micheli G et al (2007) Dynamic simulation of regulatory networks using SQUAD. BMC Bioinformatics 8:462. doi:10.1186/1471-2105-8-462
3. Zhao Y (2010) Auxin biosynthesis and its role in plant development. Annu Rev Plant Biol 61: 49–64
4. Naseem M, Dandekar T (2012) The role of auxin-cytokinin antagonism in plant-pathogen interactions. PLoS Pathog 8:e1003026
5. Mashiguchi K, Tanaka K, Sakai T et al (2011) The main auxin biosynthesis pathway in Arabidopsis. Proc Natl Acad Sci 108: 18512–18517
6. Fdos Maraschin S, Memelink J, Offringa R (2009) Auxin-induced, SCF(TIR1)-mediated poly-ubiquitination marks AUX/IAA proteins for degradation. Plant J 59:100–109

7. Vidhyasekaran P (2015) Auxin signaling system in plant innate immunity. http://link.springer.com/book/10.1007/978-94-017-9285-1
8. Gray WM, Estelle I (2000) Function of the ubiquitin-proteasome pathway in auxin response. Trends Biochem Sci 25:133–138
9. Dharmasiri N, Dharmasiri S, Estelle M (2005) The F-box protein TIR1 is an auxin receptor. Nature 435:441–445
10. Naseem M, Kaltdorf M, Dandekar T (2015) The nexus between growth and defence signalling: auxin and cytokinin modulate plant immune response pathways. J Exp Bot 66:4885–4896
11. Naseem M, Srivastava M, Tehseen M, Ahmed N (2015) Auxin crosstalk to plant immune networks: a plant-pathogen interaction perspective. Curr Protein Pept Sci 16:389–394
12. Grant MR, Jones JDG (2009) Hormone (dis) harmony moulds plant health and disease. Science 324:750–752
13. Robert-Seilaniantz A, Grant M, Jones JDG (2011) Hormone crosstalk in plant disease and defense: more than just JASMONATE-SALICYLATE antagonism. Annu Rev Phytopathol 49:317–343
14. Mutka AM, Fawley S, Tsao T, Kunkel BN (2013) Auxin promotes susceptibility to Pseudomonas syringae via a mechanism independent of suppression of salicylic acid-mediated defenses. Plant J 74:746–754
15. Hwang I, Sheen J, Müller B (2012) Cytokinin signaling networks. Annu Rev Plant Biol 63: 353–380
16. Argueso CT, Ferreira FJ, Epple P et al (2012) Two-component elements mediate interactions between cytokinin and salicylic acid in plant immunity. PLoS Genet 8:e1002448
17. Choi J, Huh SU, Kojima M et al (2010) The cytokinin-activated transcription factor ARR2 promotes plant immunity via TGA3/NPR1-dependent salicylic acid signaling in arabidopsis. Dev Cell 19:284–295
18. Naseem M, Philippi N, Hussain A et al (2012) Integrated systems view on networking by hormones in Arabidopsis immunity reveals multiple crosstalk for cytokinin. Plant Cell 24: 1793–1814
19. Sardesai N, Lee L-Y, Chen H et al (2013) Cytokinins secreted by Agrobacterium promote transformation by repressing a plant myb transcription factor. Sci Signal 6:ra100
20. Giron D, Frago E, Glevarec G et al (2013) Cytokinins as key regulators in plant-microbe-insect interactions: connecting plant growth and defence. Funct Ecol 27:599–609
21. Walters DR, McRoberts N (2006) Plants and biotrophs: a pivotal role for cytokinins? Trends Plant Sci 11:581–586
22. Karl S, Dandekar T (2015) Convergence behaviour and control in non-Linear biological networks. Scientific reports 5: 9746
23. Karl S, Dandekar T (2013) Jimena: efficient computing and system state identification for genetic regulatory networks. BMC Bioinformatics 14:306
24. Kanehisa M, Goto S (2000) KEGG: kyoto encyclopedia of genes and genomes. Nucleic Acids Res 28:27–30
25. Kanehisa M, Goto S, Sato Y et al (2014) Data, information, knowledge and principle: back to metabolism in KEGG. Nucleic Acids Res 42: 199–205
26. Szklarczyk D, Franceschini A, Wyder S et al (2015) STRING v10: protein-protein interaction networks, integrated over the tree of life. Nucleic Acids Res 43:447–452
27. Franceschini A, Szklarczyk D, Frankild S et al (2013) STRING v9.1: protein-protein interaction networks, with increased coverage and integration. Nucleic Acids Res 41: 808–815
28. Plant Metabolic Network (PMN), http://www.plantcyc.org/tools/tools_overview.faces on www.plantcyc.org. 28 Feb 2008
29. Karl S, Dandekar T (2015) Convergence behaviour and control in non-linear biological networks. Sci Rep 5:9746
30. Matsuoka Y, Funahashi A, Ghosh S, Kitano H (2014) Modeling and simulation using Cell Designer. Methods Mol Biol 1164:121–145

Chapter 7

Interplay Between Auxin and Cytokinin and Its Impact on Mitogen Activated Protein Kinase (MAPK)

Pallavi Singh and Alok Krishna Sinha

Abstract

Plant physiology, in particular, is governed by a repertoire of endogenous as well as environmental cues. Auxin and cytokinin constitute an indispensable phytohormonal system required for plant growth and development. Another pivotal aspect of plant physiological process that thoroughly affects various plant growth and developmental attributes is the signaling network, majorly comprising the canonical mitogen activated protein kinase (MAPK) cascade. Striking a fine balance between the phytohormonal and signaling components could be adopted as an intricate strategy by plants to counteract various stresses in question. Thus, a brief understanding of this multifaceted complex could be of use for delineating numerous plant physiological and developmental phenomena. Thus, the present section discusses the various MAPK related assays in context to auxin and cytokinin crosstalk. Briefly, this chapter outlines the discrete MAPK methods to better understand the fundamentals of MAPK signaling network in auxin and cytokinin treated rice seedlings. Further, various phenotypic, genomic as well as proteomic protocols are discussed for a better understanding of MAPK networks in the backdrop of auxin and cytokinin interplay.

Key words Auxin, Cytokinin, Mitogen activated protein kinase (MAPK), MAPK assays, In-gel kinase assay, Immunoblotting, qRT-PCR, Root structure architecture (RSA)

1 Introduction

Rice has strongly emerged as a global food staple, catering to the food demands of more than half of the present world population. The surging global population demands have made it daunting for crop breeders and plant biologists to focus their research endeavors on nutritional and food security issues. Plant hormonal signaling networks play decisive roles during the complete life span of plants. Indole-3-acetic acid (IAA) is the predominant form of auxin in plants, while cytokinins, the adenine derivatives are implicated in regulating many developmental aspects. These two pivotal phytohormones play a cardinal role in regulation of root growth, root architecture, vascular and root development. Both auxin and cytokinins regulate root gravitropic responses [1, 2]. An intricate

Thomas Dandekar and Muhammad Naseem (eds.), *Auxins and Cytokinins in Plant Biology: Methods and Protocols*, Methods in Molecular Biology, vol. 1569, DOI 10.1007/978-1-4939-6831-2_7,

transporting array of auxin efflux carriers, i.e., PIN proteins as well as influx carriers, i.e., AUX/LAX proteins which help in substantiating a local maxima and minima of auxin. This localized variation in auxin concentrations is instrumental in mediating numerous downstream effects of auxin signaling.

Besides these pivotal phytohormones, other physiological factor affecting a myriad of environmental, endogenous and developmental cues is the Mitogen Activated Protein Kinase (MAPK) cascade. MAPK cascade is conventionally described as a three-tier phospho-relay signaling module that is evolutionarily conserved across all eukaryotes. Eukaryotic MAPK cascade transduces environmental and developmental triggers into intracellular responses and thus, in turn, play a central role as the controller of gene expression [3–6]. Comprehensively, this divergent signal transduction network causes the activation of various downstream transcription factors and cytosolic proteins, which cause a wide array of transcriptomic, cellular, and physiological responses. Conventionally, this cascade is triggered by activation of mitogen activated protein kinase kinase kinase (MAP3K/MAPKKK/MEKK/MKKK), which phosphorylates and activates the downstream mitogen activated protein kinase kinase (MAPKK/MEKs/MKK) which in turn activates mitogen activated protein kinase (MAPK/MPK) upon phosphorylation [6–8].

Thus, plant physiology is governed by phytohormonal as well as signal transduction interplay. Thus, a thorough inspection in this realm of research is of particular pertinence for understanding plant physiology. This in turn has paved way to better understanding of diverse biological networks and their interplay, resulting in a dramatic drift to identification of multidisciplinary research tools and methods. A deeper and profounder understanding of plant physiology and convergence of diverse pathways would require a "complete-omics approach" encompassing phenotyping both tolerant and sensitive plants, study of their genetic transcripts as well as assessing their translational machinery by analyzing the proteome. Thus, phenomics, genomics as well as proteomic aspects could be helpful in unraveling the complexities and convergence of diverse physiological processes. This approach could further be harnessed to increase crop yield and well-being. With this in the backdrop the present section tries to assess the implications of MAPK signal transduction pathway on auxin and cytokinin crosstalk.

2 Materials

1. *GiA Roots Software Framework*: GiA Roots is a software framework which is especially formulated for high-throughput analysis of root system architecture [9]. This software framework is particularly designed to be user friendly and helps in assessing

Root System Architecture (RSA) traits of rice seedlings. The software is freely accessible at the link http://giaroots.biology.gatech.edu/. The software along with the manual can easily be downloaded in windows as well as Mac operating system compatible versions. The GiA roots software can easily assess around a score of root-specific phenotypic traits which can further help to delineate auxin and cytokinin dependent phenotype influenced by the presence of MAPK signal transduction pathway in the present context.

Note: All buffers are prepared using deionized ultrapure MQ grade water with a sensitivity of 18.2 MΩ cm at 25 °C and analytical grade reagents.

2. *MAP Kinase (MAPK) compatible crude protein extraction buffer*: 50 mM HEPES pH 7.5, 5 mM EDTA, 5 mM EGTA, 1 mM DTT, 10 mM Na_3VO_4, 10 mM NaF, 50 mM β-glycerol-phosphate, 2.5% PVPP, 10% (v/v) glycerol, 1 mM phenylmethylsulfonyl fluoride, and 25 μl of proteinase inhibitor cocktail.
3. *SDS PAGE resolving gel buffer (10%)*: 1.7 ml of 30% acrylamide, 1.3 ml of 1.5 M Tris–HCl, pH 8.8, 50 μl of 10% SDS, 50 μl of ammonium persulfate, and 4 μl of TEMED. The final volume of 5 ml is adjusted with water.
4. *SDS PAGE stacking gel buffer (5%)*: 330 μl of 30% acrylamide, 250 μl of 1.0 M Tris–HCl, pH 6.8, 20 μl of 10% SDS, 20 μl of ammonium sulfate, and 2 μl of TEMED. The final volume of 2 ml is adjusted with water.
5. *Tris–glycine gel running buffer*: A working concentration of 5 mM Tris–HCl, 250 mM glycine, and 0.1% SDS pH adjusted to 8.0. Note: Generally, a stock of 10× of the Tris-glycine gel running buffer is prepared and diluted to 1× for running the SDS-PAGE at the required time.
6. *Protein loading SDS dye*: 0.225 mM Tris-Cl (pH 6.8), 50% Glycerol, 5% SDS, 0.05% bromophenol blue, and 0.25 M DTT.
7. *In-solution kinase reaction buffer*: 25 mM Tris–HCl pH 7.5, 1 mM EGTA, 5 mM $MgCl_2$, 1 mM DTT, 1 μM ATP, and 0.10 μCi/μl γ^{32}P-ATP.
8. *Immunoblotting buffers*:

   Transfer buffer: Tris 48 mM, 39 mM glycine, and 20% methanol

   TBST buffer: 10 ml of Tris–HCl pH 7.5, 37.5 ml of 4 M NaCl, and 1 ml of 20% Tween 20 are mixed to a final volume for 1 L.
9. *In-gel kinase buffers*:

   Wash buffer: 25 mM Tris–HCl pH 7.5, 0.5 mM DTT, 5 mM Na_3VO_4, 0.1 mM NaF, 0.5 mg/ml BSA, and 0.1% Triton

X-100. Renaturation buffer: 25 mM Tris–HCl pH 7.5, 0.5 mM DTT, 5 mM Na_3VO_4, and 0.1 mM NaF. Reaction buffer: 25 mM Tris–HCl pH 7.5, 2 mM EGTA, 12 mM $MgCl_2$, 1 mM DTT, 0.1 mM Na_3VO_4, 1 μM ATP, and 50 μCi of γ^{32}P-ATP (3000 Ci/mmol).

3 Methods

3.1 Plant Growth Conditions and Phytohormonal Treatments

1. For exogenous phytohormonal treatments grow rice seedlings in ½ MS (Murashige and Skoog) media in sterile large glass containers in growth chamber at 30 °C with 16/8 day light condition for the stipulated period of time (*see* **Note 1**).
2. Give exogenous hormone treatments of auxin and cytokinin by germinating and growing plants in the presence of 1 and 5 μM of indole-3-acetic acid (IAA) and 6-benzylaminopurine (BAP) supplemented in ½ MS media, respectively.
3. Complete rice seedlings, roots, or shoots in particular can be used for the assays as per the experimental demands.

3.2 Phenomic Analysis of Rice Seedlings Post Auxin and Cytokinin Treatment Using GiA Roots Software

1. The phytohormone-treated rice roots can be analyzed by rotating at a definitive angel of 360° and capturing an image for every 18°, resulting in the generation of a total of 20 snap shots (*see* Fig. 1).
2. All these 20 images are first cropped and processed by the initial section of the software. Further these cropped images are processed for generation of threshold images which serve as tools for analyzing various phenotypic parameters like average root width (diameter), network bushiness, number of connected components, network depth, ellipse axes ratio, network length distribution, major ellipse axis, maximum number of roots, network width, median number of roots, minor ellipse axis, network area, network convex area, network perimeter, network solidity, specific root length, network surface area, network length, network volume, and network width-to-depth ratio (*see* Fig. 1).
3. All these factors or a few of them could be monitored as per the experimental design and requirements.

3.3 Genomic Analysis of Rice Seedlings Post Auxin and Cytokinin Using Quantitative Real Time PCR Assay

1. After total RNA isolation (*see* **Notes 2, 3**) post hormone treatment, synthesize first strand cDNA using any commercially available first strand cDNA synthesis kit following the directions of the manufacturer.
2. Before starting with the cDNA synthesis, treat total RNA with 10 U of RNase-free DNase I. Further, combine total RNA (1–5 μg) with 0.5 μg of oligo$(dT)_{18}$ and DEPC treated water

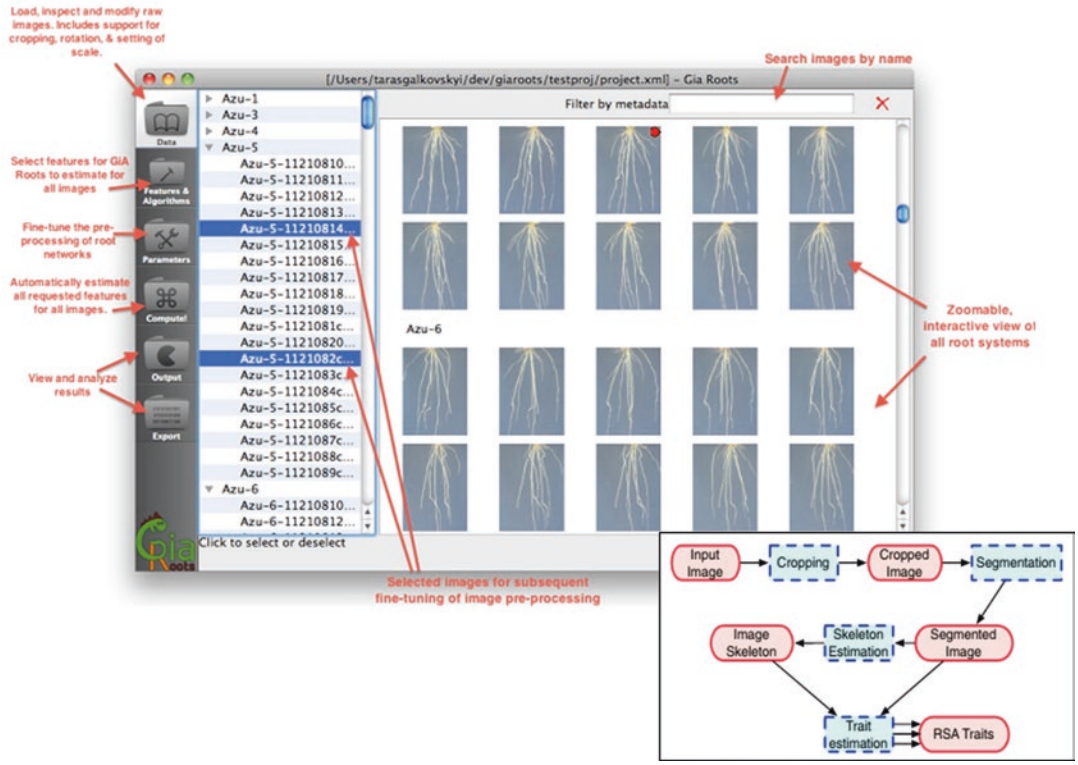

Fig. 1 An annotated snapshot of GiA roots software framework [9]. GiA Roots is an application that provides a user interface to manage input images, define a processing pipeline and manage output. It features a main window with several task windows that can be accessed through the left sidebar. Sequential access to each window page accomplishes major tasks: managing data; selecting traits to measure; tweaking parameters; performing processing; reviewing the results. This linear design helps users to keep track of progress and proceed intuitively with processing of the data. The *lower panel* depicts data types enclosed in *ellipses*, interactions are enclosed in *rectangles*. Interactions are realized by plugins, and have several variants [9]

to make the reaction volume upto 12 μl and incubate the reaction mix at 70 °C for 5 min followed by chilling on ice and briefly centrifuged.

3. Add 5× reaction buffer (4 μl), 10 mM dNTP mix (2 μl), Ribolock Ribonuclease inhibitor (1 μl), mix gently, and incubate at 37 °C for 5 min.
4. Finally, add 1 μl reverse transcriptase (200 U/μl) and incubate the components at 42 °C for 1 h and finally reaction is stopped by heating at 70 °C for 10 min.

3.4 Quantitative-Real Time PCR Analysis

1. Perform qRT-PCR in a 10-μl reaction using SYBR Green PCR master mix. Carry out the qRT-PCR in 384-well plate in the sequence detection system, as described previously [6, 10].
2. Calculate the relative expression level of each gene using the $2^{-\Delta\Delta CT}$ method [11] and by normalizing against an internal reference in accordance with the experimental setup. Use specific

primer pairs for qRT-PCR analyses of different genes that are designed by the specific software provided with the qRT-PCR system (*see* **Note 4**).

3.5 Proteomic Analysis of Rice Seedlings Post Auxin and Cytokinin Treatment Using Various Kinase Assays

1. *SDS-PAGE*
   SDS-PAGE is performed using 10% gels using the composition described in Subheading 2. The protein samples are denatured by adding the protein SDS dye and boiling for 5 min. After running the gel is either stained in Coomassie brilliant blue R-250 (CBB-0.2%, 50% methanol, 10% acetic acid) and destained by destaining solution (40% methanol, 10% HCOOH) for visualizing the proteins or transferred to the nitrocellulose membrane for immunoblotting protocols.
2. *MAPK Activity Assay*
   Grind rice seedlings post auxin and cytokinin treatment for the stipulated time point in liquid nitrogen. Isolate proteins by using MAP kinase compatible protein extraction buffer and then quantify them by using Bradford assay [12]. Separate total protein (30–40 μg) by 10% sodium dodecyl sulfate–polyacrylamide gel electrophoresis (SDS-PAGE), and later perform immunoblotting analysis by using the desired MAPK specific antibodies. Transfer the proteins from the gel to the membrane at 100 mA for 1 h in transfer buffer in a semidry transferring module as per manufacturer's instructions. After the transfer of proteins, stain the membrane with Ponceau to confirm the transfer of proteins. Incubate the membrane for 1 h in blocking buffer (5% nonfat dry milk in TBST pH 7.4) at room temperature. Then incubate the membrane in primary antibody diluted according to manufacturer's instructions in TBST-milk buffer for 2 h at room temperature. Wash the membrane with TBST five times (10 min of every single wash). Add secondary antibody conjugated with HRP diluted in TBST-milk as per instruction and add again for 2 h at room temperature. Wash the membrane three times with TBST buffer and perform western blot using western chemiluminescent HRP substrate kit according to manufacturer's instructions.
3. *In-gel kinase assay*
   Carry out in-gel kinase assay [13–15] by fractionating 20 μg of total protein on a 10% polyacrylamide gel containing 0.1% SDS and 0.5 mg/ml bovine brain myelin basic protein (MBP). After electrophoresis, remove the SDS from the gel with serial incubations with wash buffer for 30 min, 1 h at RT. Then perform renaturation in renaturation buffer at 4 °C first for 1 h then 2 h and lastly overnight. Perform MBP phosphorylation by incubating the gel in 20 ml of reaction buffer for 1 h at room temperature. Wash the gel three times with 5% TCA and 1% sodium pyrophosphate and autoradiographed.

4 Notes

1. Estimation of Root System Architecture (RSA) traits may give a deeper understanding of rice phenotype and in turn physiology. The elucidation of phenotypic characters may be helpful in deciphering various complex nexuses of plant growth and development [6].
2. Isolation of total RNA by TRIzol method. Prior to RNA isolation by TRIzol method. All the glassware and plasticware used are treated with 3% H_2O_2 to avoid RNase contamination. Tissue samples (100–250 mg) are pulverized with liquid N_2 and homogenized properly with 1 ml TRIzol reagent (phenol-guanidine isothiocyanate). For separation of aqueous and organic phases, 200 μl chloroform is added, mixed well and incubated at room temperature for 15 min. The mixture is centrifuged at 12,000 rpm for 15 min. The aqueous phase containing RNA is collected in fresh microcentrifuge tube and precipitated with isopropanol on ice for 10 min followed by centrifugation at 13,000 rpm for 15 min. The RNA pellet is further washed with 70% ethanol at $6000 \times g$ for 10 min followed by air drying the pellet. Finally, the pellet is dissolved in 20 μl of DEPC treated sterile water. The intactness of RNA is determined by separating on a 1.5% agarose gel.
3. RNA quantification. The quality and quantity of RNA are determined by measuring the absorbance at 260 and 280 nm. The concentration of RNA is calculated by comparing with the standard value, i.e., 1 $OD_{260} = 40$ μg/ml. The purity of RNA is determined by calculating the ratio A_{260}/A_{280} for each sample. The RNA samples with A_{260}/A_{280} ratio of 1.8–2.0 are considered pure.
4. Note: the primers are cross-checked for secondary structures as well as dimerization properties. Primers have no or negligible structure and those not forming primer dimers are preferred over the other pairs.

Acknowledgments

The authors extend their gratitude to the Department of Biotechnology (DBT), Government of India and National Institute of Plant Genome Research (NIPGR), New Delhi, India for financial support. Council of Scientific and Industrial Research (CSIR), Government of India is duly acknowledged for providing fellowship to PS.

References

1. Muller B, Sheen J (2008) Cytokinin and auxin interaction in root stem-cell specification during early embryogenesis. Nature 453:1094–1097. doi:10.1038/nature06943, PMID: 18463635
2. Bishopp A, Benkova E, Helariutta Y (2011) Sending mixed messages: auxin-cytokinin crosstalk in roots. Curr Opin Plant Biol 14:10–16. doi:10.1016/j.pbi.2010.08.014, PMID: 20926335
3. Colcombet J, Hirt H (2008) Arabidopsis MAPKs: a complex signalling network involved in multiple biological processes. Biochem J 413:217–226. doi:10.1042/BJ20080625, PMID: 18570633
4. Taj G, Agarwal P, Grant M, Kumar A (2010) MAPK machinery in plants: recognition and response to different stresses through multiple signal transduction pathways. Plant Signal Behav 5:1370–1378, PMID: 20980831
5. Doczi R, Okresz L, Romero AE, Paccanaro A, Bogre L (2012) Exploring the evolutionary path of plant MAPK networks. Trends Plant Sci 17:518–525. doi:10.1016/j.tplants.2012.05.009, PMID: 22682803
6. Singh PS, Mohanta TK, Sinha AK (2015) Unraveling the intricate nexus of molecular mechanisms governing rice root development: OsMPK3/6 and auxin-cytokinin interplay. PLoS One 10(4):e0123620. doi:10.1371/journal.pone.0123620
7. Sinha AK, Jaggi M, Raghuram B, Tuteja N (2011) Mitogen-activated protein kinase signaling in plants under abiotic stress. Plant Signal Behav 6:196–203
8. Rodriguez MC, Petersen M, Mundy J (2010) Mitogen-activated protein kinase signaling in plants. Annu Rev Plant Biol 61:621–649. doi:10.1146/annurev-arplant-042809-112252, PMID: 20441529
9. Galkovskyi T, Mileyko Y, Bucksch A, Moore B, Symonova O, Topp CN et al (2012) GiA Roots: software for the high throughput analysis of plant root system architecture. BMC Plant Biol 12:116. doi:10.1186/1471-2229-12-116, PMID: 22834569
10. Raghuram B, Sheikh AH, Sinha AK (2014) Regulation of MAP kinase signaling cascade by microRNAs in Oryza sativa. Plant Signal Behav 9
11. Livak KJ, Schmittgen TD (2001) Analysis of relative gene expression data using real-time quantitative PCR and the 2(−Delta Delta C(T)). Methods 25:402–408, PMID: 11846609
12. Bradford MM (1976) A rapid and sensitive method for the quantitation of microgram 882 quantities of protein utilizing the principle of protein-dye binding. Anal Biochem 72:248–254
13. Raina SK, Wankhede DP, Jaggi M, Singh P, Jalmi SK, Raghuram B et al (2012) CrMPK3, a mitogen activated protein kinase from Catharanthus roseus and its possible role in stress induced biosynthesis of monoterpenoid indole alkaloids. BMC Plant Biol 12:134. doi:10.1186/1471-2229-12-134, PMID: 22871174
14. Rao KP, Vani G, Kumar K, Wankhede DP, Misra M, Gupta M et al (2011) Arsenic stress activates MAP kinase in rice roots and leaves. Arch Biochem Biophys 506:73–82. doi:10.1016/j.abb.2010.11.006, PMID: 21081102
15. Sethi V, Raghuram B, Sinha AK, Chattopadhyay S (2014) A. mitogen-activated protein kinase cascade module, MKK3-MPK6 and MYC2, is involved in blue light-mediated seedling development in Arabidopsis. Plant Cell 26:3343–3357. doi:10.1105/tpc.114.128702, PMID: 25139007

Chapter 8

Quantification of Cytokinin Levels and Responses in Abiotic Stresses

Alfonso Albacete

Abstract

Since their discovery in the 1950s, it has been established that cytokinins (CKs) play important regulatory roles in various physiological processes in plants. Only recently have CKs been also implicated in the response of plants to biotic and abiotic stresses. During the last years, several analytical methods have been developed to determine CK concentrations in plant tissues. Here we present a simple and robust method for CK extraction, purification and analysis in plant tissues, using ultrahigh-performance liquid chromatography coupled to high resolution mass spectrometry (U-HPLC-HRMS). The main advantage of this methodology is the simplicity of the purification protocol and the possibility to extend it to the analysis of other plant hormones and derivatives.

Key words Plant hormones, Cytokinins, Abiotic stress, Quantification, Internal standards, High-resolution mass spectrometry

1 Introduction

Cytokinins (CKs) are plant hormones implicated in many aspects of plant growth and development, including cell division, shoot initiation and growth, leaf senescence, apical dominance, source–sink relationships, nutrient uptake, phyllotaxis, vascular, gametophyte, and embryonic development, as well as in the response to biotic and abiotic factors [1, 2]. To date, naturally occurring CKs are adenine derivatives carrying either an isoprene-derived or an aromatic side chain at the N^6 terminus [3]. They are conventionally called "isoprenoid CKs" or "aromatic CKs," respectively, based on the nature of their side chain (Fig. 1). An isoprenoid CK is either an isopentenyladenine (iP)-type CK, which carries an isopentenyl N^6 side chain, or a zeatin-type CK, which carries a hydroxylated isopentenyl N^6 side chain. The side chain of a zeatin-type CK occurs in either the *cis* or *trans* configuration, depending on

Thomas Dandekar and Muhammad Naseem (eds.), *Auxins and Cytokinins in Plant Biology: Methods and Protocols*, Methods in Molecular Biology, vol. 1569, DOI 10.1007/978-1-4939-6831-2_8,

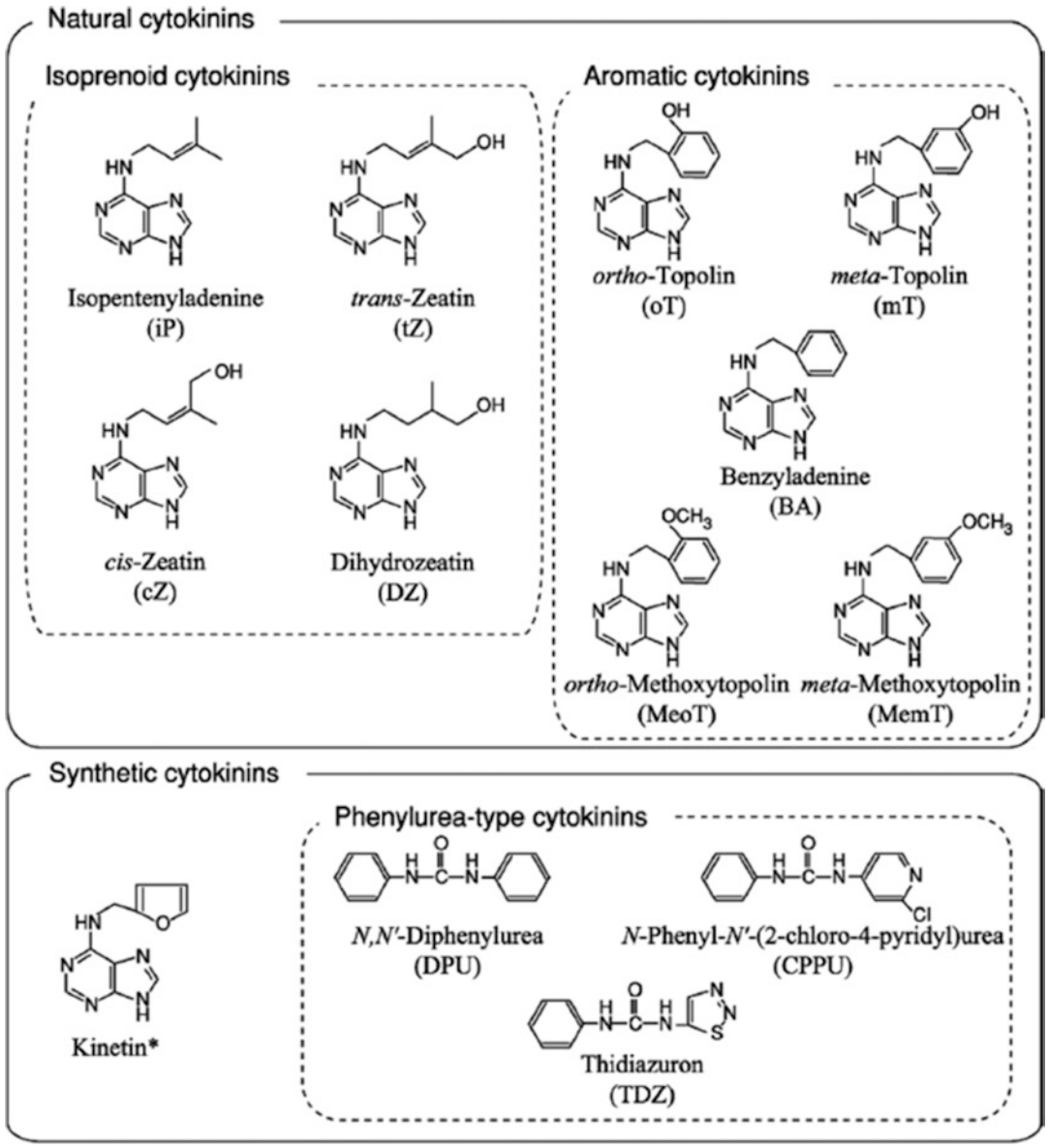

Fig. 1 Structures of representative active and synthetic cytokinin species; only trivial names are shown. Commonly used abbreviations in *parentheses*

which of the two methyl groups of the side chain is hydroxylated [4]. In most cases, naturally occurring CKs are also present in plant tissues as the corresponding nucleosides, nucleotides and glycosides.

Abiotic stresses modify source–sink relations which influence plant growth and adaptation to stress, thus affecting plant productivity [5–7]. Growth regulation under abiotic stress conditions is mediated primarily by the stress-related hormones abscisic acid

(ABA) and ethylene [8–10]. However, other hormones, such as auxins and CKs are also involved [6, 7, 9, 11–16], and therefore, an appropriate manipulation of CK levels is necessary to increase not only leaf longevity and photosynthetic capacity but also growth of sink organs under abiotic stress.

Diverse analytical methods have been developed in the past few decades for the accurate identification and quantitative determination of plant hormones and related compounds. Each class of phytohormones possesses its specific chemical characteristic as well as its physiological effect at trace concentrations, which makes their identification and quantification difficult [17]. In many cases though, a profiling of a single phytohormone class, for example CKs [18] or an analysis of the most active or most analysis-technique suitable compound of the selected class is used in such studies [19]. However, various phytohormones are being involved in many different processes and they do not act in isolation, but are prone to crosstalk in a way of modulating each other's biosynthesis or responses [20]. Therefore, although this chapter focuses on the quantification of CKs, the method described here is also valid for simultaneous profiling of multiple classes of plant hormones.

The determination of plant hormones, in general, and CKs, in particular, in complex biological samples requires extensive sample preparation techniques prior to instrumental analysis. Sample preparation has become a major bottleneck, with a wide array of techniques being used, including sampling, extraction, purification, derivatization and concentration methods [18, 21–24]. Detection techniques generally involve bioassays, immunoassays, electroanalysis, and most importantly, chromatographic methods such as capillary electrophoresis or high-performance liquid chromatography (HPLC) connected to various detectors. Especially HPLC coupled to mass spectrometry has shown good separation, robustness and qualitative abilities, therefore representing a powerful and up-to-date tool for the detection of various phytohormones in complex plant samples [18, 21–23]. Particularly, coupling (ultra) HPLC to high resolution mass spectrometry (HRMS) performed with the Orbitrap Mass Spectrometer facilitates the quantification of plant hormones and metabolites present at relatively low concentrations in plant extracts with respect to hundreds of other more abundant compounds [25].

2 Materials

The solvents utilized in this protocol are of HPLC-MS grade. Water used is deionized, using a Milli-Q system (18.2 MΩ cm at 25 °C). All chemicals and solvents are used as received, without further purification.

2.1 CK Extraction and Purification

1. *Solution of plant hormones*: This solution contains the following CKs at a concentration of 0.4 μg/ml in methanol–water (80:20, v/v): *trans*-zeatin (Z), isopentenyladenine (iP), dihydrozeatin (DHZ), isopentenyladenine 9-glucoside (iP9G), *trans*-zeatin riboside (ZR), *trans*-zeatin 9-glucoside (Z9G) (OlChemIm Ltd., Olomouc, Czech Republic) (*see* **Note 1**).
2. *Solution of internal standard*: This solution contains the following deuterated version of the CKs at a concentration of 0.4 μg/ml: [$^2H_5$]*trans*-zeatin (D-tZ), [$^2H_6$]N^6isopentenyladenine (D-iP), [$^2H_3$]dihydrozeatin (D-DHZ), [$^2H_6$]N^6-isopentenyladenine 9-glucoside (D-iP9G), [$^2H_5$]*trans*-zeatin riboside (D-ZR), [$^2H_5$]*trans*-zeatin 9-glucoside (D-Z9G) (OlChemIm Ltd., Olomouc, Czech Republic) (*see* **Note 2**).
3. *Extraction solvent*: The solvent used for CK extraction is methanol–water (80:20, v/v) (*see* **Note 3**).
4. Ready-to-use solid phase extraction (SPE) C_{18} cartridges (Chromafix, Macherey-Nagel, Düren, Germany) (*see* **Note 4**).
5. *Equilibrating solution*: The solution used for the equilibration of the SPE C_{18} cartridges is the extraction solvent.
6. *Eluting solution*: The solvent used for eluting dry pellets prior HPLC-MS injection is methanol–water (20:80, v/v) (*see* **Note 5**).

2.2 LC-MS Analysis and Quantification

1. The U-HPLC-MS system consists of an Accela Series U-HPLC (ThermoFisher Scientific, Waltham, MA, USA) coupled to an Exactive mass spectrometer (Orbitrap technology, ThermoFisher Scientific, Waltham, MA, USA) using a heated electrospray ionization (HESI) interface (*see* **Note 6**).
2. Accucore reversed-phase column (50 × 2.1 mm) which contains solid core particles, engineered to a diameter of 2.6 μm and a very narrow particle size distribution (*see* **Note 7**).
3. *Calibration solutions*: Six to eight calibration solutions should be prepared in order to adequately describe the calibration equations for each CK analyzed. These standard solutions should contain each hormone in equal concentration, in the range of concentration expected for the samples (from 0.1 to 100 ng/ml), along with 10 ng/ml of each internal standard (*see* **Note 8**).

3 Methods

This method is applicable to a variety of plant tissues and organs, such as leaves, roots, stems, seeds, fruits, flowers, and requires a minimum of 75 mg fresh weight or 20 mg dry weight of plant material. The main advantage of this method is the simplicity of the extraction and purification protocol, which takes only a few

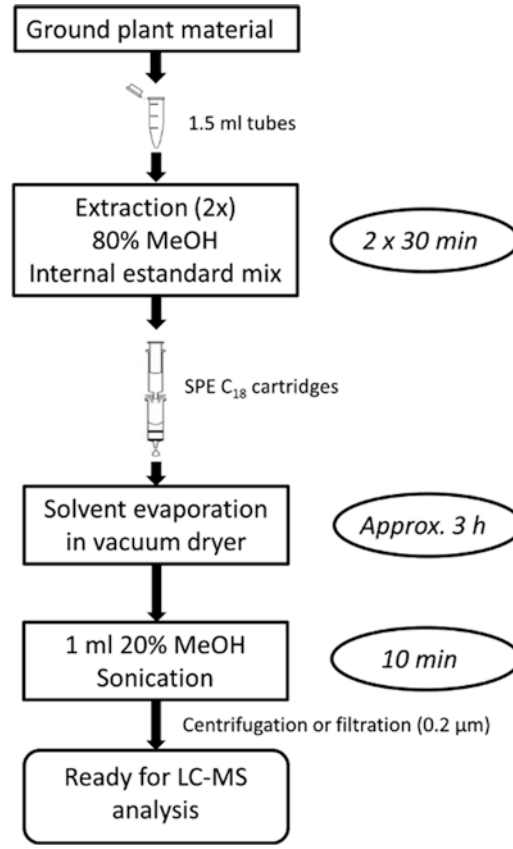

Fig. 2 Flowchart showing the individual steps of cytokinin extraction and purification

hours (the most time consuming step is the dryness process under vacuum), while the HPLC-MS analysis takes only 10 min. A schematic flow chart of the extraction and purification procedure is shown in Fig. 2. However, due to the number of CKs (and other potential analytes), an initial tuning of the mass spectrometer parameters is required, which could take some weeks to be accomplished. Another important advantage of this method is that it could be extended to the analysis of other plant hormone classes and derivatives, as a simple and robust protocol for simultaneous analysis of complex plant matrixes.

3.1 CK Extraction and Purification

1. Collect plant tissues and immediately freeze them by immersing in liquid nitrogen, and store at −80 °C until analysis. Alternatively, samples could be lyophilized in a freeze-drier and stored in the fridge at 4 °C until analysis.
2. Grind the frozen or lyophilized plant material to a fine and homogenous powder in a ball mill (*see* **Note 9**).

3. Weigh out the homogenized fresh or lyophilized plant material in a 1.5 ml tube. Add 4 ml of internal standard mix at a concentration of 10 ng/ml and 5 or 20 µl of extraction solution per mg of fresh or lyophilized plant material, respectively. Shake the tubes in a vortex for at least 30 s and place them on an orbital shaker at 4 °C for 30 min (*see* **Note 10**).
4. After extraction, shake the tubes in a vortex for 30 s, and centrifuge them at 20,000 × *g* and 4 °C for 15 min. Transfer the supernatant to a glass test tube (13 × 100 mm), and keep at 4 °C.
5. Re-extract the pellets with the same amount of extraction solution, repeating the two previous steps, and mix the two supernatants obtained per sample.
6. Equilibrate each SPE cartridge with 3 ml of equilibrating solution.
7. Pass each supernatant through a SPE C_{18} cartridge (*see* **Notes 11** and **12**), and collect them in glass test tubes (13 × 100 mm).
8. Evaporate the solvents of the samples in a vacuum dryer (*see* **Note 13**) at 40 °C and 400 rpm for 3 h (*see* **Note 14**).
9. Elute the residue with 1 ml of eluting solution in a 1.5 ml tube.
10. Sonicate the tubes in an ultrasonic bath for 10 min at room temperature (*see* **Note 15**) to facilitate the resuspension of the dried residue in the eluting solution.
11. Centrifuge the samples at 20,000 × *g* for 15 min (*see* **Note 16**).
12. Pipet the samples in a 96-well plate together with the calibration solutions, cover with plastic film and store at −80 °C until analysis (*see* **Note 17**).

3.2 LC-MS Analysis and Quantification

1. Set the pump flow to 300 µl/min in order to equilibrate the HPLC column during 15 min with the initial mobile phase (80 % water) (*see* **Note 18**).
2. Put the 96-well plate in the auto-sampler and define the sequence with the Excalibur software (ThermoFisher Scientific, Waltham, MA, USA).
3. Load the previously optimized HPLC method in the Excalibur software (ThermoFisher Scientific, Waltham, MA, USA). We used a gradient with two mobile phases (aqueous and organic, *see* **Note 19**).
4. Load the previously optimized MS method in the Exactive Tune software (ThermoFisher Scientific, Waltham, MA, USA). We perform the analyses in the negative mode $[M\text{-}H]^-$ because the method has been optimized for a vast range of hormones and derivatives, and not only for CKs (*see* **Notes 20** and **21**).

5. Run the sequence. The time of analysis per sample is 10 min (*see* **Note 22**).
6. Record the total ion chromatograms of the samples and extract the specific chromatogram of each compound with a mass tolerance of 5 ppm, using the Excalibur software (ThermoFisher Scientific, Waltham, MA, USA) (Fig. 3, *see* **Note 23**). Table 1 shows the exact mass of the CKs analyzed.
7. Set up the retention times and exact masses of the different CKs and define the calibration levels of the analytes and internal standards, prior to the quantification of CK concentrations (*see* **Note 24**).
8. Concentrations and recovery rates of the different CKs in the samples are calculated according to the internal standard method (*see* **Note 25**).

4 Notes

1. This standard solution should be freshly prepared before use, from stock solutions of the different hormones at higher concentrations (typically 50 mg/l or higher). These are the most representative CKs, but other CKs and derivatives could be also included in the analysis.
2. The internal standard mix should be also freshly prepared before use, from stock solutions of the different deuterated compounds at higher concentrations (typically 50 mg/l or higher).
3. Different percentages of organic solvent/water could be also used. The extraction solution could be slightly acidified with 1 % of acetic acid (glacial) 99.9+% purity.
4. Any other SPE C_{18} cartridge of similar characteristics could be used.
5. The percentage of organic solvent/water should be similar to that of the initial conditions of the (U)-HPLC mobile phase gradient.
6. Triple-quadrupole mass spectrometers are also widely used, but the molecules must be fractionated (MS/MS) because the resolution is lower than that of the Orbitrap spectrometer.
7. Other columns are also suitable depending on the (U)-HPLC system used (normally reversed-phase columns).
8. This is a typical calibration range in the plant material, but can be adjusted to the characteristics of the samples analyzed.
9. Samples can also be ground with a mortar.

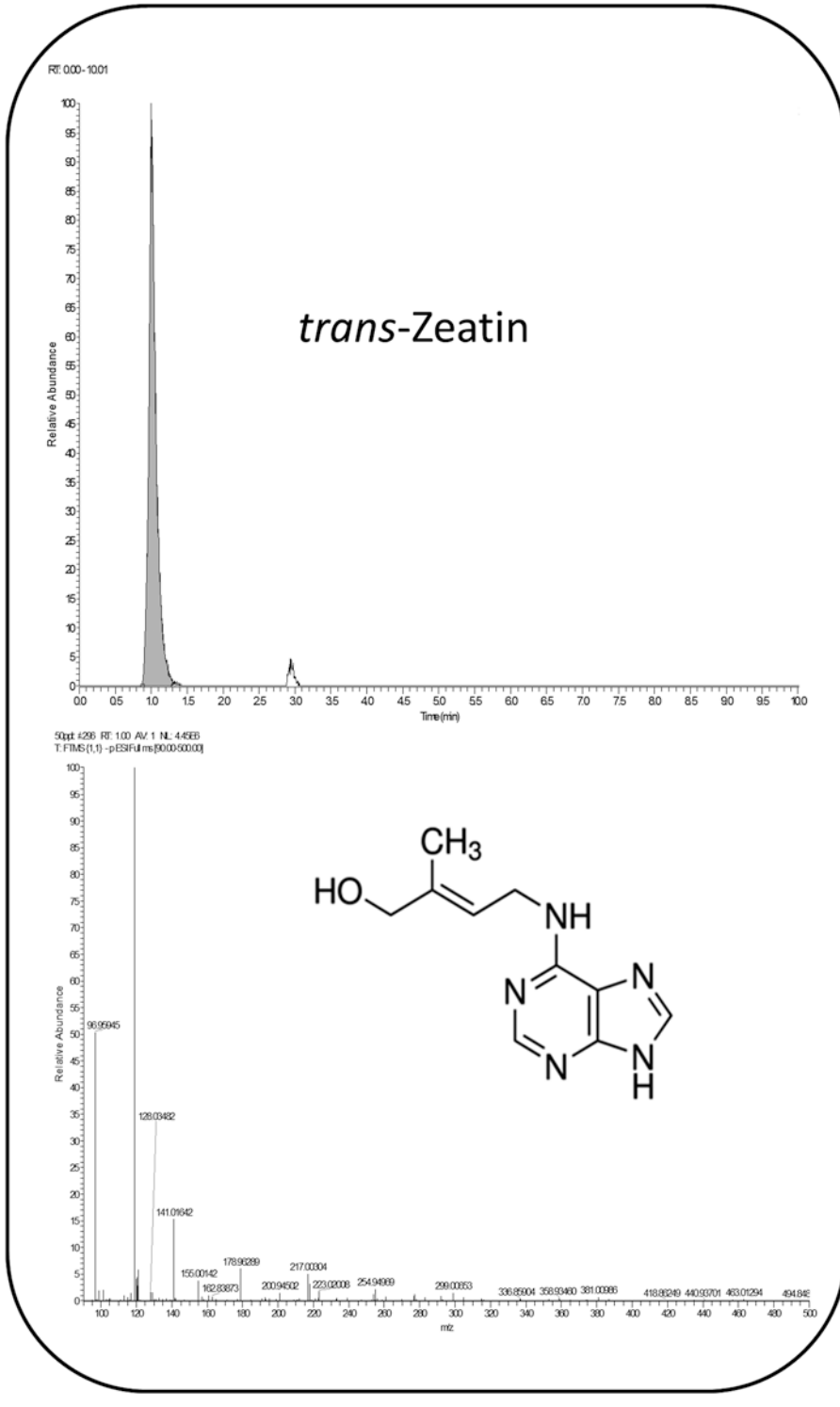

Fig. 3 Representative chromatogram (*upper panel*) and spectrum (*lower panel*) of *trans*-zeatin

Table 1
List of representative cytokinins (CKs) and exact masses of the corresponding negative ions

CKs	Molecular formula	$[M-H]^-$
trans-zeatin (Z)	$C_{10}H_{13}N_5O$	218.10473
Isopentenyladenine (iP)	$C_{10}H_{13}N_5$	202.10982
Dihydrozeatin (DHZ)	$C_{10}H_{15}N_5O$	220.12038
Isopentenyladenine 9-glucoside (iP9G)	$C_{16}H_{23}N_5O_5$	364.16264
trans-zeatin riboside (ZR)	$C_{15}H_{21}N_5O_5$	350.14699
trans-zeatin 9-glucoside (Z9G)	$C_{16}H_{23}N_5O_6$	380.15756
D-CKs	Molecular formula	$[M-H]^-$
$[^2H_5]$*trans*-zeatin (D-Z)	$C_{10}H_8{}^2H_5N_5O$	223.13612
$[^2H_6]$isopentenyladenine (D-iP)	$C_{10}H_7{}^2H_6N_5$	208.14748
$[^2H_3]$dihydrozeatin (D-DHZ)	$C_{10}H_{12}{}^2H_3N_5O$	223.13921
$[^2H_6]$isopentenyladenine 9-glucoside (D-iP9G)	$C_{16}H_{17}{}^2H_6N_5O_5$	370.20030
$[^2H_5]$*trans*-zeatin riboside (D-ZR)	$C_{15}H_{16}{}^2H_5N_5O_5$	355.17838
$[^2H_5]$*trans*-zeatin 9-glucoside (D-Z9G)	$C_{16}H_{18}{}^2H_5N_5O_6$	385.18894

10. It is desirable that the whole extraction and purification process is done under low light conditions, since some hormones are very sensitive to light.
11. This process should be carried out slowly. It removes proteins, lipids, and pigments, which may interfere in the analysis by HPLC-MS.
12. In the case of technical or biological replicates of plant material, the cartridges can be reused up to three times.
13. We use a Univapo 150 ECH vacuum dryer coupled to a Unicryo MC2L (−60 °C) unit (Uniequip, Planegg, Germany), but any similar vacuum dryer of similar characteristics could be employed.
14. The time needed for total dryness depends on the amount of solvent and the sample characteristics.
15. The ultrasonic bath that we use to resuspend the samples is an Ultrasons H-D system (Selecta, Barcelona, Spain). Any other similar ultrasonic bath is also suitable for eluting the samples.
16. Alternatively, samples could be also filtrated through 13 mm diameter Millex filters with 0.22 μm pore size and nylon membrane (Millipore, Bedford, MA, USA).
17. The ACCELA auto-sampler allows the use of different plates, facilitating the final preparation of the samples, but normal HPLC vials could be also use.

18. These parameters could be modified and adjusted depending on the (U)-HPLC system employed.
19. The method should be optimized for the specific (U)-HPLC used.
20. In fact, the MS tune will vary depending on the analyte and the MS used, so it has to be optimized before. The typical instrument settings include: sheath gas flow rate = 35 ml/min, auxiliary gas flow rate = 10 ml/min, spray voltage = 2.5 kV, capillary temperature = 275 °C, capillary voltage = −40 V, tube lens voltage = −110 V, skimmer voltage = −20 V.
21. Due to the high resolution of the Orbitrap, we record the total ion chromatogram of the samples and do not fragmentate the molecules. However, it is also possible to fragmentate to distinguish between two different CKs with the same *m/z*.
22. The time of analysis could vary depending on the LC system used. In the case of ultra-HPLC systems this time could be reduced up to less than 10 min. In the normal HPLC systems the time of analysis is 30 min or even higher.
23. We detect the ions by exact mass due to the high resolution of the Orbitrap (up to 100,000) and it is therefore possible to set a mass tolerance window of 5 ppm. With other lower resolution mass spectrometers (i.e., triple quadrupole), ion fragmentation is required.
24. This processing setup allows the determination of the limit of detection (LOD) and limit of quantification (LOQ) of each compound analyzed.
25. Acceptable recovery rates are those higher than 75 %.

Acknowledgments

I would like to thank CSIC (Spain) for a postdoc research grant (JAE program), Prof. Francisco Pérez-Alfocea for supporting my research, and Ms. Cristina Soriano-Carpena for her help in editing the English version of the manuscript. Research funded by the Spanish MINECO-FEDER (project AGL2014-59197-JIN).

References

1. Sakakibara H (2006) Cytokinins: activity, biosynthesis, and translocation. Annu Rev Plant Biol 57:431–449
2. Kieber JJ, Schaller GE (2014) Cytokinins. The Arabidopsis Book 12:e0168
3. Mok DWS, Mok MC (2001) Cytokinin metabolism and action. Annu Rev Plant Biol 52:89–118
4. Kakimoto T (2001) Identification of plant cytokinin biosynthetic enzymes as dimethylallyl diphosphate: ATP/ADP isopentenyltransferases. Plant Cell Physiol 42:677–685
5. Albacete A, Martínez-Andújar C, Pérez-Alfocea F (2014) Hormonal and metabolic regulation of source–sink relations under

salinity and drought: from plant survival to crop yield stability. Biotechnol Adv 32:12–30

6. Albacete A, Cantero-Navarro E, Großkinsky DK, Arias CL, Balibrea ME, Bru R, Fragner L, Ghanem ME, González MC, Hernández JA, Martínez-Andújar C, van der Graaff E, Weckwerth W, Zellnig G, Pérez-Alfocea F, Roitsch T (2015) Ectopic overexpression of the cell wall invertase gene CIN1 leads to dehydration avoidance in tomato. J Exp Bot 66:863–878
7. Albacete A, Cantero-Navarro E, Balibrea ME, Großkinsky DK, de la Cruz González M, Martínez-Andújar C, Smigocki AC, Roitsch T, Pérez-Alfocea F (2014) Hormonal and metabolic regulation of tomato fruit sink activity and yield under salinity. J Exp Bot 65: 6081–6095
8. Dodd IC, Davies WJ (1996) The relationship between leaf growth and ABA accumulation in the grass leaf elongation zone. Plant Cell Environ 19:1047–1056
9. Albacete A, Ghanem ME, Martínez-Andújar C, Acosta M, Sánchez-Bravo J, Martínez V, Lutts S, Dodd IC, Pérez-Alfocea F (2008) Hormonal changes in relation to biomass partitioning and shoot growth impairment in salinized tomato (*Solanum lycopersicum* L.) plants. J Exp Bot 59:4119–4131
10. Ghanem ME, Albacete A, Martínez-Andújar C, Acosta M, Romero-Aranda R, Dodd IC, Lutts S, Pérez-Alfocea F (2008) Hormonal changes during salinity-induced leaf senescence in tomato (*Solanum lycopersicum* L.). J Exp Bot 59:3039–3050
11. Magome H, Yamaguchi S, Hanada A, Kamiya Y, Oda K (2004) Dwarf and delayed-flowering 1, a novel Arabidopsis mutant deficient in gibberellin biosynthesis because of overexpression of a putative AP2 transcription factor. Plant J 37:720–729
12. Achard P, Cheng H, De Grauwe L, Decat J, Schoutteten H, Moritz T, Van Der Straeten D, Peng J, Harberd NP (2006) Integration of plant responses to environmentally activated phytohormonal signals. Science 311:91–94
13. Rivero RM, Kojima M, Gepstein A, Sakakibara H, Mittler R, Gepstein S, Blumwald E (2007) Delayed leaf senescence induces extreme drought tolerance in a flowering plant. Proc Natl Acad Sci U S A 104:19631–19636
14. Magome H, Yamaguchi S, Hanada A, Kamiya Y, Oda K (2008) The DDF1 transcriptional activator upregulates expression of a gibberellin-deactivating gene, GA2ox7, under high-salinity stress in Arabidopsis. Plant J 56: 613–626
15. Pérez-Alfocea F, Albacete A, Ghanem ME, Dodd IC (2010) Hormonal regulation of source-sink relations to maintain crop productivity under salinity: a case study of root-to-shoot signalling in tomato. Funct Plant Biol 37:592–603
16. Ghanem ME, Albacete A, Smigocki AC, Frébort I, Pospisilová H, Martínez-Andújar C, Acosta M, Sánchez-Bravo J, Lutts S, Dodd IC, Pérez-Alfocea F (2011) Root-synthesized cytokinins improve shoot growth and fruit yield in salinized tomato (*Solanum lycopersicum* L.) plants. J Exp Bot 62:125–140
17. Pan X, Wang X (2009) Profiling of plant hormones by mass spectrometry. J Chromatogr B Analyt Technol Biomed Life Sci 877:2806–2813
18. Novák O, Hauserová E, Amakorová P, Doležal K, Strnad M (2008) Cytokinin profiling in plant tissues using ultra-performance liquid chromatography-electrospray tandem mass spectrometry. Phytochemistry 69:2214–2224
19. Kojima M, Kamada-Nobusada T, Komatsu H, Takei K, Kuroha T, Mizutani M, Ashikari M, Ueguchi-Tanaka M, Matsuoka M, Suzuki K, Sakakibara H (2009) Highly sensitive and high-throughput analysis of plant hormones using ms-probe modification and liquid chromatographytandem mass spectrometry: an application for hormone profiling in *Oryza sativa*. Plant Cell Physiol 50:1201–1214
20. Pieterse CMJ, Leon-Reyes A, Van Der Ent S, Van Wees SCM (2009) Networking by small-molecule hormones in plant immunity. Nat Chem Biol 5:308–316
21. Du F, Ruan G, Liu H (2012) Analytical methods for tracing plant hormones. Anal Bioanal Chem 403:55–74
22. Tarkowski P, Ge L, Yong JWH, Tan SN (2009) Analytical methods for cytokinins. TrAC Trends Anal Chem 28:323–335
23. Hoyerová K, Gaudinová A, Malbeck J, Dobrev PI, Kocábek T, Šolcová B, Trávníčková A, Kamínek M (2006) Efficiency of different methods of extraction and purification of cytokinins. Phytochemistry 67:1151–1159
24. Dobrev PI, Kamínek M (2002) Fast and efficient separation of cytokinins from auxin and abscisic acid and their purification using mixed-mode solid-phase extraction. J Chromatogr 950:21–29
25. Van Meulebroek L, Bussche JV, Steppe K, Vanhaecke L (2012) Ultra-high performance liquid chromatography coupled to high resolution Orbitrap mass spectrometry for metabolomic profiling of the endogenous phytohormonal status of the tomato plant. J Chromatogr 1260:67–80

Chapter 9

Assessment of Cytokinin-Induced Immunity Through Quantification of *Hyaloperonospora arabidopsidis* Infection in *Arabidopsis thaliana*

Ruth A. Watson and Cristiana T. Argueso

Abstract

Cytokinins have been shown to regulate plant immunity. Application of high levels of cytokinin to plants leads to decreased susceptibility to pathogens. In this chapter, we describe a fast and accurate protocol for assessment of cytokinin-induced immunity in *Arabidopsis* plants against an oomycete plant pathogen.

Key words Cytokinins, Immunity, Defense responses, *Hyaloperonospora arabidopsidis*, *Arabidopsis*

1 Introduction

Known mostly for its role in the promotion of cell division, the plant hormone cytokinin has recently been shown to participate in the regulation of plant immunity. Application of high concentrations of cytokinin (in the micromolar range) to *Arabidopsis* plants leads to decreased susceptibility to biotrophic and hemibiotrophic pathogens [1–3]. Similar to application of exogenous cytokinin to *Arabidopsis*, rice and tobacco plants also lead to a potentiation of defense responses [1, 2, 4, 5], an effect similar to defense priming [6]. In this chapter, we describe an assay for the priming of *Arabidopsis* plants with cytokinin, followed by inoculation with the oomycete *Hyaloperonospora arabidopsidis* (henceforth, *Hpa*) and assessment of cytokinin-induced immunity.

Hpa is an obligate biotrophic pathogen, depending upon a living tissue to feed and reproduce [7]. Several isolates of *Hpa* have been identified that are virulent in different *Arabidopsis* accessions [8]. Its true biotrophic nature makes it an excellent pathogen for studies of cytokinin-induced immunity. However, *Hpa* can only be grown *in planta*, complicating pathogen quantification and consequently the assessment of plant resistance or susceptibility. Several assays have been described to measure *Hpa* growth in plants, based

Thomas Dandekar and Muhammad Naseem (eds.), *Auxins and Cytokinins in Plant Biology: Methods and Protocols*, Methods in Molecular Biology, vol. 1569, DOI 10.1007/978-1-4939-6831-2_9,

on the counting of *Hpa* asexual spores (sporangiospores) [9], the tree-shaped sporangiophores that harbor sporangiospores [10, 11], or measurement of total *in planta Hpa* growth by qPCR [12]. While these assays are generally accurate and widely used, they are inherently laborious and time consuming, enabling the comparisons of only a few plant genotypes at a time. Here we describe a protocol that allows quantification of *Hpa* asexual spores by an automated cell counter, allowing for fast determination of pathogen growth, and amenable for high-throughput screenings of a large number of plants for differential susceptibility to *Hpa*. This method can be used to document how plants respond to *Hpa* infection, as well as determine the effects of cytokinin-induced immunity by assaying pathogen growth.

2 Materials

2.1 Growing Plants for Priming and Hpa Inoculation

1. 15 mL conical tubes.
2. 0.1% (w/v) sterile agarose solution.
3. Plastic transfer pipettes.
4. Fafard 4P soil mix (Sungro, Inc.).
5. Three inch (8 cm) diameter round pots.
6. 10″ × 20″ (25 cm × 50 cm) flats and transparent plastic domes.
7. Spray bottle with water.
8. Growth chamber set at short days (8 h light/16 h dark, 22 °C, 150 μmol/m^2/s light intensity, 65% humidity).

2.2 Priming Plants with Cytokinin

1. 15 mL conical tubes.
2. Dimethyl sulfoxide (DMSO).
3. 6-Benzylaminopurine (BA) (Sigma, cat. #B3408-1G) (*see* **Note 1**).
4. Preval™ sprayers (Preval, Inc.) (*see* **Note 2**).
5. 10″ × 10″ (25 cm × 25 cm) or 10″ × 20″ (25 cm × 50 cm) flats and transparent plastic domes. You need one flat and dome for each chemical treatment.
6. Healthy, susceptible, 2-week-old *Arabidopsis* plants.
7. Growth chamber set on short days (8 h light/16 h dark, 22 °C, 150 μmol/m^2/s, 65% humidity).

2.3 Inoculating Plants with Hpa and Maintaining Hpa Isolates

1. Ice.
2. 50 mL conical tubes.
3. Distilled deionized water.
4. Forceps.

5. Vortex mixer.
6. Preval™ sprayers (Preval, Inc.) (*see* **Note 2**).
7. Three inch (8 cm) diameter round pots.
8. 10″ × 10″ (25 cm × 25 cm) flats and transparent plastic domes (*see* **Note 3**).
9. Spray bottle with water.
10. Labeling tape.
11. Healthy, susceptible, 2-week-old *Arabidopsis* plants.
12. Dedicated space for working with the pathogen.
13. Dedicated growth chamber for growing pathogen (8 h light/16 h dark, 18 °C day/16 °C night, 100 μmol/m^2/s light intensity, ambient humidity).
14. *Hpa* isolate growing on susceptible accession (for most of our assays we use isolate Noco2, which successfully grows on the Col-0 accession).
15. Headband magnifying glasses (Lehle Seeds, Inc.).
16. Counting device (either hemacytometer or TC20 automated cell counter).

2.4 Quantifying Hpa Infection

1. 1.5 mL microcentrifuge tubes.
2. Distilled deionized water.
3. Analytical balance (readability of 0.1 mg).
4. Forceps.
5. Vortex mixer.
6. Microcentrifuge.
7. Hemacytometer (Hausser Scientific Bright-Line Counting Chamber, improved Neubauer ruling pattern, cat. #0267110).
8. Compound microscope (40×–100× total magnification).
9. 95 % ethanol.
10. Tissue wipes.
11. Bio-Rad TC20 automated cell counter (*see* **Note 4**).
12. Bio-Rad cell counting slides, dual chamber for cell counter (cat. #145-0011).
13. Flash drive (optional).

3 Methods

All methods are done cleanly, but non-sterilely, at room temperature, unless otherwise specified.

3.1 Growing Plants for Priming and Hpa Inoculation

1. We use three pots per plant genotype to be analyzed, each containing 35 seeds per pot. Prepare seeds for stratification by adding seeds to a 15 mL conical tube containing 7 mL of 0.1% sterile agarose. Shake to disperse seeds and stratify for 2 days at 4 °C in the dark. As a negative control, include a wild type genotype that is not susceptible to the *Hpa* isolate being used.
2. Prior to sowing seeds, hydrate Fafard 4P soil mix (Sungro, Inc.), until media is completely wet, but not dripping. Prepare 3 in. round pots by putting media into pots and smoothing out the top. Sow seeds onto pots using disposable plastic transfer pipettes. Evenly distribute the seeds among the pots.
3. Place pots in 10″ × 20″ flats and cover with transparent plastic domes sprayed with water. Place covered flats in a growth chamber set for short days (*see* Subheading 2). Leave the dome over the germinating plants to maintain high humidity until the first true leaves start to emerge (usually 5–6 days). Water as needed.
4. Fourteen to sixteen days after sowing seeds on soil, inoculate plants with *Hpa*. Plants should be thinned out before inoculation, if needed, to obtain about 25 plants per pot. *See* Subheading 3.3 for how to inoculate plants with *Hpa*.

3.2 Priming Plants with Cytokinin

1. In order to prime plants, use Preval™ sprayers to spray chemicals (i.e., cytokinin) onto plants.
2. Prepare a 10 mM stock solution of BA by dissolving 6-Benzylaminopurine (Sigma Aldrich cat. #B3408-1G) in DMSO. Store this solution at −20 °C.
3. Prepare a fresh working stock of 100 μM BA by diluting the 10 mM BA in deionized water, just before spraying plants. For a control, dilute an equivalent volume of DMSO in water (this works out to be a 1% (v/v) solution of DMSO in water). We typically use about 5–7 mL of solution to spray two pots or a 30–40 mL solution to spray a 10″ × 20″ flat containing 18 pots.
4. Keep plants to be primed with 100 μM BA and control plants in separate flats to avoid unintentional contamination with the wrong chemical when spraying.
5. Use dedicated Preval™ sprayers for each solution. Working with one chemical at a time, spray the plants until the liquid almost runs off the leaves. Make a circular motion while spraying each pot in order to evenly coat the plants.
6. After each set of plants is sprayed with its appropriate chemical treatment, cover the flat with a dome.
7. Clean sprayers by rinsing the dip tubes with water and running water through the sprayers to rinse. Allow sprayers to air dry.

8. Place flats in a growth chamber set for short days (*see* Subheading 2), keeping the domes on for 12 h after priming plants.
9. Two days after spraying plants, inoculate with *Hpa* using the protocol described in Subheading 3.3.

3.3 Inoculating Plants with Hpa and Maintaining Hpa Isolates

1. These instructions will guide in the inoculation of healthy, 2-week-old plants with *Hpa* using asexual spores from sporulating tissue from a previous infection. For best results, inoculations should be performed between 11:00 am and 1:00 pm (*see* **Note 5**).
2. Because *Hpa* is an obligate biotroph, it needs to be propagated weekly on living plant tissue. A typical *Hpa* life cycle takes approximately 7 days from the inoculation of plants with asexual spores until new asexual spores are produced in large quantity. Alternatively, plant tissue containing *Hpa* spores can be frozen at −80 °C and revived to be used in inoculations, although it may take several weeks to obtain a heavily sporulating *Hpa* population [11].
3. Plants to be inoculated should be 14–16 days old. On inoculation day, water the plants to be inoculated in the morning. You want the plants to be well hydrated before you inoculate them with *Hpa*.
4. Use a 7-day old sporulating *in planta* culture of *Hpa* inoculated on plants 1 week earlier as a source of inoculum (*see* **Note 6**). Carefully carry sporulating plants from the previous week to your work area so as to not shake asexual spores off the sporangiophores.
5. Fill a 50 mL conical tube with some distilled deionized water. The volume of water needed depends on how many plants will be inoculated. About 5–7 mL can be used to inoculate two pots, and 30–40 mL can be used to inoculate a $10'' \times 20''$ flat containing 18 pots. We typically add 5–10 mL of water to the tube initially and dilute as needed to achieve the final spore concentration and/or volume. Keep the conical tube on ice to keep the water cold while sporulating tissue is collected.
6. Using small forceps, carefully snip off sporulating true leaves from susceptible plants and place them into the 50 mL tube with water. Make sure the leaves submerge into the water. Try to get green, sporulating leaves, and avoid transferring soil. Work with one pot at a time and leave all other sporulating plants under the dome in humid conditions. Sporangiophores on leaves can be seen by the naked eye or with the aid of a headband magnifying glass.

7. Keep adding leaves to the tube until enough tissue has been obtained to inoculate plants. Vortex the capped tube for 45 s at the highest setting.
8. Check the concentration of spores in the suspension before spraying onto plants. A hemacytometer or a TC20 automated cell counter (Bio-Rad) can be used to check the concentration of spores in the suspension. *See* Subheading 3.4 for how to use the hemacytometer and TC20. Adjust the spore concentration by either adding more sporulating leaves or by diluting the spore suspension with water to achieve the standard concentration of 5×10^4 spores/mL (*see* **Note 7**).
9. Place healthy, 2-week-old plants onto 10″ × 10″ flats to get them ready for inoculation. When ready to spray the healthy, susceptible plants, vortex the spore suspension briefly because spores tend to sink to the bottom of the tube. Using a Preval™ sprayer, spray the pathogen onto the 2-week-old plants (*see* **Note 2**). Spray the plants with the spore suspension until the liquid almost runs off the leaves. Make a circular motion while spraying each pot in order to evenly coat the plants. It is a good idea to include a wild type genotype that is not susceptible to the *Hpa* isolate being used, as a negative control for infection.
10. Spray domes with water and cover 10″ × 10″ flats containing the sprayed plants. Use labeling tape to tape the domes to the flats to ensure a high level of humidity for the first 2 days post-inoculation (dpi). Place flats in a growth chamber that is dedicated for *Hpa* growth. Keep one flat of the recently harvested, wild-type, sporulating plants as a backup for the next week's inoculations in case something happens to the newly inoculated *Hpa* (*see* **Note 8**). Spray and tape the dome and place in the pathogen growth chamber.
11. Clean-up after *Hpa* inoculation involves rinsing scissors, forceps, conical tube, and sprayer with tap water and allowing to air dry. Run tap water through the sprayer to rinse out the inside of it. Discard infected plants in biohazard waste, or according to your institution's guidelines. Pots, flats, and domes should be washed and sterilized before the next use.
12. If using more than one isolate of *Hpa* to inoculate plants, make sure to spray different isolates in different rooms/locations or on a different time of day, to prevent cross-contamination of airborne spores.
13. Check the domes for high humidity at 1 dpi. If needed, spray domes with water and tape back down.
14. At 2 dpi, in the afternoon, remove tape and crack open the domes to decrease the level of humidity (*see* **Note 9**).

15. Leave the domes cracked (or off) until 5 dpi (morning). Spray the domes with water and cover flats in order to drastically increase the humidity around the plants. Tape the domes to the flats again.
16. At 6 dpi, check the domes for high humidity. At this point, *Hpa* sporangiophores carrying asexual spores should be seen on the leaves. Handle the flats gently after sporulation begins, but in our experience, at this point in the *Hpa* life cycle, the spores are not easily released from the sporangiophores, thus allowing for a reliable count of spores. *See* Subheading 3.4 for how to harvest tissue for assaying pathogen growth.
17. By 7 dpi, sporulation should be at its maximum. Harvest tissue to be used in the inoculation of more 2-week-old plants.

3.4 Quantifying Hpa Infection

1. The first part of quantifying *Hpa* infection is harvesting sporulating plant tissue from the 6-day old, *in planta Hpa* culture. Prepare 1.5 mL microcentrifuge tubes containing 300 μL of distilled deionized water, using 10 tubes per genotype of plant used in the experiment (*see* **Note 10**). Use an analytical balance to get an initial weight of the tubes containing 300 μL of water. Record weight.
2. Carefully snip off sporulating leaves using forceps and place into pre-weighed 1.5 mL microcentrifuge tubes, putting six leaves per tube. Make sure leaves get submerged in the water by flicking and tapping the capped tubes. Make sure to not touch the forceps to the water, so as to not remove any liquid from the tube, and thereby changing its mass. Work with one genotype at a time and try to harvest leaves randomly from the pots (*see* **Note 11**). The goal is to get a representative sporulation for that genotype. For each plant to be sampled, pick true leaves 1 and 3. Try to not harvest more than two leaves per plant and to pick plants at random. Be careful to not shake off spores from nearby leaves nor to intentionally pick only well-sporulating leaves (*see* **Note 12**).
3. After harvesting tissue, weigh tubes again, obtaining the total fresh weight of the plant tissue collected. Store the tubes at 4 °C until ready to proceed with counting spores (*see* **Note 13**).
4. The second part of quantifying *Hpa* infection is releasing the spores from the leaves so that they can be counted (*see* **Note 14**). Vortex tubes containing sporulating leaf tissue at maximum speed for 45 s to release spores from sporangiophores.
5. After vortexing, centrifuge the tubes for 10 min using a microcentrifuge, at room temperature, set for 5000 rpm (2348 rcf) to concentrate the spore suspension (*see* **Note 15**). Carefully pipette out 200 μL (or 2/3) of the supernatant, leaving 100 μL of spore suspension to work with to count spores, and leaving

the leaf tissue in the tubes (*see* **Note 16**). Prepare all tubes for counting (by vortexing, spinning, and concentrating) before performing any spore counts. Store tubes at 4 °C if not proceeding to spore counts right away (*see* **Note 13**).

6. The final step in quantifying *Hpa* infection is counting spores, which can be done using either a hemacytometer or a Bio-Rad TC20 automated cell counter. In general, the TC20 gives similar results as the hemacytometer and is a best option for high-throughput counting (*see* **Note 17**).
7. Using the hemacytometer: You will need a compound microscope with 40–100× total magnification to view the spores on the hemacytometer. Rinse off the hemacytometer and glass cover slip with 95 % ethanol, blot with a tissue wipe, and allow to fully dry. Place the cover slip onto the hemacytometer to prep for sample loading. Vortex one of the 1.5 mL microcentrifuge tubes containing the concentrated spore suspension for 10 s and quickly pipette 9 μL onto each side of the hemacytometer. The spore suspension fills the chamber via capillary action. Avoid pipetting from the very bottom of the tube because debris tends to accumulate there, and you can get an artificially high concentration of spores at the bottom of the tube (*see* **Note 18**). Place the hemacytometer under the microscope and count the spores on each side of the hemacytometer using the 1 mm × 1 mm squares. Spores look like colorless, perfect circles with thick walls, 11–17 μm in diameter. Only count spores that are in the middle of the 1 mm × 1 mm square or those that are touching the top or left borders of the square so as to avoid counting spores twice. Clean the hemacytometer and cover slip by rinsing with 95 % ethanol, blotting with a tissue wipe, and allowing to fully dry. Repeat this procedure for each sample to get two technical replicates of each tube (*see* **Note 21**).
8. Using the TC20: Pull out a dual chamber counting slide. Vortex one of the 1.5 mL microcentrifuge tubes containing the concentrated spore suspension for 10 s and quickly pipette 10 μL onto each side of the counting slide. The spore suspension fills the chamber via capillary action. Avoid pipetting from the very bottom of the tube because debris tends to accumulate there, and you can get an artificially high concentration of spores at the bottom of the tube (*see* **Note 18**). Load the slide into the front of the machine and follow the prompts on the machine. We prefer to use the "gated counts" so that the machine only counts objects that are 11–17 μm in size. The machine counts an equivalent of four squares on a hemacytometer and will report the spore concentration in cells/mL. The TC20 has a few benefits over using a hemacytometer: (a) it is faster and easier to use; (b) it can use size gates to eliminate background noise in counting; and (c) image data from each spore count can be

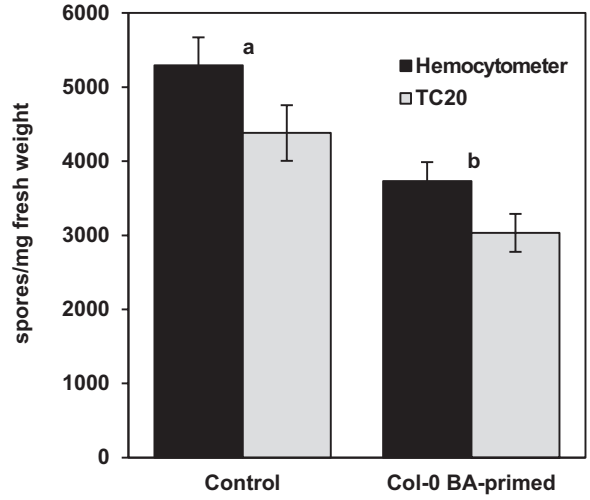

Fig. 1 Comparison of quantification of cytokinin-induced immunity against the oomycete *Hyaloperonospora arabidopsidis* isolate Noco2 by counts of asexual spores using a hemacytometer or a TC20 automated cell counter. Col-0 plants were sprayed with 100 μM BA (BA-primed) or DMSO (control) 48 h prior to inoculation with *Hpa* isolate Noco2. Error bars represent SE ($n=9$). Samples were counted with either a hemacytometer or the TC20 automated cell counter, following the protocol described here. Different letters indicate statistically significant differences ($p<0.05$, one-way ANOVA, Tukey's HSD test)

saved onto a flash drive to refer back to later or to verify the machine counts (*see* **Notes 19** and **20**).

9. If the technical replicates of spore counts were not similar to each other, then load the hemacytometer or TC20 cell counter again with the same sample and count again. Use an average of the technical replicates for each tube before continuing to other calculations.
10. Calculate the number of spores per mg of fresh weight for each tube (*see* **Note 21**). Graph the data using a bar chart to compare the differences in susceptibility between your chosen genotypes. We have found that it is best to use ANOVA as a residual diagnostic and to use the Dunnett's test or Tukey's HSD test as post hoc tests (Fig. 1) when determining which samples show a statistically significant difference (*see* **Note 22**).

4 Notes

1. 6-Benzylaminopurine (BA) is a form of cytokinin that we use for priming plants. Because BA is synthetic, it is not metabolized by the plants, allowing for a continuous cytokinin signal throughout the experiment.

2. We use Preval™ paint sprayers to spray the spore suspension onto 2-week-old plants. These sprayers atomize the suspension and allow you to evenly coat the plants. We have dedicated sprayers for each isolate of *Hpa* and each chemical treatment used in priming.
3. We use Jiffy brand 10″ × 10″ flats and domes. These work well to keep the moisture level high because the domes click into place on the inside of the flats rather than on the outside of the flats. They hold moisture in especially well if the domes are taped down to the flats. The use of a flat and dome combination that is able to hold in moisture replaces the need for a humidity feature on the pathogen growth chamber.
4. We tested several automated cell counters, and chose the TC20 from Bio-Rad, because it is compatible with a broad range of cell sizes and types. It also allows us to specify the size of cells to be counted to match the average size of *Hpa* asexual spores (11-17 μm).
5. Defense responses, including salicylic acid accumulation, have recently been found to follow a circadian pattern [13–15]. Pathogen inoculations performed at midday (11:00 am–1:00 pm) tend to result in stronger *Hpa* sporulation.
6. We usually use a 7-day-old *in planta* culture of *Hpa* as source of inoculum, as this guarantees fresh and viable spores.
7. When preparing the inoculum for propagation, leaves should be removed from tubes after vortexing, to prevent the release of more spores into solution once the desired spore concentration has been reached.
8. We keep one flat of sporulating plants of each isolate of *Hpa* in the growth chamber for 1 week longer after sporulation, as a backup source of spores for future inoculations. These flats are kept under high humidity, using the procedures described above. After 1 week, if these plants are not needed for the next inoculation cycle, they should be discarded in the biohazard waste or according to your institution's guidelines.
9. Because Colorado (USA) is quite arid, we find that just cracking the domes is enough to decrease the humidity around the plants. If the environment where you work is generally humid, then it is best to take the dome completely off at this point.
10. You can use either distilled deionized water or tap water to suspend spores.
11. This part of the protocol is prone to human bias so one must be careful when harvesting tissue. The eye generally falls to well-sporulating leaves first, but the leaves harvested should represent the entire sporulation for that genotype, which includes leaves with not as much sporulation. When using a virulent isolate,

leaves without any sporulation should be avoided, as they may represent unintentionally non-inoculated plants.

12. When harvesting tissue, it is important to make sure that all tubes have equally sporulating tissue in them and that the sporulation does not taper off with the later tubes.
13. The spores are kept well if they are stored at 4 °C, but ideally, spores should be counted within 5 days of harvesting sporulating tissue. We have counted spores up to 14 days post-harvesting and have noticed degradation in the quality of the spores by then.
14. Having 300 μL of water in the tube seems to be an optimal amount of liquid for the leaves to get shaken up during vortexing. More or less liquid volume in the tube does not work as well at releasing the spores.
15. We have found that concentrating the spore suspension before counting the spores gives more reliable and consistent results. Additionally, it gets the concentration of spores in the tubes within the optimal counting ranges for the hemacytometer and the TC20 automated cell counter (*see* **Note 17**). We have found that when using the stated protocol for concentrating, very few spores are lost to the supernatant if pipetting is done slowly and carefully.
16. We leave the leaf tissue in the tubes because we have noticed that the liquid clings to the leaves when pipetting the spore suspension into a new tube. This results in removing an unknown number of spores with the leaf tissue, which we prefer not to do.
17. The TC20 and the hemacytometer both have similar upper and lower limits of counting to be within the range of statistical significance. The lower limit on each device is about 5×10^4 cells/mL, and the upper limit on each device is about 1×10^7 cells/mL. The TC20 has an optimal counting range of 1×10^5 to 5×10^6, and the hemacytometer has a similar optimal counting range of 1×10^5 to 2×10^6. Dilution or concentration may be required in order to get the spore suspensions within these countable ranges. We have found that *Hpa* spore suspensions tend to be on the lower end of the spectrum, so we have taken to concentrating our samples.
18. Vortexing causes the spores to be randomly distributed in the water, which is ideal for pipetting onto a counting slide. Shortly after vortexing, the spores will sink to the bottom of the tube, causing a temporary concentration gradient. This is why it is important to pipette quickly after vortexing and to not pipette from the very bottom of the tube.
19. We describe here the settings that we recommend for the TC20 automated cell counter. Under “gating setup,” enable

"user-defined gates" and use "saved gates." This allows setting the size range of cells to be counted. Using "Saved Gates" tells the machine to remember the size range used during the previous count. This way you do not have to enter the sizes each time. Image data can be saved to a flash drive using "Options," then "Autosave/Sample Name." Enable "Autosave" so that it will automatically export the image data to a flash drive. Alternatively, image data can be manually exported each time. We prefer to give a name to each sample counted so that it is recognizable on the flash drive. To do this, enable "Sample Name" under "Autosave/Sample Name."

20. Bio-Rad offers a TC20 Data Analyzer program on their website that you can download to a PC computer to use with the TC20 automated cell counter. We have found that this program can be helpful when verifying the counts made by the TC20. To verify counts, load saved image data onto the program and it will circle the cells that were counted, allowing the verification of whether the correct objects (spores) have been counted. We have noticed that the most common mistake the machine makes when counting is missing spores rather than counting objects that are not spores. It especially does not do well with large clumps of spores, which in our observations tends to be rare.
21. The following formulas can be used to calculate the final concentration of spores/mg of fresh weight:

$$[\text{spores}]\left(\frac{\text{cells}}{\text{mL}}\right)=\left(\frac{\#\text{spores}}{\#\text{squares counted}}\right)\times 10{,}000\times \text{dilution factor}$$

$$\text{total}\,\#\,\text{spores}=[\text{spores}]\times \text{volume}\,(\text{mL})$$

$$\frac{\#\,\text{spores}}{\text{mg}}=\frac{\text{total}\,\#\,\text{spores}}{\text{mg fresh weight}}$$

The first equation gives the average concentration of spores in one 1 mm × 1 mm × 0.1 mm square on the hemacytometer. Our dilution factor is always 1 because we do not dilute our samples before counting. The TC20 counts an equivalent of four squares, and using the hemacytometer one should count from three to nine squares, trying to count at least 100 spores in each counting chamber. This number is then multiplied by 10,000 because the volume of each square counted is equal to 0.1 μL, which is 1/10,000 mL. An average of technical replicates should be taken before calculating number of spores/mg. In the second equation, the volume of the spore suspension is 0.1 mL after concentrating.

22. Analysis of variance (ANOVA) can be used as a residual diagnostic to test the hypothesis that there is a difference between the means of the different genotypes tested. If the data fails the ANOVA test by showing a p-value < 0.05, then the null hypothesis that all the means are equal can be rejected. A post hoc test (such as Dunnett's test or Tukey's HSD test) is only used if a statistically significant difference between the means can be shown after ANOVA (Fig. 1). These post hoc tests allow the determination of which samples show a statistically different mean from other sample(s) by performing pairwise comparisons.

Acknowledgments

We thank Phil Turk from the Franklin Graybill Statistical Laboratory at Colorado State University for the help with statistical analysis and Bettina Broeckling for comments on the manuscript.

References

1. Choi J, Huh SU, Kojima M, Sakakibara H, Paek K-H, Hwang I (2010) The cytokinin-activated transcription factor ARR2 promotes plant immunity via TGA3/NPR1-dependent salicylic acid signaling in Arabidopsis. Dev Cell 19:284–295
2. Argueso CT, Ferreira FJ, Epple P, To JPC, Hutchison CE, Schaller GE, Dangle JL, Kieber JJ (2012) Two-component elements mediate interactions between cytokinin and salicylic acid in plant immunity. PLoS Genet 8:e1002448
3. Naseem M, Philippi N, Hussain A, Wangorsch G, Ahmed N, Dandekar T (2012) Integrated systems view on networking by hormones in Arabidopsis immunity reveals multiple crosstalk for cytokinin. Plant Cell 24:1793–1814
4. Grosskinsky DK, Naseem M, Abdelmohsen UR, Plickert N, Engelke T, Zeier J, Novak O, Strnad M, Pfeifhofer H, Van der Graaf E, Simon U, Roitsch T (2011) Cytokinins mediate resistance against Pseudomonas syringae in tobacco through increased antimicrobial phytoalexin synthesis independent of salicylic acid signaling. Plant Physiol 157:815–830
5. Jiang C-J, Shimono M, Sugano S, Kojima M, Liu X, Inoue H, Sakakibara H, Takatsuji H (2013) Cytokinins act synergistically with salicylic acid to activate defense gene expression in rice. Mol Plant Microbe Interact 26:287–296
6. Conrath U, Beckers GJM, Langenbach CJG, Jaskiewicz MR (2015) Priming for enhanced defense. Annu Rev Phytopathol 53:97–119
7. Coates ME, Beynon JL (2010) Hyaloperonospora arabidopsidis as a pathogen model. Annu Rev Phytopathol 48:329–345
8. Holub EB, Beynon LJ, Crute IR (1994) Phenotypic and genotypic characterization of interactions between isolates of Peronospora parasitica and accessions of Arabidopsis thaliana. Mol Plant Microbe Interact 7:223–239
9. Feys BJ, Moisan LJ, Newman MA, Parker JE (2001) Direct interaction between the Arabidopsis disease resistance signaling proteins, EDS1 and PAD4. EMBO J 20:5400–5411
10. Tome D, Steinbrenner J, Beynon JL (2014) A growth quantification assay for Hyaloperonospora arabidopsidis isolates in Arabidopsis thaliana. Methods Mol Biol 1127:145–156
11. McDowell JM, Hoff T, Anderson RG, Deegan D (2011) Propagation, storage, and assays with Hyaloperonospora arabidopsidis: a model oomycete pathogen of Arabidopsis. Methods Mol Biol 712:137–151
12. Anderson RG, McDowell JM (2015) A PCR assay for the quantification of growth of the oomycete pathogen Hyaloperonospora arabidopsidis in Arabidopsis thaliana. Mol Plant Pathol 16:893–898
13. Zheng X-Y, Zhou M, Yoo H, Pruneda-Paz JL, Spivey NW, Kay SA, Dong X (2015) Spatial and temporal regulation of biosynthesis of the plant immune signal salicylic acid. Proc Natl Acad Sci U S A 112:9166–9173

14. Wang W, Barnaby JY, Tada Y, Li H, Toer M, Caldelari D, Lee D-U, Fu X-D, Dong X (2011) Timing of plant immune responses by a central circadian regulator. Nature 470: 110–U126

15. Zhang C, Xie Q, Anderson RG, Ng G, Seitz NC, Peterson T, McClung CR, McDowell JM, Kong D, Kwak JM, Lu H (2013) Crosstalk between the circadian clock and innate immunity in Arabidopsis. PLoS Pathog 9:e1003370

Chapter 10

Real-Time Genetic Manipulations of the Cytokinin Pathway: A Tool for Laboratory and Field Studies

Martin Schäfer and Stefan Meldau

Abstract

Although many established tools for cytokinin (CK) pathway manipulations are well suitable for the analysis of molecular interactions, their use on a whole plant scale is often limited by the induction of severe developmental defects. To circumvent this problem, different methods were developed that allow for a more precise manipulation of the CK pathway. Here we present one of these systems, the pOp6/LhGR system for chemically inducible gene expression. This system allows regulation on a spatial, temporal, and quantitative scale and therefore provides a superior tool for analyzing the role of CKs in the interactions of plants with their environment. The pOp6/LhGR system was tested for RNAi-mediated gene silencing and heterologous gene expression and was successfully used for CK pathway manipulations in different model organisms (*Arabidopsis thaliana*, *Nicotiana tabaccum*, *Nicotiana attenuata*, *Citrus sinensis*× *C. trifoliate*). Here we describe specific aspects of the screening procedure and present an experimental setup that can not only be used in the laboratory but is also applicable under field conditions.

Key words Cytokinins, Isopentenyl transferase, pOp6, LhGR, Dexamethasone, Stress response, Ecology, Fieldwork

1 Introduction

Genetic manipulations have proven to be an important tool not only for in-depth molecular investigations but also for research that focuses on higher organizational levels such as tissue functions and whole organisms, as well as on the interaction of multiple organisms. For investigation of plant hormones, such as cytokinins (CK), genetic methods are used to up- or downregulate their abundance and to manipulate their signaling. This can be achieved, for example, by overexpression, heterologous expression, RNAi-mediated gene silencing, or knockout of genes coding for rate-limiting biosynthetic enzymes (e.g., ISOPENTENYL TRANSFERASES, IPTs; [1]), degradation enzymes (e.g., CYTOKININ OXIDASES/REDUCTASES, CKX; [2]), CK receptors (CHASE DOMAIN-CONTAINING HISTIDINE

Thomas Dandekar and Muhammad Naseem (eds.), *Auxins and Cytokinins in Plant Biology: Methods and Protocols*, Methods in Molecular Biology, vol. 1569, DOI 10.1007/978-1-4939-6831-2_10,

KINASES, CHKs; [3]), or constituents of the signaling output (e.g., CK-related RESPONSE REGULATORS, RRs; [4]). Genetic manipulations are often done in a constitutive way (e.g., using T-DNA insertion lines or constitutive overexpression). However, there are many cases where this is not suitable, especially if the permanent manipulation is lethal. Constitutive manipulations of growth regulators may also interfere with the transformation and regeneration procedure, impair the propagation of plants, or cause other severe pleiotropic effects. If not controlled precisely, unfettered CK production can induce hypersensitive-like processes [5], impair callus regeneration procedures [3], and cause severe developmental effects (Fig. 1a, b; [3]). Therefore, CK manipulations are often done in a more refined manner, e.g., by the use of conditional expression systems. Prominent examples include the IPT expression driven by senescence and stress-activated promoters, such as p_{SAG} (*senescence-associated gene 12*; [6]) or p_{SARK} (*senescence-associated receptor kinase*; [7]). Still these methods do not allow for direct control by the researcher and such constructs might be activated under multiple environmental conditions. Chemically inducible expression systems in contrast allow direct influence on the target expression. However, establishing and using an inducible system is often more laborious and should therefore be mainly used for scientific questions that require this level of control.

Here we used the pOp6/LhGR expression system that is one of the most widely used chemically inducible expression systems. It is characterized by a low background expression and a high expression capacity and is not associated with the plethora of side effects that are reported for other systems (e.g., chimeric patterns or elicitor-mediated side effects to the plant; [8, 9]). The system is comprised of the target construct under the control of the pOp6 promoter and the steroid-regulated transcription regulator, LhGR. The pOp6 promoter consists of a minimal CaMV promoter downstream of an array of lac operator repeats. Due to the lack of plant inherent transcription activators, it is inactive under normal conditions. LhGR is a chimeric transcription factor that consists of a high-affinity DNA-binding region of the lac repressor, a Gal4 transcription activator domain and the ligand-binding region of a glucocorticoid receptor. LhGR is constitutively expressed, but in the absence of a suitable ligand remains inactive. In the presence of dexamethasone (DEX), the transcription factor binds to the lac operator region of the pOp6 promoter and activates the transcription of the target construct. It was shown that the pOp6/LhGR expression system can be applied to heterologous gene expression [10–12] and RNAi-mediated gene silencing [12–14]. The successful establishment in different plant species, including *Arabidopsis thaliana* [10], *Nicotiana tabaccum* [11], *Nicotiana attenuata* [12], and Citrange (*Citrus sinensis* × *C. trifoliate*; [14]), indicates the broad applicability of this method.

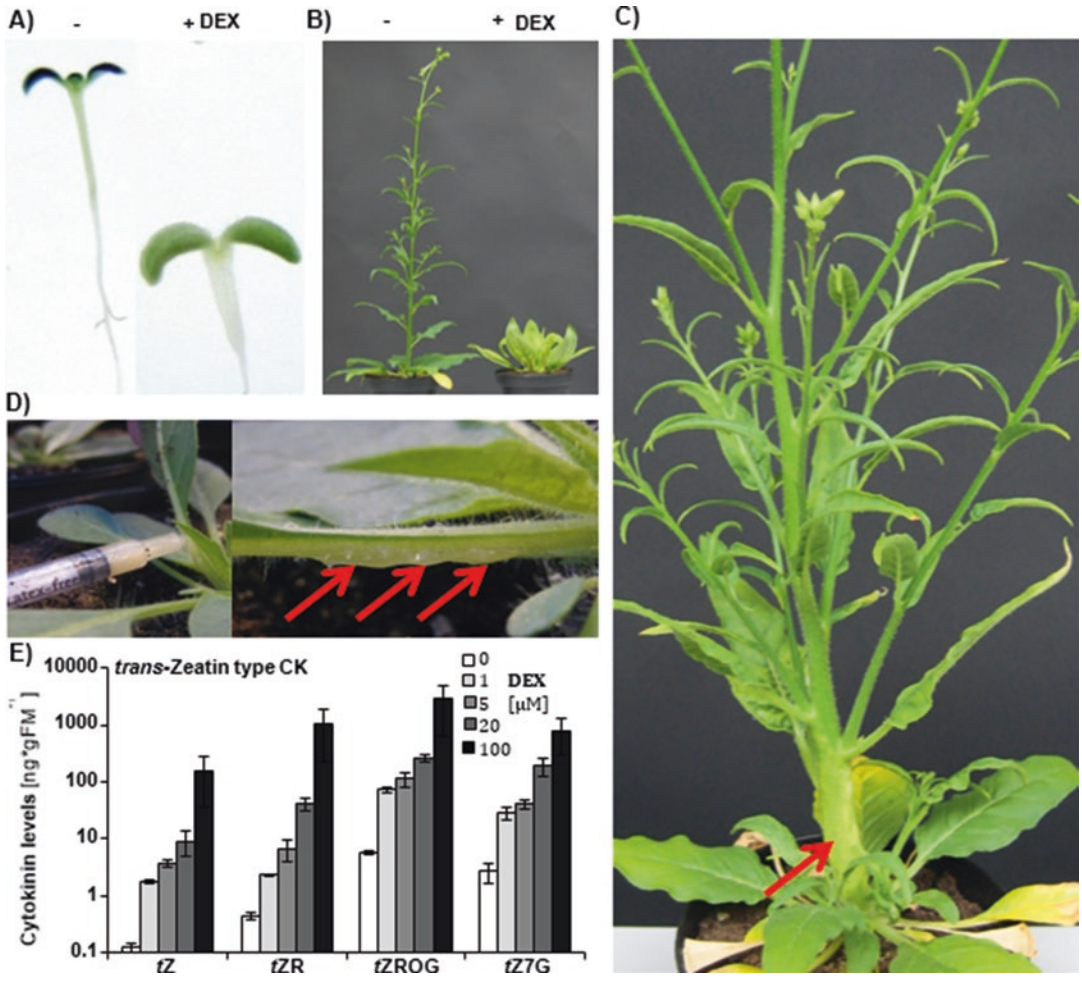

Fig. 1 pOp6/LhGR-mediated CK level changes. (**a**) i-ov*ipt* seedlings were germination on GB5 plates containing 20 μM DEX (+ DEX) or the same concentration of DMSO without DEX (−). The picture was taken after 2 weeks. (**b**) i-ov*ipt* plants 12 days after application of 0 (−) or 100 μM DEX (+ DEX)-containing lanolin paste to all leaves. Treatment was done in the rosette stage. (**c**) i-ov*ipt* plant 12 days after application of 1 μM DEX-containing lanolin paste to a lower section of the stem (indicated by an *arrow*). (**d**) Application of lanolin paste to a leaf petiole. *Arrows* indicate the applied lanolin paste. (**e**) CK level 12 days after application of differentially concentrated DEX-containing lanolin paste to i-ov*ipt* plants. *Trans*-zeatin (tZ), *trans*-zeatin riboside (tZR), *trans*-zeatin riboside *O*-glycoside (tZROG), and *trans*-zeatin 7-glycoside (tZ7G). Error bars show standard errors ($n \geq 3$). *FM* fresh mass. **a**, **d**, and **e** were modified from [12]. **b** was not shown in [12], but originates from one of the presented experiments

Different methods were applied until now for DEX treatments, including agar incorporation, soil drenching, spray application, and painting. The application method should be selected according to the developmental stage of the plants and the level of regulation that has to be applied. Besides the scientific constrains, it also has to be taken into account that DEX is bioactive in humans and can also affect other organisms [15, 16]. Probably, one of the

most common methods for the induction of full-grown plants is spraying with aqueous DEX solutions. However, this method is inappropriate for fieldwork because of the high risk of contamination to the environment and the researcher and should therefore only be conducted under controlled conditions [17, 18]. Additionally, it might complicate the work with herbivorous organisms, since coating plants with DEX will likely result in intensive DEX exposure. Even the work under laboratory conditions could become complicated since additional safety measures, such as the use of a fume hood, might be necessary. To prevent these problems, we developed a lanolin-based application method and showed its suitability for plant-herbivore interaction studies under field conditions [12]. Importantly, the method supports spatial, temporal, and quantitatively regulated construct expression with the pOp6/LhGR system.

The system might allow us to gain further understanding of local vs. systemic effects, the consequences of the heterogeneous distribution of CKs within a plant, development-dependent CK functions, short- vs. long-term effects of CKs, and finally their quantity dependencies.

2 Materials

1. Dexamethasone (DEX; Enzo Life Sciences).
2. Dimethyl sulfoxide (DMSO; Sigma-Aldrich).
3. Lanolin (Sigma-Aldrich).
4. Gamborg B5 medium including vitamins (GB5; Duchefa Biochemie).
5. Phytagel (Sigma-Aldrich).
6. Syringes (1 mL, Omnifix).

3 Methods

3.1 Screening and Line Optimization: Specific Features

For the general screening procedures of transgenic lines, protocols are already available [19]. However, some specificities of the system have to be taken into account and the protocol should be adjusted accordingly. We separately transformed and screened plants with the vectors for LhGR (pSOL9LHGRC, GenBank JX185747) and the pOp6 driven *ipt* gene (pPOP6IPT, GenBank JX185749). Because of their double hemizygous nature, the resulting crosses (abbreviated as i-ov*ipt*) are less prone for insertion site effects and transgene silencing [20]. Another advantage of this procedure is that both parts of the expression system can be

screened separately, and an optimized inducer line could be combined with multiple pOp6 constructs. Additionally, by employing different inducer lines (e.g., the constitutive active LhG4 reported by Moore et al. [21] or tissue-/stress-specific expressed variants), a huge pool of transgenic lines could be established with relatively few transformations and screenings (e.g., each four different inducer and pOp6 lines would result in 16 crosses with specific expression characteristics). In contrast, double transformation of both parts of the construct into one line would allow completing the screening within fewer generations and would allow generating homozygous lines that could be used for crosses with other transgenic lines (Fig. 2). Additionally, Wielopolska et al. [13] present a vector that contains both parts of the system on the same plasmid.

To easily determine the efficiency of an inducer or pOp6 line, we used a phenotypic screening procedure (*see* **Note 1**). It allows analysis of the induction capacity of a LhGR or pOp6 line and can be used to identify the zygosity of the parent plants. This method can partially replace antibiotic screening as proposed in Fig. 2 (*see* **Note 2**). There are also vectors available that already contain GUS as a reporter system under the control of a bidirectional pOp6 promoter [10, 11, 13]; however a high correlation to the expression of the target construct was not reported in all cases given.

3.2 Phenotypic Screening

1. Cross the lines that are to be tested (LhGR or pOp6) with their respective homozygous counterpart (not necessary to be fully optimized at this stage).
2. After seed collection, cut the parent plants back to prevent them from senescing and to induce regrowth, which will still allow use of the plants for crossings and seed collection at later time point.
3. Prepare germination media according to the used plant species, e.g., GB5 plant agar for *N. attenuata* (*see* **Note 3**). After sterilization of the media in the autoclave, let it cool to 65 °C (still solid), add 2000× concentrated DEX in DMSO (*see* **Note 4**) to reach a final concentration of 20 μM, and pour the media into petri dishes. As a control, prepare the media with the same amount of pure DMSO. After solidifying, the plates can be stored in the fridge until use.
4. Germinate the sterilized seeds (*see* **Note 5**) on a DEX-containing plate and a respective control and observe the potential phenotypical changes within the next few days. Determine the intensity of changes and the percentage of plants that are affected.
   Plants that already show changes on the control plates should be discarded because of high background expression or insertion site effects. Calculate the zygosity of parent lines (based

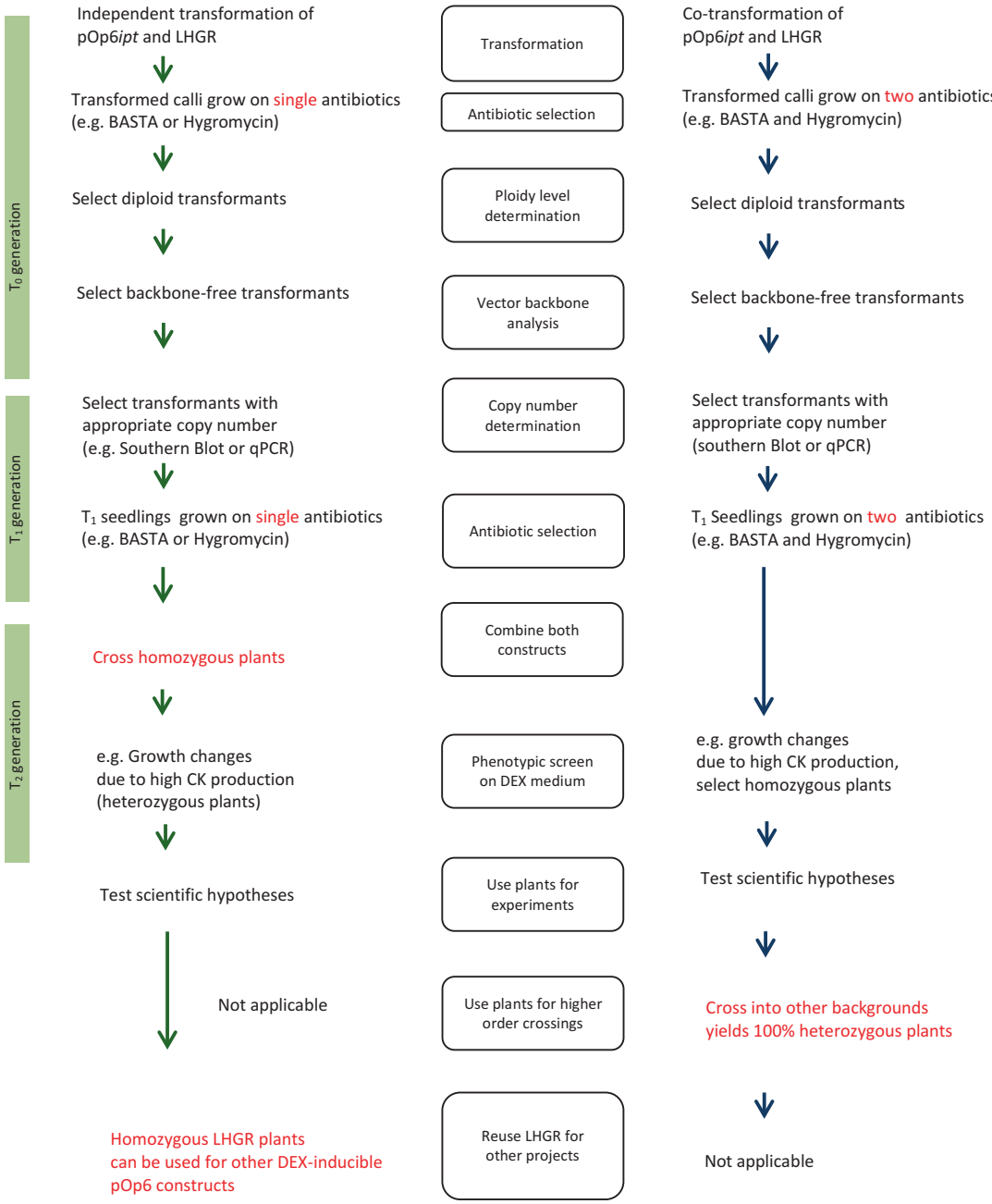

Fig. 2 Simplified scheme for screening transgenic plants with pOp6*ipt*/LHGR constructs. Differences between the two strategies are outlined in *red color*

on Mendelian inheritance). Lines that cannot be explained by a Mendelian inheritance for a single copy gene should be discarded to reduce the chance of lines with multiple insertions.

5. If parental plants with a desired zygosity are identified, transfer them to bigger planting pots to support their regrowth and use them to continue the screening.

3.3 Lanolin-Based Application

For the induction of full-grown plants, we used a lanolin-based DEX application method. Lanolin is an often used matrix for the application of hydrophobic compounds to plants [22–25]. Compared to spray applications, it has a strongly reduced risk for self-contamination and allows for locally restricted treatment. Additionally, it is expected to continuously supply the respective chemical to the plant. For plant treatments with DEX, it additionally offers the advantage that it likely reduces the light-dependent DEX degradation (*see* **Note 6**; [12]). Importantly, its preparation and application has minimal demands on the equipment and environmental conditions, supporting its suitability for fieldwork.

1. Melt an aliquot of lanolin in a water bath at 60 °C (*see* **Notes 7** and **8**).
2. Add the respective amount of 100× concentrated DEX in DMSO (*see* **Note 4**; final DEX concentrations commonly between 0.1 and 100 μM). As a control, prepare a lanolin paste containing the same amount of pure DMSO.
3. Thoroughly mix the paste, e.g., with a vortexer.
4. While the paste is still liquid, fill the paste into the syringes and allow it to solidify.
5. Prevent the paste from extensive exposure to strong sunlight until use (*see* **Note 9**).
6. Apply the lanolin directly with the syringe to the plant (e.g., to the lower side of the leaf petiole; *see* Fig. 1d).

3.4 Expression Characteristics

In the following part, we describe a procedure to analyze the induction characteristics of a fully screened line. The presented screening is based on the previously described DEX application method (*see* Subheading 3.3). The system should be analyzed according to its spatial, temporal, and quantitative expression characteristics. For locally restricted changes, the transport of the DEX, as well as the expressed construct and its consequences (e.g., small RNAs from an RNAi construct or increased CK levels as a result of IPT expression), should be taken into account. For temporal characteristics, the stability of the target compound and its metabolism play an important role.

An example is DEX-mediated elevation of the CK level. For pOp6/LhGR-mediated heterologous expression of the *Agrobacterium tumefaciens* IPT *tumor morphology root* (*tmr*; [26]), proceed as follows:

1. Apply different amounts of DEX-containing lanolin paste (e.g., 1, 5, 20, and 100 μM DEX) to single leaves, an intermediate part of the stem or a complete branch.
2. Since low amounts of CKs are already sufficient to induce visible morphological changes [27, 28], heterologous *ipt* expression allows for a phenotypic prescreening. Determine when

the treated areas show the first phenotypic changes and compare their intensity relative to the used DEX concentration. Additionally, observe the nontreated plant tissues/organs for phenotypic changes.

3. Based on the phenotypic results, preselect the treatment conditions. For example, systemic phenotypic changes after treatment of an intermediate part of the stem (Fig. 1c) rule out this treatment for an intended local manipulation.
4. Verify the results by qPCR against the *IPT* transcript and by analyzing the CK levels (example shown in Fig. 1e).

The expression of *tmr* was reported to result in an increase in *trans*-zeatin type CKs [29]. They are mainly transported in the xylem by the transpiration stream [1]. Similarly, DEX was indicated by soil-drenching experiments to be transported at least in a basipetal direction [30]. Therefore, the expression of such a construct likely allows leaf and side-branch-specific CK level manipulation, whereas it is not suitable for manipulating intermediate parts of a stem. The use of substances with inhibitory effects on the pOp6/LhGR-mediated transcript expression, such as isopropyl-b-d-thiogalactopyranoside (IPTG; [10]), might be used to gain additional regulatory control for the intended manipulation.

3.5 Effects on Herbivores

The biological activity of DEX should not only be considered in respect to the personal safety of the researcher but also for other organisms that interact with the plant. It was reported that DEX can suppress the immune responses of herbivorous insects such as the tobacco hornworm, *Manduca sexta*, by inhibiting the phospholipase A2 and the eicosanoid biosynthesis [15]. Additionally, lanoline might function like an adhesive trap for smaller insects. For investigations on plant interaction with other organisms, it is therefore important to conduct respective control experiments.

1. Treat plants without a fully functional pOp6/LhGR construct (e.g., a LhGR line or wild-type plants) with DEX-containing lanolin paste, and compare the performance of the interacting organism to a lanolin control. Plant growth might influence the effective DEX concentration for the interaction partner ("dilution effect"). Therefore, it is recommended to include DEX concentrations higher than intended for the actual investigation to compensate for potential growth variations.
2. In case of small insects, additionally check if they adhere to lanolin paste or if it otherwise influences them (e.g., stick their wings together).

Under the experimental conditions tested by Schäfer et al. [12], the *M. sexta* performance was not affected even for treatments with up to 100 μM DEX-containing lanolin paste. Next to *M. sexta*, the experimental setup was successfully applied for investigations with

the small mirid bug, *Tupiocoris notatus*. Additionally, in our fieldwork in the Great Basin Desert (UT/USA), we observed no obvious negative effect of lanolin itself on small insects.

3.6 Application

Below we describe two experimental setups that were used for pOp6/LhGR-mediated CK manipulation to investigate CK-mediated effects on plant defense responses.

The first one was used under laboratory conditions and put a special focus on the prevention of developmental alterations [31]. The second setup was done under field conditions and more generally examined differences between plant parts with CK level differences [12]. For this experiment, the changes were also applied over a longer period of time, and the setup was adjusted to compensate for some of the problems that can occur under field conditions; high spatial variability and work demand dependent limitations in plant number. The experiments were performed with the i-ov*ipt* line.

3.6.1 Single-Leaf Treatment (Laboratory)

Choose a young, but fully expanded leaf of a rosette stage plant and apply ~20 μL of 5 μM DEX-containing lanolin past to the lower side of the leaf petiole. As a control, treat some plants with lanolin paste without DEX instead. Treat the plants 1 day before the simulated herbivory induction is conducted to allow the CKs to accumulate (*see* Fig. 3a).

3.6.2 Side-Branch Treatment (Field)

Elongation stage plants were decapitated and then allowed to grow until similar sized side branches exceeded a length of 3–5 cm. Subsequently, one side branch per plant was treated with different concentrations of DEX-containing lanolin paste (e.g., 0 and 0.1 μM DEX). The lanolin paste was applied to all leaf petioles per branch and renewed every 3 days. The treatment was continued for 15 days until simulated herbivory induction was then conducted (*see* Fig. 3b).

3.6.3 Simulated Herbivory

The defense responses of the plant were induced by rolling a fabric pattern wheel three times on each side of a leaf, and subsequently 20 μL of 5x diluted *M. sexta* oral secretions were added to the puncture holes (→ simulated herbivory). After 2 days/1 h (single-leaf treatment/side-branch treatment), the leaf was collected and immediately frozen (in liquid nitrogen or on dry ice). The leaf tissue was subjected to a secondary metabolite or phytohormone analysis [12, 31, 32], respectively.

Figure 3c, d shows exemplary results for DEX-induced CK level elevation in i-ov*ipt* plants under the presented experimental conditions, as well as the subsequent elevation of herbivory-induced defense responses.

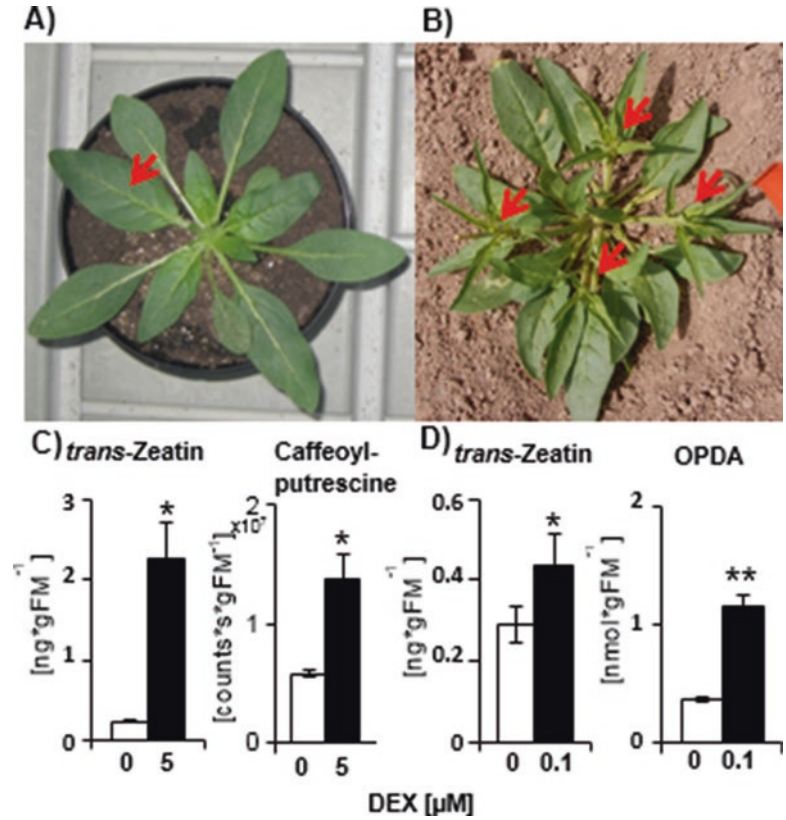

Fig. 3 Application of the pOp6/LhGR expression system for the analysis of CK-mediated effects on plant defense responses. (**a**) Exemplary plant for single-leaf treatments of rosette stage plants. The *arrow* indicates a potential treatment position. (**b**) Exemplary plant for side-branch-specific treatments. *Arrows* indicate similar sized side branches that elongated after decapitation of the plant. (**c**) *Trans*-zeatin level of i-ov*ipt* plants 1 day after pretreatment with 0 or 5 μM DEX-containing lanolin paste in the single-leaf design. Caffeoylputrescine levels were measured 2 days after simulated herbivory. (**d**) *Trans*-zeatin level of i-ov*ipt* plants 15 days after pretreatment with 0 or 0.1 μM DEX-containing lanolin paste in the side-branch design. 12-oxo-phytodienoic acid (OPDA) levels were measured 1 h after simulated herbivory. *Asterisks* indicate significant differences between DEX-treated samples and the control (**c**, independent samples *t*-test: $*P<0.05$; **d**, paired samples *t*-test: $*P<0.05$; $**P<0.01$). Error bars show standard errors (**c**, $n\geq 4$; **d**, $n\geq 7$). *FM* fresh mass. **c** was modified from [31] and **b** and **d** from [12]. The OPDA levels in **d** were not shown in [12], but originate from one of the presented experiments

4 Notes

1. For the phenotypic screening, the manipulation should result in an obvious seedling phenotype. Good examples are developmental disturbance after *ipt*-mediated CK level elevation (Fig. 1a) and photo bleaching after *phytoene desaturase* silencing

[12, 13]. Phenotypic changes that occur in later stages or that are laborious to monitor are not suitable.

2. During the screening of our pOp6-ipt lines and also a line for pOp6/LhGR-mediated *phytoene desaturase* silencing, we observed a high degree of gene silencing (perhaps mediated by DNA methylation; [33]) of the used resistance marker, *hygromycin phosphotransferase* (*hptII*; [12]). Currently, it is not clear if this is related to the construct itself. However, the pOp6-driven expression of the target construct was not noticeably affected.
3. Prepare 1× strength GB5 (3.16 g/L) in 1000 mL distilled water, adjusted to pH 6.80 with 6 g phytagel. Autoclave at 121 °C for 20 min.
4. Dilute the DEX in DMSO. In contrast to ethanol, it does not affect the plant at low concentrations [11, 34]. Additionally, it might improve the uptake of the DEX by the plant [35].
5. Sterilize seeds for 5 min in an aqueous dichloroisocyanuric acid solution (0.02 g/mL) with 0.005% Tween-20. After washing the seeds three times with sterilized water, incubate them for 1 h in 50× diluted liquid smoke (House of Herbs) containing 1 mM GA_3 (sterilize the diluted liquid smoke by autoclaving before addition of the GA_3 from a 0.1 M concentrated stock in ethanol). Wash the seeds three times with sterilized water before placing them onto the germination medium.
6. While DEX seems to be stable for several days under ambient temperatures and for short periods (30 min) at 60 °C, it shows a pronounced light-dependent degradation [12]. Prevent intensive light exposure, e.g., by treating the plant at shaded positions, such as below the leaf petiole.
7. Lanolin can easily be handled by melting a larger aliquot in the water bath (60 °C) and subsequently pouring it into 50 mL Falcon tubes using its inherent volume scale (amounts around 5 mL work best for the subsequent vortexing step). Alternatively, take up 1 mL with a syringe and mix it with the syringe in a 2 mL reaction tube. From experience, this is more accurate than pipetting because of the high viscosity of melted lanolin.
8. If necessary (e.g., for field work), the lanolin paste can be prepared with minimal equipment. The water bath can easily be exchanged by a pot of hot water or by placing the lanolin at a sun-exposed position (works only in regions with sufficient sun intensity, e.g., Great Basin Desert UT/USA), and vortexing can be adequately replaced by thorough manual shaking.
9. The exact durability of DEX in a lanolin paste is not clear at the moment. Prepare the paste as fresh as possible. However, the single time point treatments shown in Schäfer et al. [12] indicate that it stays stable for several days on the plant and probably even longer if cooled and protected from light.

References

1. Kudo T, Kiba T, Sakakibara H (2010) Metabolism and long-distance translocation of cytokinins. J Integr Plant Biol 52:53–60
2. Werner T, Nehnevajova E, Köllmer I, Novak O, Strnad M, Krämer U, Schmülling T (2010) Root-specific reduction of cytokinin causes enhanced root growth, drought tolerance, and leaf mineral enrichment in Arabidopsis and tobacco. Plant Cell 22:3905–3920
3. Riefler M, Novak O, Strnad M, Schmülling T (2006) Arabidopsis cytokinin receptor mutants reveal functions in shoot growth, leaf senescence, seed size, germination, root development, and cytokinin metabolism. Plant Cell Online 18:40–54
4. Argueso CT, Ferreira FJ, Epple P, To JPC, Hutchison CE, Schaller GE, Dangl JL, Kieber JJ (2012) Two-component elements mediate interactions between cytokinin and salicylic acid in plant immunity. PLoS Genet 8: e1002448
5. Novák J, Pavlů J, Novák O, Nožková-Hlaváčková V, Špundová M, Hlavinka J, Koukalová Š, Skalák J, Černý M, Brzobohatý B (2013) High cytokinin levels induce a hypersensitive-like response in tobacco. Ann Bot 112:41–55
6. Gan SS, Amasino RM (1995) Inhibition of leaf senescence by autoregulated production of cytokinin. Science 270:1986–1988
7. Qin H, Gu Q, Zhang J, Sun L, Kuppu S, Zhang Y, Burow M, Payton P, Blumwald E, Zhang H (2011) Regulated expression of an isopentenyltransferase gene (*IPT*) in peanut significantly improves drought tolerance and increases yield under field conditions. Plant Cell Physiol 52:1904–1914
8. Camargo SR, Cancado GM, Ulian EC, Menossi M (2007) Identification of genes responsive to the application of ethanol on sugarcane leaves. Plant Cell Rep 26:2119–2128
9. Guo HS, Fei JF, Xie Q, Chua NH (2003) A chemical-regulated inducible RNAi system in plants. Plant J 34:383–392
10. Craft J, Samalova M, Baroux C, Townley H, Martinez A, Jepson I, Tsiantis M, Moore I (2005) New pOp/LhG4 vectors for stringent glucocorticoid-dependent transgene expression in Arabidopsis. Plant J 41:899–918
11. Samalova M, Brzobohaty B, Moore I (2005) pOp6/LhGR: a stringently regulated and highly responsive dexamethasone-inducible gene expression system for tobacco. Plant J 41:919–935
12. Schäfer M, Brütting C, Gase K, Reichelt M, Baldwin I, Meldau S (2013) "Real time" genetic manipulation: a new tool for ecological field studies. Plant J 76:506–518
13. Wielopolska A, Townley H, Moore I, Waterhouse P, Helliwell C (2005) A high-throughput inducible RNAi vector for plants. Plant Biotechnol J 3:583–590
14. Rossignol P, Orbović V, Irish VF (2014) A dexamethasone-inducible gene expression system is active in Citrus plants. Sci Hortic 172:47–53
15. Miller JS, Nguyen T, Stanley-Samuelson DW (1994) Eicosanoids mediate insect nodulation responses to bacterial infections. Proc Natl Acad Sci U S A 91:12418–12422
16. Walton CH (1959) Clinical experience with dexamethasone. Can Med Assoc J 81: 724–726
17. Corrado G, Karali M (2009) Inducible gene expression systems and plant biotechnology. Biotechnol Adv 27:733–743
18. Moore I, Samalova M, Kurup S (2006) Transactivated and chemically inducible gene expression in plants. Plant J 45:651–683
19. Gase K, Weinhold A, Bozorov T, Schuck S, Baldwin IT (2011) Efficient screening of transgenic plant lines for ecological research. Mol Ecol Resour 11:890–902
20. Velten J, Cakir C, Youn E, Chen J, Cazzonelli CI (2012) Transgene silencing and transgene-derived siRNA production in tobacco plants homozygous for an introduced AtMYB90 construct. PLoS One 7:e30141
21. Moore I, Galweiler L, Grosskopf D, Schell J, Palme K (1998) A transcription activation system for regulated gene expression in transgenic plants. Proc Natl Acad Sci U S A 95:376–381
22. Baldwin I (1996) Chap. 49. In: Städler E, Rowell-Rahier M, Bauer R (eds) Proceedings of the 9th international symposium on insect-plant relationships, vol 53. Methyl jasmonate-induced nicotine production in Nicotiana attenuata: Inducing defenses in the field without wounding. Springer, Netherlands, pp 213–220
23. Kallenbach M, Bonaventure G, Gilardoni PA, Wissgott A, Baldwin IT (2012) *Empoasca* leafhoppers attack wild tobacco plants in a jasmonate-dependent manner and identify jasmonate mutants in natural populations. Proc Natl Acad Sci U S A 109:E1548–E1557
24. Kessler A, Baldwin IT (2001) Defensive function of herbivore-induced plant volatile emissions in nature. Science 291:2141–2144
25. Meldau S, Baldwin IT, Wu J (2011) SGT1 regulates wounding- and herbivory-induced jasmonic acid accumulation and *Nicotiana*

attenuata's resistance to the specialist lepidopteran herbivore *Manduca sexta*. New Phytol 189:1143–1156

26. Heidekamp F, Dirkse WG, Hille J, van Ormondt H (1983) Nucleotide sequence of the *Agrobacterium tumefaciens* octopine Ti plasmid-encoded *tmr* gene. Nucleic Acids Res 11:6211–6223
27. Bohner S, Gatz C (2001) Characterisation of novel target promoters for the dexamethasone-inducible/tetracycline-repressible regulator TGV using luciferase and isopentenyl transferase as sensitive reporter genes. Mol Gen Genet 264:860–870
28. Medford JI, Horgan R, El-Sawi Z, Klee HJ (1989) Alterations of endogenous cytokinins in transgenic plants using a chimeric isopentenyl transferase gene. Plant Cell 1:403–413
29. Ueda N, Kojima M, Suzuki K, Sakakibara H (2012) *Agrobacterium tumefaciens* tumor morphology root plastid localization and preferential usage of hydroxylated prenyl donor is important for efficient gall formation. Plant Physiol 159:1064–1072
30. Aoyama T, Chua N-H (1997) A glucocorticoid-mediated transcriptional induction system in transgenic plants. Plant J 11:605–612
31. Schäfer M, Meza-Canales ID, Brütting C, Baldwin IT, Meldau S (2015) Cytokinin concentrations and CHASE-DOMAIN CONTAINING HIS KINASE 2 (NaCHK2)- and NaCHK3-mediated perception modulate herbivory-induced defense signaling and defenses in *Nicotiana attenuata*. New Phytol 207(3):645–658
32. Kallenbach M, Alagna F, Baldwin IT, Bonaventure G (2010) *Nicotiana attenuata* SIPK, WIPK, NPR1, and fatty acid-amino acid conjugates participate in the induction of jasmonic acid biosynthesis by affecting early enzymatic steps in the pathway. Plant Physiol 152:96–106
33. Weinhold A, Kallenbach M, Baldwin IT (2013) Progressive 35S promoter methylation increases rapidly during vegetative development in transgenic *Nicotiana attenuata* plants. BMC Plant Biol 13:99
34. Robison MM, Smid MPL, Wolyn DJ (2006) Organic solvents for the glucocorticoid inducer dexamethasone: are they toxic and unnecessary in hydroponic systems? Can J Bot 84: 1013–1018
35. Williams AC, Barry BW (2012) Penetration enhancers. Adv Drug Deliv Rev 64(Suppl): 128–137

Chapter 11

Modulating the Levels of Plant Hormone Cytokinins at the Host-Pathogen Interface

Muhammad Naseem, Shabana Shams, and Thomas Roitsch

Abstract

Cytokinins are adenine and non-adenine derived heterogeneous class of regulatory molecules that participate in almost every aspect of plant biology. They also affect plant defense responses as well as help microbial pathogens to establish pathogenesis. The functional approaches that ensure desired and subtle modulations in the levels of plant cytokinins are highly instrumental in assessing their functions in plant immunity. Here, we describe a detailed working protocol regarding the enhanced production of cytokinins from plants that harbor *isopentenyltransferase* (*IPT*) enzyme gene under the control of 4xJERE (jasmonic acid and elicitor-responsive element) pathogen-inducible promoter. Our devised expression system is a context-dependent solution when it comes to investigating host-pathogen interactions under the modulated conditions of plant cytokinins.

Key words Cytokinins, Pathogen-inducible promoter, Host-pathogen interaction, Transient plant transformation

1 Introduction

Plant hormones are a shared weaponry which is utilized by the pathogen to propagate and is deployed by the host to mitigate the infection. Phytohormones act in concert and their signaling crosstalk highly modulates immune networks in plants [1–3]. The antagonism between salicylic acid (SA) and jasmonate/ethylene (JA/Et) being a central backbone of plant immune system has long been established [1, 2]. However, the detailed implications of other growth-related hormones such as auxin, cytokinins, and gibberellin for plant immunity are still not fully understood [1, 2, 4]. In order to optimally propagate the infection, plant pathogens intervene in the actions of phytohormones and thereby counter regulate the host defense responses [5]. Plant hormone cytokinins are adenine-derived regulatory molecules that control almost every aspect of plant growth and development [6]. Despite their potential for a broader crosstalk to host immune networks, only recently

Thomas Dandekar and Muhammad Naseem (eds.), *Auxins and Cytokinins in Plant Biology: Methods and Protocols*, Methods in Molecular Biology, vol. 1569, DOI 10.1007/978-1-4939-6831-2_11,

has it become known that cytokinins synergistically interact with SA-mediated defense pathway in *Arabidopsis* [3, 7]. Also, SA-independent but phytoalexin-based cytokinin protection mechanism against pathogen infection in tobacco has been reported [8]. Many plant microbial pathogens such as fungal biotrophs and tumor-causing bacteria also exploit the anti-senescent and pro-organogenesis functions of cytokinins in establishing pathogenesis of the host plant [9–12]. Therefore, cytokinins participate in plant protection mechanisms but equally give benefits to certain class of plant pathogens in causing infection. Assessment of the multifaceted functioning of cytokinins in various plant-pathogen interaction systems demands the availability of robust molecular tools that should ensure desired modulation in the levels of cytokinins in plants.

Conventionally, higher endogenous levels of cytokinins can be maintained by overexpressing the cytokinin pathway enzyme gene *isopentenyltransferase* (*IPT*) under the control of a constitutive promoter (CaMV35S) in plants [7]. Likewise, key cytokinin catabolic enzyme (cytokinin oxidase, CKX) can be overexpressed when a decrease in the level of plant cytokinins is desired [7]. However, at times, these practices bring about non-subtle changes that may result in an undesirable phenotype due the over- or underproduction of cytokinins in a plant tissue [13]. Alternatively, tight gene expression under the control of chemically inducible promoters (such as tetracycline, ethanol, or dexamethasone-inducible promoters) is a tangible solution that can address the issue of leaky expression of the transgene [14, 15]. However, in case of plant-pathogen interactions, the antimicrobial nature of these chemicals (even in very low concentration) can create a bias whether reduction in the spread of the pathogen is an intrinsic host immune response or is due to the toxicity of the underlying induction of agents [14, 15]. To address this issue, the expression of hormone biosynthesis pathway gene(s) under the control of pathogen-inducible promoters is a plausible solution that can induce the transgene only upon infection of the host plant with pathogens such *Pst* DC3000.

To date, many native and synthetic pathogen-inducible promoters have been identified [14–16]. The jasmonic acid and elicitor-responsive element (4xJERE: 4xAGACCGCC) is one among these promising synthetic pathogen-inducible promoters [8, 14, 16]. We chose 4xJERE promoter to modulate the levels of cytokinins at the host-pathogen interface due to (1) broader range of pathogens and elicitors that can induce it, (2) minimal background expression, and (3) context (plant-pathogen interaction)-dependent usage. Here, we exemplify this expression system on the production of *trans*-zeatin by *Arabidopsis* and tobacco plants upon infection with *Pseudomonas syringae* pv. *tomato* DC3000 (*Pst* DC3000) and *Pseudomonas syringae* pv. tabaci (*Ps* tabaci), respectively.

2 Materials

1. 4xJERE:IPT (promoter-gene cassette) binary construct (pCAMBIA1380-4xJERE-IPT).
2. *Agrobacterium tumefaciens* strain ABL4404.
3. LB liquid medium for the growth of *A. tumefaciens* cells.
4. LB plates supplemented with streptomycin (50 mg/l).
5. YEB medium to grow *A. tumefaciens* cells.
6. TE buffer (Tris-Cl and EDTA pH 8).
7. 15% Glycerin to store *A. tumefaciens* competent cells.
8. Kanamycin (50 mg/l) for the selection of *A. tumefaciens* ABL4404 containing pCAMBIA1380-4xJERE-IPT plasmid.
9. Incubator with adjustable temperature for giving heat shock to *A. tumefaciens* cells and other necessary incubations.
10. Autoclaved flasks for growing overnight bacterial cultures, sterile eppi tubes, and 50 and 15 ml culture tubes.
11. Centrifuges for harvesting *A. tumefaciens* cells from overnight grown bacterial cultures and their distribution in 50 ml, 15 ml culture tubes, and minimum as 2 and 1.5 ml eppi cups.
12. 10 mM MES (pH 5.5) as an ingredient of *Agrobacterium*-mediated plant transient transformation cocktail.
13. 10 mM $MgCl_2$ for bacterial resuspension and mock inoculation on plant leaves.
14. Acetosyringone to increase the transformation efficiency of plant cell.
15. Spectrophotometer for measuring bacterial growth through optical density.
16. 9–10-week-old wild-type tobacco plants (*Nicotiana tabacum* cv. W38).
17. 5-week-old wild-type *Arabidopsis* plants (*Arabidopsis thaliana* ecotype Col-0).
18. Bacterial strain of *Pseudomonas syringae* pv. tabaci (*Ps* tabaci) for the induction of cytokinin production from *IPT* gene-transformed tobacco leaves.
19. Bacterial strain of *Pseudomonas syringae* pv. *tomato* DC3000 (*Pst* DC3000) for the induction of cytokinin production from the *Arabidopsis IPT* gene-transformed leaves.
20. Scissor, needleless syringes, protection glasses, and gloves.

3 Methods

3.1 Transformation of A. tumefaciens with pCAMBIA1380-4xJERE-IPT Binary Vector

1. Inoculate freshly prepared 3 ml streptomycin (100 mg/l)-enriched LB medium with *A. tumefaciens* strain ABL 4404 as starter culture.
2. Shake this starter culture at 28 °C on a shaker for 16 h.
3. Take 1 ml of the overnight grown starter culture into 100 ml YEB medium supplemented with 100 mg/l streptomycin and further shake it on a shaker for 3–4 h at 28 °C.
4. Shift this freshly grown *A. tumefaciens* culture into two falcon tubes and centrifuge them at 4,500 × *g* at 4 °C for 20 min.
5. Wash the pellet with 5 ml cold TE buffer. Repeat centrifugation as mentioned in **step 4** and resuspend the pellet in 10 ml Tris-EDTA and again centrifuge it.
6. Finally, resuspend the clean *A. tumefaciens* pellet in 10 ml YEB supplemented with 2 ml of 15% ice cold glycerin. Make small (200–500 µl) aliquots and freeze them in liquid nitrogen or store at −80 °C and label as *Agrobacterium tumefaciens* strain ABL 4404 competent cells for subsequent use.
7. Next day, take two aliquots (200 µl) of *A. tumefaciens* strain ABL 4404 competent cells and thaw them on ice.
8. Add 2 µl (25–50 ng/µl) of pCAMBIA1380-4xJERE-IPT plasmid (*see* Subheading 4.1) to 200 µl competent cells. Keep it on ice for 5 min, then shift the tubes to 37 °C for 5 min, and afterward feed the cells with 1 ml YEB medium.
9. Keep on feeding the cells for 2–3 h. Collect the cells with brief centrifugation, then spread them on LB plates enriched with kanamycin (100 mg/l), and let them grow overnight at 28 °C.
10. The 4xJERE:IPT (cytokinin gene-pathogen-inducible promoter cassette)-transformed colonies of *A. tumefaciens* can subsequently be confirmed through standard method of colony PCR.

3.2 Transient Transformation of Tobacco Leaves with IPT Transgene and the In Planta Accumulation of Cytokinin upon Pathogen Infection

1. Grow pCAMBIA1380-4xJERE-IPT containing *A. tumefaciens* strain ABL 4404 in 5 ml LB medium (enriched with kanamycin 50 mg/l) as overnight starter culture at 28 °C. Also grow *A. tumefaciens* strain ABL 4404 with no pCAMBIA-4xJERE-IPT plasmid as negative control for transient plant transformation (*see* Subheading 4.2).
2. Shift 1 ml of the starter culture (pCAMBIA1380-4xJERE-IPT plasmid containing *A. tumefaciens* strain ABL 4404) to 50 ml LB medium-containing kanamycin (50 mg/l), 10 mM MES (pH 5.5), and acetosyringone (20 µM). Likewise, add starter culture of the *A. tumefaciens* strain ABL 4404 (with no pCAMBIA1380-4xJERE:IPT plasmid) into 50 ml LB medium-containing kanamycin (50 mg/l), 10 mM MES (pH 5.5), and 20 µM acetosyringone.

3. Grow *A. tumefaciens* cells to a level until both of these cultures attain an optical density (OD) of 0.8.
4. Separately harvest the *A. tumefaciens* culture by centrifuging at 5000 rpm at 4 °C for 20 min.
5. Resuspend the pallet of these two different cultures separately each in 50 ml $MgCl_2$ (10 mM), MES (10 mM, pH 5.5), acetosyringone (200 μM).
6. Keep the resuspended *A. tumefaciens* cells for 2 h at room temperature.
7. Arrange three tobacco wild-type (genotype W38) plants and three *Arabidopsis* Col-0 plants (*see* Subheadings 4.2 and 4.3).
8. Infiltrate ca. 300 μl (from **step 6**) of pCAMBIA1380-4xJERE-IPI plasmid containing *A. tumefaciens* strain ABL 4404 with a needleless syringe at two to three sites on one side of the tobacco leaf (Fig. 1b, d). Likewise, infiltrate *A. tumefaciens* strain ABL 4404 (no binary plasmid) into the other side of the leaf across the midrib as negative control (*see* Subheading 4.3).
9. In case of *Arabidopsis*, infiltrate 100 μl of the pCAMBIA1380-4xJERE-IPI plasmid containing *A. tumefaciens* strain ABL 4404 suspension to one side of the leaf (*see* Subheading 4.3), and for negative control infiltrate *A. tumefaciens* strain ABL 4404 without pCAMBIA1380-4xJERE-IPI plasmid suspension on a similar position leaf of another *Arabidopsis* plant of the same age (Fig. 1e) (*see* Subheading 4.3, **Note 5**).
10. Keep the *A. tumefaciens*-infiltrated transformed plants at long day conditions (16 h light and 8 h dark) for 24 h.
11. Induce the previously transformed sites with infection of *Ps* tabaci (1×10^4 CFU/ml) in case of tobacco (Fig. 1b; *see* Subheading 4.3, **Notes 1–4**) plants and with *Pst* DC3000 (1×10^4 CFU/ml) in case of *Arabidopsis* plants (Fig. 1e; *see* Subheading 4.3, **Note 5**).
12. Excise infiltrated patches (leaf segments) with the help of a scissor for further analyses (Fig. 1c) at desired intervals (*see* Subheading 4.3).

4 Notes

4.1 Description of the Cloning Strategy of Promoter Gene Cassette (4xJERE:IPT) into a Suitable Plant Transformation Vector

1. A vector construct harboring gene for the rate limiting cytokinin pathway enzyme (*IPT*) as detailed by Grosskinsky et al. [8] was previously generated. The bacterial *IPT* gene was PCR amplified along with the insertion of restriction sites of XhoI and SacI enzymes. The amplified *IPT* gene fragment with inserted restriction sites was then cloned into pGEMT easy cloning vector. It was then restricted from pGEMT-IPT and cloned at the sites of XhoI and SacI by replacing GUS gene in

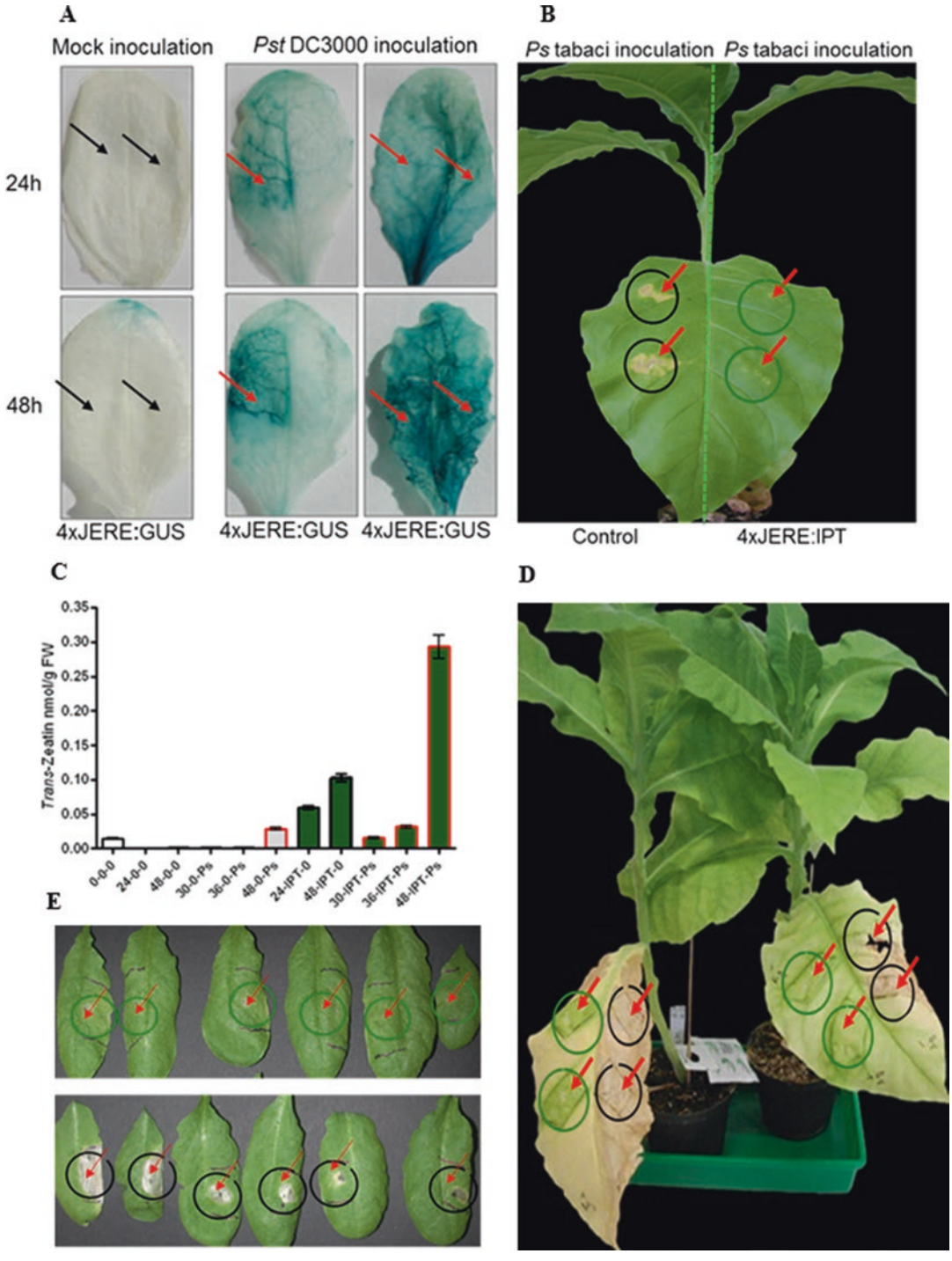

Fig. 1 Pathogen-inducible promoter system for the modulation of cytokinins at the host-pathogen interface. (**a**) The pathogen-inducible promoter 4xJERE drives the expression of *IPT* gene in leaves of promoter-reporter GUS (4xJERE::GUS) lines upon inoculation with *Pst* DC3000. The 5-week-old *Arabidopsis* 4xJERE::GUS plants were syringe infiltrated with *P. syringae* pv. tomato DC3000 (10^6 CFU/ml) at the right half of the leaf (*middle panel*: *red arrows*) as well as whole leaf (*both halves*: *right panel red arrows*). For mock induction, we use 10 mM $MgCl_2$ instead of *Pst* DC3000 (*left panel*: *black arrows*). GUS staining is performed 24 and 48 h post pathogen and

4xJERE containing pBT10-4xJERE plasmid. Subsequently, both 4xJERE and *IPT* gene cassette was removed from pBT10 vector and cloned it into pCAMBIA-1380 at the sites of BgI II and HindIII restriction enzymes.

2. The resulting final binary plasmid pCAMBIA1380-4xJERE-IPT [8] can be used to engineer stable as well as transiently transformed plants with modulated cytokinin levels upon pathogen infection.

4.2 Optimization of Incubation Period for the Induction of 4xJERE Promoter in Transgenic Plants After Pathogen Infection

1. To get functional insight into the induction of a transgene (GUS: beta-glucuronidase reporter gene as an example in this case) under the control of 4xJERE promoter, we inoculate the leaves of 5-week-old *Arabidopsis* 4xJERE:GUS plants with *Pst* DC3000 (10^6 CFU/ml) with the help of a needleless syringe. Infiltration of mock solution (10 mM $MgCl_2$ is agent that does not provoke immune from the plant) into the leaves of 4xJERE:GUS plants gives an estimate of the background expression of the transgene. We chose 24 and 48 h post pathogen infiltration (PPI) as two distinct incubation time points after pathogen infection (Fig. 1a). The pathogen and mock-infiltrated *Arabidopsis* 4xJERE:GUS plants are then subjected to GUS activity staining test as described by Naseem et al. [3].
2. Strong GUS activity was observed at *Pst* DC3000-infiltrated 4xJERE:GUS leaves as compared to that of mock-infiltrated sites (Fig. 1a). It is noteworthy that areas on 4xJERE:GUS leaves away from the site of *Pst* DC3000 infection showed faint GUS activity (Fig. 1a: middle and left panel). The extent of

Fig. 1 (continued) mock induction. (**b**) Transient expression of *IPT* gene in tobacco leaf under the control of pathogen-inducible promoter. Two sites on *right half* of the leaf are infiltrated with *Agro*. strain ABL 4404 containing the plasmid pCAMBIA1380-4xJERE-IPT (*right half*: *green circle*). The equivalent opposite sites in the *left half* are infiltrated with the same *Agro* strain but with no pCAMBIA1380-4xJERE-IPT vector (*left half* in *black circle*). After 24 h, these sites are inoculated with *P. syringae* pv. *tabaci* (*red arrow bold*). (**c**) The determination of *trans*-zeatin (nmol/g fresh weight, *y*-axis) in IPT expressing sites (4xJERE::IPT) in tobacco leaf samples induced with pathogen infection at various time points (30-IPT-Ps, 36-IPT-Ps, and 48-IPT-Ps) with and without *Ps* tabaci inoculation (24-IPT-0 and 48-IPT-0) as well as without *Agro*. strain ABL 4404 infiltration but with *Ps tabaci* inoculation (30-0-Ps, 36-0-ps, and 48-0-Ps) and untouched control samples (0-0-0) ($P < 0.05$, $n = 3$). (**d**) Spread of *Ps* tabaci (*red bold arrows*) in 4xJERE::IPT sites (*left half* of the leaf with *green circles*) and no IPT expressing sites (*black circles* on the *right half*). The IPT expressing sites 3 months post *Ps tabaci* infiltration (*left half* of the leaf) are still juvenile in comparison to non-IPT expressing sites (*right half* of the leaf). (**e**) Transient transformation of the bacterial *IPT* gene under the control of 4xJERE promoter in *Arabidopsis* leaves confer resistance against *Pst* DC3000. In *upper inset* 5-week-old wild-type *Arabidopsis* Col-0 leaves are infiltrated with *Agro*. strain ABL 4404 containing the plasmid pCAMBIA1380-4xJERE-IPT, and the treatment of *Pst* DC3000 (10^6 CFU/ml) showed minor bacterial symptoms (resistance phenotype), while the *lower inset* shows the same accession infiltrated with *Agro.* strain ABL 4404 devoid of pCAMBIA1380-4xJERE-IPT plasmid depicts susceptible phenotype (appearance of diseased symptoms on leaves) after infection with *Pst* DC3000

GUS staining at 48 h time point for *Pst* DC3000 infection is stronger than 24 h incubation time post pathogen infection.

3. These measures provide insights into to the optimization of 4xJERE promoter activity after pathogen inoculation and give a hint on optimal time to modulate endogenous gene expression as well as gene product (metabolite or protein: Fig. 1) accumulation. In our experience, 48 h post pathogen infiltration culminates in sufficient promoter activity that leads to higher cytokinins accumulation.

4.3 Cytokinin Production by Transiently Transformed 4xJERE:IPT Tobacco Leaves upon Pathogen Infection

1. To show enhanced cytokinin production at the host-pathogen interface upon infection of tobacco leaves with hemibiotrophic pathogen *Ps* tabaci, the *A. tumefaciens* strain ABL 4404 was transformed with previously generated pCAMBIA1380-4xJERE-IPT binary vector (*see* Subheading 3.1).
2. Transient transformation of restricted leaf areas of wild-type tobacco (genotype: W38) by a local infiltration of *A. tumefaciens* strain ABL 4404 containing the plasmid pCAMBIA1380-4xJERE-IPT is accomplished as per the above-described protocol (*see* Subheading 3.2). Infiltrate the comparable sites on other half of the leaf with *A. tumefaciens* strain ABL 4404 devoid of pCAMBIA1380-4xJERE-IPT for control purpose (Fig. 1b, d). To induce the *IPT* gene under the control of 4xJERE promoter, challenge these infiltrated areas with *Ps* tabaci (1×10^6 CFU/ml) at various time points such as 30, 36, and 48 h post pathogen infection (Fig. 1).
3. To assess the time-dependent effect of 4xJERE promoter on the accumulation of cytokinins, we specifically analyzed the levels of *trans*-zeatin with and without the infiltration of *Ps* tabaci (source of the induction of 4xJERE promoter). These experiments clearly indicate that accumulation of cytokinin in *IPT* gene-transformed regions is highly pathogen dependent (Fig. 1c). The level of cytokinin accumulation is significantly higher at 48 h post the inoculation of *Ps* tabaci as compared to early time points (Fig. 1c). Moreover, the difference for cytokinin accumulation at 48 h time point with and without *Ps* tabaci inoculation is also highly significant in our experiment (Fig. 1c).
4. Much intriguingly, on prolonged incubation (more than a month), *IPT* gene-induced areas under the control of 4xJERE promoter exhibited phenotype reminiscent of plants with delayed senescence. On the contrary, corresponding sites devoid of 4xJERE::IPT construct went through complete maceration owing to a full loss of chlorophyll (Fig. 1d) in the infected areas. These observations substantiate the notion that our devised pathogen-inducible cytokinin production system is an efficient cytokinin modulatory tool for the investigation of plant-pathogen interactions.

5. We also transformed *Arabidopsis* leaves with *IPT* gene under the control of 4xJERE promoter, and subsequent (24 h later) induction by infiltration with *Pst* DC3000 failed to show disease symptoms (Fig. 1e: upper panel), otherwise seen on control leaves (Fig. 1e: lower panel).
6. A cautionary note is that tissue wounding during pathogen infiltration and elicitation effects of *Agrobacterium* must be considered when transient expression assay is performed in perspective of plant-pathogen interaction.

Acknowledgments

We are thankful to Anwar Hussain and Markus Kirschke for their help in analyzing tobacco samples for cytokinin determination. We appreciate DAAD (Deutscher Akademischer Austauschdienst) for providing doctoral fellowship to MN. This work was supported by funding from the Czech Ministry of Education, Youth and Sports of CR within the National Sustainability Program I (NPU I), grant number LO1415, to T.R.

References

1. Pieterse CM, Leon-Reyes A, Van der Ent S, Van Wees SC (2009) Networking by small-molecule hormones in plant immunity. Nat Chem Biol 5:308–316
2. Robert-Seilaniantz A, Grant M, Jones JDG (2011) Hormone crosstalk in plant disease and defense: more than just salisylate-jasmonate antagonism. Annu Rev Phytopathol 49:317–343
3. Naseem M, Philippi N, Hussain A, Wangorsch G, Ahmed N, Dandekar T (2012) Integrated systems view on networking by hormones in Arabidopsis immunity reveals multiple crosstalk for cytokinins. Plant Cell 5:1793–1814
4. Naseem M, Kaltdorf M, Dandekar T (2015) The nexus between growth and defence signalling: auxin and cytokinin modulate plant immune response pathways. J Exp Bot 66:4885–4896
5. Kazan K, Lyons R (2014) Intervention of phytohormone pathways by pathogen effectors. Plant Cell 26:1–26
6. Hwang I, Sheen J, Müller B (2012) Cytokinin signaling networks. Annu Rev Plant Biol 63:353–380
7. Choi J, Huh SN, Kojima M, Sakakibara H, Paek KH, Hwang I (2010) The cytokinin-activated transcription factor ARR2 promotes plant immunity via TGA3/NPR-1-dependent salicylic acid signalling in Arabidopsis. Dev Cell 19:284–295
8. Grosskinsky DK, Naseem M, Abdelmohsen UR, Plickert N, Engelke T, Griebel T, Zeier J, Novák O, Strnad M, Pfeifhofer H, van der Graaff E, Simon U, Roitsch T (2011) Cytokinins mediate resistance against Pseudomonas syringae in tobacco through increased antimicrobial phytoalexin synthesis independent of salicylic acid signalling. Plant Physiol 157:815–830
9. Naseem M, Wölfling M, Dandekar T (2014) Cytokinin for immunity beyond growth, galls and green-islands. Trends Plant Sci 19:481–484
10. Hinsch J, Vrabka J, Oeser B, Novák O, Galuszka P, Tudzynski P (2015) De novo biosynthesis of cytokinins in the biotrophic fungus Claviceps purpurea. Environ Microbiol 8:2335–2351
11. Radhika V, Ueda N, Tsuboi Y, Kojima M, Kikuchi J, Kudo T, Sakakibara H (2015) Methylated cytokinins from the phytopathogen Rhodococcus fascians mimic plant hormone activity. Plant Physiol. doi:10.1104/pp.15.00787
12. Sardesai N, Lee LY, Chen H, Yi H, Olbricht GR, Stirnberg A, Jeffries J, Xiong K, Doerge RW, Gelvin SB (2013) Cytokinins secreted by Agrobacterium promote transformation by repressing a plant myb transcription factor. Sci Signal 302:1–12

13. Novák J, Pavlů J, Novák O, Nožková-Hlaváčková V, Špundová M, Hlavinka J, Koukalová Š, Skalák J, Černý M, Brzobohatý B (2013) High cytokinin levels induce a hypersensitive-like response in tobacco. Ann Bot 112:41–55
14. Bonfig KB, Berger S, Fatima T, González MC, Roitsch T (2006) Metabolic control of seedling development by invertases. Funct Plant Biol 34:508–516
15. Patro S, Kumar D, Ranjan R, Maiti IB, Dey N (2012) The development of efficient plant promoters for transgene expression employing plant virus promoters. Mol Plant 4:941–944
16. Rushton PJ, Reinstädler A, ReinLipka V, Lippok B, Somssich IE (2002) Synthetic plant promoters containing defined regulatory elements provide novel insights into pathogen- and wound-induced signaling. Plant Cell 14:749–762

Chapter 12

Analyzing Cytokinin Responses During Plant-Nematode Interactions

Florian M.W. Grundler and Shahid Siddique

Abstract

Cyst nematodes are obligate biotrophs that induce the formation of a hypertrophied and hypermetabolic syncytial-feeding site in roots of the host plants. Cytokinin signaling is activated at the site of infection and contributes significantly to the formation of syncytium. Here, we describe a protocol for visualizing cytokinin signaling activation in *Arabidopsis* upon infection with cyst nematode *Heterodera schachtii* using promoter reporter lines, *TCSn:GFP* and *ARR5:GUS*.

Key words Cytokinins, Nematode, Giant cells, Syncytium, Cell cycle, *TCSn:GFP*, *ARR5:GUS*

1 Introduction

Plant parasitic nematodes are destructive pests that severely damage crop plants either directly or as virus vectors. Most of this damage is caused by a small group of sedentary cyst (*Globodera* spp. and *Heterodera* spp.) and root-knot nematodes (*Meloidogyne* spp.) [1]. Infective stage juveniles of cyst nematodes (J2s) enter the roots in the elongation zone and move through different cell layers until they reach the vascular cylinder where they induce an initial syncytial cell (ISC) for feeding. The ISC expands through incorporation of neighboring cells by local dissolution of cell walls leading to the formation of a hypertrophied syncytium. Two days after selection of an ISC, cells incorporated into syncytium are enlarged and exhibit features of a typical syncytium. The cytoplasm is strongly condensed and rich in mitochondria, plastid, and ribosomes. Further, nuclei are enlarged and a larger central vacuole is replaced by several smaller vacuoles. Since nematode become immobile, syncytium serves as the sole nutrient source for nematodes throughout their life span of several weeks [2, 3]. During the following 2 weeks, nematodes feed from syncytium and molt three times (J3, J4, adult) to develop into males or females. The development of syncytium in host plants is accompanied by profound

Thomas Dandekar and Muhammad Naseem (eds.), *Auxins and Cytokinins in Plant Biology: Methods and Protocols*, Methods in Molecular Biology, vol. 1569, DOI 10.1007/978-1-4939-6831-2_12,

transcriptomic, metabolomics, and proteomic changes that have been previously investigated [4–7]. Nevertheless, the mechanism by which nematode transform initial root cell into a highly active feeding site is not fully understood.

Cytokinins are adenine derivatives with either an isoprene-derived or aromatic side chain that regulates a number of developmental and physiological processes, including cell division, senescence, root growth, branching, and various stress responses [8, 9]. Cytokinin signaling in *Arabidopsis* is mediated by a complex phosphorelay system (also called two-component signaling) in which the signal is perceived by membrane-localized histidine kinases (AHKs) and transmitted to the nucleus via phosphotransmitter proteins (AHPs). Inside the nucleus, transcription factors known as response regulators (ARRs) become activated and induce or suppress the transcription of cytokinin target genes [10–13].

One of the first events induced by cyst nematodes in the infected tissues is activation of the cell cycle [14, 15]; therefore, cytokinins have long been suggested of playing a role in syncytium formation. Indeed, our recent study provided evidence that cytokinin signaling is not only induced but also contributes significantly to cell cycle activation during the syncytium formation [4]. The activation of cytokinin signaling in *Arabidopsis* is widely assessed using two promoter reporter lines: (a) *ARR5:GUS* and (b) *TCSn:GFP* [16, 17]. Both of these reporter lines have been previously used under various conditions and have helped describe novel cytokinin functions. However, nematode root infection is a complex process consisting of different stages of parasitism including migration, ISC selection, syncytium expansion, and maintenance. This has motivated us to develop a standard protocol for cytokinin visualization during different stages of nematode infection. Although this procedure is primarily developed to visualize cytokinin signaling activation in *Arabidopsis* upon infection with beet cyst nematode *Heterodera schachtii*, it may also be used in other types of plant-nematode interactions.

2 Materials

Prepare all solutions using double distilled water and analytical grade reagents. Perform all steps under sterile conditions using autoclaved pipette tips and glassware. Store all solutions at room temperature (unless otherwise stated). Follow all waste disposal procedures required by local laws and regulations.

2.1 Knop Agar Medium

1. Five different stock solutions I–V (*see* **Note 1**). Store at 4 °C.
2. Daishin agar (catalogue number 025, Brunschwig Chemie, Amsterdam, The Netherlands).

3. Sucrose.
4. 3 M KOH.
5. Gamborg's vitamin solution (catalogue number G1019, Sigma-Aldrich, Munich, Germany). Store at 4 °C.
6. 6.1 L autoclavable clear glass bottles.
7. pH meter.
8. Autoclave.
9. Petri dishes (9 cm).
10. Cover slips (24 × 60 mm).

2.2 Arabidopsis Growth

1. 0.6% Sodium hypochlorite (NaOCl).
2. *Arabidopsis* seeds.
3. Growth chamber.

2.3 Nematode Infection

1. 12-day-old *Arabidopsis* plants.
2. Sterilized J2 of *H. schachtii* (*see* **Note 2**).
3. 0.7% Gelrite in water (catalogue number G1101, Haarlem, The Netherlands).
4. Binocular microscope.

2.4 Microscopy

1. X-GLUC solution (*see* **Note 3**).
2. Propidium iodide solution (catalogue number P4864, Sigma-Aldrich, Munich, Germany). Store at 4 °C.
3. Binocular microscope.
4. Fluorescent microscope.

3 Methods

3.1 Plant Growth

1. Prepare 1 L of Knop medium by mixing 2 mL of stock solution I, 2 mL of stock solution II, 2 mL of stock solution III, 0.4 mL of stock solution, and 0.2 mL of stock solution V in a 1 L clear autoclavable glass bottle. Add 20 g of sucrose and 8 g of Daishin agar; add double distilled water until the solution is 1 L. Autoclave the media at 121 °C for 20 min. Let the media cool down to 60 °C, and then add 1 mL of Gamborg's vitamin solution through sterile filtration. For *ARR5:GUS* assays, pour 20 mL of Knop medium into a 9 cm petri dish. For a *TCSn:GFP* analysis, pour 3 mL of Knop medium into a microscopy cover slip (24 × 60 mm). Let the media solidify for 1–2 h.
2. Collect approximately 100 *Arabidopsis* seeds (*TCSn:GFP* or *ARR5:GUS*) in a 2-mL Eppendorf tube. Add 1.8 mL 0.6% NaOCL to the tube and shake it for 5 min. Wait until the seeds

accumulate at the bottom of the tube. Carefully remove the NaOCl from the tube without disturbing the seeds. Add 1.8 mL of 70% ethanol and shake it for 5 min. Afterward, remove the ethanol and wash the seeds five times with double distilled autoclaved water. Spread the seeds on autoclaved filter paper in a petri dish and let them dry for 1–2 h. Grow the plants under long-day conditions (16 h light and 8 h dark) at 23 °C.

3.2 Nematode Infection and Microscopic Observations

3.2.1 ARR5:GUS Assays

Grow four plants per petri dish in a Knop medium as described above. Release two drops of 0.7% Gelrite containing 60–70 sterile J2 nematodes onto the surface of a Knop agar medium containing 12-day-old plants (Fig. 1). J2 search for roots guided by root exudates and may require several hours before they invade the roots. Mark the nematode infection sites with a permanent marker on the back of the petri dishes using a binocular microscope. Submerge the agar medium within the root system in an X-GLUC solution and incubate it for 6 h at 37 °C. Remove the GUS solution and wash the root system three times with 70% ethanol. Count the number of positively and negatively stained infection sites using binocular microscope (up to 50 infection sites in total). Carefully cut a root piece containing a nematode infection site from the agar medium to mount on glass slides with water. Examine them under a light microscope. Repeat the experiments three times independently. To perform a time-course analysis covering different stages of infection, we recommend staining at 24 hai (migratory), 3 dai (early J2s), 5 dai (late J2s), 7 dai (J3s), 10 dai (J3s, J4s, male, female), and 15 dai (male and females).

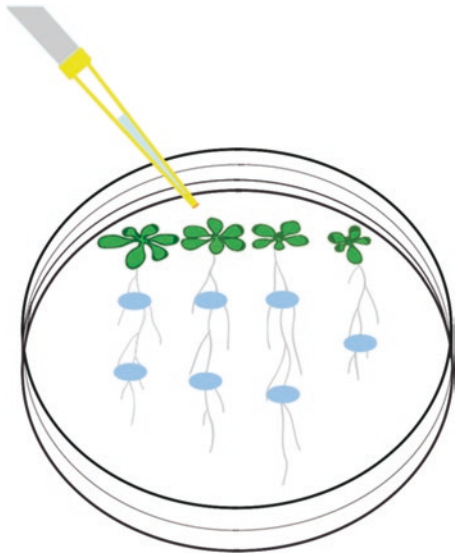

Fig. 1 Infection of 12-day-old *Arabidopsis* plants with nematode J2 for ARR5:GUS analysis

3.2.2 TCSn:GFP Analysis

Place a single seed on a cover slip with Knop medium to the short edge, allowing the roots to grow straight (Fig. 2). Keep the cover slips under sterile conditions in petri dishes. Release two drops of 0.7% Gelrite containing 60–70 sterile J2 nematodes onto the surface of the Knop agar medium containing 12-day-old plants (Fig. 3). Carefully remove the agar from the root especially around

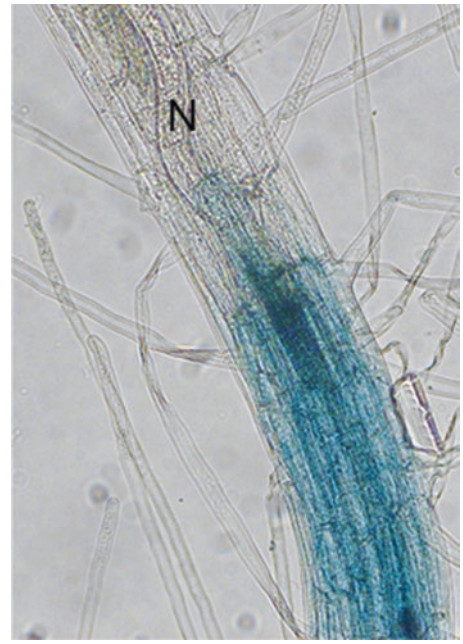

Fig. 2 Activation of cytokinin signaling in *Arabidopsis* roots upon nematode infection. Cytokinin-mediated expression of ARR5:GUS reporter upon infection with cyst nematode *H. schachtii* at 3 dpi is shown. *N* nematode

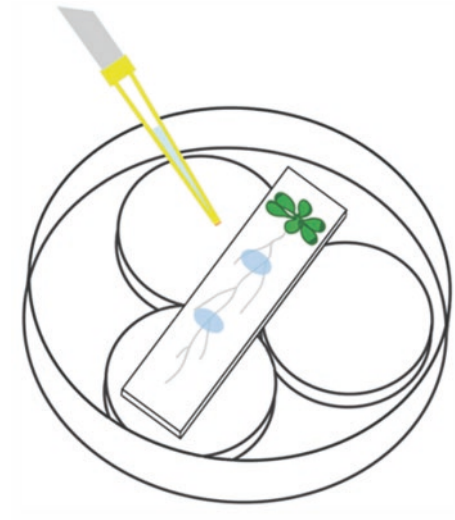

Fig. 3 Infection of 12-day-old *Arabidopsis* plants with nematode J2 for *TCSn:GFP* observations

Table 1
Stock solutions

Stock solution	Chemical	Amount (g/L)
I	KNO_3	121.32
	$MgSO_4 \cdot 7H_2O$	19.71
II	$Ca(NO_3)_2 \cdot 4H_2O$	120.0
III	KH_2PO_4	27.22
IV	FeNaEDTA	7.34
V	H_3BO_3	2.86
	$MnCl_2$	1.81
	$CuSO_4 \cdot 5H_2O$	0.07
	$ZnSO_4 \cdot 7H_2O$	0.36
	$CoCl_2 \cdot 6H_2O$	0.03
	H_2MoO_4	0.05
	NaCl	2.0

the infection sites with the help of a razor blade under binocular. To visualize the root anatomy, counterstaining with membrane-impermeable dye propidium iodide (PI) is recommended (*see* **Note 4**). Subsequently wash the root twice with water, mount the samples using a second cover slip, and examine the samples with a fluorescent microscope. Use water for mounting and don't let the samples dry.

4 Notes

1. Table of stock solutions (*see* Table 1) for Knop medium. The stock solutions are prepared by combining the chemicals as stated in the table. The values are for of 1 L stock solution.
2. X-Gluc solution:100 mM $NaPO_4$ buffer (pH 7.0) containing 10 mM EDTA, 0.01% Triton X-100, 0.5 mM $K_3(Fe(CN)_6)$, 0.5 mM $K_4(Fe(CN)_6)$, and 1 mg/mL 5-bromo-4-chloro-3--indolyl glucuronide.
3. Collect and surface sterilize the J2s of *H. schachtii* using HgCl2 as described previously [18]. The sterilization of J2s can be skipped if observations have to be made during early stages of infection (within 48 h). Add 0.7% Gelrite to larvae before inoculation.

4. Add 200 μL PI (10 μg/mL) directly to the root and incubate samples for 10 s. Do not press cover slips; otherwise, PI may penetrate the root cells and stain xylem. Additionally, nematodes may be damaged by pressing of cover slips. Don't analyze samples which are in PI for more than 20 min.

Acknowledgment

We are grateful to Zoran Radakovic, Julia Holbein, Christiane Matera, and Thomas Gerhardt for helping in various steps of protocol.

References

1. Sasser JN, Freckman DW (1986) A world perspective on nematology—the role of the society. J Nematol 18:596
2. Wyss U, Grundler FMW (1992) Feeding behavior of sedentary plant parasitic nematodes. Neth J Plant Pathol 98:165–173
3. Golinowski W, Grundler FMW, Sobczak M (1996) Changes in the structure of *Arabidopsis thaliana* during female development of the plant-parasitic nematode *Heterodera schachtii*. Protoplasma 194:103–116
4. Siddique S, Radakovic ZS, De La Torre CM, Chronis D, Novak O, Ramireddy E, Holbein J, Matera C, Hütten M, Gutbrod P, Anjam MS, Rozanska E, Habash S, Elashry A, Sobczak M, Kakimoto T, Strnad M, Schmulling T, Mitchum MG, Grundler FMW (2015) A parasitic nematode releases cytokinin that controls cell division and orchestrates feeding site formation in host plants. Proc Natl Acad Sci U S A 112:12669–12674
5. Hütten M, Geukes M, Misas-Villamil JC, Habash S, Elashry A, van der Hoorn RAL, Grundler FMW, Siddique S (2014) Activity profiling reveals changes in the diversity and activity of proteins in Arabidopsis roots in response to nematode infection. J Nematol 46:177–178
6. Szakasits D, Heinen P, Wieczorek K, Hofmann J, Wagner F, Kreil DP, Sykacek P, Grundler FMW, Bohlmann H (2009) The transcriptome of syncytia induced by the cyst nematode *Heterodera schachtii* in Arabidopsis roots. Plant J 57:771–784
7. Hofmann J, El Ashry A, Anwar S, Erban A, Kopka J, Grundler FMW (2010) Metabolic profiling reveals local and systemic responses of host plants to nematode parasitism. Plant J 62:1058–1071
8. Ha S, Vankova R, Yamaguchi-Shinozaki K, Shinozaki K, Tran LSP (2012) Cytokinins: metabolism and function in plant adaptation to environmental stresses. Trends Plant Sci 17:172–179
9. Kieber JJ, Schaller GE (2014) Cytokinins. Arabidopsis Book 12:e0168
10. Inoue T, Higuchi M, Hashimoto Y, Seki M, Kobayashi M, Kato T, Tabata S, Shinozaki K, Kakimoto T (2001) Identification of CRE1 as a cytokinin receptor from Arabidopsis. Nature 409:1060–1063
11. Riefler M, Novak O, Strnad M, Schmulling T (2006) Arabidopsis cytokinin receptor mutants reveal functions in shoot growth, leaf senescence, seed size, germination, root development, and cytokinin metabolism. Plant Cell 18:40–54
12. Higuchi M, Pischke MS, Mahonen AP, Miyawaki K, Hashimoto Y, Seki M, Kobayashi M, Shinozaki K, Kato T, Tabata S, Helariutta Y, Sussman MR, Kakimoto T (2004) In planta functions of the Arabidopsis cytokinin receptor family. Proc Natl Acad Sci U S A 101:8821–8826
13. Nishimura C, Ohashi Y, Sato S, Kato T, Tabata S, Ueguchi C (2004) Histidine kinase homologs that act as cytokinin receptors possess overlapping functions in the regulation of shoot and root growth in Arabidopsis. Plant Cell 16:1365–1377
14. Goverse A, Engler JD, Verhees J, van der Krol S, Helder J, Gheysen G (2000) Cell cycle activation by plant parasitic nematodes. Plant Mol Biol 43:747–761

15. Engler JD, De Vleesschauwer V, Burssens S, Celenza JL, Inze D, Van Montagu M, Engler G, Gheysen G (1999) Molecular markers and cell cycle inhibitors show the importance of cell cycle progression in nematode-induced galls and syncytia. Plant Cell 11: 793–807
16. D'Agostino IB, Deruere J, Kieber JJ (2000) Characterization of the response of the Arabidopsis response regulator gene family to cytokinin. Plant Physiol 124:1706–1717
17. Zurcher E, Tavor-Deslex D, Lituiev D, Enkerli K, Tarr PT, Muller B (2013) A robust and sensitive synthetic sensor to monitor the transcriptional output of the cytokinin signalling network in planta. Plant Physiol 161:1066–1075
18. Siddique S, Matera C, Radakovic ZS, Shamim MH, Gutbrod P, Rozanska E, Sobczak M, Torres MA, Grundler FMW (2014) Parasitic worms stimulate host NADPH Oxidases to produce reactive oxygen species that limit plant cell death and promote infection. Sci Signal 7(320):ra33

Chapter 13

Examining H_2O_2 Production in *Arabidopsis* Leaves Upon Challenge by Cytokinin

Shahjahan Shabbir Ahmed, Ihsan Ullah, Shazia Irfan, and Nazeer Ahmed

Abstract

Plant cells respond to stresses and exogenous environmental stimuli. Production of altered levels of reactive oxygen species (ROS) is one of a typical cellular responses against such stimuli. These responses are detectable through various techniques including luminol-based bioassays. Luminol-based bioassays provide an excellent opportunity for detection of ROS in plant leaf tissue when challenged with some exogenous stimuli like phytohormones, cytokinins, auxins, ABA, etc. The luminol-based protocol in point aims at measuring changes in the H_2O_2 levels of *Arabidopsis* leaf discs when exposed to phytohormone cytokinins. However, utility of the luminol-based ROS determination protocol is quite wide. We specifically optimized this protocol to quantify the effect of cytokinins on ROS production by *Arabidopsis* leaves.

Key words Cytokinin, Reactive oxygen species, H_2O_2, Signaling, Luminol, Scintillation counter

1 Introduction

Owing to the sessile nature of plants, development of sophisticated mechanisms to cope with biotic and abiotic stresses is a logical evolutionary outcome. Sensing and responding aptly and swiftly to various stress factors thus become part of the plant survival system. The survival instincts of the plants depend, among others, on different signaling molecules including reactive oxygen species (ROS) which in turn are responsible for activation of complex signaling pathways [1–5]. ROS are oxygen (O_2) molecules having the ability to readily oxidize other molecules. They include both free radicals and nonradical species such as hydrogen peroxide, superoxide, hydroxyl radical, and singlet oxygen. ROS have established roles in growth, development, and biotic and abiotic stresses [6]. At the organelle level in plants, they are produced in mitochondria, chloroplast, and peroxisome, while plasma membrane together with apoplast is the other main site involved in ROS generation particularly when challenged with some endogenous signals or exogenous environmental stimuli. Keeping in view the production of ROS

Thomas Dandekar and Muhammad Naseem (eds.), *Auxins and Cytokinins in Plant Biology: Methods and Protocols*, Methods in Molecular Biology, vol. 1569, DOI 10.1007/978-1-4939-6831-2_13,

particularly H_2O_2 in response to a variety of stimuli, it is not unlikely to consider H_2O_2 as one of the key players mediating cross-talk between signaling pathways [7]. An effective signaling molecule is produced quickly and efficiently whenever needed. It can induce distinct effects within the cell and is removed quickly when needed no further [8]. ROS possess these characteristics besides being very reactive.

The interplay between ROS and phytohormones is another area of interest for plant scientists. Roles of various phytohormones are well investigated in growth, development, and defense mechanisms of plants. Traditionally, in defense responses, roles of phytohormones like jasmonates (JAs), salicylates (SAs), and ethylene (ET) have extensively been documented [9]. Similarly, incoming evidence suggests the involvement of other phytohormones, such as abscisic acid (ABA), auxins (indole-3-acetic acid [IAA]), brassinosteroids (BRs) gibberellins (GA), and cytokinins (CKs) in defense strategies employed by plants [10, 11]. Allied regulatory roles of ROS and different phytohormones have been suggested [12, 13]. Cytokinins and ROS, for example, are found interacting in various growth, development, and stress mechanisms [14–17]. Here, we describe a detailed protocol to monitor the impact of cytokinins on ROS production as well as to quantify how they inhibit ROS when plant tissue is pretreated with ROS producing agents.

2 Materials

The use of analytical grade reagents and double-distilled water is recommended for preparation of all solutions. Maintaining sterile conditions and using autoclaved pipette tips, glassware, etc. are advised. All solutions be stored at room temperature (unless indicated otherwise). Safety precautions should be followed as per recommendations of the supplier. In vogue laws and regulations regarding waste disposal procedures should strictly be observed.

2.1 Growing Arabidopsis

1. *Arabidopsis* seeds.
   (a) Col 0, wild type.
   (b) Elongation factor receptor (*efr*) mutants.
   (c) *Arabidopsis* ecotype Wassilewskija (*Ws*).
2. Greenhouse.
3. Pots with soil.

2.2 Measuring H_2O_2 Production

1. Six-week-old *Arabidopsis* plants.
2. Sterilized water.
3. 96-well microplate.

4. Round leaf discs excision tool.
5. Scintillation counter or luminometer.
6. Luminol.
7. Horseradish peroxide.
8. An elicitor (flg22, elf18 or any other) as positive control.
9. Zeatin or other cytokinins.
10. Elicitor flg22.
11. Elicitor elf18.
12. Micropipette.

3 Methods

3.1 Plant Growth

Grow *Arabidopsis thaliana*

1. Accession Columbia-0 (Col-0).
2. Its T-DNA insertion line elongation factor receptor (efr) mutant.
3. *Arabidopsis* ecotype Wassilewskija (Ws) in pots for 6 weeks.

3.2 Validation of the Experimental System

1. Flg22, a 22-amino-acid-long peptide from *Pseudomonas spec.* acts as a potent elicitor inducing oxidative burst in cells of different plant species [4]. However, *Arabidopsis* ecotype *Ws-0* is insensitive to perceive flg22 due to mutation in the kinase domain of its flagellin receptor FLS2 [18]. Similarly, another microbial MAMP the elongation factor Tu (EF-TU) activates signaling events and defense responses that are common to flg22 [19]. The *Arabidopsis efr* mutant lacks the functional EFR receptor and is unable to recognize the elicitor elf18.
2. Conduct baseline experiments to confirm the proper functionality of experimental system being used.
3. Cut round leaf discs of the size of the well of 96-well plates and incubate overnight in sterilized water either in a petri plate or directly in a 96-well microplate. Each well should contain 100 µl of sterilized water. Next day, add 50 µl of reaction mix (20 µl/ml each of luminal 20 mM and horseradish peroxidase 1 mg/ml) to each well and incubate the leaf disc for 30 min.
4. As a positive control, apply 500 nM of flg22 or elf18 in wells containing leaf tissues of wild-type Col-0 plants. Typically, it should induce a transient oxidative burst.
5. If the same experiment is repeated while changing the wild-type plants with receptor mutant plants (*efr* and WS-0 ecotypes for elf18 and flg22, respectively), no production of H_2O_2 is expected.

6. In another scenario, when *efr* and WS-0 ecotypes are challenged by flg22 and elf18, respectively, oxidative burst response is elicited.

3.3 ROS Measurements Upon Challenge by Phytohormones

Similar protocol as described above is to be followed here (Fig. 1). Briefly:

1. Cut round leaf discs of the size of the well of 96-well microplate with an appropriate tool.
2. Incubate the leaf tissues overnight in sterilized water preferably in a petri plate.
3. Next day, gently shift the discs in microplate, each well containing 50 μl of reaction mix (20 μl/ml each of luminal 20 mM and horseradish peroxidase 1 mg/ml).
4. Incubate for 30 min.
5. Assay for different treatment/concentrations of cytokinins or other phytohormones on scintillation counter.
6. Record the chemiluminescent signals in the form of counts per second (CPS1) for 45 cycles (Fig. 1).

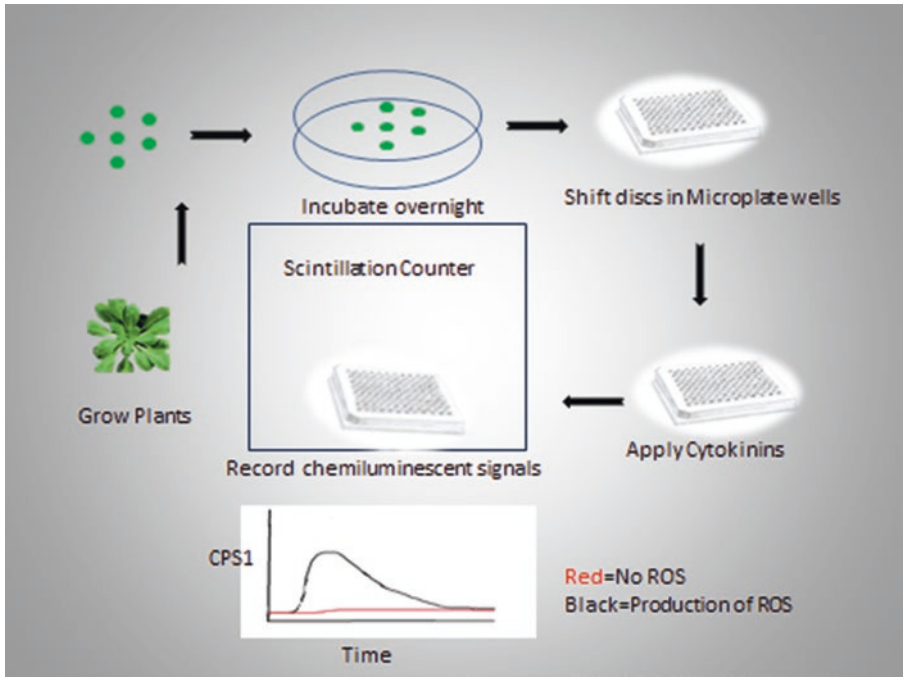

Fig. 1 ROS detection assay and the effect of cytokinins. Round *Arabidopsis* leaf discs of the size of well of 96-well microtiter plate left overnight in sterilized water leaf discs are then shifted into 96-well microtiter plate for luminol-based assay. Leaf discs incubated overnight are shifted in plate wells, and elicitors such as flg22 with and without cytokinin in defined concentration are added to the *Arabidopsis* segments. Subsequently the microtiter plate is subjected to luminol-based ROS counting equipment (scintillation counter)

References

1. Albert M, Jehle AK, Fürst U, Chinchilla D, Boller T, Felix G (2013) A two-hybrid-receptor assay demonstrates heteromer formation as switch-on for plant immune receptors. Plant Physiol 163:1504–1509
2. Koller T, Bent AF (2014) FLS2-BAK1 extracellular domain interaction sites required for defense signaling activation. PLoS One 9:e111185
3. Butenko MA, Wildhagen M, Albert M, Jehle A, Kalbacher H, Aalen RB, Felix G (2014) Tools and strategies to match peptide-ligand receptor pairs. Plant Cell 26:1838–1847
4. Felix G, Duran JD, Volko S, Boller T (1999) Plants have a sensitive perception system for the most conserved domain of bacterial flagellin. Plant J 18:265–276
5. Halter T, Imkampe J, Mazzotta S, Wierzba M, Postel S, Bücherl C, Kiefer C, Stahl M, Chinchilla D, Wang X (2014) The leucine-rich repeat receptor kinase BIR2 is a negative regulator of BAK1 in plant immunity. Curr Biol 24:134–143
6. Mittler R, Vanderauwera S, Suzuki N, Miller G, Tognetti VB, Vandepoele K, Gollery M, Shulaev V, Van Breusegem F (2011) ROS signaling: the new wave? Trends Plant Sci 16:300–309
7. Neill SJ, Desikan R, Clarke A, Hurst RD, Hancock JT (2002) Hydrogen peroxide and nitric oxide as signalling molecules in plants. J Exp Bot 53:1237–1247
8. Neill SJ, Desikan R, Hancock JT (2003) Nitric oxide signalling in plants. New Phytol 159:11–35
9. Kazan K, Lyons R (2014) Intervention of phytohormone pathways by pathogen effectors. Plant Cell 26:2285–2309
10. Robert-Seilaniantz A, Grant M, Jones JD (2011) Hormone crosstalk in plant disease and defense: more than just jasmonate-salicylate antagonism. Annu Rev Phytopathol 49:317–343
11. Naseem M, Wölfling M, Dandekar T (2014) Cytokinins for immunity beyond growth, galls and green islands. Trends Plant Sci 19:481–484
12. Mur LA, Kenton P, Atzorn R, Miersch O, Wasternack C (2006) The outcomes of concentration-specific interactions between salicylate and jasmonate signaling include synergy, antagonism, and oxidative stress leading to cell death. Plant Physiol 140:249–262
13. Mhamdi A, Hager J, Chaouch S, Queval G, Han Y, Taconnat L, Saindrenan P, Gouia H, Issakidis-Bourguet E, Renou J-P (2010) Arabidopsis GLUTATHIONE REDUCTASE1 plays a crucial role in leaf responses to intracellular hydrogen peroxide and in ensuring appropriate gene expression through both salicylic acid and jasmonic acid signaling pathways. Plant Physiol 153:1144–1160
14. O'Brien JA, Benková E (2013) Cytokinin cross-talking during biotic and abiotic stress responses. Front Plant Sci 4:451
15. Mlejnek P, Doležel P, Procházka S (2003) Intracellular phosphorylation of benzyladenosine is related to apoptosis induction in tobacco BY-2 cells. Plant Cell Environ 26:1723–1735
16. Wang Y, Shen W, Chan Z, Wu Y (2015) Endogenous cytokinin overproduction modulates ROS homeostasis and decreases salt stress resistance in Arabidopsis thaliana. Front Plant Sci 6:1004
17. Liu W-Z, Kong D-D, Gu X-X, Gao H-B, Wang J-Z, Xia M, Gao Q, Tian L-L, Xu Z-H, Bao F (2013) Cytokinins can act as suppressors of nitric oxide in Arabidopsis. Proc Natl Acad Sci 110:1548–1553
18. Gomez-Gomez L, Felix G, Boller T (1999) A single locus determines sensitivity to bacterial flagellin in Arabidopsis thaliana. Plant J 18:277–284
19. Zipfel C, Kunze G, Chinchilla D, Caniard A, Jones JD, Boller T, Felix G (2006) Perception of the bacterial PAMP EF-Tu by the receptor EFR restricts Agrobacterium-mediated transformation. Cell 125:749–760

Chapter 14

A Systems Biology Methodology Combining Transcriptome and Interactome Datasets to Assess the Implications of Cytokinin Signaling for Plant Immune Networks

Meik Kunz, Thomas Dandekar, and Muhammad Naseem

Abstract

Cytokinins (CKs) play an important role in plant growth and development. Also, several studies highlight the modulatory implications of CKs for plant-pathogen interaction. However, the underlying mechanisms of CK mediating immune networks in plants are still not fully understood. A detailed analysis of high-throughput transcriptome (RNA-Seq and microarrays) datasets under modulated conditions of plant CKs and its mergence with cellular interactome (large-scale protein-protein interaction data) has the potential to unlock the contribution of CKs to plant defense. Here, we specifically describe a detailed systems biology methodology pertinent to the acquisition and analysis of various omics datasets that delineate the role of plant CKs in impacting immune pathways in *Arabidopsis*.

Key words Cytokinins, Plant immunity, Transcriptomes, Interactomes, Plant hormones

1 Introduction

Cytokinins (CKs) are adenine-derived regulatory molecules that regulate many important functions in plants and are also implicated in plant-pathogen interactions [1–6]. In *Arabidopsis thaliana* (Hereafter: *Arabidopsis*), the signaling of CKs is mediated by a two-component system (TCS) involving a canonical phosphorelay mechanism. The binding of CKs to the central CHASE (cyclases/histidine kinases associated sensory extracellular) domain of the HISTIDINE KINASE 2–4 (AHK2–4) receptors initiates a downstream phosphotransfer cascade [2, 7]. This results in the phosphorylation of response regulators (ARRs) through histidine phosphotransfer proteins (AHPs). ARRs are categorized into two types: type-B ARRs which function as transcription factors and positively regulate CK signaling and type-A ARRs which negatively regulate CK responses and are transcriptionally regulated by type-B ARRs [2, 8]. The isopentenyltransferase (IPT) and cytochrome P450 monooxygenase (CYP735A) are important rate-limiting key

Thomas Dandekar and Muhammad Naseem (eds.), *Auxins and Cytokinins in Plant Biology: Methods and Protocols*, Methods in Molecular Biology, vol. 1569, DOI 10.1007/978-1-4939-6831-2_14,

enzymes that are involved in the biosynthesis of plant CKs. However, the final conversion of CK nucleotides into active form (iP: isopentenyladenine and tZ: *trans*-zeatin) is catalyzed by a CK-specific phosphoribohydrolase activity enzyme LONELY GUY (LOG). CKs are catabolized by cytokinin oxidase/dehydrogenase (CKX) [2, 9]. In comparison to their well-established role in regulating dynamics of plant growth and development, their functions in mediating plant immunity are not fully explored.

The increase in *Arabidopsis* resistance against infection with hemibiotrophic pathogen *Pseudomonas syringae* pv. tomato DC3000 (*Pst* DC3000) [3, 4, 10] and biotrophic pathogen *Hyaloperonospora arabidopsidis* (*Hpa*: [6]) with higher plant CK concentration points to positive crosstalk between CKs and salicylic acid (SA) defense pathway in plants. However, increased CK responses are also shown to inhibit the sporulation of necrotrophic pathogen *Alternaria brassicicola* [3, 10], and CK overproduction was coupled with protection against *Botrytis* infection [11]. Also, increased plant CK levels and susceptibility to gall-causing pathogens such as *Rhodococcus fascians* [12] and root-knot nematode (RKN: [13]) and fungal biotrophs such as *Claviceps purpurea* [9] reflect an antagonistic interaction between CK- and SA-mediated defenses. Moreover, the mutual interaction between CKs and auxin has its impact on immune balance in plants [4, 14]; however, the underlying molecular mechanisms are yet to be determined. It is therefore inferred that CKs play an important role in mediating dynamics of tradeoff between growth and defense and needs systems biology approaches to better decipher these vital functions. Here, we describe a multi-omics systems biology approach to highlight important hubs and modules that impact defense responses during increased CK status of the plant.

2 Materials

2.1 Databases

1. AINM (http://interactome.dfci.harvard.edu/A_thaliana/): *Arabidopsis* interactome database.
2. BioGRID (http://thebiogrid.org/): interactome database for several organisms including *Arabidospis*.
3. GEO (http://www.ncbi.nlm.nih.gov/geo/): a database of experimental datasets on quantitative transcriptomes.
4. GeneVestigator (https://genevestigator.com/gv/doc/intro_plant.jsp): a database of transcriptome datasets under various biotic and abiotic conditions.

2.2 Software/Programs

1. phpMyAdmin (MySQL database; https://www.phpmyadmin.net/): data management software tool.

2. Cytoscape 2.8.2 (http://www.cytoscape.org/): system biology software for visualization and analysis of biological networks.

2.3 Plugins/Tools

1. BiNGO [15]: tool to identify overrepresented Gene Ontology (GO) terms.
2. NetworkAnalyzer [16]: tool to calculate topological properties of the network.
3. AllegroMCODE [17, 18]: tool to find highly connected functional modules.
4. ClueGO [19]: tool to identify biological signaling pathways and processes.

3 Methods

3.1 Data Preparation

1. Exploit the well-known databases such as AINM or BioGRID to download high-confidence protein-protein interaction (PPI: interactome data) datasets of *Arabidopsis* (*see* **Note 1**).
2. Generate a table containing three columns: **column 1**, node A; **column 2**, interaction type; and **column 3**, node B (*see* **Note 1**).
3. Upload the table to phpMyAdmin (MySQL database).
4. Name the table as "**Interactome**."
5. Select differentially expressed genes (DEGs) (e.g., p-Value < 0.05, logFC ≥ 1, logFC ≤ 1) from the gene expression (*see* **Note 1**) dataset on the external application of CK to *Arabidopsis* seedlings (for instance, using GEO or GeneVestigator) (*see* **Note 4**).

3.2 Transcriptome-Interactome-Mapping and Reconstruction of an Immune-Specific Subnetwork

1. Select direct interaction partners of DEGs by mapping them to the interactome data in phpMyAdmin using the command: Select * From "Interactome" WHERE (nodeA = "DEG1" OR nodeB = "DEG1" ORnodeA = "DEG2" ORnodeB = "DEG2"); do this for each selected DEGs.
2. Save the interactions as .sif (simple interaction file) format by opening the identified interaction partners in phpMyAdmin as .csv table and then upload the interactions into a text editor and save the interactions as "**Network.sif**."
3. Upload and visualize the reconstructed network: Open Cytoscape software version 2.8.2 and click "File" then click "Import" and then click "Network" (Multiple File Types) and then select "Network.sif" and click "Import."
4. Analyze the network for immune-relevant processes: Click "Plugins" and then click "BiNGO" and there select organism "*Arabidopsis thaliana*" and furthermore select "Biological Processes." From the BiNGO table, list all statistically signifi-

cant (p-Value < 0.05) immune-relevant functions and their corresponding genes.

5. Reconstruct an immune-specific subnetwork using direct interaction partners of the immune genes from the BiNGO analysis (*see* **Note 2**) by mapping them to the interactome data.

3.3 Topological and Functional Analysis of the Reconstructed Immune-Specific Subnetwork and Functional Insights

1. Analyze the network topology: Click "Plugins," then "Network Analysis," and then "Analyze Network," select "Treat the network as untreated," and then select network parameters such as average number of neighbors, network centralization, and network heterogeneity (*see* **Note 3**).
2. Analyze the network for functional modules: Click "Plugins" and then "AllegroMCODE" and then click "AnalyzeNetwork," and there select significant (e.g., Score > 1) clusters (*see* **Note 1**).
3. Analyze the network for relevant signaling pathways and processes: Select all nodes in the network (or cluster nodes or nodes of interest) and click "Plugins" and then click "ClueGO + CluePedia" and then select in the column "organism" "*Arabidopsis thaliana*" and then put the selected nodes in the text field and then select in the column ClueGO "Settings of interest," e.g., "Biological Process," "KEGG," "Reactome," and "WikiPathways," and click "Show only Pathways with $p \leq 0.05$" and then opt "Start" and select from the output table list of relevant immune signaling pathways and functions as well as the associated genes (*see* **Note 1**).
4. Based on the results (network topology and AllegroMCODE and ClueGO), important functional hub nodes for CK-mediated plant immune defense (*see* **Note 5**) can be figured out.

4 Notes

We established a methodology by combining different network biology tools for elucidating the functional role of large-scale expression datasets [20]. In this context, our integrated transcriptome-interactome analysis allows investigation of changes in CK signaling upon pathogen infection and can contribute to detect relevant functional modules and hub nodes for CK-mediated defense responses in *Arabidopsis* (*see* Fig. 1).

1. Transcriptome data (microarrays or RNA-Seq) of *Arabidopsis* plants can be generated either by own experiments and/or can be downloaded from public databases such as Gene Expression Omnibus (GEO; http://www.ncbi.nlm.nih.gov/geo/). High-confidence PPI data (interactome) of *Arabidopsis* can be acquired from different databases such as the BioGRID database (http://thebiogrid.org/) and from the Arabidopsis

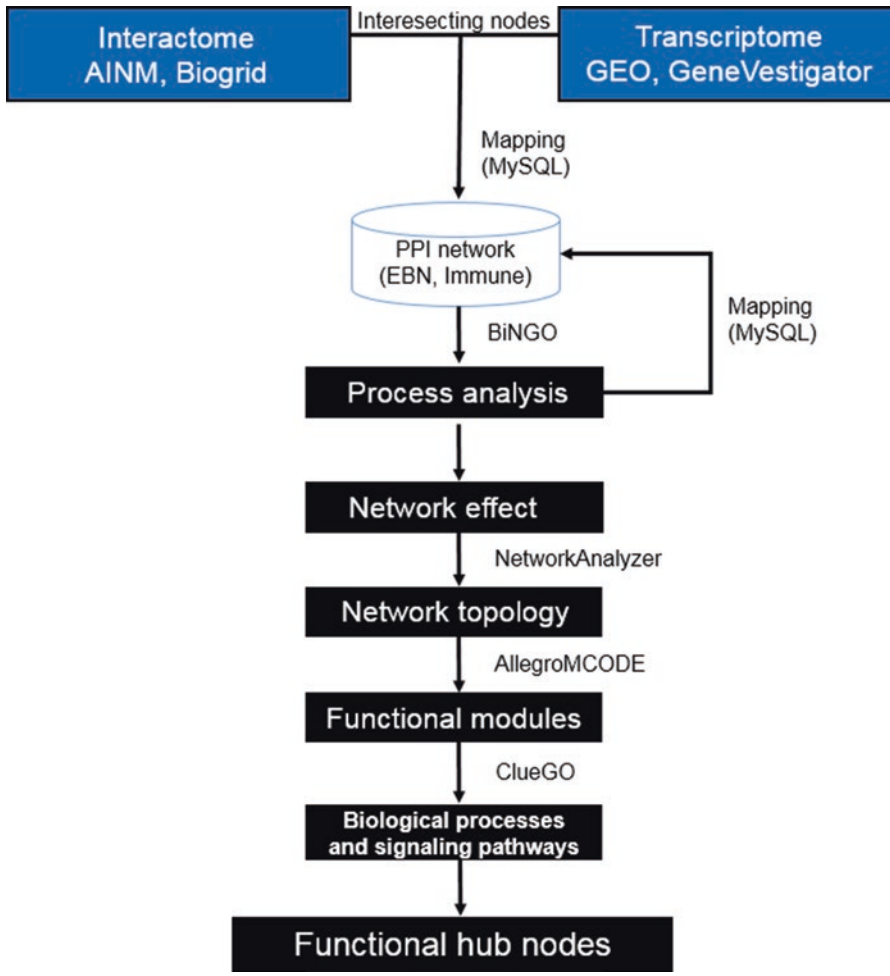

Fig. 1 Overview of the methodology. The methodology combines transcriptome and interactome data to analyze the topology and function as well as to find important functional hub nodes

Interactome Network Map (*Arabidopsis* Interactome Mapping Consortium, Science 2011, http://interactome.dfci.harvard.edu/A_thaliana/). Transcriptome and interactome data can further be warehoused in a MySQL database for an efficient data management (*see* Fig. 1).

2. Significantly DEGs from the transcriptome (data normalization, preparation, and filtering [20] here not described) reflecting changes in CK-mediated gene expression can be mapped to the entire *Arabidopsis* interactome to identify intersecting nodes (transcriptome-interactome-mapping). The reconstructed expression-based network on the shared nodes between the transcriptome and interactome and their direct interaction partners can be detected by using the Cytoscape [15]. The Cytoscape software is an open source platform for the visualization and analysis of biological networks using several plugins

(http://www.cytoscape.org/). For example, the BiNGO plugin tool identifies overrepresented Gene Ontology (GO) terms in a set of genes or a given biological network and maps them into a GO term hierarchy network. Based on this GO term analysis, statistically enriched biological processes relevant for the immune system and their participating nodes can be selected, which additionally reduced the complexity and number of nodes from the transcriptome-interactome mapping (*see* Fig. 2, three example immune processes out of 110 immune functions from the BiNGO analysis; here we used transcriptome data (GSE 6832.I) of 2-week-old wild-type *Arabidopsis* plants treated with *trans*-Zeatin for 1 h in comparison to mock treatment). Next, these immune-relevant functions and corresponding nodes can be integrated into an immune-specific subnetwork (immune network) considering all direct protein interacting nodes (direct neighbors) through mapping to the whole interactome (visualization of the network using Cytoscape) (*see* Fig. 2; example immune network based on 310 immune-relevant nodes contains 1216 nodes and 1596 edges; 310 immune nodes in green, nodes from the interactome in blue). In addition, both reconstructed networks can also be subdivided into pathogen-regulated networks based on their up- and downregulated DEGs and their interactors (*see* Fig. 1).

3. Subsequently, the reconstructed immune-specific subnetwork can be analyzed for their topological behavior. Therefore, the network topology can be analyzed using the plugin NetworkAnalyzer [16], allowing the determination of different network properties such as the average number of neighbors, network centralization, and network heterogeneity. These parameters give a better insight into the connectivity and topology as well as the network tendency to contain hub nodes [21], for instance, immune-relevant nodes with maximum connectivity from the network (*see* Fig. 1).
4. As a next step, the immune-specific subnetwork can be investigated for functional modules (called clusters) using the Cytoscape plugin AllegroMCODE [17, 18]. Functional clusters are highly connected subgraphs which have a strong impact on the whole network [17, 18] (*see* Fig. 2; example cluster with 11 nodes in brown). In addition, the subnetwork and/or identified clusters can be further analyzed for associated biological signaling pathways and processes using the Cytoscape plugin ClueGO [19]. ClueGO works similar to BiNGO but performs functionally grouped networks of GO terms and pathways that includes data from KEGG, WikiPathways, and Reactome databases and allows comparison of gene lists [19], for example, differences between the subdivided up- and downregulated pathogen-mediated networks (*see* Fig. 1).

p-Value	x	n	Biological Process
1,43E-05	9	39	cytokinin mediated signaling pathway
7,09E-08	54	637	defense response
1,02E-02	19	272	immune response

Immune network

Highly connected cluster

Hub node	Nr.	p-Value	logFC	Name	Description
AT1G80840	7	3,56E-04	3,86	WRKY40	putative WRKY transcription factor 40
AT1G32640	12	3,45E-06	3,95	MYC2	transcription factor MYC2
AT1G64280	15	2,65E-02	1,12	NPR1	Regulatory protein NPR1
AT1G19180	21	2,66E-05	4,59	JAZ1	jasmonate-zim-domain protein 1
AT1G74890	7	2,22E-04	-3,67	ARR15	two-component response regulator ARR15

Fig. 2 An example output from the BiNGO analysis (3 out of 110 immune functions) and a reconstructed immune network (containing 1216 nodes and 1596 edges, 310 immune-relevant nodes in *green*) with a highly connected cluster and hub nodes are shown. Here we analyzed a transcriptome dataset from GEO transcriptome depository (GSE 6832.l) of 2-week-old wild-type *Arabidopsis* plants treated with *trans*-Zeatin for 1 h in comparison to mock treatment

5. Finally, by combining both results from AllegroMCODE and ClueGO with the network topology analysis, important functional hub nodes for the plant defense can be identified that will result in the identification of network connections as well as bystander nodes. Hence, this can support the importance of different pathways and/or functional modules in the subnetwork and highlight potential targets and new insights into previously unknown cellular context (*see* Fig. 2; example immune-relevant hub nodes with additional information).

The described systems biology methodology integrates gene expression and *Arabidopsis* interactome data to analyze the changes in CK signaling upon pathogen infection. Thus, it allows a better elucidation of gene expression datasets leading to the identification of relevant functional modules and hub nodes for further experimental characterization of previously unknown interactions.

Acknowledgments

We thank DFG for funding (FungiNet124/B1).

References

1. Kunz M, Ahmed N, Dandekar T, Naseem M (2013) Hormone signaling networks open multiple routes for immunity and disease in plants. Biohelikon Immunity and Diseases 1:2
2. Hwang I, Sheen J, Muller B (2012) Cytokinin signaling networks. Annu Rev Plant Biol 63:353–380
3. Choi J, Choi D, Lee S, Ryu CM, Hwang I (2011) Cytokinins and plant immunity: old foes or new friends? Trends Plant Sci 16:388–394
4. Naseem M, Philippi N, Hussain A, Wangorsch G, Ahmed N, Dandekar T (2012) Integrated systems view on networking by hormones in Arabidopsis immunity reveals multiple crosstalk for cytokinin. Plant Cell 24:1793–1814
5. Naseem M, Kunz M, Ahmed N, Dandekar T (2013) Integration of boolean models on hormonal interactions and prospects of cytokinin-auxin crosstalk in plant immunity. Plant Signal Behav 8:e23890
6. Argueso CT, Ferreira FJ, Epple P, To JP, Hutchison CE, Schaller GE, Dangl JL, Kieber JJ (2012) Two-component elements mediate interactions between cytokinin and salicylic acid in plant immunity. PLoS Genet 8:e1002448
7. Schaller GE, Bishopp A, Kieber JJ (2015) The yin-yang of hormones: cytokinin and auxin interactions in plant development. Plant Cell 27:44–63
8. Naseem M, Wolfling M, Dandekar T (2014) Cytokinins for immunity beyond growth, galls and green islands. Trends Plant Sci 19:481–484
9. Hinsch J, Vrabka J, Oeser B, Novak O, Galuszka P, Tudzynski P (2015) De novo biosynthesis of cytokinins in the biotrophic fungus Claviceps purpurea. Environ Microbiol 17:2935–2951
10. Choi J, Huh SU, Kojima M, Sakakibara H, Paek KH, Hwang I (2010) The cytokinin-activated transcription factor ARR2 promotes plant immunity via TGA3/NPR1-dependent salicylic acid signaling in Arabidopsis. Dev Cell 19:284–295
11. Swartzberg D, Kirshner B, Rav-David D, Elad Y, Granot D (2008) Botrytis cinerea induces senescence and is inhibited by autoregulated expression of the IPT gene. Eur J Plant Pathol 120:289–297
12. Radhika V, Ueda N, Tsuboi Y, Kojima M, Kikuchi J, Kudo T, Sakakibara H (2015) Methylated cytokinins from the phytopathogen Rhodococcus fascians mimic plant hormone activity. Plant Physiol 169:1118–1126
13. Siddique S, Radakovic ZS, De La Torre CM, Chronis D, Novak O, Ramireddy E, Holbein J, Matera C, Hütten M, Gutbrod P, Anjam MS, Rozanska E, Habash S, Elashry A, Sobczak M, Kakimoto T, Strnad M, Schmülling T,

Mitchum MG, Grundler FM (2015) A parasitic nematode releases cytokinin that controls cell division and orchestrates feeding site formation in host plants. Proc Natl Acad Sci U S A 112:12669–12674
14. Naseem M, Dandekar T (2012) The role of auxin-cytokinin antagonism in plant-pathogen interactions. PLoS Pathog 8:e1003026
15. Maere S, Heymans K, Kuiper M (2005) BiNGO: a Cytoscape plugin to assess overrepresentation of gene ontology categories in biological networks. Bioinformatics (Oxford, England) 21:3448–3449
16. Assenov Y, Ramirez F, Schelhorn SE, Lengauer T, Albrecht M (2008) Computing topological parameters of biological networks. Bioinformatics (Oxford, England) 24:282–284
17. Bader GD, Hogue CW (2003) An automated method for finding molecular complexes in large protein interaction networks. BMC Bioinformatics 4:2
18. Saito R, Smoot ME, Ono K, Ruscheinski J, Wang PL, Lotia S, Pico AR, Bader GD, Ideker T (2012) A travel guide to Cytoscape plugins. Nat Methods 9:1069–1076
19. Bindea G, Mlecnik B, Hackl H, Charoentong P, Tosolini M, Kirilovsky A, Fridman WH, Pagès F, Trajanoski Z, Galon J (2009) ClueGO: a Cytoscape plug-in to decipher functionally grouped gene ontology and pathway annotation networks. Bioinformatics (Oxford, England) 25:1091–1093
20. Naseem M, Kunz M, Dandekar T (2014) Probing the unknowns in cytokinin-mediated immune defense in Arabidopsis with systems biology approaches. Bioinformatics Biol Insights 8:35–44
21. Dong J, Horvath S (2007) Understanding network concepts in modules. BMC Syst Biol 1:24

Chapter 15

Monitoring of Crosstalk Between Jasmonate and Auxin in the Framework of Plant Stress Responses of Roots

Víctor Carrasco Loba, Marta-Marina Pérez Alonso, and Stephan Pollmann

Abstract

Over the last few years, it became more and more evident that plant hormone action is to great parts determined through their sophisticated crosstalk, rather than by their isolated activities. Thus, the parallel analysis of interconnected phytohormones in only very small amounts of tissue developed to an important issue in the field of plant sciences. In the following, a highly sensitive and accurate method is described for the quantitative analysis of the plant hormones jasmonic acid and indole-3-acetic acid in the model plant *Arabidopsis thaliana*. The described methodology is, however, not limited to the analysis of *Arabidopsis* samples but can also be applied to other plant species. The presented method is optimized for the working up of as little as 20–50 mg of plant tissue. Thus, it is well suited for the analysis of plant hormone contents in plant tissue of only little biomass, such as roots. The presented protocol facilitates the implementation of the method into other laboratories that have access to appropriate laboratory equipment and comparable state-of-the-art gas chromatography-mass spectrometry (GC-MS) technology.

Key words Jasmonic acid, Auxin, Crosstalk, Electron impact tandem mass spectrometry (EI-GC-MS/MS), Solid-phase extraction, Stable isotopes, Derivatization, Plant hormone analysis

1 Introduction

Plant hormones are involved in the regulation of virtually all aspects of plant growth and development, as well as in plant responses to environmental stimuli. Up to date, a small number of such signaling molecules are known, including among others auxins, cytokinins, gibberellins, abscisic acid, salicylic acid, jasmonates, and ethylene [1]. Initially, the various plant hormones have been studied in an isolated fashion. Deeper insight into their mode of action and their pivotal impact on plant development and responses toward external stimuli, however, revealed a high degree of interaction between the different phytohormones [2, 3]. To date, it is commonly accepted that the plant hormone network can affect both plant growth and development as well as their physiological

Thomas Dandekar and Muhammad Naseem (eds.), *Auxins and Cytokinins in Plant Biology: Methods and Protocols*, Methods in Molecular Biology, vol. 1569, DOI 10.1007/978-1-4939-6831-2_15,

responses to external cues on different levels involving, e.g., the control of mRNA and protein synthesis, the activity and turnover rate of proteins, hormone transport, and the reversible or irreversible inactivation of active signaling molecules [4].

In this context, the mechanistic and conceptual crosstalk between jasmonic acid (JA) and indole-3-acetic acid (IAA) is particularly interesting because, at first glance, those two plant hormones possess antagonistic properties. While IAA is generally considered the plant's most important growth factor, JA is commonly associated with growth inhibitory effects. However, it has been shown that the two plant hormones share components of the perception and signal transduction machinery [5–7], which was among the first evidence that highlighted a tight and intimate interconnection of JA and IAA. Later on, further research substantiated those findings, disclosing an important impact of jasmonates and their precursors on the biosynthesis of IAA [8–12]. It is suggested that the crosstalk between JA and IAA plays an important role in plant stress responses, particularly toward biotic foes. As an example, mechanical wounding, which is known to trigger the rapid production of JA, is capable to induce gene expression of *YUC9*, a flavin-containing monooxygenase involved in auxin biosynthesis [11]. So far, the role of auxin in plant stress responses and the importance of JA/IAA crosstalk are not well established, but it is considered that alterations in auxin homeostasis in the course of stress responses of the root have a substantial impact on root architecture. In this context, the response toward the endophyte *Piriformospora indica* is a very good example since the main target of the fungus in the roots is auxin homeostasis [13, 14]. For further reading on this particular topic, we refer to Chapter 3.

However, whole-genome covering transcriptomics approaches, comparing transcriptional responses in wild-type *Arabidopsis* to those in a number of available mutants, provided a wealth of very valuable information on the mechanism through which JA may impact on auxin homeostasis, incrementing IAA biosynthesis. At this point, we have to put emphasis on the fact that final proof for such a described impact has to come from the quantification of the corresponding plant hormone levels in the responding tissue, because this is the ultimate readout that matters. Bearing in mind that particularly JA, but also IAA, abundance in plant tissues is fairly low, the quantitative analysis of those signaling molecules still remains a challenging task.

To overcome this problem, modern methods for the quantitative analysis of trace substances nowadays rely on highly sensitive mass spectrometric techniques. In combination with internal standardization using stable isotope-labeled compounds, mass spectrometry offers not only the unambiguous identification of

plant hormones but also their absolute quantitation within a given sample. It has to be remarked that the extraction and pre-purification protocol presented here is suitable to enrich all kinds of acidic plant hormones at once, which in fact makes multiplex analysis of several acidic phytohormones, such as auxins, jasmonates, salicylic acid, abscisic acid, and those with modifications of gibberellins, from one sample possible if required GC-MRM-MS/MS equipment is available [15–17]. Apart from very few entry-level GC-MS machines, modern GC-MS setups generally possess tandem MS (MS/MS or MS^n) capacities. In brief, working in MS/MS mode refers to the selection of suitable parent or precursor ions in the first MS step, which are then fragmented through the collision with a noble gas, most commonly argon. The resulting so-called fragment, daughter, or product ions are finally recorded in a second MS step. The upside of this methodology is the substantial improvement of the signal-to-noise ratio that offers the possibility to obtain clean spectra for given target compounds even from very complex samples. On the downside, utilizing a very sensitive technique such as GC-MS makes the establishment of an efficient pre-purification/sample preparation protocol mandatory, because primary extracts are generally not considered suitable for direct assessment by GC-MS, even though exactly this would be desirable. In this respect, it has to be noted that there is no one universal method that facilitates the simultaneous pre-purification of all plant hormones at the same time, due to their very different chemical properties. However, mainly because of major advances in sensitivity, liquid chromatography-mass spectrometry (LC-MS) moves more and more into the limelight, also in the field of plant hormone quantification. This can likely be attributed to the fact that the LC-MS setup is less prone to malfunction and long-lasting contamination of the hardware when sample quality is slightly on the low side. In any case, it has to be emphasized that also in LC-MS comprehensive sample preparation protocols are sometimes required to facilitate analysis of the desired target substances [18–22].

The method presented in this chapter facilitates the parallel quantitative analysis of JA and IAA in small tissue samples. As stated above, the described purification procedure is also suitable for several other acidic phytohormones and related substances. The method has been validated and successfully used for a number of plant species, for instance, *Arabidopsis*, barley, tobacco, potato, tomato, corn, and rice. It is, however, not appropriate to purify basic plant hormones, such as cytokinins and related derivatives. In this case, the reader is referred to advanced literature for further reading [23–28].

2 Material

2.1 Plant Hormone Extraction, Pre-purification, and Derivatization

All solvents should be prepared using exclusively reagents in pro analysis or at least high-performance liquid chromatography (HPLC) grade. If not directly using the pure reagents, it is recommended to prepare the solvents freshly and to use them at room temperature (if not explicitly stated otherwise). All reagents should be stored at room temperature.

1. Acetic acid (Sigma Chemical Company, St. Louis, MO, USA).
2. Acetone (Sigma Chemical Company, St. Louis, MO, USA).
3. Methanol (Sigma Chemical Company, St. Louis, MO, USA).
4. Diethyl ether, dry, free of peroxides (Sigma Chemical Company, St. Louis, MO, USA).
5. Chloroform (Sigma Chemical Company, St. Louis, MO, USA).
6. 2-Propanol (Sigma Chemical Company, St. Louis, MO, USA).
7. (Trimethylsilyl)diazomethane solution, 2.0 M in diethyl ether (Sigma Chemical Company, St. Louis, MO, USA).
8. Washing solvent for solid-phase extraction: chloroform/2-propanol [2:1, v/v].
9. Elution solvent for solid-phase extraction: diethyl ether + 2% acetic acid [v/v].
10. Thermomixer (Thermomixer comfort, Eppendorf AG, Hamburg, Germany).
11. Aminopropyl solid-phase extraction columns (Chromabond NH_2 shorty 10 mg, Macherey-Nagel GmbH, Düren, Germany).
12. Centrifuge and corresponding rotor (1-15PK with rotor 12024-H, Sigma Laborzentrifugen GmbH, Osterode am Harz, Germany).
13. Speed-vac concentrator (Concentrator Plus 5305, Eppendorf AG, Hamburg, Germany).
14. Extraction vacuum manifold (20-port, Waters Corporation, Molford, MA, USA).
15. Membrane vacuum pump stand (PC 620 NT, Vacuubrand, Wertheim, Germany).
16. Ball mill with Eppendorf cup adaptor (Retch MM300, purchased from Qiagen, Hilden, Germany).
17. Stainless steel balls, 3 mm diameter (Retsch, Haan, Germany).
18. Ultrasonic bath (Bansonic 5510E-DTH, Branson Ultrasonics Corporation, Danbury, CT, USA).

2.2 Stable Isotope-Labeled Internal Standard

Stable isotope-labeled indole-3-acetic acid ([$^2H_2$]-indole-3-acetic acid) and jasmonic acid ([$^2H_5$]-jasmonic acid), respectively, to be used as internal standards in the mass spectrometric analysis are commercially available and can be purchased, e.g., from CDN isotopes (Pointe-Claire, Canada) or OlChemIm Ltd. (Olomouc, Czech Republic). There is the possibility to use standards from other vendors (*see* **Note 1**) given that the isotopic enrichment of the substance is higher than 96% and the compound does neither decay nor detectably exchange the heavy isotopes during the sample preparation and analysis process. Please note that it is highly recommended that the mass difference between internal standard and analyte is not less than two AMU.

3 Methods

3.1 Extraction of Plant Tissue

If not explicitly specified otherwise, all steps can be carried out at room temperature.

1. Weigh between 20 and 50 mg of plant tissue (fresh weight) into a 1.5 ml disposable reaction tube (*see* **Note 2**). Add 1 ml of methanol, 30 pmol of [$^2H_5$]-jasmonic acid and 50 pmol of [$^2H_2$]-indole-3-acetic acid internal standard (*see* **Note 3**), and three steel balls.
2. Use a thermomixer to heat the sample to 60 °C and incubate it under gentle agitation for 3 min, then homogenize by heavy vortexing or shaking for several minutes. Optimally, a vibrating-ball micro-mill (Retsch MM300) can be utilized, subjecting the sample to two rounds of 3 min, each at 30 Hz (*see* **Note 4**). Further extraction will take place at room temperature for at least 1 h. Over the course of the incubation, the sample should be vortexed or inverted a couple of times.
3. Remove the steel balls by using a magnetic tool and centrifuge the sample (14,000 × *g*, 1 min) to sediment cell wall debris and other floating particles. Carefully transfer the supernatant to a fresh reaction tube, omitting to pick up parts of the pellet. Take the sample to complete dryness using a speed-vac set to 60 °C (*see* **Note 5**) and maximum vacuum. Please note that after drying the sample can be stored at −80 °C until further processing.

3.2 Pre-purification and Enrichment of Acidic Compounds by Solid-Phase Extraction

1. Thoroughly dissolve the crude residue in 50 µl methanol, then add 200 µl of diethyl ether. Sonify the sample for 5 min in an ultrasonic bath, before centrifuging it for 5 min at 14,000 × *g*.
2. During the preparation of the sample, already start with the equilibration of the aminopropyl solid-phase extraction column (*see* **Note 6**). To do so, wash the column with 2 × 200 µl diethyl ether.

3. Transfer the entire sample onto the conditioned column and let the sample pass the matrix by gravity flow without applying vacuum to the SPE manifold. This is likely to improve the association of acidic compounds to the NH_2 matrix.
4. After passage of the sample, wash the column twice with 200 µl freshly prepared washing solvent (chloroform/2-propanol). Clean the tip of the plastic insert holding the column with some white laboratory paper.
5. Elute the sample from the matrix into a fresh reaction tube by adding 2 × 200 µl of the elution solvent (acidified diethyl ether, containing 2% acetic acid [v/v]). Finally, dry the combined eluates using a speed-vac concentrator (10 mbar, 60 °C). Remove residual acetic acid in a gentle stream of nitrogen.

3.3 Derivatization of the Sample Prior to GC-MS Analysis

The contained acidic plant hormones are preferentially analyzed by gas chromatography-mass spectrometry (GC-MS) in the form of their methyl esters, which are characterized by a substantially lower melting point and, thus, better vaporization properties during the subsequent GC-MS analysis (*see* **Note 7**).

1. Prepare 10 ml of an acetone/methanol [9:1 (v/v)] solution. When kept in darkness and in an airtight vessel, the mixture can be stored at room temperature over a longer period of time.
2. To prepare the derivatization solvent for the methylation of organic acids, mix 220 µl of the acetone/methanol solution with 27 µl diethyl ether and 3 µl of the (trimethylsilyl)diazomethane solution (*see* **Note 8**). The resulting 250 µl are sufficient for the chemical modification of at least ten samples (*see* **Note 9**).
3. Dissolve the sample in 25 µl methanol and transfer the solution into a 600 µl crimp top conical microvial (Chromacol Uni-VL Supelco #27312). Dry completely in a gentle stream of nitrogen.
4. Add 20 µl of the freshly prepared derivatization solvent to the sample. Immediately close the vial with a suitable 8 mm crimp seal with PTFE/rubber septa. Let the sample rest for 30 min at room temperature before proceeding with the GC-MS analysis.

3.4 Gas Chromatographic-Mass Spectrometric Assessment

From the derivatized sample, a 1 µl aliquot is injected into the GC-MS system for gas chromatographic separation and subsequent mass spectrometric analysis.

3.4.1 GC Setup

Injection of the sample was carried out in splitless mode. A pressure pulse of 25 psi over 1 min was used to force the transfer of compounds from the injector into the column. After that time, the

split was fully opened for 1.5 min before it was set to a split ratio of 20% for the remaining run time. The injector temperature was 250 °C and the column temperature was held at 50 °C for 1.2 min. Then, it was increased by 30 °C/min to 120 °C, followed by a further increase to 325 °C by 10 °C/min. Finally, a temperature of 325 °C was held for another 4 min. Separation was achieved by using a 30 m × 0.25 mm i.d. fused silica capillary column with a chemical bond 0.25 μm ZB35 stationary phase (Phenomenex, Torrance, USA) (*see* **Note 10**). Helium at a flow rate of 1 ml/min served as the mobile phase.

3.4.2 Mass Spectrometer Setup

The method described here is optimized for triple-quadrupole mass spectrometers run with positive polarity. The mass spectrometer was operated in EI-MRM mode. The transfer line temperature was set to 250 °C, while the ion source temperature was set to 200 °C. Ions were generated with −70 eV at a filament emission current of 80 μA. The dwell time was 175 ms. Argon set at 2.0 mTorr was used as the collision gas. For the target compounds, derivatized endogenous IAA and JA as well as the two deuterated internal standards, at least two transitions were recorded. One transition was used as the quantifier ion, whereas the others served as qualifier ion providing additional information about the analyte as well as indicating the presence of possible impurities. The selected precursor ions and corresponding diagnostic product ions are listed in Table 1.

The amount of the endogenous compound was calculated from the signal ratio of the unlabeled over the stable isotope-containing mass fragment observed in the parallel measurements (Table 1).

4 Notes

1. Stable isotope-labeled indole-3-acetic acid is also available from Cambridge Isotopes (www.isotope.com), Isotec (Sigma-Aldrich; www.isotec.com, www.sigma-aldrich.com), while both labeled indole-3-acetic acid and jasmonic acid are commercially available from Medical Isotopes (www.medicalisotopes.com).
2. It has to be noted that jasmonic acid production is strongly induced by mechanical wounding. In case that organ-specific plant hormone analysis is desired, which involves dissection of the plants, fast quenching of the metabolism is required. We strongly recommend freeze the harvested tissue directly in reaction tubes containing liquid nitrogen. By this measure, corruption of the obtained data by self-induced JA production can largely be avoided.

Table 1
Characteristic precursor and product ions used for the detection of methylated jasmonic and indole-3-acetic acid and its internal standards

Compound	Retention time (min)	Retention time window (min)	Precursor ion (*m/z*)	Product ion (*m/z*)	Collision energy	Scan time (%)	Quantifier ion
MeIAA	13.42	1	189	130	10	50	X
	13.42	1	130	103	15	50	
[$^2H_2$]-MeIAA	13.42	1	191	132	10	50	X
	13.42	1	132	103	15	50	
MeJA	11.25	1	151	108	10	50	X
	11.25	1	224	151	10	50	
[$^2H_5$]-MeJA	11.25	1	154	111	10	50	X
	11.25	1	229	154	10	50	

It has to be noted that the retention time for the target compound may moderately shift due to system-dependent parameters. It is recommended to use reference compounds to determine retention times for the actual setup prior to the analysis (*see* **Note 10**)

3. Note that it is mandatory to determine the appropriate amount of internal standard to be used in preliminary experiments. The necessary standard content can change for different tissues and developmental stages, respectively. It is recommended that the amount of standard added to the sample should neither exceed the endogenous content of the analyte by five times, nor should it be less than 1/5 of the respective analyte to be analyzed.
4. More rigid plant organs, e.g., more lignified tissues such as stems or seeds, may require longer vibration times. If no vibrating-ball micro-mill is available, the tissue can alternatively be ground in liquid nitrogen using micro-pistils and standard reaction tubes. The resulting powder must not thaw before the addition of the methanol.
5. It is important that the sample is completely dried with no traces of water left. Unnecessary processing in the speed-vac concentrator, however, should be avoided as over-drying may result in analyte loss. Given the fact that indole-3-acetic acid and jasmonic acid have their melting points between 160 and 169 °C, the risk of analyte loss by evaporation is low though. To our experience, processing times of up to 2 h do not negatively affect analyte contents.
6. It is possible to use commercially available microtips from other vendors, e.g., from Glygen Corp., Columbia, USA, or Chromacol

Ltd., Welwyn Garden City, UK, for solid-phase extraction. Please note, however, that the presented protocol has not been optimized for such type of pipet microtips and, thus, needs to be adapted in case that usage of microtips is desired.

7. As an alternative to the methylation using (trimethylsilyl) diazomethane solution, other reagents for the derivatization of indole-3-actic acid and jasmonic acid can be used. In our hands, trimethylsilylation using *N*,*O*-bis(trimethylsilyl)trifluoroacetamide (BSTFA) + trimethylsilyl chloride (TMCS), 99:1 [v/v] (Supelco, Bellefonte, PA, USA) proved to be very effective. However, it has to be taken into account that BSTFA does not only react with the –OH group of carboxy functions, but with all type of alcohol, phenol, carboxyl, amine, amide, and thiol groups at different reaction velocities, which sometimes results in nonuniform derivatization of compounds that carry more than one group prone to the reaction with the reagent. For example, in case of IAA, it can lead to the formation of TMS-IAA and $(TMS)_2$-IAA due to the rapid derivatization of the carboxy function, whereas derivatization of the –NH group in the heterocycle takes considerably longer. For this reason, we recommend to allow a derivatization time of at least 45 min at 60 °C to ensure uniform and complete derivatization of target compounds.
8. Alternatively, ethereal diazomethane can be used for the methylation. Ethereal diazomethane can be prepared from *N*-nitrosomethylurea recrystallized from methanol. *N*-Nitrosomethylurea can be obtained from Sigma-Aldrich. However, in any case, when preparing and/or handling diazomethane containing solutions, safety precautions should strictly be obeyed. All steps have to be performed in a well-ventilated laboratory fume hood.
9. It is recommended to prepare only the amount of derivatization solution required for immediate use. The solvent should only be used freshly prepared.
10. GC capillary columns with an intermediate polarity similar to that of the here used ZB-35 column (35 % phenyl–65 % dimethylpolysiloxane, low bleeding) are standard for acidic phytohormone profiling. However, other stationary phases (e.g., containing 5 or 50 % phenyl) that provide either lower or higher polarity can also be used. It has to be noted that such columns may need a slightly different temperature program than the one reported here to achieve satisfying separation of the analytes.

Acknowledgments

This work was supported by MINECO grant BFU2014-55575-R and Marie Curie career integration grant FP7-PEOPLE-CIG-2011 303744 to SP.

References

1. Davies PJ (ed) (2010) Plant hormones. Biosynthesis, signal transduction, action! 3rd edn. Kluwer, Dordrecht
2. Kazan K, Manners JM (2008) Jasmonate signaling: toward an integrated view. Plant Physiol 146:1459–1468
3. Wolters H, Jürgens G (2009) Survival of the flexible: hormonal growth control and adaptation in plant development. Nat Rev Genet 10:305–317
4. Hoffmann M, Hentrich M, Pollmann S (2011) Auxin-oxylipin crosstalk: relationship of antagonists. J Integr Plant Biol 53:429–445
5. Tiryaki I, Staswick PE (2002) An Arabidopsis mutant defective in jasmonate response is allelic to the auxin-signaling mutant *axr1*. Plant Physiol 130:887–894
6. Ren C, Pan J, Peng W, Genschik P, Hobbie L, Hellmann H, Estelle M, Gao B, Peng J, Sun C, Xie D (2005) Point mutations in Arabidopsis *Cullin1* reveal its essential role in jasmonate response. Plant J 42:514–524
7. Szemenyei H, Hannon M, Long JA (2008) TOPLESS mediates auxin-dependent transcriptional repression during Arabidopsis embryogenesis. Science 319:1384–1386
8. Dombrecht B, Xue GP, Sprague SJ, Kirkegaard JA, Ross JJ, Reid JB, Fitt GP, Sewelam N, Schenk PM, Manners JM, Kazan K (2007) MYC2 differentially modulates diverse jasmonate-dependent functions in Arabidopsis. Plant Cell 19:2225–2245
9. Sun J, Xu Y, Ye S, Jiang H, Chen Q, Liu F, Zhou W, Chen R, Li X, Tietz O, Wu X, Cohen JD, Palme K, Li C (2009) Arabidopsis ASA1 is important for jasmonate-mediated regulation of auxin biosynthesis and transport during lateral root formation. Plant Cell 21:1495–1511
10. Sun J, Chen Q, Qi L, Jiang H, Li S, Xu Y, Liu F, Zhou W, Pan J, Li X, Palme K, Li C (2011) Jasmonate modulates endocytosis and plasma membrane accumulation of the Arabidopsis PIN2 protein. New Phytol 191:360–375
11. Hentrich M, Böttcher C, Düchting P, Cheng Y, Zhao Y, Berkowitz O, Masle J, Medina J, Pollmann S (2013) The jasmonic acid signaling pathway is linked to auxin homeostasis through the modulation of *YUCCA8* and *YUCCA9* gene expression. Plant J 74:626–637
12. Hentrich M, Sanchez-Parra B, Perez Alonso MM, Carrasco Loba V, Carrillo L, Vicente-Carbajosa J, Medina J, Pollmann S (2013) YUCCA8 and YUCCA9 overexpression reveals a link between auxin signaling and lignification through the induction of ethylene biosynthesis. Plant Signal Behav 8:e26363
13. Lee Y-C, Johnson JM, Chien C-T, Sun C, Cai D, Lou B, Oelmüller R, Yeh K-W (2011) Growth promotion of Chinese cabbage and Arabidopsis by *Piriformospora indica* is not stimulated by mycelium-synthesized auxin. Mol Plant Microbe Interact 24:421–431
14. Dong S, Tian Z, Chen PJ, Senthil Kumar R, Shen CH, Cai D, Oelmüllar R, Yeh KW (2013) The maturation zone is an important target of *Piriformospora indica* in Chinese cabbage roots. J Exp Bot 64:4529–4540
15. Müller A, Düchting P, Weiler EW (2002) A multiplex GC-MS/MS technique for the sensitive and quantitative single-run analysis of acidic phytohormones and related compounds, and its application to *Arabidopsis thaliana*. Planta 216:44–56
16. Schmelz EA, Engelberth J, Alborn HT, O'Donnell P, Sammons M, Toshima H, Tumlinson JH III (2003) Simultaneous analysis of phytohormones, phytotoxins, and volatile organic compounds in plants. Proc Natl Acad Sci U S A 100:10552–10557
17. Birkemeyer C, Kolasa A, Kopka J (2003) Comprehensive chemical derivatization for gas chromatography-mass spectrometry-based multi-targeted profiling of the major phytohormones. J Chromatogr A 993:89–102
18. Chiwocha SD, Abrams SR, Ambrose SJ, Cutler AJ, Loewen M, Ross AR, Kermode AR (2003) A method for profiling classes of plant hormones and their metabolites using liquid chromatography-electrospray ionization tandem mass spectrometry: an analysis of hormone regulation of thermodormancy of lettuce (*Lactuca sativa* L.) seeds. Plant J 35:405–417
19. Ziegler J, Qwegwer J, Schubert M, Erickson JL, Schattat M, Burstenbinder K, Grubb CD, Abel S

(2014) Simultaneous analysis of apolar phytohormones and 1-aminocyclopropan-1-carboxylic acid by high performance liquid chromatography/electrospray negative ion tandem mass spectrometry via 9-fluorenylmethoxycarbonyl chloride derivatization. J Chromatogr A 1362:102–109
20. Strehmel N, Böttcher C, Schmidt S, Scheel D (2014) Profiling of secondary metabolites in root exudates of *Arabidopsis thaliana*. Phytochemistry 108:35–46
21. Wang X, Zhao P, Liu X, Chen J, Xu J, Chen H, Yan X (2014) Quantitative profiling method for phytohormones and betaines in algae by liquid chromatography electrospray ionization tandem mass spectrometry. Biomed Chromatogr 28:275–280
22. Novak O, Henykova E, Sairanen I, Kowalczyk M, Pospisil T, Ljung K (2012) Tissue-specific profiling of the *Arabidopsis thaliana* auxin metabolome. Plant J 72:523–536
23. Astot C, Dolezal K, Moritz T, Sandberg G (1998) Precolumn derivatization and capillary liquid chromatographic/frit-fast atom bombardment mass spectrometric analysis of cytokinins in *Arabidopsis thaliana*. J Mass Spectrom 33:892–902
24. Jameson PE, Zhang H, Lewis DH (2000) Cytokinins. Extraction, separation, and analysis. Methods Mol Biol 141:101–121
25. Farrow S, Emery RN (2012) Concurrent profiling of indole-3-acetic acid, abscisic acid, and cytokinins and structurally related purines by high-performance-liquid-chromatography tandem electrospray mass spectrometry. Plant Methods 8:42
26. Kojima M, Sakakibara H (2012) Highly sensitive high-throughput profiling of six phytohormones using MS-probe modification and liquid chromatography–tandem mass spectrometry. In: Normanly J (ed) High-throughput phenotyping in plants. Humana, New York, pp 151–164
27. Takei K, Yamaya T, Sakakibara H (2003) A method for separation and determination of cytokinin nucleotides from plant tissues. J Plant Res 116:265–269
28. Novák O, Hauserová E, Amakorová P, Doležal K, Strnad M (2008) Cytokinin profiling in plant tissues using ultra-performance liquid chromatography–electrospray tandem mass spectrometry. Phytochemistry 69: 2214–2224

Chapter 16

High-Throughput Protoplast Trans-Activation (PTA) Screening to Define Transcription Factors in Auxin-Mediated Gene Regulation

Nora Wehner, Jörn Herfert, Wolfgang Dröge-Laser, and Christoph Weiste

Abstract

Genome sequencing and annotation studies clearly highlight the impact of transcriptional regulation in plants. However, functional characterization of the majority of transcriptional regulators remains elusive. Hence, high-throughput techniques are required to facilitate their molecular analysis. Here, we provide a detailed protocol to conduct a high-throughput protoplast trans-activation (PTA) screening, which enables simultaneous analysis of up to 95 individual transcription factor activities on a customizable promoter:*LUCIFERASE* reporter. This system is well suited to decipher complex transcriptional networks such as that triggered by the phytohormone auxin.

Key words Transcription factor, Screening, High throughput, Protoplast, Gene regulation, Auxin

1 Introduction

At the beginning of this century, comprehensive genome sequencing projects and gene annotation studies let to the identification of roughly 27,500 protein-coding genes in *Arabidopsis thaliana* [1–4]. Over 9 % (2492) of these genes are thought to encode for transcription factors (TFs) [5], thereby constituting one of the largest functional classes in eukaryotic genomes [6]. Although, this clearly accentuates the impact of gene regulation in plant evolution, only a limited number of TF genes have been functionally characterized, to date [5]. In order to enable molecular and biochemical analysis on a genomic scale, joint efforts were undertaken to generate large TF open reading frame (ORF) compilations [7–10]. Building upon these repositories, a high-quality, sequence-validated *Arabidopsis* TF ORF collection was recently generated, covering almost 80 % (1956) of all currently annotated transcriptional regulators [5]. Employing the GATEWAY® recombination system, the deposited TF coding regions can be readily transferred

Thomas Dandekar and Muhammad Naseem (eds.), *Auxins and Cytokinins in Plant Biology: Methods and Protocols*, Methods in Molecular Biology, vol. 1569, DOI 10.1007/978-1-4939-6831-2_16,

from their recombination-compatible donor to expression vectors, thereby highly facilitating the ensuing functional analysis [5, 11].

Due to their high quantity, individual characterization of TF genes is laborious and time-consuming. As moreover highly related TFs frequently exhibit pronounced functional redundancy and sophisticated TF networks cooperate in controlling promoter activity, high-throughput strategies are essential to screen large TF collections for their impact on gene regulation [12–14].

In this respect, classical yeast-1-hybrid screening approaches proved to be powerful tools [15–18]. However, analysis of TF activities on full-length promoters faces several limitations in this heterologous system [12].

Arabidopsis mesophyll protoplasts are an ideal high-throughput applicable system for studying plant signal transduction pathways [12–19]. Indeed, protoplasts can be easily isolated and transfected [19, 20] and display physiological responses to a wide array of endogenous [21–23] and environmental [12, 24] stimuli. In particular, they were found to be a valuable tool to decipher hormone-triggered signaling events as they react sensitively and specifically to treatments with phytohormones such as ethylene [23], abscisic acid [21], cytokinin [25], or auxin [22].

Based on a previously published, highly efficient protoplast transfection protocol [19], we established a high-throughput protoplast trans-activation (PTA) screening platform [12]. By co-transfecting protoplasts with a promoter:*LUCIFERASE* (*LUC*) reporter, a normalization plasmid, and individual TF effector constructs in a 96-well microtiter plate format, this system allows the simultaneous and quantitative examination of up to 95 TF activities on a given promoter (Fig. 1). Thus, highly complex signal integration processes can be readily assessed.

Transcription mediated by the phytohormone auxin serves as an example for complex gene regulation. In this context, it has been shown that auxin qualitatively controls auxin-responsive gene expression by interfering with the activity of *AUXIN RESPONSE FACTOR* (*ARF*) and *AUXIN/INDOLE-3-ACETIC ACID* (*Aux/IAA*) proteins [26]. In *Arabidopsis* both types of regulators belong to large gene families encoding for 23 ARFs [27] or 29Aux/IAAs [28], respectively. Moreover, several reports revealed a quantitative impact of specific MYB [29] and basic leucine zipper (bZIP) TFs [22, 30, 31] on auxin-responsive genes. Making use of the described high-throughput PTA screening platform, we could unravel a selective impact of members of the bZIP TF family on the well-characterized auxin-responsive GRETCHEN HAGEN 3.3 promoter (Pro*GH3.3*) (Fig. 2), demonstrating the systems' high capacity. In this chapter, we provide a detailed protocol to analyze TF activities on any given promoter using the PTA screening system.

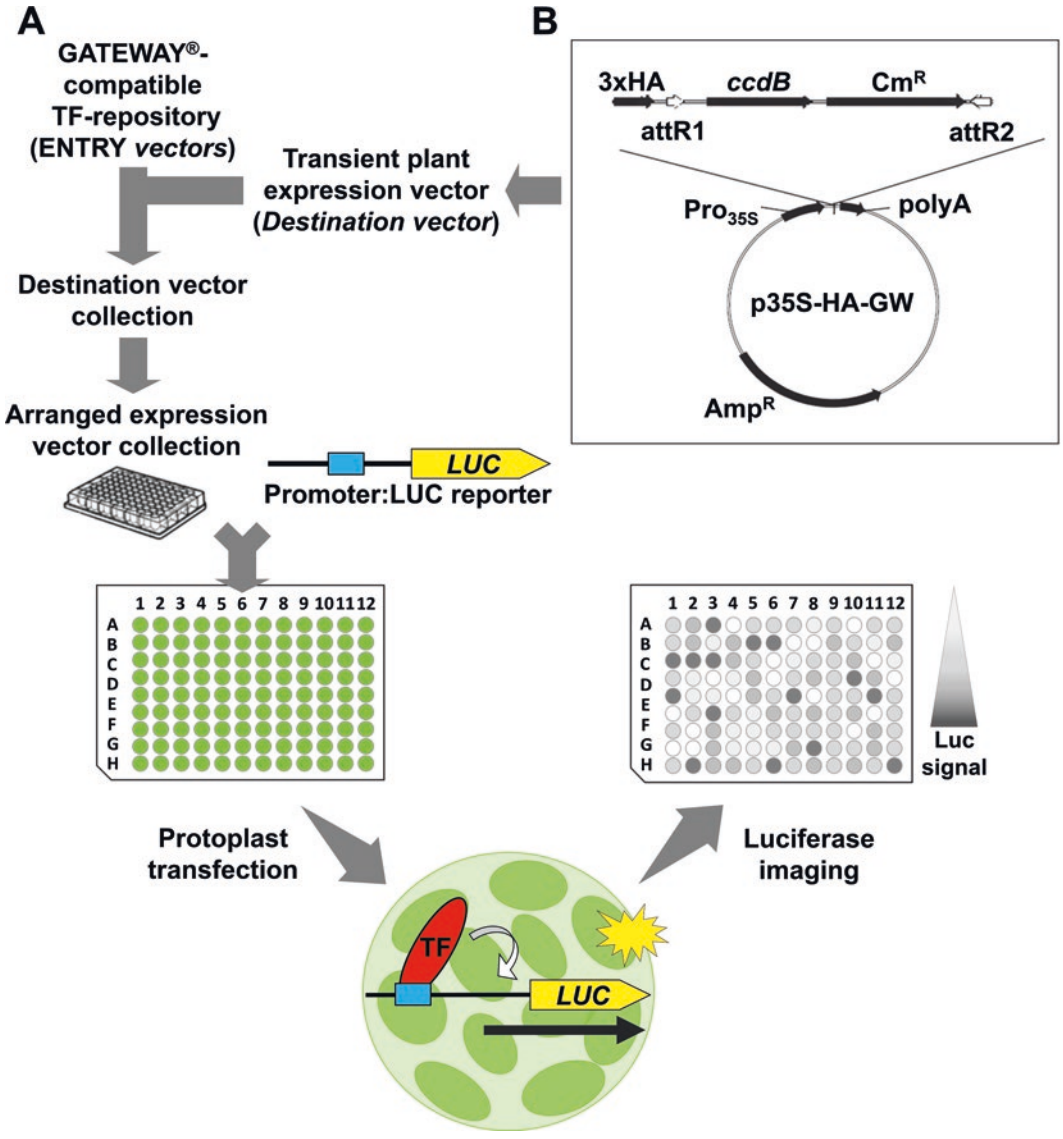

Fig. 1 Schematic overview of the protoplast trans-activation (PTA) system. (**a**) Detailed presentation of the PTA screening procedure [13]. To examine the activation or repression potential of up to 95 TFs on a promoter of choice at a time, protoplast transfections are carried out in a standard microtiter plate. Therefore, a predefined GATEWAY®-compatible TF collection is recombined in the plant expression vector p35S-HA-GW (**b**) [32], which enables transient expression in protoplasts. Trans-activation of the promoter:*LUC* reporter can be readily determined by quantitative luciferase imaging

2 Materials

2.1 Generation of Reporter and TF Effector Constructs

1. Reporter construct (pBT10-*fLUC*) (*see* **Note 1**).
2. Effector construct (p35S-HA-GW, GATEWAY®-compatible destination vector) (*see* **Note 2**).

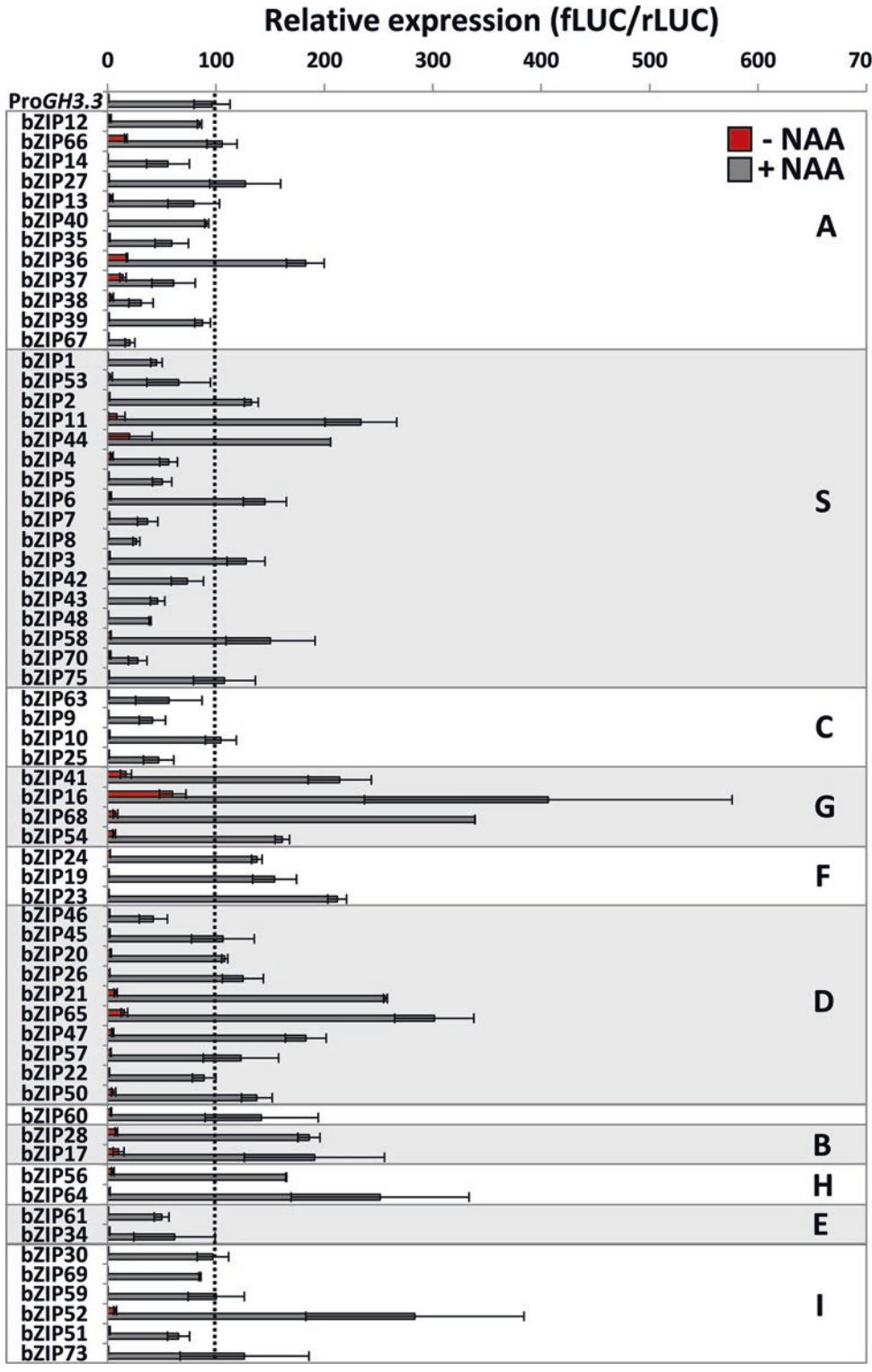

Fig. 2 PTA screen to identify bZIP TFs controlling auxin-responsive *GH3.3* promoter activity. Trans-activation properties of 63 individual bZIP TFs on the full-length (−2000 bp) *GH3.3* promoter [22] were analyzed in the

3. TF ORF collection in GATEWAY®-compatible ENTRY vector (*see* **Note 3**).
4. GATEWAY®-compatible ENTRY vectors (Thermo Fisher Scientific).
5. Phusion® High-Fidelity DNA Polymerase (New England Biolabs).
6. PrimeScript First Strand cDNA synthesis kit (Clontech).
7. GATEWAY® BP Clonase® 2 Enzyme Mix (Thermo Fisher Scientific).
8. GATEWAY® LR Clonase® 2 Enzyme Mix (Thermo Fisher Scientific).
9. Selected restriction endonucleases (Thermo Fisher Scientific).
10. T4 DNA Ligase (New England Biolabs).
11. NucleoSpin® Gel and PCR Clean-Up Kit (Macherey-Nagel).
12. NucleoSpin® Plasmid Kit (Macherey-Nagel).
13. Plasmid Plus Midi Kit (Qiagen, Cat. no. 12945) (*see* **Note 4**).

2.2 Arabidopsis Mesophyll Protoplast Preparation

1. 4–5-week-old *Arabidopsis thaliana* plants grown on soil under a 12-h light/12-h dark regime (*see* **Note 5**).
2. Forceps and scalpel.
3. Standard plastic petri dish (9 cm diameter).
4. Cellulase Onozuka R-10 (Serva).
5. Macerozyme R-10 (Serva).
6. Enzyme solution (1.25 % (w/v) Cellulase R-10, 0.3 % (w/v) Macerozyme R-10, 0.4 M mannitol, 20 mM KCl, 20 mM 4-morpholineethanesulfonic acid (MES), 10 mM $CaCl_2$, pH 5.7). Sterile-filtered stocks can be stored at 4 °C for 2 weeks (*see* **Note 6**).
7. Exsiccator with vacuum pump.
8. Steel mesh (aperture 63 μm).
9. Falcon tube (50 mL).
10. Serological pipet (10 mL).
11. Isotonic washing buffer (154 mM NaCl, 125 mM $CaCl_2$, 5 mM KCl, 2 mM MES, pH 5.7), treat by autoclave.
12. Cell-saver pipet tips, wide bore, 1 mL (Axygen).
13. Ice.

Fig. 2 (continued) absence (*red bars*) or presence (*gray bars*) of 0.3 μM of the synthetic auxin 1-naphthaleneacetic acid (NAA) in *Arabidopsis* mesophyll protoplasts. Given is the mean *firefly LUCIFERASE* (*fLUC*) reporter gene expression from two independent transfection events (±SD) relative to promoter 35S-driven *renilla LUCIFERASE* (*rLUC*) expression. All results were normalized to *GH3.3* promoter activity in the presence of NAA (set to 100%), which is indicated by a *dashed line*. bZIP TFs are arranged in subgroups (A–I, S) according to their phylogenetic relationship [33]

2.3 High-Throughput Protoplast Transfection

1. Normalization construct (pHBT-Pro35S:*rLUC*) (*see* **Note 7**).
2. Empty vector DNA (pHBT).
3. 96-well microtiter plate (transparent, round bottom).
4. Protoplast transfection buffer 1 (0.4 M mannitol, 15 mM $MgCl_2$, 4 mM MES, pH 5.7). Sterile-filtered stocks can be stored at 4 °C for 2 weeks.
5. Protoplast transfection buffer 2 (40 % (w/v) polyethylene glycol (PEG) 4000, 0.2 M mannitol, 100 mM $CaCl_2$) (*see* **Note 8**).
6. Multichannel pipet (8 or 12 channels).
7. Cell-saver pipet tips, wide bore, 200 µL (Axygen).
8. Reagent reservoir for multichannel pipets, 25 mL (Thermo Fisher Scientific).
9. Timer.
10. Isotonic washing buffer (see protoplast preparation).
11. Incubation buffer (0.5 M mannitol, 4 mM MES, 20 mM KCl, pH 5.7). Sterile-filtered stocks can be stored at 4 °C for 2 weeks.
12. 1-naphthaleneacetic acid (NAA) (Sigma-Aldrich) in DMSO. Stocks (10 mM) can be stored at −20 °C for a few months (*see* **Note 9**).

2.4 Quantitative and Semiquantitative Luciferase Imaging

1. 96-well microtiter plate (Nunc PP 0.5 mL, white, round bottom, Thermo Fisher Scientific).
2. Luminometer plate reader (Robion Solaris, Stratec).
3. Lysis buffer (2× concentrated Lysis-Juice 2, PJK GmbH).
4. Firefly luciferase substrate (Beetle-Juice BIG KIT, PJK GmbH).
5. d-Luciferin potassium salt (SYNCHEM OHG).
6. Renilla luciferase substrate (Renilla-Juice BIG KIT, PJK GmbH).
7. 75 % ethanol.

3 Methods

3.1 Generation of Reporter Constructs

Reporter constructs for the PTA screening platform can be easily assembled by inserting a PCR-amplified promoter region of choice directly upstream of the *fLUC* reporter gene in the pBT10-*fLUC* vector [12]. The following step-by-step protocol describes a general construct preparation.

1. Define the promoter region which should be screened. Using a roughly 1500 bp intergenic region upstream of the translational start site is a good starting point (*see* **Note 10**).
2. Design oligonucleotides to PCR-amplify the promoter region of choice. Introduce restriction sites 5′ of each primer, which

are present in the multiple cloning site (mcs) upstream of the *fLUC* reporter gene in the pBT10-*fLUC* vector. Restriction sites should be unique and not cut outside the vectors' mcs or within the desired promoter region (*see* **Note 11**).

3. Amplify promoter region from *Arabidopsis* genomic DNA using a high-fidelity DNA polymerase, following the manufacturer's protocol (*see* **Note 12**). Isolate the PCR fragment of correct size by performing agarose gel electrophoresis and subsequent gel extraction using a commercial kit (e.g., NucleoSpin® Gel and PCR Clean-Up Kit, Macherey-Nagel).
4. Digest pBT10-*fLUC* vector and isolated promoter fragment using the selected restriction endonucleases (*see* **step 2**), following the manufacturer's instructions. Clean up vector backbone and promoter fragment by gel electrophoresis and subsequent gel extraction using a commercial kit (e.g., NucleoSpin® Gel and PCR Clean-Up Kit, Macherey-Nagel).
5. Ligate pBT10-*fLUC* vector backbone and promoter fragment using high-quality T4 DNA Ligase (New England Biolabs), following the manufacturer's instructions. A 1:3 molar ratio of vector to promoter fragment DNA is a good starting point for the ligase reaction.
6. Transform highly chemically competent *E. coli* cells (e.g. DH5α) with half of the ligation reaction using a standard heat-shock transformation protocol [34]. Plate the transformation reaction on LB agar plates (10 g/L NaCl, 10 g/L tryptone, 5 g/L yeast extract, 15 g/L agar) containing 100 mg/L ampicillin. Incubate plates overnight at 37 °C.
7. Identify five individual bacterial colonies and inoculate with each 5 mL of liquid LB medium containing 100 mg/L ampicillin. Incubate overnight at 37 °C in a shaker incubator.
8. Prepare reporter plasmid DNA from individual *E. coli* cultures using a commercial kit (e.g., NucleoSpin® Plasmid Kit, Macherey-Nagel), following the manufacturer's manual. Validate promoter sequence by Sanger sequencing using vector-specific primers (*see* **Note 13**).
9. Prepare highly pure plasmid DNA from a sequence-validated clone using the Plasmid Plus Midi Kit from Qiagen, following the manufacturer's instructions (*see* **Note 4**).

3.2 Generation of TF Effector Constructs

In order to express TF transgenes in protoplasts, TF coding sequences (CDS) need to be cloned into a transient plant expression vector. Required TF CDS can be either obtained by PCR amplification from *Arabidopsis* cDNA preparations or taken from already existing TF CDS collections [5, 7–10]. In the following protocol, we describe both procedures using the GATEWAY® cloning technology.

3.2.1 Cloning of TF CDS from cDNA Using GATEWAY®

1. Determine under which growth conditions or in which developmental stage your TF of interest is expressed at high levels (*see* **Note 14**.
2. Cultivate *Arabidopsis* under selected growth conditions and prepare RNA from plants of the appropriate developmental stage (*see* **step 1**). Highly pure RNA from *Arabidopsis* tissues can be extracted using a TRIzol-based RNA isolation protocol [35].
3. Prepare cDNA from extracted RNA using a cDNA synthesis kit (e.g., PrimeScript First Strand cDNA synthesis kit, Clontech), following the manufacturer's manual.
4. Design transgene-specific primers to PCR-amplify your TF CDS from prepared cDNA. Primers need to contain GATEWAY® *attB* attachment sites for integrating the PCR product into the GATEWAY®-compatible ENTRY vector pDONR201 (*see* **Note 15**).
5. PCR-amplify TF CDS using the GATEWAY®-compatible primers (*see* **step 4**). Clean up PCR product by agarose gel electrophoresis and subsequent gel extraction using a commercial kit (e.g., NucleoSpin® Gel and PCR Clean-Up Kit, Macherey-Nagel).
6. Perform GATEWAY® BP reaction using 200 ng of PCR product, 200 ng of ENTRY vector, and 2 μL of GATEWAY® BP Clonase® Enzyme Mix 2 in 10 μL sample volume. Incubate reaction overnight at room temperature (*see* **Note 15**).
7. Transform highly chemically competent *E. coli* cells (e.g. DH5α) with 10 μL BP reaction using a standard heat-shock transformation protocol [34]. Plate the transformation reaction on LB agar plates (10 g/L NaCl, 10 g/L tryptone, 5 g/L yeast extract, 15 g/L agar) containing 50 mg/L kanamycin. Incubate plates overnight at 37 °C.
8. Choose two colonies and inoculate each with 5 mL of liquid LB medium containing 50 mg/L kanamycin. Incubate overnight at 37 °C in a shaker incubator.
9. Prepare donor vector DNA from individual *E. coli* cultures using a commercial kit (e.g., NucleoSpin® Plasmid Kit, Macherey-Nagel), following the manufacturer's manual. Validate TF CDS by Sanger sequencing using vector-specific primers (*see* **Note 16**).

3.2.2 Transfer of TF CDS from GATEWAY® Donor to a GATEWAY®-Compatible Plant Expression Vector

1. Perform GATEWAY® LR reaction using 200 ng of TF CDS containing donor vector, 200 ng of p35S-HA-GW destination vector, and 2 μL of GATEWAY® LR Clonase® Enzyme Mix 2 in 10 μL sample volume. Incubate reaction overnight at room temperature (*see* **Note 15**).

2. Transform highly chemically competent *E. coli* cells (e.g. DH5α) with 10 μL LR reaction using a standard heat-shock transformation protocol [34]. Plate the transformation reaction on LB agar plates (10 g/L NaCl, 10 g/L tryptone, 5 g/L yeast extract, 15 g/L agar) containing 100 mg/L ampicillin. Incubate plates overnight at 37 °C.
3. Choose two colonies and inoculate each with 5 mL of liquid LB medium containing 100 mg/L ampicillin. Incubate overnight at 37 °C in a shaker incubator.
4. Prepare effector construct DNA from individual *E. coli* cultures using a commercial kit (e.g., NucleoSpin® Plasmid Kit, Macherey-Nagel), following the manufacturer's manual. Validate correct construct assembly by determining its specific restriction pattern (*see* **Note 17**).
5. Prepare highly pure plasmid DNA from a validated effector clone using the Plasmid Plus Midi Kit from Qiagen, following the manufacturer's instructions (*see* **Note 4**).

3.3 Arabidopsis Mesophyll Protoplast Preparation

The following protocol describes the isolation of *Arabidopsis* mesophyll protoplasts. However, it can be readily adapted to other plant tissues such as roots [36] or other plant species [20]. The whole procedure takes about 7 h.

1. Cultivate soil-grown *Arabidopsis* plants for 4–5 weeks in a growth incubator under a 12 h light (8000 lx)/12 h dark regime at 20 °C and a relative humidity of ~60 % (*see* **Note 5**.
2. To avoid leaf wilting, take plants out of the growth incubator, water them, and let them acclimatize to lab conditions for ½ hour.
3. Cut the petiole of two healthy, not serrated true leaves with a scalpel and place them bottom-side up on the lid of a petri dish. Do not remove more than two leaves at a time, as this would result in severe leaf wilting.
4. Hold the petiole of the leaf with forceps and cut the leaf's abaxial side into 1 mm strips using the scalpel.
5. Turn the leaf around and place the sliced abaxial side into a petri dish filled with 10 mL of enzyme solution. Remove encased air bubbles by sweeping over the leaf with the scalpel. For one PTA screen with 96 transfections, approximately 20–25 leaves need to be prepared.
6. To ensure efficient penetration of the enzyme solution, leaves are vacuum infiltrated in the dark for 5 h using an exsiccator.
7. Release protoplasts by gently swirling the enzyme solution for up to 3 min. Greening of the enzyme solution indicates successful protoplast recovery (*see* **Note 18**).

8. Place the 63 μm metal mesh on a 50 mL falcon tube and wet it with 1 mL of ice-cold isotonic washing buffer. Afterwards clean protoplasts from residual leaf material by filtration.
9. Centrifuge the solution for 2 min at 100 × *g* using a swing-out rotor (*see* **Note 19**).
10. Remove as much supernatant as possible using a standard lab pipet with wide bore tips.
11. Gently resuspend the protoplast pellet in 10 mL of ice-cold isotonic washing buffer (*see* **Note 20**).
12. Repeat **steps 9–11**. Place the solution on ice for 30 min and let protoplasts settle by gravity.

3.4 High-Throughput Protoplast Transfection Protocol

The following universal protocol describes the procedure to simultaneously perform up to 96 independent *Arabidopsis* mesophyll protoplast transfection reactions at a time [12]. The whole procedure takes about 2 h.

1. For quantitative PTA assays, a total of 5 μg vector DNA in 5 μL of water are used for each transfection reaction. In detail, 2 μg of a selected promoter:*fLUC* reporter plasmid and 1 μg of a transfection normalization construct are combined in each well of a standard 96-well, round-bottom microtiter plate. In order to determine the promoter's background activity, one of the wells is supplemented with 2 μg of an empty vector DNA, whereas the remaining 95 wells are supplied with 2 μg of individual TF effector constructs, enabling screening of their transactivation properties on the given reporter (*see* **Note 4**).
2. Remove as much isotonic washing buffer as possible from the protoplast pellet and adjust protoplasts to a final concentration of 4×10^5 mL^{-1} by gently resuspending protoplasts in protoplast transfection buffer 1 (*see* **Notes 20** and **21**).
3. Add 30 μL of protoplast solution (approximately 1×10^4 cells) to each well using a multichannel pipet and wide bore tips. Gently mix protoplasts and DNA by pipetting up and down twice (*see* **Note 22**).
4. Add 33 μL of protoplast transfection buffer 2 to each well using a multichannel pipet and wide bore tips. Gently mix protoplasts and DNA by slowly pipetting up and down eight times (*see* **Notes 21–24**).
5. Incubate transfection reactions for 20 min at room temperature.
6. Stop the reaction by adding 120 μL of isotonic washing buffer to each well using a multichannel pipet and wide bore tips. Gently mix the solutions by slowly pipetting up and down five times (*see* **Notes 21–24**).

7. Seal microtiter plate with Parafilm and centrifuge it for 1 min at 100 × *g* using a swing-out rotor (*see* **Note 19**).
8. Remove 175 µL of the supernatant and add 100 µL of incubation buffer to each well using a multichannel pipet. Gently mix the settled protoplasts by slowly pipetting up and down five times using wide bore tips (*see* **Notes 21–25**).
9. Incubate transfected protoplasts overnight in the same growth incubator as used for cultivating the plants for protoplastation.

3.5 Determination of Reporter Activity via Dual Luciferase Imaging

In order to quantitatively assess the trans-activation properties of a selected set of TFs on a given promoter:f*LUC* reporter, differences in protoplast transfection efficiencies among the 96 individual reactions need to be taken into account. Hence, we routinely perform dual luciferase imaging to analyze both: (1) the activity of the reporter-driven *firefly LUCIFERASE* and (2) for normalization the activity of a *renilla LUCIFERASE* gene, controlled by the strong constitutive CaMV 35S promoter. The ratio between firefly and renilla luciferase activity has been found to be a reliable quantitative readout for TF activities on a given promoter [12]. The described dual luciferase imaging procedure is generally performed in around 2 h.

1. Carefully remove 90 µL of supernatant from the settled transfected protoplasts.
2. Add 22 µL of the 2× concentrated Lysis-Juice 2 to each well using a multichannel pipet and gently mix by pipetting up and down eight times.
3. Incubate the microtiter plate for 15 min on ice to ensure proper protoplast lysis.
4. Seal microtiter plate with Parafilm and centrifuge it for 10 min at 4000 × *g* using a swing-out rotor.
5. Transfer 10 µL of cell lysate into the wells of two new white round-bottom microtiter plates that are kept on ice. One plate is used to measure firefly luciferase (*see* **step 7**) and the other to determine renilla luciferase (*see* **step 9**) activity, respectively.
6. Clean injectors of the plate reader luminometer with 75 % ethanol and distilled water and fill 6 mL of firefly luciferase substrate (Beetle-Juice BIG KIT) into the injector reservoir.
7. Let the liquid handling robotic device of the luminometer add 50 µL of firefly luciferase substrate to each well and directly measure the upcoming luminescence.
8. Clean again the injectors of the plate reader luminometer (*see* **step 6**) and fill 6 mL of renilla luciferase substrate (Renilla-Juice BIG KIT) into the injector reservoir.
9. Let the liquid handling robotic device of the luminometer add 50 µL of renilla luciferase substrate to each well and directly measure the upcoming luminescence.

10. Calculate the ratio between *fLUC* and *rLUC* activity. The resulting relative luminescence intensity serves as a quantitative measure for TF trans-activation properties on the given promoter.

3.6 Semiquantitative Determination of Reporter Activity via Firefly Luciferase Imaging

Quantitative dual luciferase imaging is cost-intensive. Experienced users will also obtain reliable semiquantitative results by performing at least triplicate *fLUC* activity measurements. We strongly recommend this procedure if large screening collections are handled.

1. Clean injectors of the plate reader luminometer with 75 % ethanol and distilled water and fill 5 mL of firefly luciferase substrate (1 mM d-luciferin potassium salt dissolved in incubation buffer) into the injector reservoir.
2. Carefully remove 90 μL of supernatant from the settled transfected protoplasts.
3. Dark-incubate the microtiter plate for 8 min in the luminometer to reduce auto-phosphorescence of living protoplasts.
4. Let the liquid handling robotic device of the luminometer add 40 μL of the firefly luciferase substrate to each well. Directly measure the upcoming luminescence with an integration time of 15 s.
5. Calculate mean *fLUC* activity.

4 Notes

1. The pBT10-*fLUC* reporter plasmid can be obtained at: http://www.pbio.biozentrum.uni-wuerzburg.de/forschungwissenschaft/prof_dr_wolfgang_droege_laser/
2. The p35S-HA-GW destination vector allows transient effector expression in protoplasts and can be obtained at: http://www.pbio.biozentrum.uni-wuerzburg.de/forschungwissenschaft/prof_dr_wolfgang_droege_laser/
3. A high-quality, sequence-validated TF ORF collection in GATEWAY®-compatible ENTRY vectors [5] is available via the Arabidopsis Biological Resource Stock Center, http://www.abrc.osu.edu
4. High DNA purity and integrity is extremely important to obtain a good protoplast transfection efficiency. We hence strongly recommend to prepare all plasmid DNA required for the PTA screening procedure making use of the Plasmid Plus Midi Kit from Qiagen (Cat. no. 12945) or by classical CsCl-based methods [34].
5. Plants should be handled with care. Protoplasts derived from plants that encountered pathogen infection or were exposed to

drought or other unfavorable conditions display poor transfection rates. The same is true for protoplasts obtained from plants older than 6 weeks.

6. Cellulase and macerozyme are provided as powder that slowly dissolves in water. Therefore, it is advisable to incubate freshly prepared enzyme solution for at least 10 h in the fridge, prior to sterile filtration.
7. In order to account for variability in transfection efficiencies, we recommend to normalize reporter gene expression to the expression of a *renilla LUCIFERASE* gene driven by the constitutive CaMV 35S promoter. The normalization plasmid (pHBT-Pro35S-*rLUC*) is available at: http://www.pbio.biozentrum.uni-wuerzburg.de/forschungwissenschaft/prof_dr_wolfgang_droege_laser/
8. We recommend to use PEG4000 from Sigma-Aldrich (St. Louis, USA) or Carl ROTH (Karlsruhe, Germany) to obtain good transfection efficiencies. Prior to sterile filtration, applying a 0.45 μm syringe-filter unit, incubate PEG solution in the fridge for at least 10 h. Do not autoclave PEG solution.
9. We recommend to use the synthetic auxin analog 1-naphthaleneacetic acid (NAA) in PTA assays as it elicits auxin responses via the natural auxin perception pathway [37] but shows an enhanced stability and membrane permeability compared to the natural auxin indole-3-acetic acid.
10. Determination of promoter boundaries is still a challenging task. Although the majority of regulatory *cis*-elements that control promoter activities have generally been found within ~100–2000 bps upstream the translational start site, important enhancer, or repressor elements might also be present in distant intergenic or coding regions. Hence, it can be advisable to analyze several promoter regions in the PTA system.
11. For primer design, the freely available Primer3 program (http://primer3.ut.ee/) can be used. To increase PCR efficiency, primers should exhibit similar melting temperatures and not show extensive inter- and intramolecular self-complementarity. Addition of 4–5 extra nucleotides 5′ to the attached restriction sites in the designed primers is generally recommended for efficient cleavage of the resulting PCR product by restriction endonucleases.
12. In order to enable discrimination between natural or PCR-mediated sequence mutations, it is advisable to perform two independent PCR reactions and compare the obtained sequences with the publicly available *Arabidopsis* genome information.
13. It is recommended to confirm the entire promoter sequence using vector-specific primers (e.g., pBT10-LUC forward,

5′-AGTCAGTGAGCGAGGAAGC-3′, and pBT10-LUC reverse, 5′-GTGATGTTCACCTCGATATGTG-3′).

14. Information on gene expression profiles can be obtained online from The Arabidopsis Information Resource (TAIR) at https://www.arabidopsis.org or from Genevestigator at https://genevestigator.com
15. A detailed description on the GATEWAY® technology including sequences of GATEWAY® attachment sites and an extensive troubleshooting guide can be found in the GATEWAY® manual at https://tools.thermofisher.com/manuals or in related publications [11]. Propagation of all GATEWAY®-compatible vectors containing the *ccdB* gene needs to be done exclusively in the *E. coli* strain DB3.1.
16. The vector-specific primers SeqL1 forward (5′-TCGCGTTAACGCTAGCATGGATCTC-3′) and SeqL2 reverse (5′-GTAACATCAGAGATTTTGAGACAC-3′) can be used to sequence-validate any TF CDS in the pDONR201 ENTRY-vector backbone.
17. GATEWAY® LR reactions do not result in sequence mutations in TF CDS. Hence, validation of vector integrity by restriction analysis is sufficient.
18. Protoplast quality should be checked under the microscope. Complete cell wall digestion results in spherical protoplasts and is crucial for efficient DNA uptake during the transfection procedure.
19. To prevent compressing or resuspension of protoplasts during centrifugation, we recommend to use extremely low centrifuge acceleration or braking rates, respectively.
20. Protoplasts are sensitive to external forces. Therefore, it is advisable to add buffers slowly and to resuspend the protoplast pellet by gentle swirling. Usage of wide bore tips prevents extensive shearing of protoplasts during pipetting.
21. It is crucial that all buffers used for protoplast transfection are kept for at least 1 h at room temperature before usage.
22. To ensure rapid and nearly simultaneous treatment of 96 transfection reactions, the usage of multichannel pipets (8 or better 12 channels) is stringently required.
23. Thorough intermixture of protoplasts and protoplast transfection buffer 2 is essential to obtain high protoplast transfection rates.
24. Buffers should always be added to the wells in the same succession to ensure equal incubation times for all reactions.
25. In order to analyze TF activity under auxin-promoted conditions, supplement the incubation buffer with a final concentration of 0.25 μM of NAA.

References

1. Berardini TZ, Reiser L, Li D, Mezheritsky Y, Muller R, Strait E, Huala E (2015) The Arabidopsis information resource: making and mining the "gold standard" annotated reference plant genome. Genesis 53:474–485.
2. Kaul S, Koo HL, Jenkins J, Rizzo M, Rooney T, Tallon LJ, Feldblyum T et al (2000) Analysis of the genome sequence of the flowering plant Arabidopsis thaliana. Nature 408:796–815.
3. Riechmann JL, Heard J, Martin G, Reuber L, Jiang C, Keddie J, Adam L, Pineda O, Ratcliffe OJ, Samaha RR, Creelman R, Pilgrim M, Broun P, Zhang JZ, Ghandehari D, Sherman BK, Yu G (2000) Arabidopsis transcription factors: genome-wide comparative analysis among eukaryotes. Science 290:2105–2110.
4. Riechmann JL, Ratcliffe OJ (2000) A genomic perspective on plant transcription factors. Curr Opin Plant Biol 3:423–434.
5. Pruneda-Paz JL, Breton G, Nagel DH, Kang SE, Bonaldi K, Doherty CJ, Ravelo S, Galli M, Ecker JR, Kay SA (2014) A genome-scale resource for the functional characterization of Arabidopsis transcription factors. Cell Rep 8:621–631.
6. Weirauch MT, Hughes TR (2011) A catalogue of eukaryotic transcription factor types, their evolutionary origin, and species distribution. Subcell Biochem 52:25–73.
7. Gong W, Shen YP, Ma LG, Pan Y, Du YL, Wang DH, Yang JY, Hu LD, Liu XF, Dong CX, Ma L, Chen YH, Yang XY, Gao Y, Zhu D, Tan X, Mu JY, Zhang DB, Liu YL, Dinesh-Kumar SP, Li Y, Wang XP, Gu HY, Qu LJ, Bai SN, Lu YT, Li JY, Zhao JD, Zuo J, Huang H, Deng XW, Zhu YX (2004) Genome-wide ORFeome cloning and analysis of Arabidopsis transcription factor genes. Plant Physiol 135:773–782.
8. Paz-Ares J, Regia C (2002) REGIA, an EU project on functional genomics of transcription factors from Arabidopsis Thaliana. Comp Funct Genomics 3:102–108.
9. Underwood BA, Vanderhaeghen R, Whitford R, Town CD, Hilson P (2006) Simultaneous high-throughput recombinational cloning of open reading frames in closed and open configurations. Plant Biotechnol J 4:317–324.
10. Yamada K, Lim J, Dale JM, Chen H, Shinn P, Palm CJ, Southwick AM, Wu HC, Kim C, Nguyen M, Pham P, Cheuk R, Karlin-Newmann G, Liu SX, Lam B, Sakano H, Wu T, Yu G, Miranda M, Quach HL, Tripp M, Chang CH, Lee JM, Toriumi M, Chan MM, Tang CC, Onodera CS, Deng JM, Akiyama K, Ansari Y, Arakawa T, Banh J, Banno F, Bowser L, Brooks S, Carninci P, Chao Q, Choy N, Enju A, Goldsmith AD, Gurjal M, Hansen NF, Hayashizaki Y, Johnson-Hopson C, Hsuan VW, Iida K, Karnes M, Khan S, Koesema E, Ishida J, Jiang PX, Jones T, Kawai J, Kamiya A, Meyers C, Nakajima M, Narusaka M, Seki M, Sakurai T, Satou M, Tamse R, Vaysberg M, Wallender EK, Wong C, Yamamura Y, Yuan S, Shinozaki K, Davis RW, Theologis A, Ecker JR (2003) Empirical analysis of transcriptional activity in the Arabidopsis genome. Science 302:842–846.
11. Katzen F (2007) Gateway ® recombinational cloning: a biological operating system. Expert Opin Drug Discov 2:571–589.
12. Wehner N, Hartmann L, Ehlert A, Bottner S, Onate-Sanchez L, Dröge-Laser W (2011) High-throughput protoplast transactivation (PTA) system for the analysis of Arabidopsis transcription factor function. Plant J 68:560–569.
13. Wehner N, Weiste C, Dröge-Laser W (2011) Molecular screening tools to study Arabidopsis transcription factors. Front Plant Sci 2:68.
14. Weiste C, Iven T, Fischer U, Onate-Sanchez L, Dröge-Laser W (2007) In planta ORFeome analysis by large-scale over-expression of GATEWAY-compatible cDNA clones: screening of ERF transcription factors involved in abiotic stress defense. Plant J 52:382–390.
15. Ito S, Song YH, Josephson-Day AR, Miller RJ, Breton G, Olmstead RG, Imaizumi T (2012) FLOWERING BHLH transcriptional activators control expression of the photoperiodic flowering regulator CONSTANS in Arabidopsis. Proc Natl Acad Sci U S A 109:3582–3587.
16. Li L, Ljung K, Breton G, Schmitz RJ, Pruneda-Paz J, Cowing-Zitron C, Cole BJ, Ivans LJ, Pedmale UV, Jung HS, Ecker JR, Kay SA, Chory J (2012) Linking photoreceptor excitation to changes in plant architecture. Genes Dev 26:785–790.
17. Niwa M, Daimon Y, Kurotani K, Higo A, Pruneda-Paz JL, Breton G, Mitsuda N, Kay SA, Ohme-Takagi M, Endo M, Araki T (2013) BRANCHED1 interacts with FLOWERING LOCUS T to repress the floral transition of the axillary meristems in Arabidopsis. Plant Cell 25:1228–1242.
18. Pruneda-Paz JL, Breton G, Para A, Kay SA (2009) A functional genomics approach reveals CHE as a component of the Arabidopsis circadian clock. Science 323:1481–1485.
19. Yoo SD, Cho YH, Sheen J (2007) Arabidopsis mesophyll protoplasts: a versatile cell system for transient gene expression analysis. Nat Protoc 2:1565–1572.

20. Sheen J (2001) Signal transduction in maize and Arabidopsis mesophyll protoplasts. Plant Physiol 127:1466–1475.
21. Fujii H, Chinnusamy V, Rodrigues A, Rubio S, Antoni R, Park SY, Cutler SR, Sheen J, Rodriguez PL, Zhu JK (2009) In vitro reconstitution of an abscisic acid signalling pathway. Nature 462:660–664.
22. Weiste C, Dröge-Laser W (2014) The Arabidopsis transcription factor bZIP11 activates auxin-mediated transcription by recruiting the histone acetylation machinery. Nat Commun 5:3883.
23. Yanagisawa S, Yoo SD, Sheen J (2003) Differential regulation of EIN3 stability by glucose and ethylene signalling in plants. Nature 425:521–525.
24. He P, Shan L, Sheen J (2007) The use of protoplasts to study innate immune responses. Methods Mol Biol 354:1–9.
25. Niu Y, Sheen J (2012) Transient expression assays for quantifying signaling output. Methods Mol Biol 876:195–206.
26. Vanneste S, Friml J (2009) Auxin: a trigger for change in plant development. Cell 136:1005–1016.
27. Okushima Y, Overvoorde PJ, Arima K, Alonso JM, Chan A, Chang C, Ecker JR, Hughes B, Lui A, Nguyen D, Onodera C, Quach H, Smith A, Yu G, Theologis A (2005) Functional genomic analysis of the AUXIN RESPONSE FACTOR gene family members in Arabidopsis thaliana: unique and overlapping functions of ARF7 and ARF19. Plant Cell 17:444–463.
28. Overvoorde PJ, Okushima Y, Alonso JM, Chan A, Chang C, Ecker JR, Hughes B, Liu A, Onodera C, Quach H, Smith A, Yu G, Theologis A (2005) Functional genomic analysis of the AUXIN/INDOLE-3-ACETIC ACID gene family members in Arabidopsis thaliana. Plant Cell 17:3282–3300.
29. Shin R, Burch AY, Huppert KA, Tiwari SB, Murphy AS, Guilfoyle TJ, Schachtman DP (2007) The Arabidopsis transcription factor MYB77 modulates auxin signal transduction. Plant Cell 19:2440–2453.
30. Heinekamp T, Strathmann A, Kuhlmann M, Froissard M, Muller A, Perrot-Rechenmann C, Dröge-Laser W (2004) The tobacco bZIP transcription factor BZI-1 binds the GH3 promoter in vivo and modulates auxin-induced transcription. Plant J 38:298–309.
31. Iven T, Strathmann A, Bottner S, Zwafink T, Heinekamp T, Guivarc'h A, Roitsch T, Dröge-Laser W (2010) Homo- and heterodimers of tobacco bZIP proteins counteract as positive or negative regulators of transcription during pollen development. Plant J 63:155–166.
32. Ehlert A, Weltmeier F, Wang X, Mayer CS, Smeekens S, Vicente-Carbajosa J, Dröge-Laser W (2006) Two-hybrid protein-protein interaction analysis in Arabidopsis protoplasts: establishment of a heterodimerization map of group C and group S bZIP transcription factors. Plant J 46:890–900.
33. Jakoby M, Weisshaar B, Dröge-Laser W, Vicente-Carbajosa J, Tiedemann J, Kroj T, Parcy F (2002) bZIP transcription factors in Arabidopsis. Trends Plant Sci 7:106–111.
34. Sambrook J, Fritsch EF, Maniatis T (1989) Molecular cloning: a laboratory manual. Cold Spring Harbour Laboratory Press, Cold Spring Harbour.
35. Chomczynski P (1993) A reagent for the single-step simultaneous isolation of RNA, DNA and proteins from cell and tissue samples. Biotechniques 15:532–534.
36. Hartmann L, Pedrotti L, Weiste C, Fekete A, Schierstaedt J, Gottler J, Kempa S, Krischke M, Dietrich K, Mueller MJ, Vicente-Carbajosa J, Hanson J, Dröge-Laser W (2015) Crosstalk between two bZIP signaling pathways orchestrates salt-induced metabolic reprogramming in Arabidopsis roots. Plant Cell 27:2244–2260.
37. Tan X, Calderon-Villalobos LI, Sharon M, Zheng C, Robinson CV, Estelle M, Zheng N (2007) Mechanism of auxin perception by the TIR1 ubiquitin ligase. Nature 446(7136): 640–645.

INDEX

A

Abiotic stress 62, 90, 102–104, 106, 107, 109, 110, 159
Arabidopsis 3, 6, 8, 11, 32, 41, 63, 75, 84, 113, 128, 142, 143, 152, 160, 161, 165, 167, 176, 187, 191
Arabidopsis thaliana 3, 6, 8, 11, 32, 41–47, 49–56, 58, 63, 74–80, 113–123, 125, 128, 143, 161, 165, 167, 168, 187, 191
ARR5:GUS 152–155
Auxin 1, 31, 43, 62, 73, 84, 93, 103, 141, 160, 166, 175, 188
  and cytokinins 3, 4, 31, 32, 61–71, 84, 90, 91, 93
  signaling and metabolism 2–11
  transport 3, 7–11, 17, 50

B

Boolean models 84, 88, 90

C

Cell cycle 152
Clubroot-disease 41, 43, 48, 49, 55, 58
Crosstalk 15, 16, 31, 84, 94, 103, 141, 166, 175–184
Cyst nematodes 74–80, 151, 152, 155
Cytokinin (CKs) 1, 31, 43, 62, 73, 84, 93, 101, 113, 127, 141, 152, 160, 165, 175, 188
  signaling 12–18, 74–80, 121, 152, 155, 166–172

D

Defense responses 113, 122, 135, 136, 141, 160, 161, 166, 168
Derivatization 32, 103, 178–181, 183
Dexamethasone (DEX) 128–131, 133–137, 142

E

Ecology 127
Electron-impact tandem mass spectrometry (EI-GC-MS/MS) 175

F

Fieldwork 130, 133, 135

G

Gene regulation 18, 58, 83, 187, 188, 190–199
Giant cells 151
ß-Glucuronidase 44, 70, 147

H

H_2O_2 ..... 99, 159–162
High resolution mass spectrometry (HRMS) 103
High-throughput 83, 94, 114, 120, 187, 188, 190–199
Hormone immune network 85, 86
Hormone responsive promoter 43
Host-pathogen interaction 142–149
Hyaloperonospora arabidopsidis 113–123, 125, 166

I

Immunity 83–91, 113–123, 125, 141, 166
Immunoblotting 98
Indole-3-acetic acid (IAA) 2–6, 8, 9, 12, 16, 31, 32, 44, 50, 52, 58, 62–64, 66–70, 73, 74, 76, 84, 93, 96, 160, 176, 177, 179, 181–183, 188, 199
Infection assay 80
In-gel kinase assay 95, 98
Interactome 83, 166–172
Internal standard 33–37, 66, 67, 71, 104, 106, 107, 176, 179, 181, 182
Isopentenyl transferase (IPTs) 16, 127

J

Jasmonic acid (JA) 44, 62, 141, 142, 160, 176, 177, 179, 181–183

L

Lateral root 10, 47, 73, 74, 76–79
LHGR 128–137
Liquid chromatography 103, 177, 178
Luminol 161, 162

M

Mass spectrometry 103, 176–177, 179–181
Mitogen activated protein kinase (MAPK) assay 94–99

N

Nematode 74–80, 151–154, 156, 157, 166
Network simulation 83, 85–87

P

Pathogen-inducible promoter 142, 144, 146–147
Pathway prediciton 84

Thomas Dandekar and Muhammad Naseem (eds.), *Auxins and Cytokinins in Plant Biology: Methods and Protocols*, Methods in Molecular Biology, vol. 1569, DOI 10.1007/978-1-4939-6831-2, © Springer Science+Business Media LLC 2017

Phytohormones 32, 37, 62, 66, 67, 69–71, 73, 84, 90, 93, 103, 135, 141, 160, 162–163, 175, 177, 183, 188
Plant hormone 1, 3, 31, 33, 43, 44, 58, 62, 70, 84–86, 91, 101, 103–105, 113, 127, 142–149, 175–181
Plant hormone analysis.....32, 181
Plant immunity 83–91, 113, 141, 166
Plant micro interactions 62
Plasmodiophora brassicae 42–47, 49–56, 58
pOp6 128–137
Protoplast 42, 187, 188, 190–199
Pseudomonas syringae..... 63, 64, 142, 143, 146–147, 166

Q

Quantification 35–36, 64, 67, 68, 98, 99, 102–104, 106, 107, 109, 110, 113–123, 125, 160, 176, 177
Quantitative-Real Time PCR analysis (qRT-PCR) 97–98

R

Reactive oxygen species (ROS)..... 159, 160, 162–163
Root-knot nematodes (RKN).....74, 76–78, 80, 151, 166
Root structure architecture (RSA)..... 47, 95, 99

S

Scintillation counter 161, 162
Screening..... 3, 6, 8, 12, 13, 66, 85, 114, 130–133, 136, 187, 188, 190–199
Signaling..... 3, 9, 10, 13–18, 43, 49, 50, 52, 62, 74–80, 83, 90, 93, 127, 141, 175, 176
Signaling network.....62, 93
Solid-phase extraction (SPE) 32, 33, 35, 37, 64, 67, 104, 106, 107, 178–180, 183
Stable isotopes 33, 37, 63, 67, 176, 179, 181
Stress response..... 152, 175–184
Syncytium.....151, 152

T

TCSn:GFP..... 152, 153, 155–156
Transcription factor 5, 6, 9, 12, 13, 16, 17, 53, 62, 90, 94, 128, 152, 165, 187, 188, 190–199
Transcriptomes 3, 14, 94, 152, 166–172, 176
Transient plant transformation 144